BIOOXIDATION KINETICS OF *LEPTOSPIRILLUM FERRIPHILUM* ATTACHED TO A DEFINED SOLID SUBSTRATE

Dissertation in partial fulfilment for the degree of

Master of Science in Chemical Engineering

By

POROGO DUKU [BSc CHEMICAL ENGINEERING]

Centre for Bioprocess Engineering Research

Department of Chemical Engineering

UNIVERSITY OF CAPE TOWN

December 2011

Dedication


FOR **MUM** AND **DAD**
ALWAYS **LOVING**,
SUPPORTING AND
ENCOURAGING ME
ANYIK AND **LEJU:**
YOU CAN ACHIEVE
ANYTHING YOU SET
YOUR MIND TO
ACHIEVE.
All GLORY GOES TO **GOD** FOR
STRENGTH AND PROVISION
THROUGH MY JOURNEY
ALLISON:
YET ANOTHER
MOUNTAIN
WE'VE CLIMBED
TOGETHER
FOR ALL THE **FRIENDS** I HAVE
MET ALONG THE WAY: MY
FAMILY AWAY FROM HOME!!!

Declaration

I know that plagiarism is wrong. Each significant contribution to, and quotation in, this study from the work, or works, of other people has been attributed, and has been cited and referenced. This dissertation is for the degree of Master of Science in Chemical Engineering at the University of Cape Town and has not been submitted for any other degree at any other university.

Porogo Duku

Signature (Porogo Duku) **.....**

Acknowledgements

I would like to acknowledge the following individuals that I have had the pleasure of working with. The journey was not always easy, with many obstacles along the way but in the end I prevailed.

- To my supervisors: **Dr Jochen Petersen, Dr Sanet Minnaar** and **Prof Sue Harrison**. Each of you played a vital role in pushing my work forward. Thank you all for giving me the opportunity to be a part of CeBER and for the ideas, encouragement and guidance throughout the duration of my studies.

- To my mentor, **Chris Bryan**, for literally teaching me everything I know about Applikon reactors and *Leptospirillum ferriphilum*. You made it so much easier for me to start my work. Thank you for your patience. To **Fran Pocock** and **Emmanuel Ngoma**, for all the assistance in the laboratory as well as the encouragement when times were difficult. You are indeed the backbone of the CeBER labs. **To Rob** for providing me with *Leptospirillum ferriphilum* at the early stages of my work. To **Sue Jobson, Candice Mazzolini** and **Bev Bailey** for all the administrative assistance. To the Centre for Bioprocess Engineering Research (**CeBER**), **BHP Billiton** and the National Research Foundation (**NRF**) for the funding throughout my studies.

- To **Elizabeth Kuiper** and **Michelle van Ryneveld** for the work they did in the laboratory towards their BSc thesis which was also useful for this study particularly chapter 5.

- To **Lerato, Gracia, Tapiwa, Rebecca, Tindi, Nozonke, Lesego, Doreen, Seun, Femi, Dion, JP and Elaine** amongst others for the motivation and companionship both at work and play. To **Allison Kasozi,** for being there always and for all the encouragement and support. For the love you have shown me. I am grateful to have you in my life.

- To my parents (**Dr and Mrs Duku**) and younger brothers (**Anyik** and **Leju**) for being the best family anyone could ever ask for. I have received all the support I need from you and more. The journey we have been through in life is amazing with all the sacrifices that have been made to give me an education. I owe a lot to you for who I am today.

- I thank the man above, for all his blessings. Because of you I am who I am today. May your name be glorified through this work as my inspiration and motivation come from you **GOD**.

Synopsis

Bioleaching can be categorized as being either stirred tank type (i.e. bio-oxidation) or irrigation type (i.e. heap/dump bioleaching) yet studies investigating the kinetics of bioleaching systems mostly use empirical data determined from stirred tank type and initial rate experiments in batch cultures or using iso-potential devices. Rate equations deduced from such empirical data is then used to model both the stirred tank type and irrigation type bioleaching systems overlooking the possibility that there may be significant differences in their environments and therefore the kinetics. Tank bioleaching systems are well mixed suspention systems dominated by planktonic microorganisms (freely suspended in the liquid medium). Heap bioleaching systems on the contrary, are heterogeneous in nature with chemical and physical conditions changing over time and are dominated by sessile microorganisms (attached microorganisms to the surface of a solid). The heap bioleaching system is therefore highly complex compared to the stirred tank-type systems. Microbial growth in bioleaching systems significantly influence the overall bioleaching kinetics yet biological kinetic effects in sessile/ attached environments are not well understood. Heap and dump leaching account for about 20% of the world's copper production and are becoming popular methods of copper production from leaching low grade ores. It is therefore important that the kinetics of irrigation type bioleaching systems are well understood.

A strategy to determine the microbial kinetics of a sessile microbial population is enforced in this study. From this, empirical data determined from irrigation type environments can then be used to derive equations which can be used to accurately model heap bioleaching systems. Three sets of experiments were conducted to try and achieve this:

i. planktonic experiments - investigating the microbial kinetics of a planktonic microbial population
ii. attachment experiments - investigating the nature of growth of the microbial population to the surface of a solid substrate during attachment to create a sessile microbial population
iii. sessile experiments - investigating the microbial kinetics of the sessile microbial population

A pure culture of *Leptospirillum ferriphilum* (a mesophilic, ferrous iron oxidizing bioleaching microorganism) was used in this study. Planktonic experiments were conducted in a completely mixed, well aerated continuous stirred tank reactor (CSTR) with a 1 litre working volume, operating at a pH of about 1.3 and temperature of 37^{o}C. Attachment and sessile experiments were conducted using a CSTR with similar conditions to the planktonic experimental, however the system was

modified by introducing a packed bed vessel (PBR) attached as a closed loop to the CSTR. Solution drawn from the CSTR was then continuously pumped through the PBR and back to the CSTR.

Planktonic experiments showed that there was wall growth in the CSTR system resulting in a deviation from Monod type behaviour. The maximum growth rate (μ_{max}) of the microbial culture used in this study where wash-out was expected was determined to be 0.0831 hr^{-1} (12 hr residence time). In this study, however, the complete wash-out of planktonic microorganisms from the CSTR did not occur. This was as a result of the microorganisms attached to the reactor wall (wall growth) which continuously eluted planktonic microorganisms into the CSTR medium. Sessile experiments were therefore conducted at conditions where the planktonic population numbers were minimal and ferrous iron was un-limited (4 and 5 hr residence time).

The attachment of the microbial population was achieved by day 2. Over 87% of the sessile population was firmly attached to the ceramic saddles. Sessile microorganisms therefore could not be easily washed out from the PBR during sessile experiments. The growth of the sessile population at specific reactor conditions (32 hr residence time in CSTR and 11.5 recycle ratio[flow rate of culture out of the CSTR through the glass vessel: the flow rate of the fresh feed into the CSTR]) reached a steady state and the population was on average 106 x 10^6 cells/g ceramic saddles. Sessile experiments showed that the recycle ratio (flow rate of culture out of the CSTR through the PBR: the flow rate of the fresh feed into the CSTR) was an important factor to consider when investigating the kinetics of the sessile microbial population. Experiments conducted at low recycle ratios (4 hr residence time-1.4 recycle ratio; 5 hr residence time-1.8 recycle ratio) showed that the kinetics in the PBR had very little influence on the CSTR. Due to ferrous iron limitations in the PBR, the PBR reached a steady state independent of the steady state conditions in the CSTR.

The specific ferrous iron oxidation rate is derived from a mass balance around the CSTR system and is dependent on the ferrous iron oxidation rate and total biomass in the system. This however, only applies when cell attachment is assumed to be negligible and therefore there is no accumulation of biomass in the system. Under this assumption, the biomass in the system can be determined using carbon dioxide uptake rates at a known dilution rate. In this study, however, wall growth was observed during planktonic experiments therefore there was an accumulation of biomass in the CSTR system. During sessile experiments, there was also an accumulation of biomass in the PBR. An accurate measure of the biomass in the reactor system therefore could not be determined using carbon dioxide uptake rates. A ratio of the ferrous iron oxidation rate rFe^{2+}: carbon dioxide uptake

rate rCO_2 ($q'Fe^{2+}$ratio) was therefore used in this study to compare the kinetic data from planktonic experiments to that from sessile experiments.

There were small difference between $q'Fe^{2+}$ratio from planktonic experiments and sessile experiments. This was because the PBR did not influence the CSTR significantly due to ferrous iron limitations (in the PBR). The $q'Fe^{2+}$ratios from sessile experiments were 152 mmolFe.hr.mmolC^{-1} (5 hr residence time, 13% decrease from planktonic ratio) and 182 mmolFe.hr.mmolC^{-1} (4 hr residence time, 4% increase from planktonic ratio). The two reactors (CSTR and PBR) could not be assumed to be in one system because the conditions in the two reactors were heterogeneous. Samples drawn from the CSTR were therefore not representative of the solution in the PBR. A sessile experiment at a 5 hr residence time using a higher recycle ratio of 21 was therefore investigated to try and achieve homogenous conditions between the PBR and CSTR solution. There were still ferrous iron limitations in the PBR and conditions in the PBR and CSTR were still heterogeneous. The system therefore could not be assumed to be one system. Differences in the conditions between the CSTR medium and the PBR medium were however reduced. The $q'Fe^{2+}$ratios from sessile experiments at a high recycle ratio was 132 mmolFe.hr.mmolC^{-1} (5 hr residence time, 27% decrease from planktonic ratio).

This study has shown that the recycle ratio determines the extent of ferrous iron limitations in the PBR. If ferrous iron is limiting then the PBR system reaches a steady state regardless of the availability of ferrous iron in the CSTR. Removing this ferrous iron limitation by increasing the recycle ratio would therefore achieve homogenous conditions between the PBR solution and CSTR solution. The study also points out the occurrence of wall growth in the CSTR system. If wall growth can be eliminated from the system, planktonic cells can be completely washed-out of the CSTR and the kinetics of the sessile population can then be accurately determined. This study has shown that the environment in bioleaching systems does affect the kinetics of the system.

Table of Contents

List of Figures

List of Tables

Glossary

Autotrophic:	Organism capable of fixing carbon dioxide for biomass production.
Abiotic	Refers to non-living physical and chemical attributes of a system.
Biotic	Refers to living factors in a system.
Brownian motion:	The random drifting of microscopic particles suspended in fluid resulting from the continuous bombardment of particles from the surrounding medium.
Chemolithotroph:	Organism capable of generating energy from inorganic compounds.
Chemotaxis:	The movement of motile organisms influenced by the concentration gradient of a particular substance.
Critical dilution rate:	Equivalent to the maximum specific growth rate at steady state conditions in ideal conditions. If the dilution rate is greater than the critical dilution rate, the death rate is greater than the growth rate and cells are unable to sustain themselves so they washout of the reactor.
Dilution rate:	The flow rate of medium per unit volume of culture in a bioreactor. The dilution rate is equal to the specific growth rate at steady state conditions.
Extracellular polymeric substances:	Substance excreted by microorganisms for attachment purposes to a solid surface. It is made of sugars, fatty acids, glucuronic acid and ferric iron.
Heap leaching:	An irrigation type hydrometallurgy method used for the extraction of metals usually from low grade ores.
Hydrometallurgy:	The extraction and purification of metals using wet methods.
Hydrophobic:	Repels/resistant to water.
Planktonic:	Microorganism freely suspended in liquid medium**.**
Residence time:	The average time a particle remains in a system.
Sessile:	A microorganism attached to a surface.
Washout:	Occurs when the rate of microorganisms flowing out of a bioreactor exceeds the rate at which microorganisms are produced in a bioreactor.

Nomenclature

ABREVIATIONS

A.D	*Anno Domini*
AAS	Atomic Absorption Spectrum spectroscopy
Af	*Acidithiobacillus ferrooxidans*
At	*Acidithiobacillus thiooxidans*
ATP	Adenosine Tri-phosphate
B.C	Before Christ
CeBER	Centre for Bioprocess Engineering Research
CSTR	Continuous Stirred Tank Reactor
EPS	Extracellular polymeric substances
Lf	*Leptospirillum ferriphilum*
NADPH	Nicotinamide Adenine Dinucleotide Phosphate
PLS	Pregnant liquor solution
PPM	Parts per million
USA	United States of America

CHEMICAL FORMULAE

a_1	Cytochrome a_1
As_2S_3	Orpiment
As_4S_4	Realgar
C	Cytochrome c
$CH_{1.8}O_{0.5}N_{0.2}$	Biomass
CO_2	Carbon dioxide
C_u	Rusticyanin
$CuFe_2S$	Chalcopyrite
E_h	Redox potential
Fe^{2+}	Ferrous iron
Fe^{3+}	Ferric iron
FeS_2	Pyrite
H^+	Hydrogen proton
H_2O	Water
H_2SO_4	Sulphuric acid
H_2S_n	Polysulphide

K_La	Overall mass transfer coefficient
MnS_2	Hauerite
MoS_2	Molybdenite
MS	Metal sulphide
NH_4^+	Ammonium ion
O_2	Oxygen
PbS	Galena
pH	Potential for hydrogen ion concentration
SO_4^{2-}	Sulphate ion
$S_2O_3^{2-}$	Thiosulphate
WS_2	Tungstenite
ZnS	Sphalerite

LIST OF SYMBOLS

SYMBOL	DESCRIPTION	UNITS
a_i	Chemical activity of relevant species i	$mole.L^{-1}$
α	Specific death rate	hr^{-1}
D	Dilution rate	hr^{-1}
D_c	Critical dilution rate	hr^{-1}
E_a	Activation energy	Joules
E_h	Redox potential	mV
E_o	Standard redox potential	mV
F	Faraday constant	$9.649C.mole^{-1}$
$[Fe^{2+}]$	Ferrous iron concentration	$mmolFe.L^{-1}$
ΔG	Gibbs free energy	$Joules.mole^{-1}$
ϒ	Activity coefficient	dimensionless
I	Ionic strength	$mole.L^{-1}$
K_m	Apparent Michaelis-Menten constant	
$K_i, K_{if}, K_{si}, K_i', K_3^*$	Model-specific inhibition constants	various
$K_s, K_m, K_{Fe^{2+}}$	Model-specific substrate affinity constants	$mmole.L^{-1}$
m_s	Maintenance	$mmolFe^{2+}.mmolC.hr^{-1}$
n	Number of electrons transferred	
μ	Microbial growth rate	hr^{-1}
μ_{max}	Maximum microbial growth rate	hr^{-1}

ρ_{O_2}	Oxygen partial pressure	Pa
$q_{Fe^{2+}}^{max}$	Maximum Specific ferrous iron utilisation rate	$mmolO_2.(mmolC.hr)^{-1}$
$q_{O_2}^{max}$	Maximum Specific oxygen utilisation rate	$mmolO_2.(mmolC.hr)^{-1}$
q_s	Specific substrate utilisation rate	$mmolS.(mmolC.hr)^{-1}$
q_s' **ratio**	rFe^{2+}: rCO_2	$mmolFe.hr.mmolC^{-1}$
R	Universal gas constant	$8.314J.mol.K^{-1}$
$-r_{CO_2}$	Carbon dioxide uptake rate	$mol.L^{-1}.hr^{-1}$
$-r_{O_2}$	Oxygen uptake rate	$mol.L^{-1}.hr^{-1}$
$-r_s$	Limiting substrate uptake rate	$mol.L^{-1}.hr^{-1}$
$[S]_{inlet}$	Substrate inlet concentration	$mmol.L^{-1}$
$[S]_{outlet}$	Substrate outlet concentration	$mmol.L^{-1}$
T	Absolute Temperature	K
τ	Residence time	hr
V	Volume	L
X	Cell concentration in reactor	$mmol.L^{-1}$
X_o	Cell concentration in inlet	$mmol.L^{-1}$
Y_{sx}^{max}	Maximum growth yield on substrate s	$mmolC.(mmolFe^{2+})^{-1}$
Z_i	Ion charge of species i	$mole.L^{-1}$

1 Introduction

1.1 Background

Historically, and even currently, the bulk of the world copper (80%) has been produced, primarily, through the pyrometallurgical process route which involves smelting and refining of copper sulphide concentrates (Lusinga, 2011). Pyrometallurgy, however, is typically capital intensive and has been historically associated with negative environmental impacts due to SO_2 emissions and high energy intensity, although some of these issues have been radically addressed in recent years (Lusinga, 2011).

Hydrometallurgical extraction technologies, more specifically heap and dump leaching, which account for about 20% of the world's copper production, are becoming popular methods of copper production (via secondary sulphide and oxide copper minerals) as they typically have relatively lower capital and operating costs compared to smelting. However, a current weakness with copper heap and dump leaching is that these methods offer low extraction rates for chalcopyrite (a primary sulphide mineral), which is the most abundant copper mineral in the world and hence present in most sulphide deposits. Chalcopyrite is extracted more efficiently in smelters. Hydrometallurgical processes can be categorised as either irrigation type (such as in situ leaching, dump leaching and heap leaching), or tank type (such as suspension leaching), with heap bioleaching as a popular option (Ojumu *et al.*, 2006; Petersen, 2009). The appropriate hydrometallurgical process depends on the grade of the ore. Suspension leaching tends to be the least popular when leaching low grade ores as it is more costly (Rawlings, 2002; Sandström, 2008). Heap bioleaching typically involves trickling an acidic solution through a stacked heap of ore that contains copper minerals and collecting the pregnant leach solution (containing dissolved copper ions) from beneath the heaps into ponds and thereafter extracting the copper ions in the form of saleable copper cathodes through solvent extraction (SX) and electrowinning (EW) technology. Bacteria catalyze the generation of the leach reagents required for the copper extraction (leaching) reactions that occur between the ore minerals and the acidic solution within the heaps.

Leaching rates of biotic systems have been found to be 10^5-10^6 times faster than abiotic leaching systems at ambient temperatures, showing the importance of the presence of microorganisms in leaching systems (Ozkaya *et al.,* 2007). Bioleaching microorganisms are acidophilic in nature, operating at pH levels as low as pH 1 (Sandström, 2008). They are also autotrophic i.e. fix atmospheric carbon dioxide for biomass generation, and are known to be chemolithotrophic as they

generate energy by oxidizing ferrous iron and/or other reduced inorganic sulphur compounds. Some of the microorganisms are capable of oxidizing either ferrous iron or sulphur, while others are capable of oxidizing both (Rawlings *et al.*, 2003; Watling, 2006). They are also sensitive to temperature and are categorized as mesophiles, moderate thermophiles or extreme thermophiles. *Acidithiobacillus ferrooxidans* was the first bioleaching microorganism to be isolated from pyrite inclusions of bituminous coal in the 1950's (Gericke *et al.*, 2009; Mathur, 2005) and has been studied extensively. It was thought to be the dominant mesophilic microorganism for a long time but *Leptospirillum* has been found to be the dominant species in many bioleaching operations instead. *Leptospirillum* can function at high redox potentials, a quality that *Acidithiobacillus ferrooxidans* does not possess, and forms part of the reason for the dominance of the *Leptospirillum* species in bioleaching systems (Rawlings *et al.*, 1999; Rawlings, 2002). Microbial growth significantly influences leaching kinetics as certain elementary processes such as direct microbial action, indirect microbial action, surface attachment of microorganisms to the ore particles, growth of microorganisms on alternative energy sources, inhibition of microbial action by ions released with the leached metal, natural oxidation, electrochemical reactions, and diffusional resistance depend on microbial action (Rossi, 1990; van Scherpenzeel *et al.*, 1998).

A number of studies from literature have proposed microbial growth and ferrous iron oxidation rate equations using empirical data from continuous systems (in absence of mineral substrate) and initial rate experiments in batch cultures or using iso-potential devices (Ojumu *et al.*, 2006). In these studies Michaelis-Menten/Monod type equations and the chemiosmotic theory or electrochemical analogies are applied to the empirical data obtained to determine rate equations. Some of these equations have been further modified by adding terms to account for inhibition by ferric and/or ferrous iron (Ojumu *et al.*, 2006). Although numerous kinetic data have been published which model the leaching process, they mostly apply to tank type leaching systems which are well mixed suspensions in nature with optimum conditions and are dominated by planktonic microorganisms. Heap leaching systems however tend to be heterogeneous in nature, with multiple sub-processes occurring simultaneously and operating far from optimum conditions (Demergasso, 2009; Rossi, 1990). In real heap systems the kinetics are also affected by both biological phenomena and mineral related chemical effects, unlike experimental tank systems where kinetics are affected by only the biological phenomena. Surface attachment is a significant factor to consider in the heap leaching environment as most microorganisms are sessile. The ratio of solution to solid is usually about 1:12 (usually 8:1 in tank leaching) resulting in the dominance of sessile microorganisms (Petersen, 2009). Extracellular polymeric substances (EPS) are released by sessile microorganisms to enhance

attachment which augments the dissolution process (Farah *et al.,* 2005; Sand and Gehrke, 2006). There have been studies on the attachment of microorganisms to the minerals surface to understand the mechanisms better; but there is still a lack of understanding of the biological kinetic effects of sessile/ attached microorganisms. It is thus questionable whether leaching kinetics obtained from planktonic systems can be used to model systems because of the differences in biological and chemical parameters.

In addition, kinetic models developed from the primarily planktonic cultures in experimental tank systems, although appropriate for fitting heap leaching models, there is still a need to predict performance under the limiting conditions in real heap environments. This is because in heaps any inadequate transportation of air up and feed solution down the heap solution influences oxygen and carbon dioxide delivery to the reactive sites. The exothermic reactions in the heap produce heat which can be removed by the air and solution passing through and influences the temperature ranges in the heap. The solution can also become stagnant in pores promoting irregular solution flow within the heap, further influencing the delivery of reagents and product removal from the reactive sites. This stagnant solution compromises inter and intra particle diffusion, microbial growth, and influences mass transfer limitations of CO_2 and O_2. The mineralogy and topology of the mineral as well as the chemical and electrochemical interactions of the mineral surface also influence the leaching rates in heap environments (Petersen and Dixon, 2003; Petersen and Dixon, 2007b). Lastly, physicochemical factors such as redox potential, temperature, acidity, oxygen concentrations, carbon dioxide concentrations, humidity and salinity vary widely and fluctuate radically with time, and various sub-processes tend to be rate controlling at different time intervals due to these fluctuations (Petersen, 2009; Pradhan *et al.*, 2008).

1.2 Problem statement

Research has been done to investigate overall leaching kinetics of a given mineral concentrate or whole low grade ore in tank or column experiments but kinetic effects attributed specifically to biological phenomena and those attributed to mineral related chemical effects are not easily differentiated and remain system specific. Since bio-oxidation kinetics derived from submerged culture chemostat systems may not necessarily be representative of those occurring in a heap, it is important that the bio-oxidation kinetics be investigated under conditions mimicking the sessile culture. This study tries to address this problem and aims to determine bio-oxidation kinetics of sessile microorganisms by investigating the kinetics of ferrous iron oxidation by sessile and planktonic cells.

1.3 Research objectives

Kinetic effects in bioleaching systems are attributed to mineral related chemical effects as well as to biological phenomena facilitated by microorganisms. In tank systems, the majority of microorganisms are usually freely suspended in a liquid medium (planktonic microorganisms). Heap leaching environments, however, are heterogeneous systems with the majority of microorganisms attached to the minerals surface (sessile microorganisms). This means they are in a different physiological state when compared to planktonic microorganisms. It is therefore important to allow for the differentiation between biological and mineral effects in heap bioleaching studies, and provide kinetic data for the biological effects with which suitable strategies for the modelling of heap reactors can be found. The main objective of this study was therefore to develop a strategy that allows for the determination of ferrous iron oxidation kinetics catalysed by a sessile microbial population as a function of population size, availability of ferrous iron and culture conditions.

This was achieved by:

- investigating the ferrous iron oxidation rates of a pure culture of planktonic *Leptospirillum ferriphilum* in a continuous stirred tank reactor (CSTR).
- investigating the nature of microbial attachment of planktonic *Leptospirillum ferriphilum* on the surface of a solid substrate (ceramic saddles) in a CSTR + Packed bed reactor (PBR) set-up.
- investigating ferrous iron oxidation rates of sessile *Leptospirillum ferriphilum* in a CSTR+PBR set-up at flow conditions typical of wash-out in the CSTR.
- comparing the kinetic data obtained from the activity of planktonic *Leptospirillum ferriphilum* as a benchmark to that of sessile *Leptospirillum ferriphilum*.

1.4 Scope and limitations

The investigation of the kinetics of a sessile microbial population in a CSTR + PBR set-up in the laboratory does not exactly mimic the conditions portrayed in heap bioleaching system. Heap bioleaching environments are highly complex with parameters such as the acidity, salinity, oxygen (O_2) and carbon dioxide (CO_2) concentrations fluctuating simultaneously over time in various regions of the heap (Pradhan *et al.*, 2008; Petersen, 2009). There are no interstitial spaces created in the same way agglomerated ore gives. The approach taken in this study was to investigate the activity of a sessile population from a fundamental point of view in a controlled environment where parameters such as the pH, CO_2 and O_2 concentrations are constant while varying only the ferrous

iron dilution rates. The most important factor was ensuring that there was a sessile population whose activity could be monitored.

1.5 Thesis outline

In this thesis, literature related to bioleaching relevant for this study is reviewed in Chapter 2. **Section 2.1** gives an overview of biomining and reports the history behind biohydrometallurgy as well as explaining biomining. **Section 2.2** focuses on the characteristics and the bioenergetics of biomining microorganisms. **Section 2.3** describes the bioleaching mechanisms. Direct and indirect dissolution mechanisms, the characteristics of metals sulphides which determine the reaction pathways during the bioleaching process; contact, non-contact and cooperative leaching and the factors influencing bacterial attachment are addressed. In **Section 2.4**, the kinetics behind the bioleaching process is addressed and previous developments of kinetic equations are reported. Rate limiting factors influencing the bioleaching process are also discussed in Section 2.4. In closing Chapter 2, **Section 2.5** addresses the thesis objectives, hypotheses and key questions based on the gaps found in literature.

Chapter 3 describes the material and the methods used in this study. Firstly in **Section 3.1**, the experimental approach is described and is linked to previous work reported from literature. **Section 3.2** follows and explains the experimental configurations for the different experiments conducted while **Section 3.3** describes the origin and maintenance of the microbial culture used during investigation as well as the constituents of the growth medium. **Sections 3.4, 3.5 and 3.6** report the experimental procedures, analytical methods and data analysis respectively.

The results and discussion is split into two chapters (Chapter 4 and 5). **Chapter 4** reports on the results obtained from experimental work investigating the kinetics of planktonic microorganisms. A comparison of the work done by Naik (2010) under non-sterile conditions and this study conducted in sterile conditions is reported in Chapter 4. The results obtained from investigating attachment and the kinetics of the sessile population are reported in **Chapter 5**. **Chapter 6** covers an integrated discussion of the results from this study and **Chapter 7** presents the overall conclusions and recommendation for future work based on the interpretation of the results. In closing, the list of references used in this study and the Appendices follow.

2 Literature Review

2.1 An overview of biomining

The extraction and purification of metals from ore is known as extractive metallurgy, which is subdivided into pyrometallurgy, hydrometallurgy and/or electrometallurgy. In pyrometallurgy ore is roasted, smelted and converted at extremely high operating temperatures. The sulphide concentrate is heated in the presence of oxygen to a metal oxide during roasting, with sulphur dioxide produced as a by-product. During smelting, slag formers are introduced to remove impurities producing matte. Oxygen is then blown through the matte to remove any remaining sulphur and this is known as converting. In hydrometallurgy, wet methods are used to recover metals from ore, concentrates and other metallurgical intermediate products. Electrometallurgy usually proceeds after pyrometallurgy in terms of electro-refining of copper, or after hydrometallurgical processing as electrowinning (Habashi, 1999; Sandström, 2008).

Pyrometallurgy has been practiced for centuries and requires high grade ores or concentrates for economic processing. The depletion of high grade mineral resources globally has however pushed mines to extend deeper underground in search of high grade ores or to milling and concentrating lower grade resources. This has resulted in environmental problems primarily high energy requirements, leading to high cost requirements to recover metals (Du Plessis *et al*., 2007; Mathur, 2005). Brierley (2009) reports that, over the last decade, there have been fluctuations in metal prices over time and production costs have increased rapidly. Lusinga (2011) reports that historically copper smelting was preferred for metal extraction but was found to have negative implications to the environment due to CO_2 and SO_2 emissions. As a result, environmental regulations were introduced which led to the development of better smelting technologies that reduced CO_2 and SO_2 emission (total sulphur capture efficiencies can be between 60-99.9% depending on the technology). The environmental regulations also led researchers to try and develop suitable hydrometallurgical processes which could be used as an alternative for metal extraction, eliminating the emission of harmful gases. Biohydrometallurgy appears to be a suitable alternative method for metal extraction. Breed and Hansford (1999b) report that bioleaching has economic, environmental and technical advantages over pressure oxidation and roasting. In terms of copper, the 1990's (especially in Chile) saw rapid adoption of the heap leaching process as the investment and operating costs of heap leach/ solvent extraction/ electrowinning plants was found to be lower than the conventional concentration/smelting/refining complexes (Davenport, 2002). This was observed relative to processing 0.75% copper oxide ore. Lusinga (2011) reports that in the case of copper extraction,

heap leaching (a hydrometallurgical method) was less cost intensive when compared to smelting projects; the only shortcoming being the low recovery of copper from chalcopyrite which is not economical and thus prohibits the use of this technology in the context of copper ores that consist primarily of chalcopyrite.

On account of the above-mentioned factors, hydrometallurgy has become popular in the mining industry and has in some cases been further modified by incorporating biological aspects in order to extract minerals from ores or concentrates. This combination is known as biohydrometallurgy and includes two main categories; stirred tank-type processing and irrigation-type processing (Akcil *et al.*, 2007; Brierley and Brierley, 2001; Fu *et al.*, 2008; Olson *et al.*, 2003; Ojumu *et al.*, 2006; Petersen, 2009; Rawlings *et al.*, 1999; Rawlings, 2002; Rawlings *et al.*, 2003; Sampson and Phillips, 2001; Sundkvist *et al.*, 2008). Collectively, all these methods are known as biomining.

2.1.1 History of hydrometallurgy

In ancient times, humans used metals such as gold and silver as found in their native state. Pyrometallurgy only began during the Bronze Age 3500 B.C and hydrometallurgy during the 7th century A.D (Habashi, 1999; Sandström, 2008). Hydrometallurgy started during the time of the alchemists who discovered that if iron was dipped into copper sulphate solution, a layer of metallic copper formed. The Chinese practiced a similar technology as far back as 100-200 B.C with no knowledge of its chemistry (Ehrlich, 2001; Habashi, 1999; Mathur, 2005; Rossi, 1990).

Heap leaching to extract copper initially began in the Harz mountains in Germany, at the Rio Tinto river in Spain, as well as in Sweden and China. Piles of pyrite containing copper sulphide minerals were exposed to open air and rain for months resulting in the dissolution of copper. Copper sulphate was then drained from the heap and collected using basins (Habashi, 1999; Olson *et al.*, 2003). Silver and copper were recovered from a mineral deposit in the Huelva province of southern Spain (from the Rio Tinto river). By 1752, heap leaching was already widely practiced by the Spanish who developed a copper leaching process from partially roasted ore (Gericke *et al.*, 2009; Mathur, 2005). The Rio Tinto river, also referred to as the red river, obtained its name from the red colour of the water caused by the presence of high concentrations of ferric ions. The water was undrinkable and contained no fish. The prime source of the water came from hills rich in sulphide ores. Due to microbial activity on these sulphide minerals, the river contained high concentrations of dissolved ferric iron (Gericke *et al.*, 2009).

In the 18th century, Quebec produced potash (used in the soap and glass industry) for export to France. The cyanidation process for gold, and the Bayer process for bauxite were discovered in the 19th century marking the beginning of modern hydrometallurgy. In France the use of ammonia for copper, nickel, and cobalt sulphide leaching was first proposed in 1903, whilst nitric acid was proposed for leaching sulphide ores in 1909. At this same time, in Chile, copper was now recovered from solution using electrowinning methods (1912) rather than using scrap metal for cementation; while in the 1940's during the Manhattan Project in the USA there was a breakthrough for uranium solvent extraction. By the mid 20th century, hydrometallurgy had begun to advance progressively (Habashi, 1999).

Pressure hydrometallurgy was introduced for leaching sulphide concentrates in the 1950's, followed by the discovery in the 1960's of the role of bacteria in leaching, with the result that heap and in-situ leaching for the extraction of copper became widespread (Ehrlich, 2001; Habashi, 1999). The first acidophilic iron- and sulphur oxidizing bacterium, *Thiobacillus ferrooxidans* (now referred to as *Acidithiobacillus ferrooxidans*), was isolated from pyrite inclusions of bituminous coal and was described in 1951 by Colmer, Temple and Hinkle (Gericke *et al.*, 2009; Mathur, 2005). Later in 1958 L.C. Bryner and J. V. Beck and their students from Brigham Young University in Provo, Utah found some bacteria (*Acidithiobacillus ferrooxidans* and *Acidithiobacillus thiooxidans*) from an acid drainage at a coal mine and showed from laboratory experiments, that *Acidithiobacillus ferrooxidans* was capable of leaching various copper sulphide minerals (Cordoba *et al.*, 2008; Ehrlich, 2001; Mathur, 2005). The commercial use of microorganisms for bioleaching only occurred in the mid-1980's in Fairview South Africa, where the first plant for the pre-treatment of refractory gold bearing concentrates was authorized (Brierley and Brierley, 2001). Since then, the use of microorganisms in hydrometallurgical operations has expanded globally (Gericke *et al.*, 2009).

2.1.2 Leaching techniques in biomining

Ore from the ground is removed by surface, underground, or solution mining. In surface mining open pits, open cast, and alluvial mining methods are used to remove soil and waste rocks found above a mineral deposit. Underground mining involves the removal of valuable ore from underground and follows surface mining (Broadhurst, 2007). In solution mining, ore is pre-treated by means of fragmentation thereafter metals can be leached out (Sandström, 2008). Except in the case of *in situ* leaching where ore is not removed from underground and leaching agents are injected directly into porous, permeable mineral deposits, several leaching methods can then be used to extract valuable metal. The other methods include dump leaching and heap leaching; both of which use irrigation

methods and suspension leaching which uses stirred tank processing either at ambient or elevated pressure. Figure 2-1 illustrates the different mining techniques that can be used to process sulphide ore deposits depending on the ore grade.

Commercially, ore is removed from the ground and is crushed, except in the case of *in situ* mining where ore is not extracted. When practicing *in situ* mining, ore is fragmented by blasting and holes are drilled into the ore body to inject acid solution which percolates down until it reaches an impermeable layer. Pregnant liquor solution (PLS) is then extracted to the surface using deeper drill holes and processed by solvent extraction and electrowinning. *In situ* mining is usually very slow with low yields and can have negative environmental impacts due to loss of leach liquor (Du Plessis *et al*., 2007; Sandström, 2008).

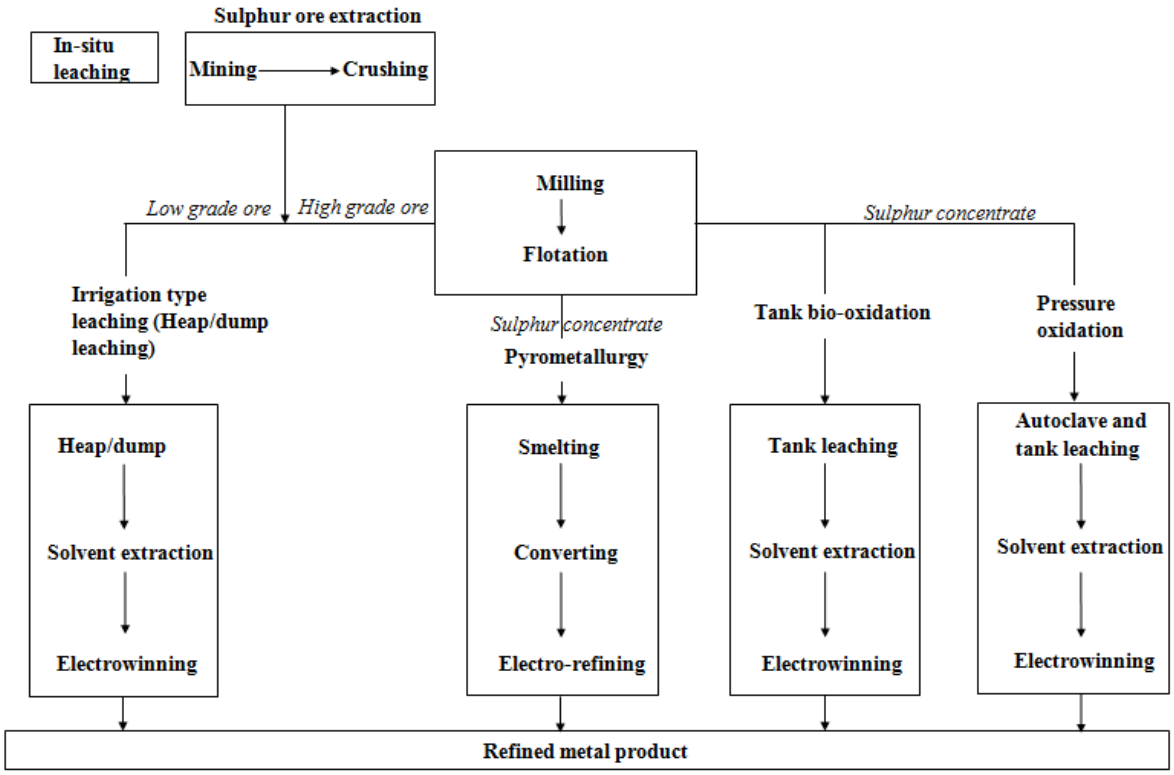

Figure 2-1: Mining and beneficiation of sulphide ore deposits (adapted from Broadhurst, 2007)

Once the ore is crushed, it is separated into either high or low grade ore. High grade ore is first milled and then goes through a flotation process to produce a concentrate which may go through either pyrometallurgical processing, pressure oxidation, or tank bio-oxidation (suspension leaching) to extract the metal. Suspension leaching tends to be very costly, especially when operating under pressure, because of the construction and operation of the reactors and is the least popular

methods for leaching low grade ores (Rawlings, 2002; Sandström, 2008). In pyrometallurgy the concentrate is fed into a smelter and is refined into the metal grade of choice with very high conversions of the metal contained in the concentrate. Any metals lost during concentration can be found in the tailings and may still go through cheaper technology options such as heap leaching for their recovery. The metal is then dissolved in an acid sulphate solution and processed by solvent extraction and electrowinning methods (Du Plessis *et al*., 2007). During pressure leaching autoclaves are used and operate at temperatures of up to 200°C and pressures of 40 atmospheres (Sandström, 2008). Stirred tank leaching can be performed as either batch or continuous at temperatures as high as 85°C and requires fine grained material when leaching (Morin, 2007). It is still relatively costly so only high grade ores or concentrates are processed using this method. If bacteria are used for mineral extraction then it becomes known as a bio-oxidation process. Solvent extraction and electrowinning follow after each of these processes to extract the metal from solution (Du Plessis *et al*., 2007; Sandström, 2008).

Low grade ore is processed via irrigation type leaching methods such as heap/dump leaching for mineral extraction. Dump leaching is used on low grade ore put aside in big dumps in mines (run-of-mine or ROM ore). Ore particle sizes tend to be large and are stacked up to heaps as high as 350m (Rawlings, 2002). Acidified water is sprinkled on the surface of the dumps and the leach solution percolates through the dump and is collected in ditches at the base of the dump. This process takes very long (usually years) to complete and metal recoveries tend to be very low (Sandström, 2008).

Heap leaching is very popular today for the extraction of metals from low grade ores especially in the copper industry. It is useful in the mining industry as it aids in achieving reasonably high metal recoveries from low grade ore which otherwise cannot be economically processed through pyrometallurgical methods. Heap bioleaching is also associated with environmental and technical advantages as it requires less energy for the crushing of the ore to produce a concentrate for alternative processes (Breed *et al.*, 1999; Breed and Hansford, 1999a; Dempers *et al.*, 2003; May *et al.*, 1997; Petersen, 2009; Rawlings *et.al.*, 2003). Figure 2-2 gives an illustration of the heap bioleaching process. Run-of-mine waste (dump / waste rock), crushed and agglomerated ores (heap), and tailings qualify to go through heap bioleaching. Wastes and tailings after pyrometallurgical processing would often otherwise simply be exposed to air and rain and undergo uncontrolled leaching resulting in acid mine drainage (Rawlings, 2002). Heap leaching operates in a similar manner to dump leaching but is pre-planned with strategies placed to optimize leaching rates

and increase efficiency - usually by crushing the ore to some degree or by leaching relatively shallow piles on carefully designed leach pads (Sandström, 2008; Rawlings, 2002).

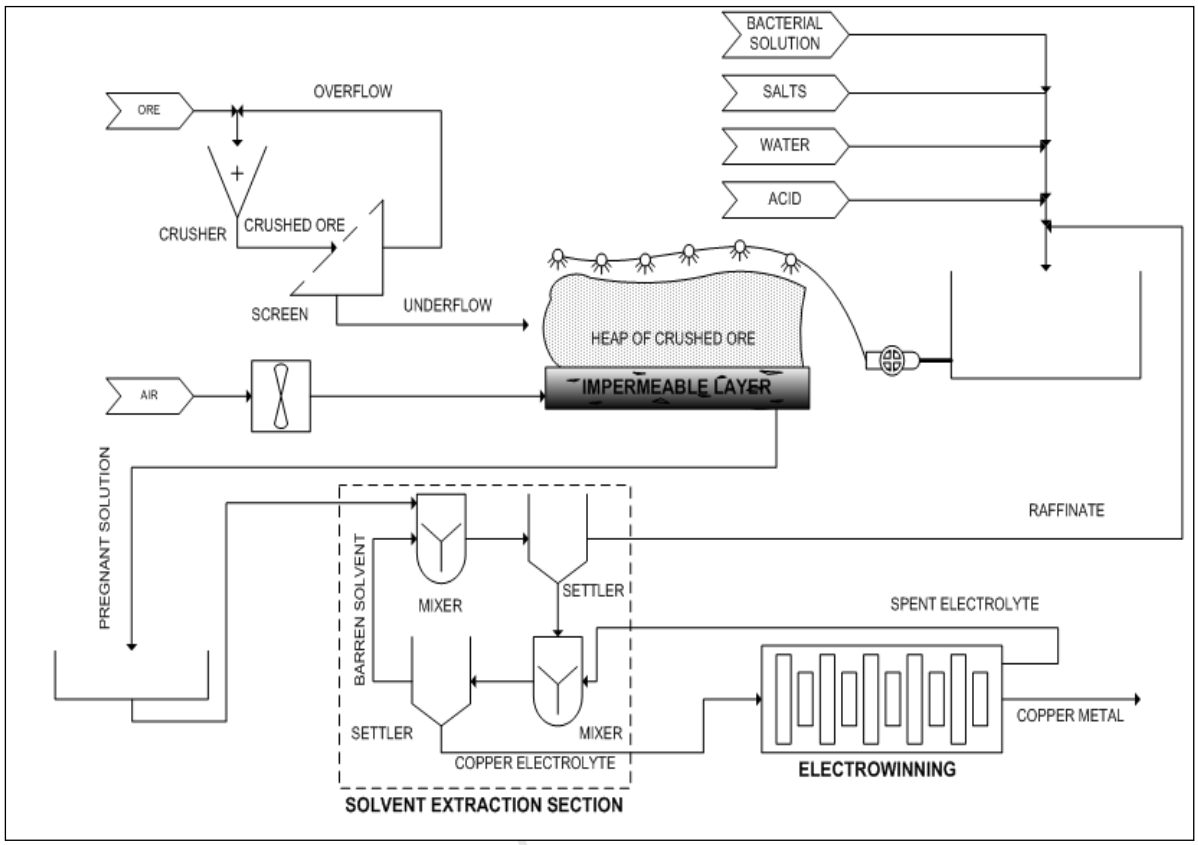

Figure 2-2: Heap bioleaching process (Pradhan *et al.*, 2008)

Crushed ore (10-30mm) is acidified using sulphuric acid and transferred to rolling drums to agglomerate particles so that fine particles bind to larger particles thus forming coarser agglomerate particles. This ensures even acidification and moisture distribution within the heap. If raffinate (recycled solution after solute has been extracted by solvent extraction) is used for agglomeration, then bacteria may be introduced into the system (Rawlings, 2002; Watling, 2006). The agglomerated ore is then stacked up on an impermeable layer fitted with a solution drainage system at heights ranging from 4-10m. The impermeable base minimises losses of the leachate and avoids pollution (Siddiqui *et al.*, 2009). Ore is arranged in heaps with perforated air pipes placed at the bottom to allow for permeability of solutions and gases within the heap (Du Plessis *et al*., 2007; Petersen and Dixon, 2007b; Sandström, 2008). Sprinklers are used to continuously irrigate over the top surface of the heaps. The solution is left to seep through the ore bed where it can react with the ore (Petersen and Dixon, 2007b; Watling, 2006). The metal rich effluent from the heap is then collected via a drainage system; thereafter it proceeds to the solvent extraction and electrowinning units to recover

the metal (Pradhan *et al.*, 2008). The barren solution (raffinate) is then recycled back to the top surface of the heap (Petersen and Dixon, 2007b).

2.2 Microorganisms used in biomining

2.2.1 Classification of microorganisms

The role of microorganisms during bioleaching is to oxidize ferrous ions to ferric iron for the chemical attack of the mineral; and for the removal of elemental sulphur which results in the production of sulphuric acid used for proton hydrolysis (Deveci, et al., 2008; Rawlings, 2002; Rawlings *et al.*, 2003; Schippers, 2007). Ferrous iron oxidation rates are increased by half a million to a million times using *Acidithiobacillus ferrooxidans* compared to abiotic chemical oxidation rates by dissolved oxygen at ambient temperatures (Rawlings, 2002). Boon and Heijnen (1998) also reported that bio-oxidation rates of pyrite were 10-20 times faster than the chemical oxidation rate of pyrite. Jones and Kelly (1983) showed that ferrous iron oxidation is 2 x 10^3 to 10^6 times faster than non-biological oxidation, and Ozkaya *et al.* (2007) also found that the microbial oxidation of Fe^{2+} occurred 10^5-10^6 times faster than chemical oxidation at pH 2-3.

Microorganisms used in biomining processes belong to both bacteria and archaea (Sandström, 2008). Their behaviour is not completely understood as they are affected by complex environmental, physico-chemical and biological factors such as redox potential, acidity, temperature, oxygen concentrations, carbon dioxide concentrations, humidity and salinity conditions which vary widely and change radically with time in leaching systems (Pradhan *et al.*, 2008). Improving the understanding of the microbiology of biomining microorganisms would however enable better control of conditions to improve leach rates, metal recoveries, and costs; so as to further advance commercial bioheap operations (Brierley, 2001).

Microbial populations are usually mixed in heaps and can either oxidize iron or sulphur, or have the ability to simultaneously oxidize both ions. They are classified as acidophilic because they grow in environments with pH levels between 1 and 3. Plumb *et al.* (2008b) report that acidophiles grow optimally at pH levels of less than 3. They are also classified as chemolithotrophs because of their ability to obtain energy from ferrous iron or reduced inorganic sulphur compounds. They grow autotrophically by fixing CO_2 from the atmosphere for the generation of cellular material. Nitrogen can also be fixed by these microorganisms (Rawlings *et al.*, 2003; Sandström, 2008; Watling, 2006). In aerated systems, oxygen from air is usually the electron acceptor. In acidic environments, ferric iron is soluble and in the event that oxygen is insufficient, sulphur oxidizing microorganisms are

capable of using ferric iron as an electron acceptor in place of oxygen (Rawlings *et al.*, 2003). The most common microorganisms involved in mineral sulphide oxidation are categorised into four broad groups, based on their optimum temperature ranges for growth. During heap leaching heat is generated due to exothermic reactions, which increases temperature within the heaps (Pradhan *et al.*, 2008). It is therefore essential that there is temperature control in the heaps as the microorganisms function at specific temperature ranges. Bacteria usually belong to the psychrophilic, mesophilic and moderately thermophilic region whilst only archaea are found under extremely thermophilic conditions (Plumb *et al.*, 2008a; Schippers, 2007; Sandström, 2008).

Psychrophiles operate at optimum temperatures of 20^{o}C and have not been found to be useful in biohydrometallurgy. Mesophiles are gram negative bacteria operating at optimum temperatures of between 20^{o}C-42^{o}C; examples include *Acidithiobacillus ferrooxidans* (iron-and-sulphur oxidizing), *Acidithiobacillus thiooxidans* (sulphur oxidizing), *Leptospirillum ferrooxidans* and *Leptospirillum ferriphilum* (both iron oxidizing). They were originally isolated from soils and sulphide deposits and are the best explored and most frequently used bioleaching microorganisms (Sandström, 2008). It is important to note that although *Leptospirillum* species are classified as mesophiles, they tend to withstand extreme conditions such as low pH, high redox potential and high temperatures compared to other mesophilic iron oxidizers (Gahan *et al.*, 2010). Moderate thermophiles are gram positive bacteria and operate at optimum temperatures of between 42^{o}C-60^{o}C; examples include *Sulfobacillus acidophilus*, *Acidimicrobium ferrooxidans*, *Sulfobacillus thermosulphidooxidans and Acidithiobacillus caldus*. They were originally isolated from autoheated coal and sulphide ore heaps. Some archaea also fall into the moderately thermophile range and belong to the genus *Ferroplasma* (Schippers, 2007). Extreme thermophiles like *Sulfolobus metallicus, Metallospaera sedula* and *Sulfolobus acidicaldarius* are archaea and operate at optimum temperature ranges of between 60^{o}C-80^{o}C (Deveci *et al.*, 2007; Rawlings *et al.*, 1999; Rawlings and Johnson, 2007; Sandström, 2008). They were originally isolated from hot springs, have a short lifespan and are relatively delicate such that if left agitated without fresh concentrate they can disappear over time. They have no cell wall, only a cell membrane and struggle with high shear rates; for this reason they are less commonly employed in tank leaching operations. They require low agitation and very dilute slurries during biohydrometallurgical processing to survive (Clark *et al.*, 2006).

Table 2-1 gives a summary of the different types of microorganisms commonly used in bioheaps and their optimum temperature and pH ranges.

Table 2-1: Examples of acidophiles and their optimum temperature and pH ranges (Schippers, 2007)

SPECIES	OPTIMUM pH	OPTIMUM TEMPERATURE RANGE (ºC)
Mesophilic and moderately thermophilic bacteria		
Acidimicrobium ferrooxidans	~2.0	45 – 50
Acidithiobacillus albertensis	3.5 – 4.0	25 – 30
Acidithiobacillus caldus	2.0 – 2.5	45
Acidithiobacillus ferrooxidans	2.5	30 – 35
Acidithiobacillus thiooxidans	2.0 – 3.0	28 – 30
Alicyclobacillus disulfidooxidans	1.5 – 2.5	35
Alicyclobacillus tolerans	2.5 – 2.7	37 – 42
Caldibacillus ferrivorus	1.8	45
Ferrimicrobium acidiphilum	2.0 – 2.5	37
Leptospirillum ferriphilum	1.3 – 1.8	30 – 37
Leptospirillum ferrooxidans	1.5 – 3.0	28 – 30
Sulfobacillus acidophilus	~2	45 – 50
Sulfobacillus montserratensis	1.6	37
Sulfobacillus sibiricus	2.2 – 2.5	55
Sulfobacillus thermosulfidooxidans	~2	45 – 48
Sulfobacillus thermotolerans	2.0 – 2.5	40
"Thiobacillus prosperus"	~2	33 – 37
Thiomonas cuprina	3.5 – 4.0	30 – 36
Mesophilic and moderately thermophilic archaea		
Ferroplasma acidarmanus	1.2	42
Ferroplasma acidiphilum	1.7	35
Ferroplasma cupricumulans	1.0 – 1.2	54
Extreme thermophilic archaea		
Acidianus brierleyi	1.5 – 2.0	~70
Acidianus infernus	~2	~90
Metallosphaera hakonensis	3.0	70
Metallosphaera prunae	2.0 – 3.0	~75
Metallosphaera sedula	2.0 – 3.0	75
Sulfolobus metallicus	2.0 – 3.0	65
Sulfolobus yangmingesis	4.0	80
Sulfurococcus mirabilis	2.0 – 2.6	70 – 75
Sulfurococcus yellowstonensis	2.0 – 2.6	60

Acidithiobacillus ferrooxidans was the first bacterium to be isolated for leaching purposes and was considered the most important microorganism for processes operating in the mesophilic region (Gericke *et al.*, 2009; Mathur, 2005). As a result of this *Acidithiobacillus ferrooxidans* has been extensively studied. *Acidithiobacillus ferrooxidans* is however not the dominant microbial species in all biomining processes, especially not in continuous stirred tank reactors. They do not operate well

in solutions with high ferric to ferrous iron ratios. *Leptospirillum* however, tends to have a high affinity for ferrous iron and can withstand ferric inhibition when at high concentrations. It is therefore the dominant iron oxidizer (Rawlings, 2002). Bacterial strains can be characterised by their affinity for ferrous to ferric iron ratio (Boon *et al.*, 1999). *Leptospirillum ferrooxidans* at low redox potentials has a specific maximum utilization rate but at higher redox potentials, can sustain higher activity compared to *Acidithiobacillus ferrooxidans* (Rawlings *et al.*, 1999).

2.2.2 Bioenergetics of bioleaching microorganisms

Ferrous iron oxidation is an essential part of the bioleaching process as energy is produced in the process which is essential for carbon dioxide fixation (as microorganisms are autotrophic), nitrogen fixation (if required), and for growth. As discussed previously, only certain bacteria can oxidize ferrous ions. Some bacteria oxidize only sulphur compounds to derive energy while others can oxidise both sulphur and ferrous ions. Studies on ferrous iron oxidation have been published mostly based on the bacterium *Acidithiobacillus ferrooxidans* which oxidizes both sulphur compounds and ferrous ions (Ingledew, 1982; Nemati *et al.*, 1998; Ojumu, 2008). Figure 2-3 gives an illustration of how ferrous iron oxidation occurs and of the transportation of protons in *Acidithiobacillus ferrooxidans* as proposed by Ingledew (1982). This assumes that all bacteria that can oxidize ferrous iron follow this same path. The oxidation of Fe^{2+} by *Acidithiobacillus ferrooxidans* results in energy production used for carbon fixation and cell growth. Oxygen (O_2) acts as an oxidizing agent during this process (Mignone and Donati, 2004; Quatrini *et al.*, 2006). This is shown by equations 2-1 to 2-3 (Ingledew, 1982). Equation 2-3 is the overall reaction from the two half cell reactions (equation 2-1 and 2-2).

$$2Fe^{2+} \longrightarrow 2Fe^{3+} + 2e^{-} \qquad E_h^o = +770mV \qquad \text{Equation 2-1}$$

$$2e^{-} + \frac{1}{2}O_2 + 2H^{+} \longrightarrow H_2O \qquad E_h^o = +1230mV \qquad \text{Equation 2-2}$$

$$2Fe^{2+} + \frac{1}{2}O_2 + 2H^{+} \longrightarrow 2Fe^{3+} + H_2O \qquad \Delta E_h^o = +460mV \qquad \text{Equation 2-3}$$

pH in the cytoplasm is maintained between 6.5 and 7.0, while the pH in the outer region (bulk region) is usually acidic at a pH of around 2 or even as low as pH 1 (Alexander *et al.*, 1987; Ingledew, 1982; Mignone and Donati, 2004; Nemati *et al.*, 1998). The difference in pH creates a proton electrochemical gradient which in turn facilitates the production of the energy carriers ATP from ADP. The protons get pumped through a partially impermeable membrane via proton channels and cannot flow into the cytoplasm except through ATP synthesis (Gahan *et al.*, 2010; Ojumu, 2008).

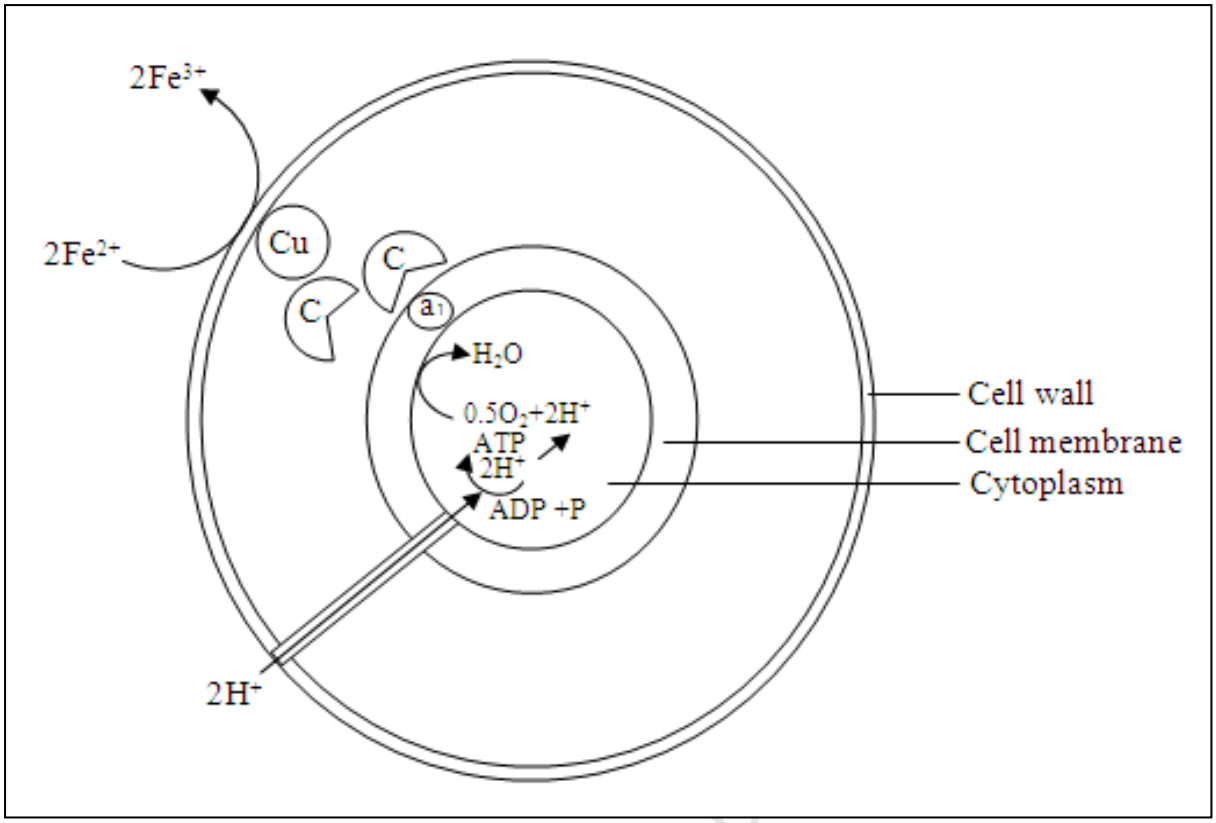

Figure 2-3: Organisation of Fe^{2+} - oxidizing chain of *At.ferrooxidans* as proposed by Ingledew. Cu – Rusticyanin; C- Cytochrome c and a_1 – cytochrome a_1. (Adapted from Nemati *et al.*, 1998)

An enzyme complex made up of rusticyanin, cytochrome c and cytochrome a_1 creates an electron chain in the periplasma. Electrons are transferred across the cell membrane through this electron chain to reduce the oxygen molecules in the cytoplasm. Once electrons have been transferred to the cytoplasm, they combine with oxygen and the protons to produce water (Ojumu, 2008). Carbon dioxide is fixed by bacteria through the Calvin-Benson-Bassham reductive pentose phosphate cycle. This cycle requires three ATP molecules and two NADPH molecules to fix one CO_2 molecule. Production of NADPH occurs by reverse electron transport also in the periplasmic region (Ingledew, 1982; Mignone and Donati, 2004; Nemati *et al.*, 1998; Ojumu 2008).

2.3 Bioleaching mechanisms

2.3.1 Direct vs. indirect dissolution mechanisms

Silverman and Ehrlich (1964) (cited by Rodríguez *et al.*, 2003a) were the first to attempt to explain bioleaching and proposed two possible mechanisms (Ehrlich, 2001; Rohwerder and Sand, 2007). The direct leaching mechanism was proposed to be a direct enzymatic oxidation process where bacterial membrane components interact directly with the metal and sulphur moiety of the ore (Rawlings,

2002; Sand *et al.,* 2001). The indirect mechanism was proposed to be a non-enzymatic oxidation process, where ferric ions and sometimes protons (depending on the type of ore) chemically oxidize the metal sulphide resulting in the dissolution of the metal sulphide and production of ferrous ions and sulphur compounds. Mineral dissolution reactions are not always similar for all metal ores, with the oxidation processes of metal sulphides proceeding via different intermediates (Rawlings *et al.*, 2003). Bioleaching microorganisms then regenerate ferric ions by oxidizing the ferrous ions produced (Sand *et al.,* 2001; Rawlings, 2002).

Some authors were in disagreement with the direct mechanism. Boon and Heijnen (1998) proved experimentally that the direct mechanism was not feasible and could not be used to determine bacterial oxidation kinetics of the metal sulphide with bacteria. They ran experiments which proved that oxygen consumption did not occur on the surface of the sulphide ore (pyrite) but in solution. Tributsch (2001) showed, using electron microscope pictures, that bacteria produced an extracellular polymeric layer as the reaction medium, therefore it could not be true that the bacterial membrane interacts with the sulphide using enzymatic substances as proposed in the direct mechanism. Today, following much debate, the direct mechanism has been rejected and studies show that the indirect bioleaching mechanism is the correct mechanism to explain bioleaching processes (Fowler *et al.*, 2001; May *et al.*, 1997; Rohwerder and Sand, 2007; Sand and Gehrke, 2006).

The indirect mechanism can be subdivided into at least three independent sequential and/or parallel processes. The overall process can therefore be separated, with the kinetics obtained from the respective sub-processes being mutually independent. The kinetics obtained from each sub-process can be studied independently to improve the bioleaching efficiency, using different operating parameters (Breed *et al.*, 1999; Breed and Hansford, 1999a). Generally during bioleaching, the metal sulphide is chemically oxidized by ferric ions to ferrous ions and sulphur (Equation 2-4). Ferrous iron is then oxidized by iron oxidizing and sulphur oxidizing microorganisms to regenerate ferric ions and to convert sulphur to sulphate (equation 2-5 and 2-6) (Boon *et al.*, 1998; Boon and Heijnen, 1998; Cruz *et al.*, 2005; Ehrlich, 2001; Rawlings, 2002; Hansford and Vargas, 2001; Ojumu *et al.*, 2006).

$$2Fe^{3+} + MS \longrightarrow 2Fe^{2+} + M^{2+} + S^0 \qquad \text{Equation 2-4}$$

$$2Fe^{2+} + 2H^{+} + 0.5O_2 \xrightarrow{\text{Iron oxidizing microorganisms}} 2Fe^{3+} + H_2O \qquad \text{Equation 2-5}$$

$$S^0 + 1.5O_2 + H_2O \xrightarrow{\text{Sulphur oxidizing microorganisms}} H_2SO_4 \qquad \text{Equation 2-6}$$

2.3.2 Characteristics of metal sulphides and reaction pathways during bioleaching

Leaching is generally achieved by a combination of proton attack and oxidation processes. The dissolution of metal sulphides follows one of two pathways, i.e. the thiosulfate or the polysulphide pathways which are mineral specific (Rawlings *et al*., 2003; Rohwerder and Sand, 2007; Sundkvist *et al.*, 2008). Figure 2-4 gives an illustration of both the thiosulphate and polysulphide pathways.

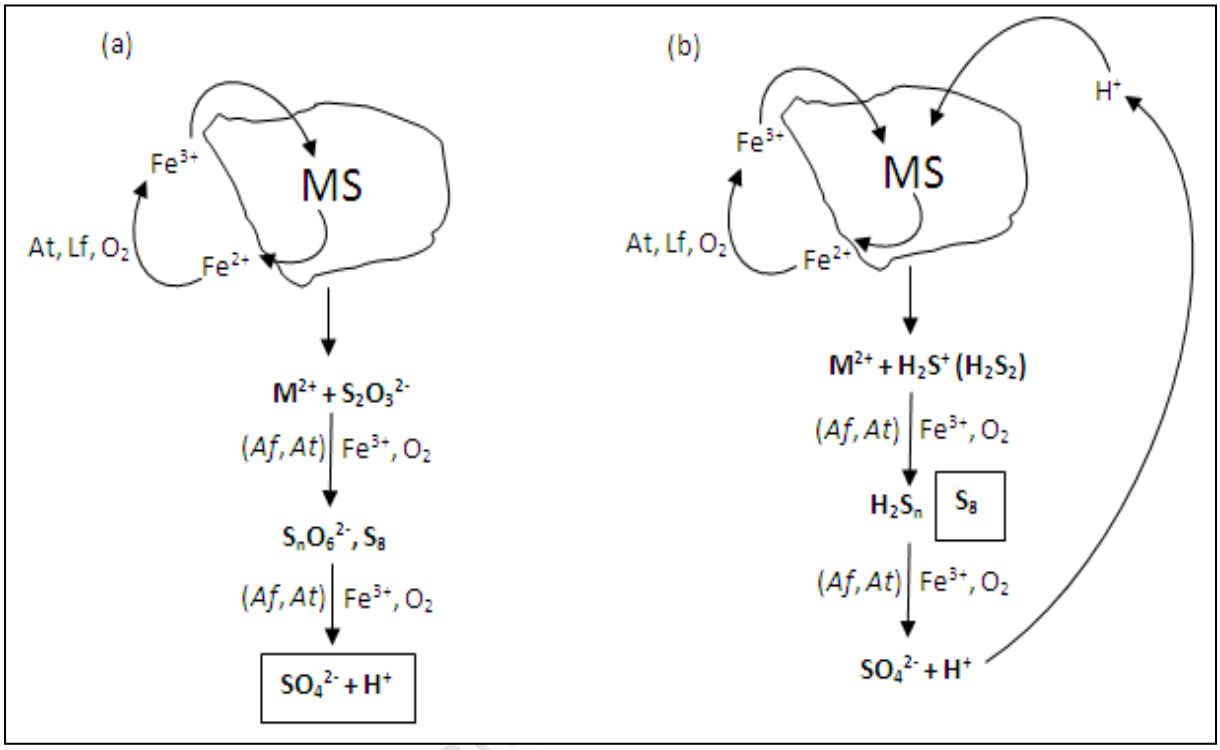

Figure 2-4: (a) - Thiosulphate mechanism (b) - Polysulphide mechanism for bacterial leaching of sulphide minerals. *Acidithiobacillus ferrooxidans* (*Af*), *Acidithiobacillus thiooxidans* (*At*) and *Leptospirillum ferrooxidans* (*Lf*) are bacteria used for ferrous iron and sulphur compound oxidation. Products in boxes represent main reaction products in the absence of sulphur compound oxidizers (Rohwerder and Sand, 2007).

Metal sulphides can either be acid soluble (e.g. chalcopyrite ($CuFe_2S$), sphalerite (ZnS), galena (PbS), hauerite (MnS_2), orpiment (As_2S_3) and realgar (As_4S_4)), or acid insoluble (e.g. pyrite (FeS_2), molybdenite (MoS_2) and tungstenite (WS_2)). Most metal sulphides have semiconducting properties. From a structural point of view, both the metal and sulphur are bound as a crystal lattice (Sand *et al.*, 1999). Acid insoluble metal sulphides have valence bands derived from the orbitals of only the metal atoms and cannot be attacked by protons. Acid soluble metal sulphides, on the contrary, derive their valence bands from both the metal and sulphide atom making them vulnerable to proton attack (Rohwerder and Sand, 2007). The crystal structure of the metal sulphide determines acid solubility and the electronic configuration determines what reaction pathway to follow (Rohwerder and Sand,

2007). When acid soluble metal sulphides are oxidized they follow the polysulphide pathway (involving formation of a polysulphide intermediate) whereas acid insoluble metal sulphides follow the thiosulphate pathway (involving formation of a thiosulphate intermediate).

The dissolution of acid soluble metal sulphides is a result of attack from both protons and ferric ions. H_2S can be liberated if two protons are bound to a metal sulphide. In the presence of ferric ions, however, the sulphur moiety is oxidised simultaneously with protons and goes through several steps via polysulfide and polysulphide radicals to elemental sulphur (Equation 2-7 to 2-9). 90% of the sulphide moiety of metal sulphides is transformed to elemental sulphur in the absence of sulphur oxidizing bacteria and other minor products formed are thiosulphate, polythionates and sulphates (Hansford and Vargas, 2001; Rawlings, 2002; Rawlings *et al.*, 2003; Rohwerder and Sand, 2007). Any ferric iron produced in this process is regenerated by iron oxidizing microorganisms (equation 2-10).

$$2MS + 2Fe^{3+} + 2H^{+} \longrightarrow 2M^{2+} + H_2S_n + 2Fe^{2+} \quad n \geq 2 \qquad \text{Equation 2-7}$$

$$0.5H_2S_n + Fe^{3+} \longrightarrow 0.125S_8 + Fe^{2+} + H^{+} \qquad \text{Equation 2-8}$$

$$0.25S_8 + 3O_2 + 2H_2O \xrightarrow{\text{Sulphur oxidizing microorganisms}} 2SO_4^{2-} + 4H^{+} \qquad \text{Equation 2-9}$$

$$2Fe^{2+} + 2H^{+} + 0.5O_2 \xrightarrow{\text{Iron oxidizing microorganisms}} 2Fe^{3+} + H_2O \qquad \text{Equation 2-10}$$

The elemental sulphur produced may exist as free aggregates or crystals, potentially affecting the dissolution processes. Elemental sulphur may form a layer on the metal sulphide surface resulting in changes in the electrochemical properties. This layer can have negative implications on leaching kinetics as it acts as a barrier reducing the diffusion rates of the ions and oxygen (Rohwerder and Sand, 2007). The dissolution process can stop due to the formation of the passive layer. Other factors that could also contribute to creating a passive layer include the formation of jarosite precipitate in the presence of ferric iron, sulphates at high pH, and intermediate metal sulphides which are less reactive than the original metal sulphide (Rodríguez *et al.*, 2003b).

The dissolution of acid insoluble metal sulphides is not complex because of the nature of its electronic structure. No intermediates or passive layers are formed to trigger a barrier effect during bioleaching (Blight *et al.,* 2000; Rodríguez *et al.*, 2003a). Ferric iron is responsible for the chemical oxidation of the mineral and is reduced to ferrous iron by receiving electrons from the valence band electrons of the metal atoms (Equation 2-11). The chemical bond between the sulphur atom and the metal atom does not break until a total of six successive one-electron oxidation steps have been conducted and thiosulphate is liberated in the process (Rohwerder and Sand, 2007). Thiosulphate is

oxidized via tetrathionate and other polythionates to sulphate (equation 2-12). Elemental sulphur may be produced in the event that there are no sulphur oxidizing bacteria and the ferric attack extracts electrons from the sulphate, or due to pH conditions which promotes abiotic oxidation. Iron oxidizing bacteria in acidic conditions, regenerate ferric iron used for the chemical oxidation of the mineral (equation 2-13) (Hansford and Vargas, 2001; Rawlings, 2002; Rawlings *et al.*, 2003; Rohwerder and Sand, 2007).

$$MS_2 + 6Fe^{3+} + 3H_2O \longrightarrow 7Fe^{2+} + S_2O_3^{2-} + 6H^+ \quad \text{Equation 2-11}$$

$$S_2O_3^{2-} + 8Fe^{3+} + 5H_2O \longrightarrow 8Fe^{2+} + 2SO_4^{2-} + 10H^+ \quad \text{Equation 2-12}$$

$$2Fe^{2+} + 2H^+ + 0.5O_2 \xrightarrow{\text{Iron oxidizing microorganisms}} 2Fe^{3+} + H_2O \quad \text{Equation 2-13}$$

2.3.3 Contact, non-contact and cooperative leaching

The indirect mechanism comprises of the sub mechanisms; contact, non-contact and cooperative leaching (Cruz *et al.*, 2005; Rawlings, 2002; Rodríguez *et al.,* 2003a; Sand and Gehrke, 2006; Tributsch, 2001). In the non-contact sub-mechanism, planktonic microorganisms in solution are responsible for ferric ion renewal. In the contact sub-mechanism, attached microorganisms/sessile microorganisms condition the mineral surface inside an Extracellular Polymeric Substance (EPS) released on the surface of the microorganisms for ferric attack through electrochemical dissolution. This conditioning is of importance as sessile microorganisms do not have to rely on other bacteria to increase ferric iron concentrations (Rawlings, 2002). If the microorganisms are sulphur oxidizing, colloidal sulphur (a temporary energy reserve) is released. Iron oxidizers like *Leptospirillum ferriphilum* accumulate ferric iron in the EPS layer for electrons extraction at sufficiently positive potentials. This induces electrochemical thiosulphate and sulphate formation. Cooperate leaching involves colloidal sulphur, globules and mineral fragments released into the environment from the EPS layer of microbes attached to the metal surface. Sulphur colloids and fragments are a wasteful way of releasing unconsumed chemical energy, which becomes useful to planktonic (non-attached) cells (Rawlings *et al.*, 1999). The sulphur particles feed planktonic iron and sulphur-oxidizing microbes to generate ferric iron and protons useful to the non-contact leaching mechanism (Tributsch, 2001). Figure 2-5 gives an illustration of the three leaching mechanisms.

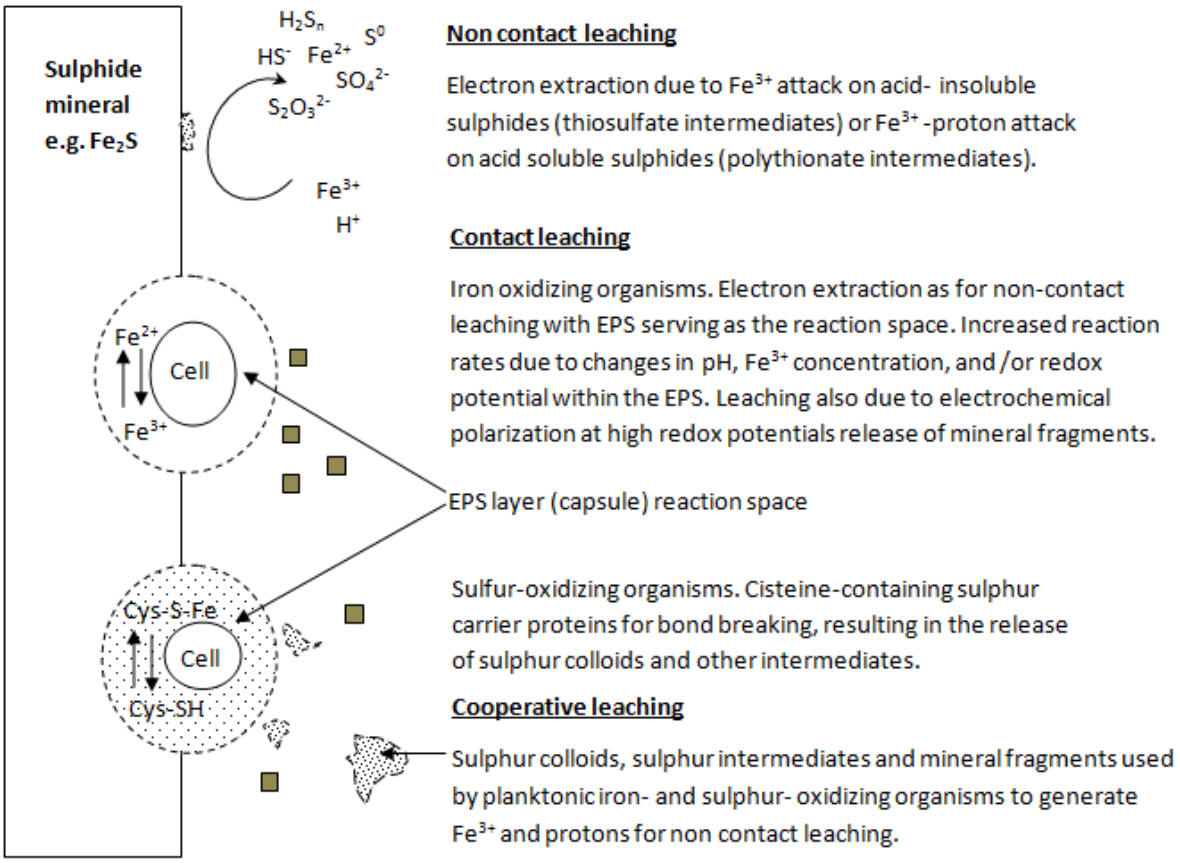

Figure 2-5: The proposed mechanisms during bio oxidation of pyrite (Rawlings, 2002)

2.3.4 Bacterial attachment

Jordan *et al.* (1993) report that cell attachment is a prerequisite for the dissolution of metal sulphides. Rawlings *et al.* (2003) mention that the interaction between attached iron oxidizing cells and sulphide surfaces plays a crucial role in oxidative dissolution. For bioleaching to begin, bacteria must first be in contact with the mineral surface and begin to multiply in order to colonise the entire surface area (Lizama *et al.*, 2003). Bacteria in mineral environments grow in biofilms which strongly adhere to surfaces (Rawlings *et al.*, 1999). The complex interaction between bacteria, a solid substrate and liquid phase results in the attachment of bacteria to solid surfaces. Attachment may occur via diffusion and convection which are random processes, and/or chemotaxis which involves the active orientation of bacteria in a chemical gradient (Sand and Gehrke, 2006). Varying environmental conditions due to one or each of these components may lead to complications in attachment (Ghauri *et al.*, 2007). The resulting colonisation of the mineral surface may occur in the following sequence; transport, initial adhesion, film attachment and surface colonisation. These are shown on Table 2-2.

Table 2-2: Sequencing steps in the colonisation of surfaces by microorganisms (van Loosdrecht *et al.*, 1990; Rossi, 1990)

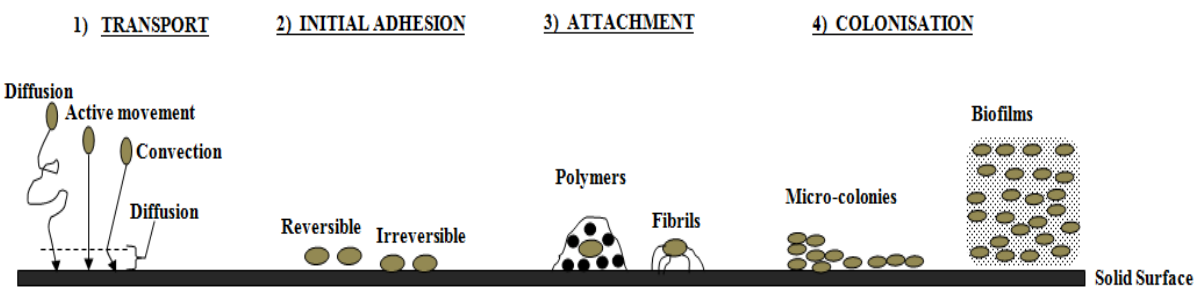

Transport

Occurs due to three different modes of transport:

- Diffusive transport

Small bacteria cross a diffusion layer. No convection can take place and bacteria randomly come into contact with the interface due to Brownian motion even in mild conditions.

- Convective

Is several orders of magnitude faster than diffusive transport and is influenced by liquid flow. In certain instances (through the diffusion sub layer) the route to the surface can be diffusion controlled.

- Active

When bacteria are close to the surface they may reach the surface by chance or chemotactically (due to a concentration gradient in the interstitial region).

Initial adhesion

Initial adhesion is a physicochemical process and is a prerequisite for EPS formation (Harneit *et al.*, 2006; Barreto *et al.*, 2005) and can be either reversible or irreversible:

- Reversible adhesion

Bacteria still exhibit Brownian motion. Rossi (1990) mentions that forces holding the cells are related to electrostatic, van der Waals forces, interfacial tension and covalent bonding and cells attached reversibly can easily be removed by mild shear. The bacteria's mobility may also influence their removal from the surface.

- Irreversible adhesion

Bacteria that adhere to the surface irreversibly do not exhibit Brownian motion. They cannot be removed except using strong shear force.

Film Attachment

Once bacteria are firm on the surface they may begin to grow fibrils and or polymers resulting in strong links to the surface.

Surface colonization

Once firmly attached, bacteria may begin to grow with new cells remaining attached to each other resulting in micro colonies or biofilm formation. If cells are attached reversibly, bacteria may be released back to the medium.

Adhesion is found to be conditional, depending on surface properties such as hydrophobic and electrostatic interaction between bacterial cells and mineral particles, which are the most important

factors governing mechanisms for bacterial adhesion (Cruz *et al.*, 2005; Ghauri *et al.*, 2007; Jordan *et al.*, 1993; Pogliani and Donati, 1999; Roberts *et al.*, 2006; Rohwerder *et al.*, 2003; van Loosdrecht *et al.*, 1990). Rossi (1990) reported that mechanisms such as chemotaxis, Brownian motion, electrostatic attractions (Sand and Gehrke, 2006), electrical double layer effects and cell surface hydrophobicity influence attachment.

Rohwerder *et al.* (2003) also note that in the case of pyrite dissolution, attachment occurs due to electrostatic interactions of positively charged bacterial cells attracted to a negatively charged pyrite surface. Ghauri *et al.* (2006) showed that *Acidithiobacillus ferrooxidans'* initial attachment is electrostatic, and explains that ferric iron forms a complex with uronic acid in the EPS and has a net positive charge while the pyrite surface is negatively charged. Cells are chemotactically responsive to the mineral surface due to surface charge before the mineral is completely covered by a monolayer of cells.

The main site for microbial activity in natural environments (which constitute of water, optimum temperatures, nutrients, minerals, carbon dioxide, oxygen and electron acceptors) is on the surface of the mineral ore although microorganisms do not have to be in contact with the mineral to improve leaching efficiency. The extra-cellular polymeric substance (EPS) excreted by microorganisms to surround all cells for attachment forms the initial location for leaching. Acid excretion, organic solvent production, slime formation, ammonia and hydrogen sulphide formation and exoenzyme excretion become active in the EPS (Sand and Gehrke, 2006). Once bacteria attach to mineral surfaces they begin to generate a matrix where cells divide resulting in biofilm formation with well developed community structures that control nutrient delivery and waste disposal. Farah *et al.* (2005) report that *A. ferrooxidans* adheres to solid substrates by means of the EPS. The EPS forms a reaction space and mediates attachment of microorganisms to a metal sulphide (electrostatic forces) where dissolution occurs (Watling, 2006; Rawlings, 2002). It is in this region that ferric/ferrous iron turnover takes place (Hansford and Vargas, 2001).

The EPS consists of sugars such as glucose, rhamnose, fructose, xylose and mannose; C12 to C20 fatty acids, glucuronic acid and ferric ions (Ghauri et al., 2007; Pogliani and Donati, 1999; Rohwerder and Sand, 2007). The formation of complexes with glucuronic acid, uronic acids or other residues maintain iron concentrations in the EPS layer at approximately 53 gL^{-1} (Rawlings, 2002). Ferric iron is concentrated within this layer and chemically attacks the valence bonds of the mineral. Iron oxidizing microorganisms then reduce the ferric iron to ferrous iron. This process increases pH levels

in the EPS which assists in mineral dissolution (Pogliani and Donati, 1999; Rawlings, 2002; Rodríguez *et al.*, 2003). Pogliani and Donati (1999) showed experimentally that the removal of the EPS layer cells resulted in no attachment to the mineral surface and attachment could only be possible once the EPS was restored. Hansford and Vargas (2001) reported that the oxidation of metal sulphides with bioleaching bacteria depended heavily on the ferric/ ferrous iron turnover ratio in the EPS. Attachment is affected by solution chemistry parameters like ferrous ion inhibition and the formation of jarosites during bioleaching. EPS production is determined by the growth medium as bacteria adapt to substrate or growth conditions. The type of mineral being leached also determines cell attachment. Some cells are mineral and site specific, for example, cells may only attach to small pyrite and chalcopyrite inclusions in low grade ore rather than to siliceous phases (Harneit *et al.,* 2006; Watling, 2006).

2.4 Kinetics of bioleaching processes

2.4.1 Factor influencing leaching kinetics

The leaching environment influences the kinetics of a system. Tank type systems have been mostly used to determine the kinetics of bioleaching systems because of their well mixed suspension nature. Irrigation type systems are more complex due to their heterogeneous nature with chemical and physical conditions changing over time. In heterogeneous environments, various sub-processes occur simultaneously at separate regions of the system (Demergasso, 2009; Rossi, 1990). A sub-process may be rate controlling at one point but in an instant another sub process may take over. The solid phase in irrigation type systems are relatively stationary compared to tank type systems, with the ratio of solution to solid being about 1:12 (tank leaching is usually 8:1). Particles are larger with a small percentage making up valuable material (Petersen, 2009). Figure 2-6 illustrates some of the interactions in heaps from macro to micro scale, some of which are not fully understood. Studies around these dynamic principles within heaps can help improve on leaching rates (Petersen and Dixon, 2007b).

Numerous elementary processes such as direct microbial action, indirect microbial action, surface attachment of microorganisms to the ore particles, growth of microorganisms on alternative energy sources, inhibition of microbial action by ions released with the leached metal, natural oxidation, electrochemical reactions, and diffusional resistance; occur simultaneously in bioleaching which sometimes also influence overall leaching kinetics (Rossi, 1990).

Scale →	Heap (Macro scale)	Stagnant cluster (Meso)	Ore particle	Mineral grain
Sub-process	Unsaturated solution flow Gas advection Water vapour transport Heat balance	Gas adsorption Inter and Intra particle diffusion Microbial growth Microbial attachment Microbial oxidation	Topological effects Intra-particle diffusion Particle size distribution	Ferric/ferrous reduction Mineral oxidation Sulphur oxidation Surface processes
Illustration	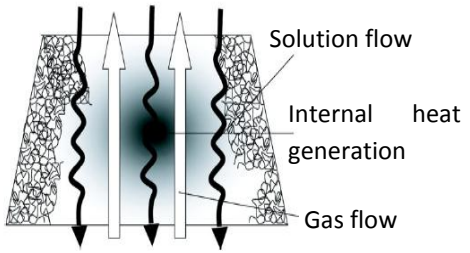	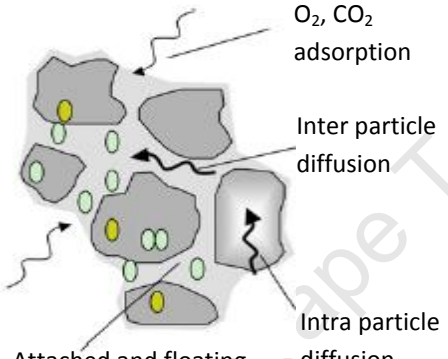	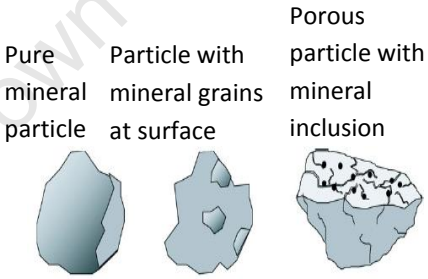	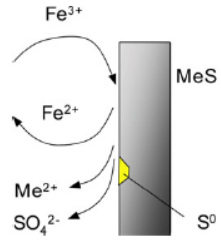
Factors affecting leaching rates	-Mass (i.e. gases and solution) and energy (i.e. heat) transportation through heap. -Inadequate gas flowing through the heap as a whole to deliver O_2 and CO_2. - Exothermic reactions within the heap release heat some of which is removed by the percolating solution downwards and humid air flowing up. This results in difficulty in controlling temperature within heap.	-Solution trickles down through heap of which some becomes stagnant in pores/ crevices on the ore (meso-scale) causing irregular solution flow. -Heap performance affected as the rate of delivering reagents and removing product from the reactive site is affected. -CO_2 and O_2 mass transfer limitations, bacterial growth as well as inter and intra particle diffusion are huge factors influencing the overall leaching rate and are all affected by stagnant solution.	-Mineralogy of gangue matrix within low grade ore. -Ore topology.	-Chemical and electrochemical interactions of the surface.

Figure 2-6: Scales and sub processes involved in heap bioleaching (Petersen and Dixon, 2003; Petersen and Dixon, 2007)

In addition, sub-processes such as chemical leaching, ferric iron inhibition of microbial growth and ferric precipitation or ions present within a leaching system may also potentially influence kinetics depending on environmental conditions. One factor however, that significantly influences kinetics is microbial growth, as certain elementary processes are mediated by microorganisms (Rossi, 1990; van Scherpenzeel *et al.*, 1998).

2.4.2 Theory behind deducing microbial growth kinetics and ferrous iron utilization

Kinetic data generated by several scientific authors for leaching processes combine respiratory and microbial stoichiometry (van Scherpenzeel *et al.*, 1998). Several assumptions are made when obtaining these stoichiometric relationships. Boon *et al.* (1998) showed through elemental balances on C, H, O, N, Fe and charge balances that equation 2-14 could be used to describe the bacterial oxidation of ferrous iron (Details on the stoichiometric equation can be found in Appendix C).

$$CO_2 + 0.2NH_4^+ + \left(\frac{1 - 4.2Y_{sX}}{4Y_{sX}}\right)O_2 + \frac{1}{Y_{sX}}Fe^{2+} + \left(\frac{1}{Y_{sX}} - 0.2\right)H^+ \xrightarrow{bacteria} CH_{1.8}O_{0.5}N_{0.2} + \frac{1}{Y_{sX}}Fe^{3+} + \left(\frac{1}{2Y_{sX}} - 0.6\right)H_2O \quad \text{Equation 2-14}$$

The microbial biomass produced is represented by $CH_{1.8}O_{0.5}N_{0.2}$ and is assumed to be entirely metabolically active. Other assumptions made are that the carbon source to the bioleaching system is CO_2 from air (van Scherpenzeel *et al.*, 1998), and that the energy required for microbial growth, maintenance and metabolic cell processes is due to ferrous ion oxidation only. The planktonic cells used during investigation do not produce extracellular polymeric substances (EPS), and CO_2 assimilation contributes to metabolically active cells. Continuous stirred tank reactors (CSTR) used during experiments are also typically operated at steady state with no significant changes in the flowrates and concentrations during sampling (Breed *et al.*, 1999a; Naik, 2010; Ojumu, 2008).

The energy required for bacterial growth and maintenance is obtained from ferrous iron oxidation. The rate of ferrous ion oxidation can be calculated from either a degree of reduction balance (equation 2-15) or from a material balance on the substrate in a continuous stirred tank reactor (CSTR) (equation 2-16). The degree of reduction balance (see Appendix C for more information) shows the relationship between oxygen and carbon dioxide consumption rates and follows from the stoichiometry of the bacterial oxidation equation (Boon *et al.*, 1998; Breed *et al.*, 1999a; van Scherpenzeel *et al.*, 1998).

$$-r_s = -4r_{O_2} - 4.2r_{CO_2}$$ Equation 2-15

$$-r_s = D([S]_{inlet} - [S]_{outlet})$$ Equation 2-16

where r_s (mmol.L^{-1}.hr^{-1}) is the oxidation rate of the substrate i.e ferrous iron; r_{O_2} (mmol.L^{-1}.hr^{-1}) is the oxygen uptake rate, r_{CO_2} (mmol.L^{-1}.hr^{-1}) is the carbon dioxide uptake rate; D (hr^{-1}) is the dilution rate; $[S]_{inlet}$ (mmolL^{-1}) is the substrate inlet concentration and $[S]_{outlet}$ (mmolL^{-1}) is the substrate outlet concentration.

In 1942, Monod proposed a model now used almost universally to describe substrate limited microbial growth. It has proved to be the most appropriate model for describing microbial growth with ferrous ions as the limiting substrate (Rossi, 1990; Sundkvist *et al.*, 2008) for leaching processes. The Monod equation's (equation 2-17) mathematical form is similar to the Michaelis and Menten model derived for enzyme-substrate interaction kinetics. Ojumu (2008) describes the Monod model as assuming that bacteria behave like a group of enzymes following the kinetic pathways used for the Michaelis and Menten model.

$$\mu = \frac{\mu_{max}[S]}{K_m + [S]}$$ Equation 2-17

μ_{max} (hr^{-1}) is the maximum specific growth rate and [S] (mmol/L) the substrate concentration. The specific growth rate - μ (1/hr) and the apparent Michaelis-Menten constant - K_m (mmole/L) need to be known if using the Monod equation as a model for microbial growth. Rossi (1990) describes them as constants that are a function of temperature, the organism, the type of medium and the growth limiting substrate contained in the medium [S]. The Monod equation is however a bad fit for systems with rapid growth conditions and it is therefore necessary in such cases to modify the model and add terms that eliminate inhibiting effects due to factors such as substrate, product or toxic effects (Sundkvist *et al.*, 2008).

A method used by many authors to obtain kinetic data has been to run continuous stirred tank reactors (CSTR) at steady state (Naik, 2010; Ojumu 2008; Rossi, 1990; Sundkvist *et al.*, 2008). Chemical conditions are maintained by adjusting the flow rates of inflowing and outflowing streams. In order to obtain kinetic data from a CSTR, the reactor is assumed to be well mixed, with insignificant variations in temperature and substrate concentration. Sterile feed is used when running experiments and contains iron sulphate solution (the culture should be substrate limited).

Cell attachment is assumed to be negligible, hence there is no supposed biomass accumulation; the formation of precipitate is also assumed negligible. Feed and discharge flow rates are the same. The volume of the reactor remains constant and the culture is in exponential growth phase. There are no growth inhibition factors and conditions must be aseptic to encourage the strong domination of one species or the strict presence of only one species in the chemostat (Ojumu, 2008; Sundkvist *et al.*, 2007). A mass balance around a CSTR with active cells is shown by equation 2-18 (Ojumu, 2008; Rossi, 1999; Sundkvist *et al.*, 2008).

$$V\frac{dX}{dt} = FX_0 - FXV + \mu XV - \alpha XV \qquad \text{Equation 2-18}$$

where V is the reactor volume; F, the flowrate; X, the cell concentration in the reactor; μ, the specific growth rate; α, the specific death rate; X_o, the cell concentration in the input stream and $\frac{dX}{dt}$ represents the accumulation of cells in the chemostat. At steady state, equation 2-19 applies where $\frac{dX}{dt}$ is zero and α is considered to be negligible because the specific growth rate is much greater than the death rate and μ >> α.

$$\frac{F}{V} = \mu = D = \frac{1}{\tau} = \frac{r_{CO_2}}{X} \qquad \text{Equation 2-19}$$

The mass balance reduces to equations 2-20 and 2-21 following these assumptions (Rossi, 1990):

$$\frac{dX}{dt} = (\mu X - \alpha X) + (DX_0 - DX) \qquad \text{Equation 2-20}$$

$$DX_0 = (D - \mu)X \qquad \text{Equation 2-21}$$

The wash-out of cells can be reached at the critical growth rate ($D_c=\mu_{max}$). D_c correlates to the flowrate where the flow of biomass out of the reactor is the same as newly formed biomass in the same interval of time. There would be a huge reduction of the biomass in the reactor if $D>D_c$ until there are no cells left, i.e. the microbial population becomes completely washed out (Rossi, 1990). For a limiting substrate such as ferrous ions, a mass balance around a CSTR is represented by (equation 2-22) (Ojumu, 2008):

$$V\frac{dS}{dt} = F[S_0] - FS + \frac{\mu X}{Y_{sX}^{max}} - m_s XV \qquad \text{Equation 2-22}$$

The fraction used for growth is represented by $\frac{\mu X}{Y_{sX}^{max}}$; and the fraction used for cell maintenance is represented by $m_s X$. Y_{sX}^{max} (mmolC.mmolS^{-1}) is the maximum yield. The maximum yield is the maximum amount of biomass that can be produced per mole of substrate consumed. The maintenance (mmolS .mmolC^{-1}hr^{-1}), m_s, is the amount of substrate required per unit of time in order to maintain one C-mole of bacteria without any growth (Boon *et al.*, 1998; van Scherpenzeel *et al.*, 1998); $\frac{dS}{dt}$ is the accumulation of the substrate in the chemostat and should be zero at steady state. Maintenance can be influenced by factors such as cell motility, cell membrane potential adjustments, solution pH and ionic strength (Sundkvist *et al.*, 2008). If maintenance is neglected, then equation 2-23 applies:

$$So - S = \frac{\mu X}{Y_{sX}^{max}} \qquad \text{Equation 2-23}$$

And if $r_X = \frac{dX}{dt} = \mu X$ then equation 2-23 can be re-written as:

$$Y = \frac{dX/dt}{-dS/dt} = \frac{r_X}{-r_s} \qquad \text{Equation 2-24}$$

Equation 2-24 only holds under certain assumptions (Ojumu, 2008; Rossi, 1990):

- The cell yield is assumed to be independent of the growth or the dilution rate.
- The absolute value of cell concentration X is independent of all nutrients except the limiting one.
- Cell yield on the limiting nutrient is affected only by the limiting nutrient under consideration and the maintenance requirements are assumed to be negligible.

Equation 2-23 was found not to correlate with empirical trends for microbial growth. It was further modified by Pirt to include the maintenance factor (Pirt, 1975). The Pirt equation relates substrate consumption, bacterial growth and maintenance (Boon *et al.*, 1998). Pirt hypothesized that energy derived during substrate utilization was used for either cell maintenance (non growth cell activities) or cell growth. Equation 2-25 shows the Pirt equation (Boon *et al.*, 1998; Breed *et al.*, 1999a):

$$-r_s = \frac{r_X}{Y_{sX}^{max}} + m_s X \qquad \text{Equation 2-25}$$

The rate of microbial growth (r_X) is directly proportional to its population (equation 2-26) and the specific substrate oxidation rate (q_s) is the rate at which the substrate is utilized per mole of biomass produced (equation 2-27). Using these relations, the Pirt equation can further be reduced to equation 2-28. Using steady state continuous culture data, Y_{sX}^{max} and m_s can be determined by plotting q_s vs. D (Breed *et al.*, 1999a).

$$r_X = \frac{dX}{dt} = \mu X \quad \text{Equation 2-26}$$

$$q_s = \frac{-r_s}{X} \quad \text{Equation 2-27}$$

$$-q_s = \mu \frac{1}{Y_{sX}^{max}} + m_s \quad \text{Equation 2-28}$$

Table 2-3 shows Lineweaver-Burk, Eadie-Hofstee or Langmuir plots used to determine μ_{max}, K_m, Y_{sX}^{max}, and m_s. If the steady state substrate and biomass concentrations are known for the different dilution rates μ_{max}, K_m, Y_{sX}^{max}, and m_s can be calculated by linearizing the Monod equation to the appropriate equations shown on Table 2-3. μ_{max} can also be calculated by plotting the natural logarithm of the cells concentration over a given period of time. In the exponential phase of microbial growth, the slope as shown by equation 2-29 is the maximum growth rate;

$$\mu_{max} = \frac{LnX_t - LnX_0}{\Delta t} \quad \text{Equation 2-29}$$

where X_0 is the initial cell concentration; X_t is the final cell concentration and t is the time. Y_{sX}^{max}, and m_s may be calculated by linearizing the Pirt equation, and plotting the specific iron utilization rate (q_s) against the dilution rate D (m_s-y intercept and 1/ Y_{sX}^{max} - gradient) (Breed *et al.*, 1999a).

Table 2-3: Plots of linearised Monod equations (Ojumu, 2008; Sundkvist *et al.*, 2008)

Linearised Equation	Plot
$\frac{1}{D} = \frac{K_m}{\mu_{max}}\left(\frac{1}{[s]}\right) + \frac{1}{\mu_{max}}$	**Lineweaver-Burk plot:** 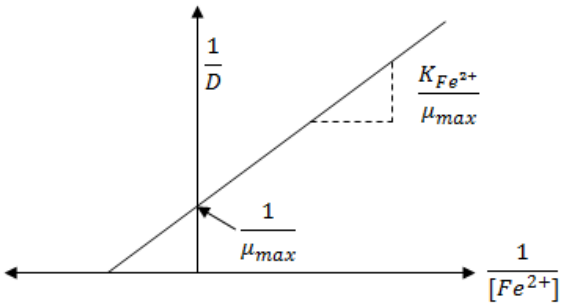
$\frac{D}{[s]} = \frac{\mu_{max}}{K_m} - \frac{D}{K_m}$	**Eadie-Hofstee:** 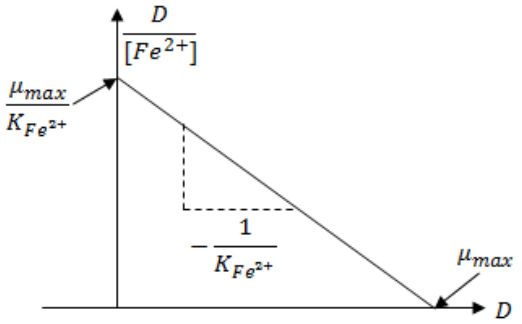
$\frac{[s]}{D} = \frac{K_m}{\mu_{max}} + \frac{[s]}{\mu_{max}}$	**Langmuir plot:** 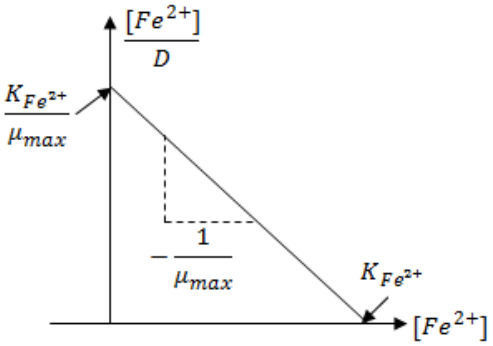

2.4.3 Development of kinetic equations for microbial ferrous iron oxidation

Rate equations are important for the design and modelling of tank and heap leaching processes. For over 30 years various authors have published work concerned with microbial ferrous oxidation kinetics and have deduced rate equations for ferrous iron oxidation which includes effects of temperature, pH, biomass concentration and ionic strength (Ojumu *et al.*, 2006; Sundkvist *et al.*, 2008). These models are classified as either empirical (using tools like logistic equations to model kinetics), or Michaelis-Menten/Monod (using traditional enzyme kinetics) based (Breed and Hansford, 1999b; Dempers *et al.*, 2003). Table 2-4 shows some of these kinetic models published.

Table 2-4: Some published kinetic models for ferrous iron oxidation with *Acidithiobacillus ferrooxidans* (Ojumu *et al.*, 2006)

Author	Model	Conditions
Lacey and Lawson (1970)	$\mu = \frac{\mu^{max}\,[Fe^{2+}]}{Y_{sX}K_m + [Fe^{2+}]}$	Batch STR, T=25-30°C, pH=2-2.3, Fe^{2+} = 6g/l
MacDonald and Clark (1970)	$\mu = \frac{\mu^{max}\,[Fe^{2+}]}{K_m + [Fe^{2+}]}$	Continuous, T=28°C, pH=2.2
Jones and Kelly (1983)	$\mu = \frac{\mu^{max}\,[Fe^{2+}]}{[Fe^{2+}] + K_m(1 + \frac{[Fe^{3+}]}{K_i})}$	Continuous, T=30°C, pH=1.6, Fe_T =5-400mM
Braddock *et al*. (1984)	$\mu = \frac{\mu^{max}([Fe^{2+}] - [Fe^{2+}]_t)}{K_m + ([Fe^{2+}] - [Fe^{2+}]_t)}$	Continuous, T=22°C, Fe_T =9-22mM, Isolate AK1
Liu *et al.* (1988)	$\mu = \frac{\mu^{max}[Fe^{2+}]}{[Fe^{2+}] + K_s(1 + K_i[Fe^{3+}])}$	Continuous, T=35°C, pH=1.8, Fe_T =0.52-3.29g/L
Lizama and Suzuki (1989)	$-r_{o_2} = \frac{k_3^{'}[X][Fe^{2+}]}{[Fe^{2+}] + K_m[1 + \frac{[X]}{K_i^{'}} + \frac{[Fe^{3+}]}{K_{if}} + \frac{[X][Fe^{3+}]}{\alpha K_i^{'} K_{if}}]}$	Continuous, T=29°C, pH=1.8-2.0, Fe_T =0.25-26mM
Nikilov and Karamanev (1992)	$\mu = \frac{\mu^{max}[Fe^{2+}]}{[Fe^{2+}] + K_s + [Fe^{3+}]\frac{K_s}{K_i} + \frac{[Fe^{3+}]}{K_{if}} + \frac{([Fe^{3+}])^2}{K_{si}}}$	Continuous, T=29°C, pH=1.8-2.0, Fe_T =2-70.8g/L
Huberts (1994)	$-r_{Fe^{2+}} = a_1(\frac{p_{o_2}}{k_B + p_{o_2}})(\frac{[Fe^{2+}]}{[Fe^{2+}] + K_{Fe^{2+}}\left(1 + \frac{[Fe^{3+}]}{K^{'}}\right]})$	Continuous, T=30°C, pH=2, *Leptospirillum ferrooxidans*
Crundwell (1997)	$-r_{Fe^{2+}} = k(\frac{p_{o_2}}{k_B + p_{o_2}})^{0.5}(\frac{[Fe^{2+}]/[H^+]}{K_{Fe^{2+}} + \frac{[Fe^{2+}]}{[H^+]} + K_i[Fe^{3+}]})^{0.5}$	Theoretical, fitted to data from Huberts
Hansford (1997)	$q_{Fe^{2+}} = \frac{q_{Fe^{2+}}^{max}}{1 + K_{Fe^{2+}}\frac{[Fe^{3+}]}{[Fe^{2+}]}}$	Only fitted to *Leptospirillum* data
Nemati and Web (1998)	$\mu = \frac{K_0 e^{\frac{E_a}{RT}}[X][Fe^{2+}]}{(K_m + [Fe^{2+}])(1 + \frac{[Fe^{3+}]}{K_i})}$	Initial rate, T=30°C, pH=2.0, Fe_T =0.45-31.5Kg/m^3
Boon *et al*. (1999)	$q_{O_2} = \frac{q_{O_2}^{max}}{1 + \frac{K_s}{[Fe^{2+}] - [Fe^{2+}]_t} + \frac{K_s}{K_i}(\frac{[Fe^{3+}]}{[Fe^{2+}] - [Fe^{2+}]_t})}$	Continuous, T=30°C, pH=1.8-1.9, Fe_T =0.05-0.36M
Meruane *et al*. (2002)	$q_{Fe^{2+}} = \frac{K_1^* \exp\left[\frac{nF}{2RT}\left(E^m - E_h^0\right)\right]\{1 - exp\left[\frac{nF}{2RT}(E^m - E)\right]\}}{1 + \frac{K_2^*}{Fe^{2+}} + K_3^* \exp\left[\frac{nF}{2RT}(E^m - E_h^0)\right]}$	Electrochemical cell, T=30°C, pH=1.8, Fe_T=0.05-1g/l

Lacey and Lawson investigated ferrous iron oxidation rates using a batch culture and used a model with Monod and Michaelis-Menten kinetics. Jones and Kelly used a continuous culture and modified the model based on ferrous iron and ferric iron inhibition (van Scherpenzeel *et al.*, 1998). Other models have been deduced from either initial rate studies in batch and continuous cultures, or using iso-potential devices (Ojumu *et al.*, 2006). Data collected from experiments have also been fitted using modified Monod or Michaelis equations or models derived from the chemiosmotic theory or electrochemical analogies. The most useful of these equations in terms of experimental measurements as well as engineering applications was the work published by Boon and co-workers whose model is in terms of specific ferrous utilization. Hansford simplified the equation to express ferric inhibition in terms of the ferric to ferrous ratio which is commensurate with solution redox potential and hence easily monitored (Breed *et al.*, 1999a; Naik, 2010; Ojumu *et al.*, 2006). The model is also listed in Table 2-4.

2.4.4 Redox potential

The ferrous iron oxidation rate is related to a ferric to ferrous iron ratio which influences redox potential. Rossi (1990) defines the redox potential of a solution as 'a measure of the tendency of the solution to be oxidized or reduced' (Naik, 2010; Ojumu, 2008). A standard solution potential is measured using a standard hydrogen electrode (SHE) and is the electrode potential measured from a solution with the concentration of solutes at 1molar, a gas pressure of 1 atmosphere and temperature of 25^{o}C (standard conditions) (Ebbing, 1993). In the laboratory, the SHE electrode is impractical and cannot be used for accurate measurements, so alternatively stable electrodes such as the silver-silver chloride electrode can be used to measure redox potential. If one wishes to calculate the solution potential relative to the standard hydrogen electrode after obtaining the redox potential using a silver-silver chloride electrode with a 3M KCL electrolyte, then the measured solution redox potential is offset from the SHE potential by 207 mV under standard conditions. This offset differs and depends on the molarity of the electrolyte in use (If the electrolyte was saturated KCL then the offset would be 197 mV) (Metrohm 827 pH meter booklet).

The Nernst equation is used to express the ferric: ferrous iron ratio in terms of the redox potential as shown by equation 2-30 (Boon and Heijnen, 1998; Breed and Hansford, 1999b; Hansford and Vargas, 2001; May *et al.*, 1997; Naik, 2010; Nemati and Webb, 1997; Ojumu, 2008; Rawlings *et al.*, 1999):

$$E_h = E_0 - \frac{RT}{nF}\ln\left(\frac{Fe^{3+}}{Fe^{2+}}\right) \qquad \text{Equation 2-30}$$

$$E_0 = \frac{\Delta G^0}{nF}$$ Equation 2-31

where E_h is the redox potential measured in mV, E_0 the standard redox potential in mV, R the universal gas constant, T the absolute temperature (K), ΔG the Gibbs free energy, n is the number of electrons transferred in the redox reaction n and F is the Faraday constant (96,485 C/mol). The redox potential depends on the ion concentrations, and therefore it is important to know how ions in leaching solutions interact with each other (Ebbing, 1993). The activity (see equations 2-32 and 2-33) gives an accurate measure of the ionic interactions in solution. The activity constants are a function of ionic strength.

$$a_i = \gamma_i C_i$$ Equation 2-32

$$I = \frac{1}{2} \sum C_i z_i^2$$ Equation 2-33

where a_i is the activity, C_i the concentration of species i, γ_i the activity coefficient of ionic species i, z the ionic charge of species i and I is the ionic strength of the electrolyte solution (mol.L^{-1}). The activity coefficient of ionic species γ_i can be determined from models such as the Debye-Huckel model. The activity coefficient of ionic species is a function of the ionic strength and can be obtained using equation 2-32. To use equation 2-32, it is assumed that the electrolyte solution is dilute (Ojumu, 2008).

2.4.5 Rate limiting factors

2.4.5.1 Temperature

Temperature levels limit the leaching process by affecting microbial oxidation kinetics and influence the economics of the process (Dopson *et al.*, 2007; Franzmann *et al.,* 2005; Ojumu *et al.,* 2009). Heat is generated in heaps due to exothermic reactions (sulphide oxidation) and contributes to irregular and wide temperature variations across the bed (Ojumu *et al.*, 2009). Heaps are usually inoculated with a consortium of microorganisms that can range from mesophilic, moderate thermophilic or to extremely thermophilic. It is therefore important to find ways of controlling temperature in heaps so that microbial activity remains uninterrupted.

The Arrhenius equation (equation 2-34) is used to show the relationship between the oxidation kinetics of ferrous iron and sulphur and temperature (Franzmann *et al.*, 2005; Nemati and Web,

1997; Ojumu *et al.,* 2009). The activation energy required by various microorganisms can be found using this relationship and indicates how much energy is required for the reactions to occur.

$$\ln k = -\frac{E_a}{RT} + lnA \qquad \text{Equation 2-34}$$

k is the first order rate coefficient, E_a the activation energy in Joules, R is the gas constant (8.314J/K.mol), A is the pre-exponential constant and T is the temperature in Kelvin.

The Ratkowsky equation is used to define operational temperature constraints on common mineral leaching organisms (equation 2-35) (Dopson *et al.*, 2007; Franzmann *et al.,* 2005; Ojumu *et al.*, 2006).

$$\sqrt{\frac{1}{t}} = b \times (T - T_{min}) \times (1 - e^{(c \times (T - T_{max}))}) \qquad \text{Equation 2-35}$$

t is the generation time to reach a specific condition, T the temperature (K), T_{MIN} the theoretical extrapolated minimum temperature for growth and T_{MAX} the theoretical extrapolated maximal temperature for growth whilst b and c are fitting parameters.

2.4.5.2 Salinity

Inorganic and organic species (toxic cations and anions) present in water bodies used during heap leaching can affect bacterial culture activity (Shiers *et al.,* 2005; Deveci *et al.*, 2008). Cations and anions inhibit bacteria at different tolerance levels and have different effects on the physiology of microorganisms. In arid regions such as Chile, heap operations may produce pregnant leach solutions (PLS) containing high concentrations of dissolved ions, including chlorides (Ojumu *et al.,* 2008).

Alexander *et al.* (1986) found that *Acidithiobacillus ferrooxidans* was resistant to cations but relatively sensitive to anions. In acidic environments (at pH of about 1), the internal pH of the cell is maintained at about 6.5. The pH difference across the cytoplasmic membrane is influenced by both the proton-electrochemical potential and the membrane potential (proton-electrochemical potential (in mV) = membrane potential (in mV) 59·ΔpH); the pH difference and membrane potential are at a balance. At inhibitory concentrations of the anion, the anion enters the cell resulting in the acidification of the cytoplasm. The movement of anions to the cell causes a greater pH difference

and protons are forced to enter the cell to maintain that balance. Alexander *et al.* (1986) and Ingledew (1982) reported that bacteria were usually tolerant to a wide range of heavy metal cations. Blight and Ralph (2008) examined effects of ions on cell replication rates of iron oxidizing bacteria and found that aluminium and nitrate ions both reduced cell replication in saline media. Inhibition by nitrates was greater than inhibition by chloride ions. The impact of aluminium was similar to salts like sodium, potassium and ammonium sulphate. Experiments by Shiers *et al.* (2005) showed that chloride ions were more toxic than sulphate ions. Cultures could adapt to low concentrations of sodium sulphate (20 gL^{-1}) with permanent inhibition at much higher concentrations (40 gL^{-1}). In the presence of sodium chloride, the culture could adapt to very low concentrations of (7 gL^{-1}) with higher concentrations resulting in permanent inhibition. Gahan *et al.* (2010) reported that high chloride ions affected bio-oxidation efficiency by influencing jarosite precipitation resulting in the removal of ferric ions from solution. (Ojumu *et al.,* 2008) also reported that the dissolution of gangue minerals from igneous ore material resulted in the build up of high concentrations of magnesium and aluminium sulphates in the recycled leach solutions. Heaps with high concentrations of ions contained in the recycled water inventory retarded colonies. Garcia and da Silva (1991) mention that metals such as silver and mercury are potentially toxic even at very low concentrations while there is resistance to metals such as zinc nickel, cobalt and copper.

Acidophiles have little tolerance for chloride ions as they inhibit cell growth and the ferrous iron oxidation enzyme system (Gahan *et al.*, 2010). Toxicity could be caused by the accumulation of anions into the cytoplasm, resulting from the combination of infinite permeability of the cytoplasmic membrane to anions, as well as the positive cytoplasmic membrane potential as mentioned earlier on (Alexander *et al.*, 1986). Baker-Austin *et al.* (2005) reported that copper at toxic concentrations was able to catalyze the synthesis of reactive oxygen species which causes severe damage to the cytoplasmic constituents by the oxidation of proteins, cleavage of DNA and RNA and lipid preoxidation. Copper also binds to histidine, cysteine and methionine with high affinity resulting in the deactivation of proteins. Salts exert different osmotic pressures on microbial cells (Ojumu *et al.*, 2006). Ions can change enzyme conformations or bind to transport sites, resulting in the disruption of the cell membrane transport process. They accumulate in the cell cytoplasm, causing loss of the membrane potential and inhibit the respiratory chain. Anions indirectly inhibit iron oxidizing bacteria by changing solution speciation that affect the ferric/ferrous couple (Ojumu *et al.,* 2008). Kinnunen and Puhakka (2005) mention that metal ions are capable of damaging cell membranes and the DNA structure; of altering enzyme specificity, and disrupting cellular functions.

Shiers *et al.* (2005) reported that ions in solution contribute to the ionic strength. The effect of salinity can be explained in terms of ionic strength. Increasing the ionic strength imposes a larger energetic load on each cell to maintain homeostasis against the osmotic gradient with less energy for cell reproduction (Blight and Ralph, 2008). The ionic gradient across the membrane, and the decrease in the concentration of dissolved gases (oxygen and carbon dioxide) results in the inhibitive effect of ionic strength, leading to a lower cell doubling rate constant (Shiers *et al.*, 2005). Increased ionic strength changes the potential of the ferric/ferrous couple. Ionic strength in solution affects the potential ΔE of the bio-electrochemical cell formed and of which energy available from the oxidation and reduction of the ferric/ferrous iron and O_2/H_2O couples is dependent (Blight and Ralph, 2008).

2.4.5.3 pH

During bioleaching, the solution pH is a measure of the balance between acid producing and acid consuming reactions. Acids or alkali may be added to the system to influence the solution pH. Ore composition (gangue components and mineral sulphides) influences solution pH as some gangue materials contain carbonates which are acid consuming (Plumb *et al.,* 2008b). Generally, leaching solutions are required to be at pH levels lower than 3 as this favours the leaching process. One important factor is that leaching microorganisms are acidophilic in nature. The high proton environment facilitates the electron transport system within bacteria for nutritional purposes (Ojumu *et al.,* 2011). Extreme thermophiles seem to have a greater tolerance for acidity than mesophiles (Deveci *et al,* 2008). Protons are required for the dissolution process of acid soluble sulphides therefore low pH levels are required (Plumb *et al.,* 2008b).

In acidic conditions, elemental sulphur is inert to abiotic oxidation and becomes a diffusion barrier affecting the dissolution process (Deveci *et al.,* 2008; Plumb *et al.*, 2008b). Sulphur oxidizing microorganisms (acidophilic in nature) can override this problem and oxidize elemental sulphur so as to avoid any barriers (equation 2-37). Oxidation of ferrous to ferric iron can result in jarosite formation. Jarosites formation usually occurs at high pH levels (Daoud and Karamanev, 2006; Deveci *et al,* 2008; Fu *et al.*, 2008). Ojumu et.al (2011) report that ferric iron precipitate was significant at pH levels above 1.3. This is shown by equation 2-38, which is reversible depending on the proton concentration (Plumb *et al.,* 2008). Jarosite formation decreases the bioleaching rate by deactivating the surface of metal sulphide particles, thus creating kinetic barriers (Daoud and Karamanev, 2006). It also diminishes ferric ions in the medium, occupies the space within biomass carrier material and

tends to block pumps and valves (Kinnunen and Puhakka, 2005). In a heap environment, the heap permeability is reduced due to ferric iron precipitation (Ojumu *et al.,* 2011).

$$4Fe^{2+} + O_2 + 4H^+ \longrightarrow 4Fe^{3+} + 2H_2O \quad \text{Equation 2-36}$$

$$2S^0 + 2H_2O + 3O_2 \longrightarrow 2SO_4^{2-} + 4H^+ \quad \text{Equation 2-37}$$

$$3Fe^{3+} + 2SO_4^{2-} + 6H_2O + M^+ \longrightarrow MFe^{3+}(SO_4)_2(OH)_6 + 6H^+ \quad \text{Equation 2-38}$$

At low pH levels, leaching microorganisms require energy to maintain the proton gradient between the cytoplasm and the bulk solution. The cell's cytoplasm must be maintained at or near neutral values while the bulk solution is at pH<3. Energy is produced due to this proton gradient as it is the driving force for ATP synthesis. Protons are a substrate in the cytoplasm and react with oxygen (electron acceptor) to produce water. High pH levels inhibit growth as there is no proton gradient for the proton transfer into the cytoplasm as well as no synthesis of ATP for energy (Ojumu *et al.*, 2006).

2.4.5.4 Ferric and ferrous iron concentration

Ferric and ferrous ions play a key role in bioleaching. Ferric ions oxidize sulphide minerals, and microorganisms aid in the regeneration of ferric ions by oxidizing ferrous ions. Microorganisms containing plenty of iron and glucuronic acid in their exopolymers contribute to high oxidation activity compared to microorganisms with low amounts. Sand and Gehrke (2006) reported that cells with a high amount of complexed ferric iron had stronger electrostatic interaction with pyrite surfaces, resulting in increased cell attachment. The solution potential is related to the ferric to ferrous iron ratio and control over the solution potential during leaching is important. This is done by controlling ferric and ferrous iron concentration levels as they can have negative impacts on the leaching process.

During dissolution, the rate of ferric iron attachment on the metal sulphide is much slower than ferrous iron oxidation by bacteria and can result in the accumulation of ferric ions in the leaching solution. High ferric ion concentrations inhibit the ferrous iron oxidizing system of bacteria (Kabawe *et al.*, 2003; Nemati and Web, 1997; van Scherpenzeel *et al.*, 1998). Córdoba *et al. (*2008) found that high ferric iron levels of up to 5 gL^{-1} were toxic for a consortium of microorganisms (*Leptospirillum ferrooxidans*, *Acidithiobacillus ferrooxidans*, *Acidithiobacillus thiooxidans* and Sulfolobus BC strain) while Nemati *et al.* (1997) found that a maximum concentration of 15.6 gL^{-1} of ferric iron caused complete inhibition with no growth of *Acidithiobacillus ferrooxidans* microorganisms. High concentrations of ferrous iron also have inhibitory effects on leaching microorganisms; for example

while it has been reported that ferrous iron concentration of up to 5.6 gL^{-1} can enhance oxygen uptake rates during leaching; higher concentrations result in a lower oxygen uptake rates (Blight and Ralph, 2008; van Scherpenzeel *et al.*, 1998).

Rodríguez *et al. (*2003a), using pyrite, showed that dissolution was controlled by competitive chemisorption between ferrous iron and ferric iron on the mineral surface layer. They explained that high ferric iron concentrations cause enzymatic ferrous ion oxidation inhibition of microorganisms. This promotes accumulation of ferrous ions on the mineral surface resulting in a diffusion barrier to ferric attack. The diffusion barrier results in the accumulation of ferric iron on the mineral surface which inhibits microbial oxidation. High ferric iron concentrations also produce chemical instabilities in the leaching system favoring the nucleation and growth of jarosites over the mineral substrate particles. This causes passivation on the mineral substrate, resulting in low reactivity of the metal surface (Córdoba *et al.,* 2008).

The response of bioleaching microorganisms to ferric and ferrous iron concentrations vary depending on their nature, and bacterial strains can be characterised by their affinity to ferrous iron (Boon *et al.*, 1999). Keeping the solution potential at the right levels is important so that dissolution is maximised, but this depends on the nature of metal sulphide. Mesophiles create a high potential environment that benefits metal sulphides such as chalcocite and pyrite whereas thermophiles create solution conditions which maintain relatively low solution potentials. Ores like chalcopyrite cannot be oxidized in moderately high potential environments as the potential influences passivation which hinders leaching (Petersen and Dixon, 2006). Microorganisms like *Leptospirillum ferrooxidans* have high affinity for ferrous iron compared to *Acidithiobacillus ferrooxidans* and are less inhibited by ferric iron (Mignone and Donati, 2004; Ojumu *et al.*, 2009). At high ferric iron concentrations (high redox potentials) *Leptospirillum ferrooxidans* can still carry on with leaching activity, while *Acidithiobacillus ferrooxidans* is unable to. At low redox potentials *Acidithiobacillus ferrooxidans* dominates (Breed and Hansford, 1999; Rawlings *et al.,* 1999; Rawlings, 2002; van Scherpenzeel *et al.*, 1998).

2.4.6 Carbon dioxide and oxygen supply

Microorganisms used for bioleaching are autotrophic aerobes therefore an adequate supply of carbon dioxide (CO_2), and oxygen (O_2) during the bioleaching process is essential for growth and survival. Oxygen can be utilized to directly oxidize sulphides during the chemical leaching process as an electron acceptor. Its reduction occurs inside the cytoplasmic membrane and it has to be

transported from the solution across the cell membrane to participate in the reaction (Ojumu *et al.*, 2006). The molecule is then reduced to water. Microorganisms also require carbon usually obtained from atmospheric carbon dioxide. This is required to produce the building blocks required for cell growth. The amount of carbon dioxide required in heap leach environments is 2.2%-5% of the amount of oxygen that is required. In air, the carbon dioxide content is 0.17% of oxygen (350ppm vs. 21%). This is based on kinetic studies of microbial ferrous iron oxidation by *Leptospirillum* and *Acidithiobacillus* species indicating a carbon yield of 0.022 to 0.05 molC /mol O_2. If all the carbon dioxide present in air is adsorbed, then the air supply rate has to be faster than what is required to satisfy the oxygen demand for the same application (Petersen and Dixon, 2007). In heap leach systems, with low aeration rates, the supply of carbon dioxide may be the overall rate limiting factor if there are no carbonates in the ore (Petersen and Dixon, 2007).

To transport oxygen and carbon dioxide it is important to ensure that there is an effective gaseous mass transfer of carbon dioxide and oxygen from the atmosphere to the gas/liquid/solid interphase in the leach pulp (Witne and Phillips, 2001). The dissolved oxygen concentration in solution is always low, due to its low solubility in water. There may be gas-liquid mass transfer limitations which govern microbial oxidation kinetics. During bioleaching, oxygen must continuously be dissolved in the liquid phase at a higher rate than the oxygen consumption rate. If oxygen becomes a limiting substrate at the critical bulk oxygen concentration, the microbial growth rate slows down. If oxygen levels are below the critical point then microbes enter a lag phase and the oxidation process stops (Ojumu *et al.*, 2006).

The gas transfer rate (GTR) of oxygen is defined as:

$$GTR = K_La(C^* - C_i) \qquad \text{Equation 2-39}$$

where K_La represents the volumetric gas transfer coefficient, depending on the geometry of the transfer system, the rheology of the liquid phase, the environmental conditions and the operating conditions; K_L is the mass transfer conditions in the liquid film and a is the gas liquid interfacial area per unit volume of liquid. C^*-C_i is the driving force of the transfer phenomenon (Acevedo and Gentina, 2007; Witne and Phillips, 2001).

De Kock *et al.* (2003a) reported that mass transfer limitations were not encountered in tank operations at mesophilic conditions but mass transfer difficulties were experienced at elevated temperatures. This was because, at thermophilic conditions, mass transfer became a limiting factor

because of the reduced solubility of oxygen. The solubility of oxygen in these conditions could not be overcome by increasing agitation speeds and aeration rates. The only way to overcome this problem was using CO_2 enriched air although there were also limitations with regards to how much enriched air was used because excess of dissolved O_2 and CO_2 can be inhibitory.

Elevated dissolved oxygen concentrations can have detrimental effects on microbial cells as the capacity to dissipate oxygen-derived free radicals enzymatically can become overloaded. Inhibition is more detrimental at low dissolved oxygen concentrations, although prolonged exposure to high dissolved oxygen concentrations also results in an eventual cessation of activity. CO_2 levels at lower levels can cause inhibition of the microbial growth rate. Petersen *et al.* (2010) found that carbon dioxide supplementation in bioheaps stimulates microbial growth but does not increase the oxygen uptake rate and hence the rate of leaching. The absence of carbon dioxide resulted in a gradual population decline and decline in leaching rates, however, if there was active biomass then oxidation would continue in the absence of carbon dioxide. Using *Acidithiobacillus ferrooxidans* they found that optimal CO_2 concentrations for growth were between 0.23-0.53%. Concentrations above 0.73% reduced bacterial growth significantly (de Kock *et al.*, 2003a). Rawlings *et al.* (2003) reported that not all microorganisms were efficient at fixing CO_2 and grew better when enriched with 0.5-5% v/v CO_2.

2.5 Thesis Objectives, Hypotheses and Key Questions

2.5.1 Conclusions from literature

From the literature it has been shown that in previous studies the bio-oxidation kinetics have been primarily investigated in agitated tank environments where the systems are well mixed suspensions in nature and kinetics are driven by planktonic microorganisms. In real life heap systems however, a substantial proportion of the microbial population is associated with or attached to the mineral surface (i.e. is sessile); the resulting leaching kinetics therefore are largely due to the sessile microorganism activity and not from planktonic cultures as have been used in the past to fit heap leaching models.

In addition, biological processes in real heap leach environments are typically operated under non-optimal conditions with respect to pH, temperature, salinity, O_2 and CO_2 concentration, whereas kinetic constants have been typically generated from chemostat culture under optimal conditions. While available kinetic models have attempted to account for these kinetic differences, there is still a lack of understanding of the kinetics of ferrous iron oxidation by sessile/attached micro-organisms.

As a result, the bio-oxidation kinetics derived from well mixed submerged culture chemostat systems may not necessarily represent those of a heap, and it is therefore important that they be investigated under conditions mimicking the sessile culture.

The present study continues from work by Maas and Paxton (2007) and by Naik (2010). Maas and Paxton (2007) attempted to investigate a possible reactor setup which could then be used to model the activity of a sessile microbial population using a continuous stirred tank reactor (CSTR) setup. Their aim was to try and quantify if the kinetics derived from tank experiments were applicable to heap conditions. The study suggested that kinetics derived from the conventional stirred tank reactor could not necessarily be applied to heaps systems. Naik (2010) investigated the effect of carbon dioxide on the growth and activity of a *Leptospirillum ferriphilum* microbial population. Part of that study included a comparison of the activity of a sessile microbial population relative to that of a planktonic microbial population. In particular the study included:

1. An investigation of a planktonic system alone (system 1). This entailed investigating the kinetics of planktonic *Leptospirillum ferriphilum* in a CSTR at 340 ppm, 100 ppm, 50 ppm and 30ppm CO_2 concentrations for residence times between 16-55 hr.
2. A study on a combined planktonic + sessile system (system 2) where a column containing a solid support was attached to a CSTR with an active planktonic culture to generate a sessile population. The kinetics of the planktonic + sessile population were investigated at 340 ppm, 100 ppm, 50 ppm and 30 ppm CO_2 concentrations for residence times between 16-55 hr.

Naik (2010) discovered from these experiments that:

i. There was very little difference in the ferrous iron oxidation rate between system 1 and 2.
ii. The amount of biomass in the planktonic + sessile system increased up to threefold when at steady state.
iii. Ferrous iron in the system was limiting, therefore it was unclear whether sessile microorganisms were able to oxidize ferrous iron at higher rates.

The findings (i), (ii) and (iii) led to a **decoupling study** (still a part of Naik's work 2010) where the objective was to investigate the performance of the sessile population in an environment that was not ferrous iron limiting. The sessile population was created in a column containing a solid support attached to a CSTR with an active planktonic culture at a 32 hr residence time. Solution was

circulated between CSTR and sessile bed at a rapid rate such that solution condition in the sessile bed and the CSTR were more or less identical. The sessile population was then detached from the CSTR and transferred to another CSTR operating abiotically at residence times of 16hrs and 32hrs. From the decoupling study, it was found that

i. a planktonic population was colonised from the sessile population, and this occurred at a faster rate than in the reverse case for both residence times of 16 hr and 32 hr. The study was dynamic, with the focus being on the initial period where the sessile population is independent of the planktonic population.
ii. increased ferrous iron oxidation activity was observed when ferrous iron was not limiting, and the study suggested that the sessile population could oxidize ferrous iron at higher rates.

Following on from the findings by Maas and Paxton (2007) and Naik (2010), the present study continued to focus on the sessile microbial population, and aimed to develop a strategy that allows the kinetics of ferrous iron oxidation catalysed by a sessile microbial population to be determined as a function of population size, availability of ferrous iron, and culture conditions. Such data would allow differentiation between the biological and mineral effects in heap bioleaching studies, and provide kinetic data for the biological effects for which suitable modelling strategies can be found.

2.5.2 Thesis Objectives

The objectives of this study were therefore threefold:

- To investigate ferrous iron oxidation rates of a pure culture of planktonic *Leptospirillum ferriphilum* microorganisms. The results would be used as a benchmark for comparison with the activity of sessile microorganisms in subsequent studies, and with previous studies run in non-sterile environments. The critical dilution rate, where washout of planktonic microorganism from the continuous stirred tank reactor would occur would also be determined from these experiments.

- To investigate the nature of attachment of a pure culture of *Leptospirillum ferriphilum* microorganisms to the surface of a solid substrate (ceramic saddles). It was important to know if, over time, cell attachment stopped once the surface area of the solid substrate was covered or if cell attachment continued indefinitely. Sessile microorganisms were created by

exposing planktonic *Leptospirillum ferriphilum* microorganisms to the solid substrate where they then began to attach.

- To investigate ferrous iron oxidation rates of a fully developed pure culture of sessile *Leptospirillum ferriphilum* microorganisms. The attached cells were contained in a glass vessel packed bed reactor (PBR) and connected to a continuous stirred tank reactor operating in the washout region (determined from experiments on planktonic *Leptospirillum ferriphilum* microorganisms). Results obtained were then compared to the rates of the planktonic culture.

2.5.3 Hypotheses and Key questions

In line with the objectives above, three working hypotheses were derived for this study and several key questions were generated from each hypothesis:

1. **Planktonic microorganisms will attach to the solid substrate of choice (ceramic saddles). Once the surface area of the solid substrate is completely covered by attached microorganisms, attachment will stop and cell numbers will plateau. A steady state (where cell numbers are consistent) will be reached.**

Key questions to explore this hypothesis include:

- During experiments will the culture attach to the inert solid support of choice? *Leptospirillum ferriphilum* has been found to be specific to attachment i.e. on pyrite ore.
- Is the sessile population firmly attached or just entrained in pore spaces in the solid support?
- How do sessile cultures grow and how does this differ from the growth of planktonic cultures?
- During colonization, will cell numbers increase until they reach steady state? Or will growth be transient? How long will steady state take to achieve? Will biofilms only cover the surface area of the solid support or will biofilms form layer on top of layer causing uncontrolled growth?
- How can cell numbers of sessile cultures be determined once attachment is established in the glass vessel?

2. **In the wash-out region, ferrous iron oxidation in the system will be driven by sessile microorganisms only.**

Key questions to explore this hypothesis include:

- At what dilution rate does the wash out of planktonic cells occur?
- To what extent are cells washed off the support, or are only as many cells released into the solution as growth on the support, leaving the sessile culture at steady state levels?

3. **Ferrous iron oxidation rates of planktonic microorganisms differ from ferrous iron oxidation rates of sessile microorganisms.**

Key questions to explore this hypothesis include:

- Are there any intrinsic differences between sessile and planktonic cultures based on the environments they are exposed to?
- If there are differences between sessile and planktonic cultures, how do these differences affect microbial kinetics?

3 Materials and methods

Chapter 3 begins with a summary of previous experimental work done to investigate the activity of sessile microbial populations, which approaches were used and built on in this study. A description of the experimental configurations utilised as well as the origins of the microbial culture and contents of the growth medium used in this study then follows. A description of the experimental procedures, analytical methods used and information on data analysis closes the chapter.

3.1 Experimental approach

3.1.1 Links to previous work

Naik (2010) performed a study to compare the activity of sessile microorganisms to that of planktonic microorganisms, aiming at obtaining ferrous iron oxidation rates influenced by only sessile microorganisms. These experiments were performed in a continuous stirred tank reactor (CSTR) in the Centre for Bioprocess Engineering Research (CeBER) laboratory at the University of Cape Town. Ferrous iron oxidation rates of a pure culture of planktonic *Leptospirillum ferriphilum* microorganisms (system 1) were compared to ferrous iron oxidation rates of a system containing a combination of both sessile and planktonic *Leptospirillum ferriphilum* microorganisms (system 2).

The sessile population was created by attaching an airtight glass column containing ceramic saddles to a CSTR with an active culture of planktonic microorganisms and circulating the culture through the glass column. This was done over a period of 3-7 residence times. It was confirmed that planktonic *Leptospirillum ferriphilum* attached to the surface of the ceramic saddles. There was no significant difference in the ferrous iron oxidation rates between the two systems due to ferrous iron limitations and this led to a decoupling study as described in section 2.5.1.

This study is a continuation of the work done by Naik (2010) and adopts part of the experimental approach taken. Experiments were conducted to: investigate the kinetics of planktonic *Leptospirillum ferriphilum* microorganisms in a CSTR for a range of residence times 4-55 hr; investigate the attachment of the microorganisms to the surface of ceramic saddles in a CSTR+PBR set-up at a fixed residence time of 32 hr, and to investigate the kinetics of the sessile population at washout (at washout conditions the growth of planktonic microorganisms is prevented) in a CSTR+PBR set-up at 4 and 5 hr residence times. Figure 3-1 shows a schematic summarizing the experimental approach taken as a whole for this study.

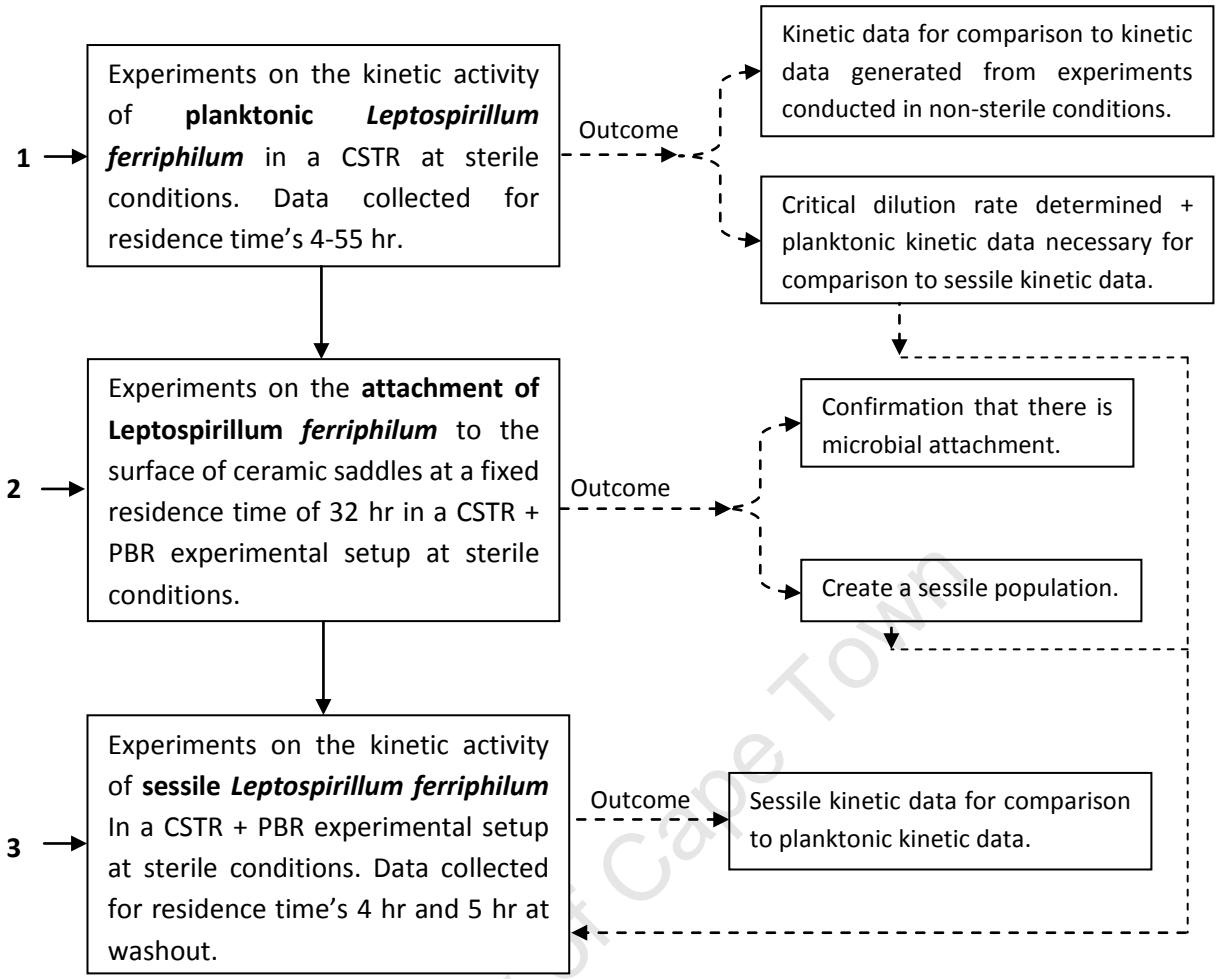

Figure 3-1: Schematic showing an overview of the approach taken in this study

3.2 Experimental configurations

Three separate experimental procedures were performed with two types of experimental configurations to:

- Determine ferrous iron oxidation rates and maximum growth rate of planktonic *Leptospirillum ferriphilum*.
- Investigate the attachment of microorganisms to a solid substrate of choice (ceramic saddles).
- Determine ferrous iron oxidation rates of sessile microorganisms.

All experiments were conducted in 2 litre Applikon® reactors (continuous stirred tank reactors-CSTR's) with 1 litre working volumes and the sessile population was colonised on the surface of ceramic saddles contained in a 200 mL glass vessel/packed bed reactor (PBR).

3.2.1 Planktonic experiments

Figure 3-2 shows the typical CSTR configuration used for planktonic experiments in this study.

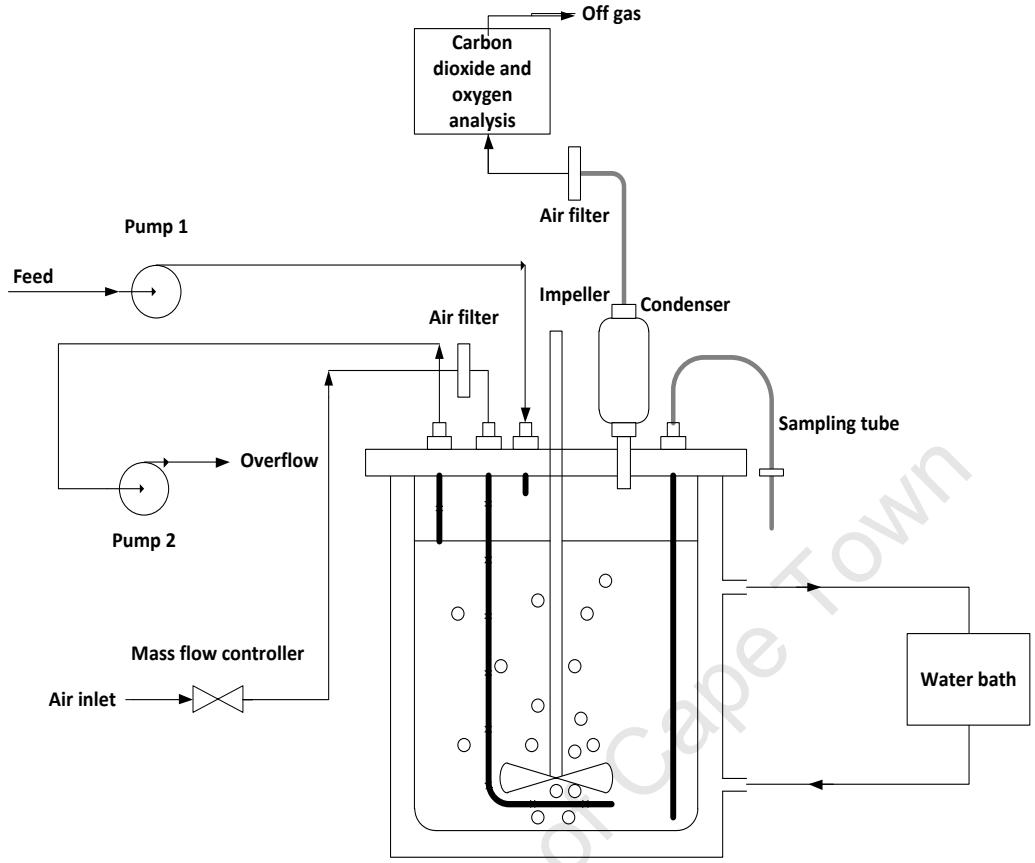

Figure 3-2 : Experimental configuration for planktonic experiments (Adapted from Ojumu *et al.*, 2009)

A 2 litre Applikon® reactor was connected to a Grant constant temperature water bath that circulates heated water through the reactor jackets to keep the system at the desired temperature of 37^{o}C. During experiments, flowrates of the feed into the reactor were variable and were used to establish the different dilution rates. Feed and effluent flow rates were controlled using a Masterflex® console pump drive. The feed was pumped using L/S™ 7013/20 standard pump heads via L/S™ 13 Norprene® food tubing and the effluent pumped out of the reactor using L/S™ 7014/20 standard pump heads via L/S™ 14 Norprene® food tubing. At the effluent port, metal tubing was inserted into the reactor and was adjusted to the same level as the 1 litre working volume. The outlet flow rate was set to pump out any overflow from the reactor at a faster rate to the feed thereby maintaining a constant volume of 1 litre within the reactor. This ensured there was no accumulation of the reactor medium in the system. Complete mixing and gas dispersion in the reactor was achieved through agitation, using a pitched 45^{o} four blade turbine impeller connected to an Applikon P100 (ADI 1032) stirrer controller rotating at 500 rpm. Dry compressed air was supplied

to the reactor at 1 bar by a Denco SN0.75 gas compressor and sparged into the bottom of the vessel underneath the impeller. Brooks model 5850S mass flow controllers and a Brooks model 0154 microprocessor control monitored gas flow rates entering the reactor at 30 $L.hr^{-1}$. Air leaving the reactor was passed through a reflux condenser, which contained ethylene glycol coming from an mrc BL-30 low temperature bath operating at 2°C. This cooled and dried the air before it entered an ABB EL3020 off-gas analyser where carbon dioxide concentrations were logged onto a computer. All air entering and leaving the reactor was filtered through 0.2 µm vent filters as the system was required to run as aseptically as possible.

3.2.2 Attachment experiments

In the reactor configuration used for attachment experiments, a 200 mL glass vessel packed with 123 g of ceramic saddles (solid substrate) was attached to a 2 litre Applikon® reactor in a closed loop. Solution from the Applikon® reactor was then pumped out at a fixed flow rate of 8.6 $Lday^{-1}$ (the maximum flowrate that the Masterflex® console pump drive could achieve) using L/S™ 7013/20 standard pump heads via L/S™ 13 Norprene® food tubing which entered the PBR from the bottom to the top. L/S™ 7014/20 standard pump heads were used to pump out the overflow from the PBR via L/S™ 14 Norprene® food tubing. The PBR was coiled with tubing connected to a Grant constant temperature water bath that circulated heated water to keep the system in the PBR at the desired temperature of 37°C.

Figure 3-3 gives an illustration of the reactor configuration used for attachment experiments. All conditions within the Applikon® reactor were identical to those described for planktonic experiments in section 3.2.1. Figure 3-4 shows the PBR dimensions and Table 3-1 gives detailed information of the design of the PBR. It was designed to have a conical shape at the bottom to prevent the build up of solution and to ensure a smooth flow of the liquid medium through the ceramic saddles. All the ceramic saddles were completely submerged by the medium and the total volume occupied by the ceramic saddles and liquid medium was 180 mL (see Appendix C for detailed information).

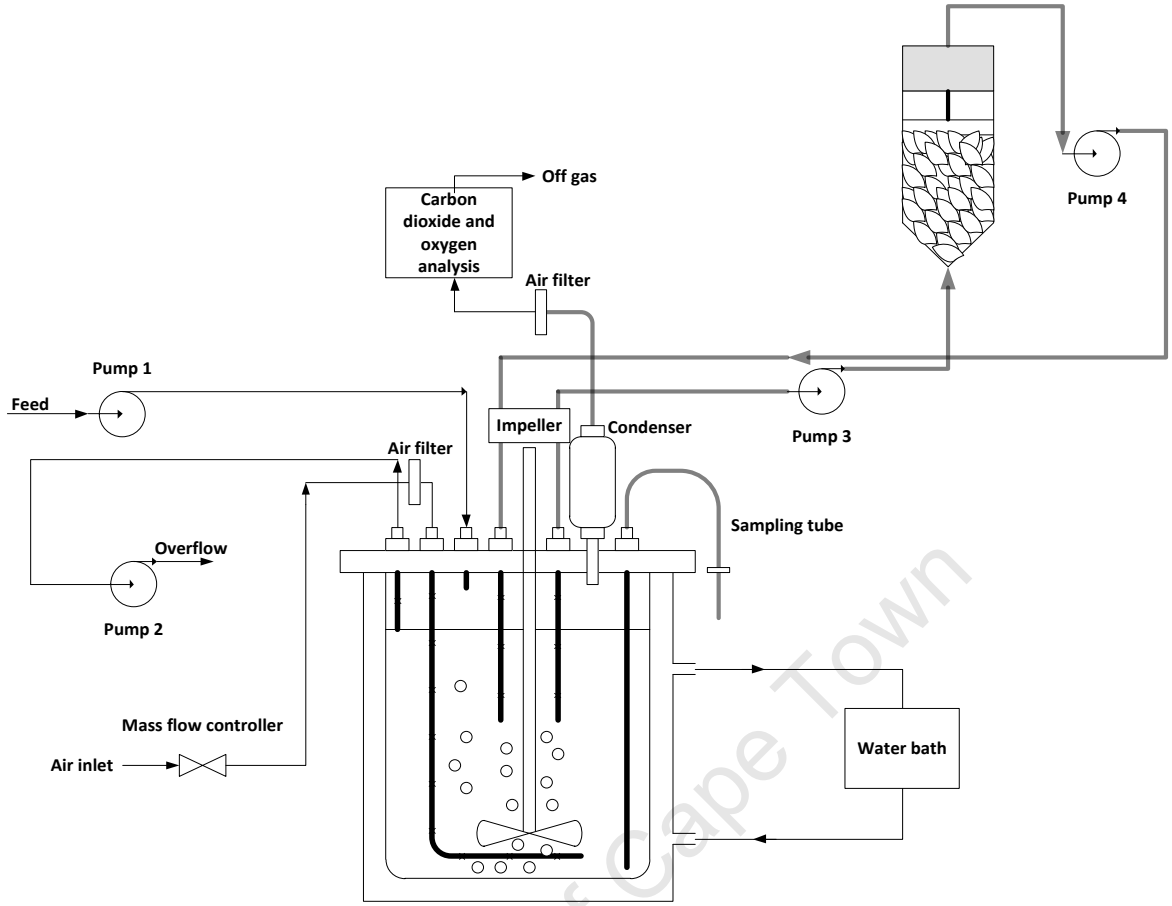

Figure 3-3: Experimental configuration for attachment and sessile experiments (Ojumu *et al*., 2009)

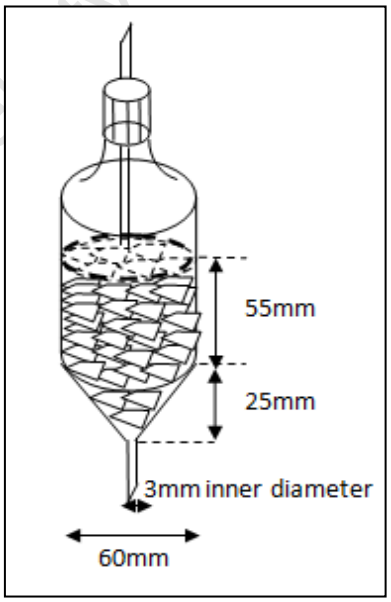

Figure 3-4: PBR configuration

Table 3-1: PBR specifications

Volume occupied by ceramics + voidage	180	cm^3
Volume occupied by ceramics	50.0	cm^3
Volume of void space	130	cm^3
Mass of ceramic saddles	123	g
Size of each ceramic saddle	12.0	mm
Specific surface area of ceramic saddle (AceChemPack)	647	m^2/m^3
Total surface area of ceramics for attachment of cells	0.117	m^2

3.2.3 Sessile experiments

The reactor configuration used during sessile experiments was identical to the configuration shown on Figure 3-3. Three experiments in total were conducted when investigating the sessile population. Two of these experiments were conducted using an identical set up as described in section 3.2.2. In the third experiment however, tubing with a bigger diameter was used to pump out a larger volume of the Applikon® reactor medium to the packed bed vessel and back to the Applikon® reactor. In this case the Applikon® reactor medium at a rate of 125 $L.day^{-1}$ was pumped using L/S™ 7016/20 standard pump heads via L/S™ 16 Norprene® food tubing which entered the packed bed vessel from the bottom to the top. L/S™ 7018/20 standard pump heads were then used to pump out the overflow from the glass vessel via L/S™ 18 Norprene® food tubing. Figure 3-5 and Figure 3-6 show pictures of the ceramic saddles, the PBR and general experimental set-up of the equipment used in the laboratory for this study.

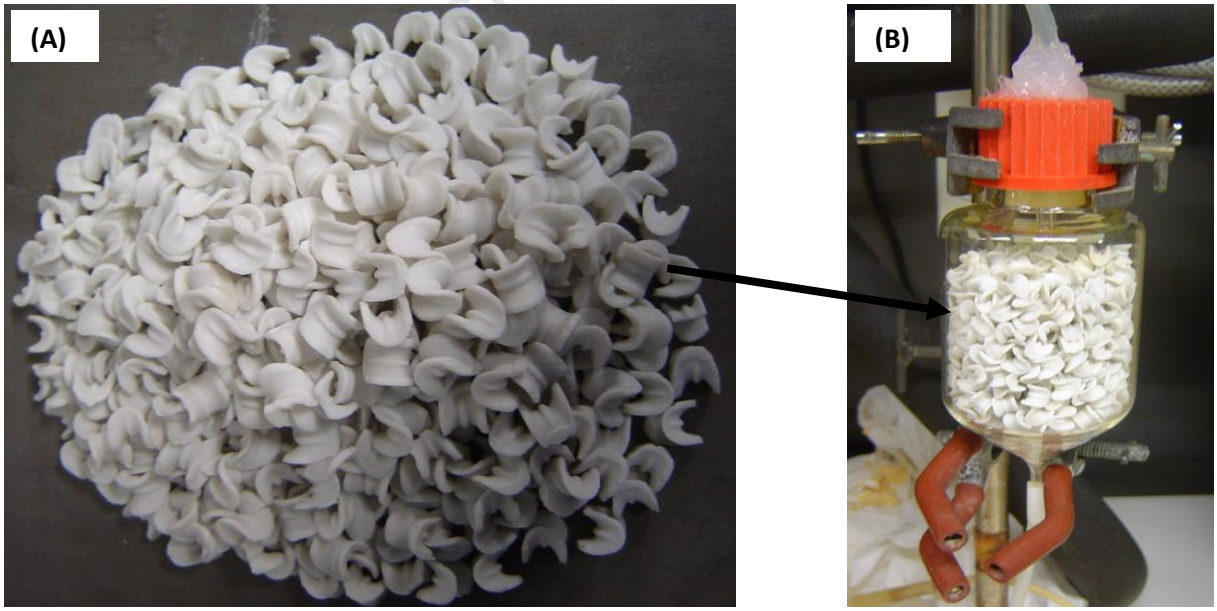

Figure 3-5: Pictures showing (A) the ceramic saddles used as the solid substrate and (B) the PBR- a glass column packed with ceramic saddles and used during attachment and sessile experiments.

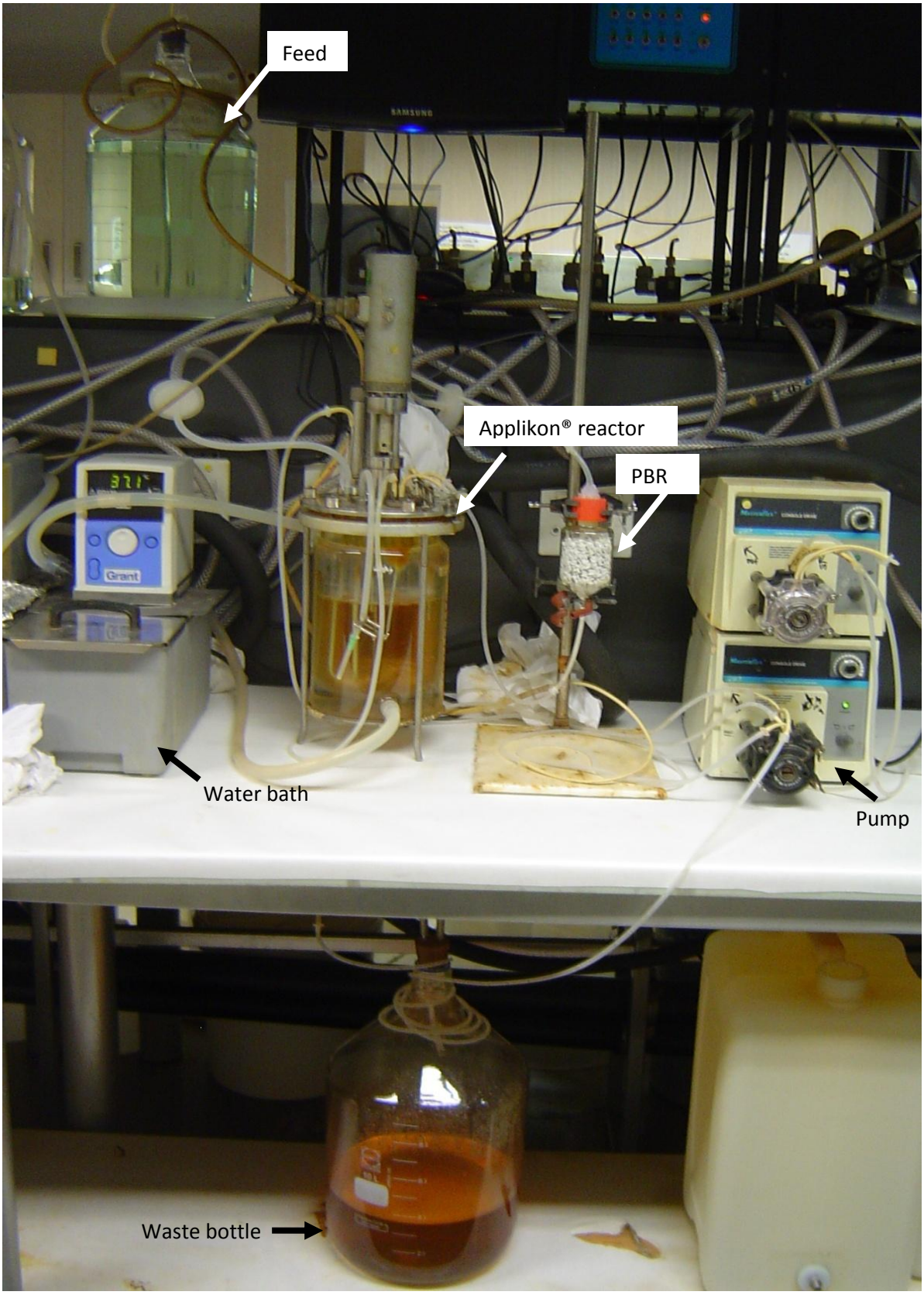

Figure 3-6: Picture showing the experimental set-up in the laboratory. The PBR was only introduced to the system as a closed loop for attachment and sessile experiments.

3.3 Microbial culture (Origin and maintenance) and growth medium

3.3.1 Microbial culture

Pure *Leptospirillum ferriphilum* of type strain ATCC 49881, originally isolated from a culture in the Centre for Bioprocess Engineering Research (CeBER) laboratory at the University of Cape Town, was used in all experiments. A stock culture was maintained in a CSTR using feed with a 5 gL^{-1} ferrous iron concentration at a 55 hr residence time. All solutions used in experiments were sterilised and the entire system kept as sterile as possible. This was done by autoclaving and filtering all solution meant to feed the microorganisms (see section 3.3.2 for more details). The morphology of the microorganisms in the reactor was checked daily under the microscope to ensure no contamination (*Leptospirillum ferriphilum* is generally spiral or comma shaped). Visual checks for any fungal infections were also investigated. DNA extraction by quantitative real time PCR (qPCR) of a sample from the reactor also confirmed the population of microorganisms in the reactor as purely *Leptospirillum ferriphilum*.

3.3.2 Growth Medium

Ten litre batches of growth medium with a final concentration of 5 gL^{-1} ferrous iron were prepared continuously to feed all reactors. Each ten litre growth medium solution consisted of 8.8 litres of distilled water, 0.2 litres of a 50x autotrophic basal salt (ABS) solution, 10 mL trace element solution and 1 litre of a 50 gL^{-1} ferrous sulphate solution. The pH was maintained at 1.1 using sulphuric acid (H_2SO_4). The solution (excluding the ferrous sulphate solution) was first autoclaved before adding sterile ferrous sulphate solution which was sterilised by filtration. Ferrous sulphate solution was rather filtered because it formed precipitate when autoclaved.

3.3.2.1 Autotrophic basal salt solution

A 50x concentrate of autotrophic basal salt (ABS) solution was made using 7.5 gL^{-1} $(NH_4)_2SO_4$, 7.5 gL^{-1} $Na_2SO_4.10H_2O$, 2.5 gL^{-1} KCl, 25 gL^{-1} $MgSO_4.7H_2O$, 2.5 gL^{-1} KH_2PO_4 and 0.7 gL^{-1} $Ca(NO_3)_2.4H_2O$. The pH was adjusted to 1.1 using concentrated sulphuric acid (H_2SO_4), thereafter, the solution was autoclaved.

3.3.2.2 Trace element solution

One mL L^{-1} of trace element solution was required for every 10 L batch of feed and was added to the diluted autotrophic basal salt solution before autoclaving. It was prepared by dissolving the following salts in 800 mL of acidified distilled water (pH 1.1 using H_2SO_4); 10 gL^{-1} $ZnSO_4.7H_2O$, 1 gL^{-1} $CuSO_4.5H_2O$, 0.64 gL^{-1} $MnSOH_2O$, 1 gL^{-1} $CoSO_4.7H_2O$, 0.5 gL^{-1} $CrK(SO_4)_2.12H_2O$, 0.6 gL^{-1} H_3BO_3, 0.5 gL^{-}

[1] $Na_2MoO_4.2H_2O$, 1 gL^{-1} $NiSO_4.6H_2O$, 1 gL^{-1} $Na_2SeO_4.10H_2O$ and 0.1 gL^{-1} $Na_2WO_4.2H_2O$. Salts were added in the order above and each salt had to dissolve before adding the next. pH was constantly checked and adjusted using H_2SO_4 to ensure it remained at 1.1. Once all the salts were dissolved, the volume of the mixture was made up to 1litre with distilled water and the pH adjusted. The solution was also autoclaved and then chilled in a refrigerator at 4℃ when not in use.

3.3.2.3 Ferrous sulphate solution

Fifty gL^{-1} of ferrous sulphate solution was made by dissolving 248.92 g of ferrous sulphate heptahydrate ($FeSO_4.7H_2O$) in about 700 mL of distilled water. The pH was adjusted to 1.1 using H_2SO_4. Once fully dissolved, the solution was topped up to 1 litre using deionised water and the pH adjusted to 1.1. The solution was then filtered (sterilised) twice using 0.22 µm filter paper in a fume cupboard before its addition to the sterilized ABS solution. The filter unit used to sterilize the solution had to be autoclaved first before use to avoid contamination as much as possible.

3.4 Experimental procedures

To start up the Applikon® reactor (inoculation), 500 mL of stock culture was added to a 2 litre Applikon® reactor containing 500 mL of fresh growth medium. This was done in a fume cupboard to prevent any possibility of contamination. The Applikon® reactor was then set up to the configurations of the experiments to be performed as described in section 3.2 in batch mode, and the redox potential (relative to Ag/AgCl) was monitored regularly until it reached 600 mV. The Applikon® reactor was then switched from batch to continuous mode and the flow rates adjusted according to the desired dilution rate. This depended on the experiment being conducted.

3.4.1 Planktonic experiments

Once in continuous mode, the activity of planktonic *Leptospirillum ferriphilum* was investigated at various dilution rates ranging between 0.0183 hr^{-1} - 0.250 hr^{-1} (55 hr - 4hr residence times) which corresponds to the Masterflex® console pump drive set points 1.16 - 6.68 respectively. For each dilution rate steady state was assumed after three residence times and an additional 12 hr. Data was then captured for analysis. Three samples at different time intervals (every hour) were collected from the Applikon® reactor and tested for ferrous and total iron concentrations. The redox potential, pH, CO_2 concentrations, dry weight analysis and cell counts were also measured.

The maximum growth rate of *Leptospirillum ferriphilum* was also required for data analysis and was determined by switching the Applikon® reactor from continuous mode back to batch mode. 500 mL of the active *Leptospirillum ferriphilum* culture was mixed with 500 mL of fresh growth medium and the redox potential (relative to Ag/AgCl) and cell concentration were monitored over a 10 hr period at 1 hr intervals.

3.4.2 Attachment experiments

All experiments were conducted at a feed dilution rate of 0.0313 hr^{-1} (32 hr residence time) to the Applikon® reactor, which corresponds to the set point 1.47 on the Masterflex® console pump drive. Once the Applikon® reactor was at steady state (ferrous iron concentration remained unchanged), the PBR was attached and the active culture pumped through it at a flowrate of 8.6 $Lday^{-1}$. The recycle ratio (flow rate of culture out of the CSTR through the PBR: the flow rate of the fresh feed into the CSTR) during the attachment experiments was thus 11.5. Attachment experiments were conducted for different time intervals each investigated in triplicates. The time intervals investigated were for 2, 4, 6, 8, 10 and 12 days respectively. The redox potential, pH, CO_2 concentrations, and cell counts were also measured for data analysis. At the end of each experiment, the ceramic saddles

were unloaded and the cells detached from the surface using the detachment protocol (Appendix B) for data analysis.

3.4.3 Sessile experiments

Following the attachment of *Leptospirillum ferriphilum* microorganisms to the surface of the ceramic saddles over a 12 day period at dilution rate 0.0313 hr^{-1} (32 hr residence time), the reactor dilution rate was switched to either 0.200 hr^{-1} (5 hr residence time) or 0.250 hr^{-1} (4 hr residence times) independently and the activity of the sessile microorganisms investigated. Dilution rates 0.0313 hr^{-1}, 0.200 hr^{-1} and 0.250 hr^{-1} corresponded to pump set points 1.47, 5.29 and 6.64 respectively. At 5 hr and 4 hr residence times the recycle ratios reduced to 1.79 and 1.43 respectively.

A third experiment, a repeat at 5 hr residence time was therefore conducted at a higher recycle ratio of 21 (achieved using a faster pump). For all experiments, the Applikon®reactor medium was analysed daily up to a point where steady state was achieved. Steady state was achieved when the ferrous iron concentration and the off gas data remained unchanged. At steady state, three samples at different time intervals (every hour) were collected and tested for ferrous and total iron concentrations. Redox potential, pH and CO_2 concentrations was also measured. The ceramic saddles were also unloaded and cells detached using the detachment protocol for data analysis of the attached cells.

3.5 Analytical methods

All the analytical methods used for the purpose of generating data are briefly described in this section. A more detailed description of some of these methods can be found in Appendix B.

3.5.1 pH

All pH measurements were carried out using a Metrohm®, 713 pH meter. The pH meter was calibrated with commercial standards at pH 1 and pH 4 every day.

3.5.2 Redox potential

A Metrohm®, 827 pH meter with a platinum ring electrode and 3M KCL + AgCL electrolyte was used for all redox potential measurements. The redox meter was calibrated daily against a standard solution (Crisson at 468mV).

3.5.3 Ferrous iron assay

Ferrous iron concentrations were determined colorimetrically using the 1-10 phenanthroline line method (Komadel and Stucki, 1988). This was done using 1-10 phenanthroline, ammonium acetate buffer solution and distilled water for dilution purposes. An orange red complex forms when ferrous ions reacts with 1-10 phenanthroline. Three molecules of 1-10 phenanthroline chelates with one ferrous ion and forms a complex which is magenta in colour and has an absorbance maximum of between 400 and 600 nm (Naik, 2010).

A standard curve was first determined for calibration purposes (relating absorbance to the ferrous iron concentration) of the Unicam®, Heλios, α.v4.04 spectrophotometer at a wavelength of 510nm. This was done by making standard solution of 10, 20, 30, 40 and 50 mgL^{-1} of ferrous iron solution. Two mL of 1-10 phenanthroline and 2 mL of ammonium acetate buffer solution was added to 5 separate test tubes. For this study, each sample was first diluted using a dilution factor of x100 (meaning 10 µL of each sample was added to 990 µL of distilled water used for dilution purposes to makes up 1 mL) before addition of the samples to respective test tubes. The solutions were then thoroughly vortexed. A **standard curve** relating the absorbance to mass concentrations was then plotted using data obtained from the spectrophotometer with respect to the different ferrous iron concentrations tested.

Ferrous iron concentrations of a sample from the reactor was tested by adding 2 mL of 1-10 phenanthroline to 2 mL of ammonium acetate buffer solution in a test tube. Using a x100 dilution

factor the sample was added to the test tube and thoroughly vortexed and the absorbance determined from the spectrophotometer. The concentration of the sample was determined using the **standard curve** (See Appendix B).

3.5.4 AAS

A Varian Spectra AAS30 Atomic absorption spectrophotometer incorporating Spectra AA100/200 version 5.1 software was used to measure total iron concentrations in the feed and samples representing the medium in the reactor.

3.5.5 Microbial cell counts

Cell counting was done using a standard Hawksley Helber counting chamber and phase contrast optical Olympus® CX40 microscope. At a magnification of 15x100 the counting chamber was seen to have 4 big squares with grids. Each big square was further divided into 4 squares each of which were subdivided into 16 tiny squares with an area of $\frac{1}{400} mm^2$ and a depth of 0.02 mm. The volume of one of the tiny square boxes was $5x10^{8}$mL. During cell counting 4 of the small squares each with 16 tiny square boxes were randomly selected and any cells observed were counted. If the cell numbers were too high, the sample was diluted further (the dilution factor was considered when calculating actual cell numbers). Equation 3-1 was used when calculating cell concentrations.

$$[cells] = Number\ of\ cells\ counted \times 312500\ \times Dilution\ factor \quad \text{Equation 3-1}$$

3.5.6 Dry weight analysis

Dry weight analysis was done by centrifuging 900 mL of an active population of *Leptospirillum ferriphilum* (collected from the overflow of the reactor system) at 9184 g (7000 rpm). The centrifuge used was a Seval RCSB plus using an SLC-4000 rotor. A microscopic cell count was performed first on a sample of the medium. Centrifuging was for 45 mins thereafter, the supernatant was discarded and cells resuspended in distilled water and recentrifuged. This procedure was repeated 3 times and the sample left to dry in an 80^{o}C oven until there was no change in mass (adapted from Naik, 2010).

3.5.7 Solid support

A detachment protocol (Bryan *et al.,* 2011) was used to investigate attachment of cells on the surface of the ceramic saddles by determining the cell numbers on the solid support. This included 4 washing steps using acidified detachment media and 3 washing steps with 0.4% (v/v) Tween 20. This process enabled microbial cells to be counted for 3 separate liquid phases: the interstitial phase, the

weakly attached phase, and the strongly attached phase detached with Tween20. A detailed description of the detachment protocol can be found in Appendix B.

3.5.8 Off-gas measurements

An ABB EL3020 off-gas analyser was used to measure carbon dioxide (CO_2) concentrations from a reference line (the reference line contains air and represents the air flowing into the reactor) and off-gas from the CSTR. All data collected from the gas analyzer was logged onto a computer.

With a given CO_2 concentration, a mass balance (see equation 3-2) around the reactor system was used to determine the uptake rates of CO_2 in the system.

$$-r_j = \frac{C_{j,0}\tilde{v}_{in} - C_j\tilde{v}_{out}}{V_R} \qquad \text{Equation 3-2}$$

where $-r_j$ is the uptake rate of species j; $C_{j,0}$ is the inlet concentration of species j; C_j is the outlet concentration of species j; $\tilde{v}_{in}$ is the volumetric flowrate of species j into the reactor; $\tilde{v}_{out}$ is the volumetric flowrate of species j out of reactor and V_R is the volume of the reactor.

The volumetric flowrate of the air entering the reactor was not equivalent to the volumetric flowrate of gas leaving the reactor and could not be assumed to be equal as this led to a systematic error in the analysis of the data (Ojumu, 2008). The off gas flowrate was therefore determined using a nitrogen balance (Equation 3-3) as the flowrate of nitrogen into and out of the reactor remained unchanged. The CO_2 concentrations measured from the gas analyzer were dimensionless, measured in volume per volume (Ojumu, 2008).

$$\tilde{v}_{gas.out} = \tilde{v}_{gas.in}\frac{1-[O_2]_{in}-[CO_2]_{in}}{1-[O_2]_{out}-[CO_2]_{out}} \qquad \text{Equation 3-3}$$

In general, CO_2 and O_2 uptake rates could therefore be determined using the relationships shown by Equations 3-4 and 3-5 which are derived in detail in Appendix B.

$$-r_{O_2} = \frac{60\times\tilde{v}_{in}}{24.5\times V_R}\left\{[O_2]_{in} - [O_2]_{out}\times\left[\frac{1-[O_2]_{in}-[CO_2]_{in}}{1-[O_2]_{out}-[CO_2]_{out}}\right]\right\} \qquad \text{Equation 3-4}$$

$$-r_{CO_2} = \frac{60\times\tilde{v}_{in}}{24.5\times V_R}\left\{[CO_2]_{in} - [CO_2]_{out}\times\left[\frac{1-[O_2]_{in}-[CO_2]_{in}}{1-[O_2]_{out}-[CO_2]_{out}}\right]\right\} \qquad \text{Equation 3-5}$$

For this study, the oxygen concentrations could not be determined using the gas analyzer due to technical issues. The inlet O_2 concentration was therefore assumed to be 21% and the outlet concentration was determined using the degree of reduction balance (Equation 3-7). This is explained in more detail in section 3.6.

3.6 Data analysis

3.6.1 Ferrous iron oxidation rates

The ferrous iron oxidation rate of a culture growing in a continuous stirred tank reactor (CSTR) can be determined either by ferrous iron concentration measurements (Equation 3-6) based on a mass balance around the reactor, or through respirometry using the degree of reduction balance (Equation 3-7):

$$-r_{Fe^{2+}} = D \cdot ([Fe^{2+}]_{inlet} - [Fe^{2+}]_{outlet}) \quad \text{Equation 3-6}$$

$$-r_{Fe^{2+}} = -4r_{O_2} - 4.2r_{CO_2} \quad \text{Equation 3-7}$$

Studies by Breed *et al*. (1999), Naik (2010) and Ojumu (2008) have shown the validity of both methods when calculating ferrous iron oxidation rates via Equation 3-6 and 3-7; therefore any one of the methods can be used to determine ferrous iron oxidation rates.

3.6.1.1 Ferrous iron oxidation rate by mass balance

Ferrous iron concentrations can be determined using atomic absorption spectroscopy (AAS), spectrophotometry or by reduction-oxidation potential. In this study the inlet feed ferrous iron concentration used in all experiments was approximately 5 g/l and was determined by AAS (Equation 3-8). AAS was found to be more accurate than spectrophotometry when measuring samples with high ferrous iron concentrations.

$$[Fe^{2+}]_{total} = [Fe^{2+}]_{inlet} \quad \text{measured by } \textbf{AAS} \quad \text{Equation 3-8}$$

Perfect mixing was assumed in a CSTR therefore the reactor outlet ferrous iron concentration was assumed to be equivalent to the ferrous iron concentration in the reactor (Equation 3-9). In this case, ferrous iron oxidation rates were measured using spectrophotometry.

$$[Fe^{2+}]_{reactor} = [Fe^{2+}]_{outlet} \quad \text{measured by } \textbf{spectrophotometry} \quad \text{Equation 3-9}$$

The ferrous iron oxidation rate could also be determined by measuring the redox potential of the reactor sample (Equation 3-10). The ratio is a measure of the ferric to ferrous iron concentration which could be calculated relative to a standard curve plotted from a relationship to the Nernst equation (Naik, 2010).

$[Fe^{2+}]_{reactor} = [Fe^{2+}]_{outlet} = \frac{[\mathrm{Fe_{total}}]}{1+\mathrm{Ratio}}$ measured by **reduction-oxidation potential** Equation 3-10

Once $[Fe^{2+}]_{inlet}$ and $[Fe^{2+}]_{outlet}$ were determined, the rate of ferrous iron oxidation could be calculated using Equation 3-8. For this study, $[Fe^{2+}]_{inlet}$ was measured using AAS and $[Fe^{2+}]_{outlet}$ was measured using spectrophotometry.

3.6.1.2 Ferrous iron oxidation rate measurements by respirometry

The ferrous iron oxidation rate could also be calculated using the carbon dioxide and oxygen uptake rates. Rates were calculated using oxygen and carbon dioxide concentrations captured using a gas analyzer (Equations 3-4 and 3-5) and applied to the degree of reduction balance (Equation 3-7). Equations 3-4 and 3-5 were derived from a mass balance (details are shown in Appendix C).

3.6.2 Biomass Calculations

3.6.2.1 Method 1: Dry mass measurements

Biomass was determined using the dry mass of a 900 mL culture collected from the reactor overflow. The dry mass per cells was first determined using the relationship shown by Equation 3-11. Cell counting under a microscope was then used to determine the cell concentration [cells.mL^{-1}], after which the 900 mL of culture was centrifuged and the biomass dried in an 80^{o}C oven before determining the dry mass [mg.L^{-1}].

$$Dry\ mass\ per\ cell = \frac{dry\ mass\ (mg/L)}{cell\ concentration\ (cells/mL)}$$ Equation 3-11

Dry biomass is typically 50% carbon by weight (adapted from Naik (2010), Caracklis and Marshall (1990)) hence the carbon equivalent of each cell was calculated using Equation 3-12;

$\text{Cell}_{\text{carbon equivalent}}$ = 0.5 x Dry mass per cell = g_{carbon} per cell Equation 3-12

3.6.2.2 Method 2: Gas analysis

Biomass could also be determined using off gas data to calculate the rate of carbon dioxide uptake via Equation 3-5 thereafter at steady state conditions in the reactor, Equation 3-13 can be applied. It is important to note, however, that this only applies if it is assumed that all CO_2 is converted to biomass at steady state. Also attachment should be assumed negligible in the CSTR therefore there is no accumulation of biomass.

$$C_x = \frac{-r_{CO_2}}{D} \qquad D = \mu \; at \; steady \; state$$ Equation 3-13

3.6.3 Specific ferrous iron oxidation rate, growth yield and maintenance coefficient

Once the rate of ferrous iron oxidation and biomass was determined, the specific ferrous iron oxidation rate was calculated using the relationship shown by Equation 3-14:

$$-q_{Fe^{2+}} = \frac{-r_{Fe^{2+}}}{C_x}$$ Equation 3-14

The specific ferrous iron oxidation rate can then used to determine the maximum yield and the maintenance by linearizing the Pirt equation (Equation 3-15).

$$-q_{Fe^{2+}} = \frac{\mu}{Y_{Fe^{2+}}^{max}} + m_{Fe^{2+}}$$ Equation 3-15

3.6.4 Maximum growth rate

For this study the maximum growth rate was determined manually by monitoring cell concentrations of *Leptospirillum ferriphilum* in a batch system over a period of time and plotting a growth curve. The natural logarithm of the cell concentration was plotted against time to determine the growth curve and the relationship shown by Equation 3-16 was used to determine the maximum growth curve.

$$\mu_{max} = \frac{LnX_t - LnX_0}{\Delta t}$$ Equation 3-16

3.6.5 Rate of dissolved carbon dioxide in the liquid medium

To account for carbon dioxide that dissolves into the reactor medium Henry's law was applied:

$$P_{CO_2} = x_{CO_2} \times P_{Tot}$$ Equation 3-17

$$[CO_{2_{aq}}] = P_{CO_2} \times K$$ Equation 3-18

$$r_{CO_{2_{dissolved}}} = \left[CO_{2_{aq}}\right] \times Residence \; time$$ Equation 3-19

All sample calculations with detailed information can be found in Appendix C.

4 Results and discussion (I)

4.1 AIM AND APPROACH

The reviewed literature has confirmed that microbial activity significantly influences bioleaching kinetics with ferrous iron oxidation rates stepping up to 10^5-10^6 times faster compared to chemical oxidation at low temperatures (Boon and Heijnen 1998; Jones and Kelly 1983; Ozkaya et al. 2007; Rawlings, 2002). In the past, bio-oxidation kinetics were primarily investigated in agitated tank systems (dominated by planktonic microorganisms) with the intention being to isolate microbial oxidation kinetics from those of the mineral. Heap bioleaching systems differ from agitated tank systems in that they are dominated by sessile microorganisms; therefore bio-oxidation kinetics from agitated tank systems may not be truly representative for modelling those in bioheap systems. The main aim of this study was to attempt to develop a strategy which allows the determination of sessile microbial kinetics as a function of population size, availability of ferrous iron and culture conditions.

This study continues from the work of Maas and Paxton (2007) and Naik (2010), and focuses on finding a strategy that allows the determination of the kinetics of the sessile population independent of the planktonic population. The approach taken was to firstly investigate the microbial activity of a pure culture of planktonic *Leptospirillum ferriphilum*. Although the investigation of the microbial planktonic cultures in continuous systems at steady state has been covered extensively in literature (e.g. Boon *et al.*, 1998; Boon and Heijnen; Breed and Hansford, 1999; Dempers *et al.*, 2003; Jones and Kelly 1983; Naik, 2010; Nemati and Web, 1996; Ojumu, 2008; Sundkvist *et al.*, 2007; van Scherpenzeel *et al.*, 1998), it was essential to generate data specific to the reactor conditions in the laboratory as a benchmark for comparison with the activity influenced by the sessile microbial population. The main objective for investigating the activity of planktonic *Leptospirillum ferriphilum* however; was to determine the critical dilution rate of the system where there is washout. This was necessary as all experiments in this study, in investigating the activity of the sessile microbial population, were required ideally to be operated at washout. Operating at washout ensured that the planktonic cells were eliminated from the system.

All experimental work in this study was conducted under sterile conditions. This was to avoid the possibility of any contamination of the culture by other ferrous iron oxidizing microorganisms as this would interfere with the kinetic data. The aim was to investigate kinetics relative to a pure culture of only one type of ferrous iron oxidizing microorganism from a fundamental point of view. A number

of studies from literature when investigating microbial kinetics have been investigated in non-sterile conditions and there has been no indication of pure culture kinetic studies with *Leptospirillum ferriphilum*. Naik's (2010) experimental work, which this study follows, was carried out in non-sterile condition but the medium was frequently checked for contaminants like fungi. In the event there was contamination, the experiment was stopped and a fresh culture was used to continue the experiment. Universal primers were used to amplify a 16s rRNA gene which was sequenced to confirm homology of the bacterial culture used which was found to have a >98% sequence homology to *Leptospirillum ferriphilum*. Although through this approach Naik (2010) attempted to keep the culture free from contamination by other microorganisms, it was possible that the culture may have still been contaminated over time. It was therefore worthwhile to compare the data obtained from the two studies to note if there were any significant differences in kinetic data based on sterility.

This chapter begins by presenting the experimental results obtained from investigating the activity of planktonic *Leptospirillum ferriphilum* in a continuous stirred tank reactor and later compares the kinetic data determined from this under sterile conditions with data from Naik's (2010) study obtained under non-sterile conditions. The following chapter 5 will then proceed to present the results from the attachment experiments and the investigation of the sessile population.

4.2 Planktonic experiments

4.2.1 Introduction

The microbial oxidation rates of planktonic *Leptospirillum ferriphilum* were investigated in a continuous stirred tank reactor (CSTR) with a working volume of 1 litre under sterile conditions. The reactor conditions are indicated on Table 4-1. Ferrous iron in the system at 5 gL^{-1} was the growth limiting substrate used as it was completely oxidized by the culture and was controlled by varying the feed flowrates. The flowrate, dilution rate and residence time are related by the relationship shown on equation 4-1:

$$\frac{Flowrate}{Volume} = Dilution\ rate\ (hr^{-1}) = \frac{1}{Residence\ time\ (hr)} \qquad \text{Equation 4-1}$$

Following the work of du Preez (1995), Pirt (1975) and Wang *et al.* (1979), when the physiological conditions in the reactor as well as the cell and product concentration were constant the system was assumed to be at steady state. The redox potential, pH and cell concentration were determined at

these steady state conditions. Figure 4-1 illustration A, shows the Monod model which is the theoretically expected behaviour of continuous cultures.

Table 4-1: CSTR reactor conditions for planktonic experiments

Operating temperature	37^{o}C
Air flowrate	30 L.hr^{-1}
Agitation rate	500 rpm
Ferrous iron inlet feed concentration	5 gL^{-1}
Inlet feed pH	1.1
Reactor pH	1.3
Steady state	3 residence times + 12 hr
Residence times varied (dilution rates varied) at steady state conditions	55 hr (0.0182 hr^{-1}), 40 hr (0.0250 hr^{-1}), 32 hr (0.0313 hr^{-1}), 24 hr (0.0417 hr^{-1}), 16 hr (0.0625 hr^{-1}), 15 hr (0.067 hr^{-1}), 14 hr (0.0714 hr^{-1}), 13 hr (0.0769 hr^{-1}), 12 hr (0.0833 hr^{-1}), 11 hr (0.090 hr^{-1}), 10 hr (0.100 hr^{-1}), 9 hr (0.111 hr^{-1}), 8 hr (0.125 hr^{-1}), 7 hr (0.143hr^{-1}), 6 hr (0.167hr^{-1}), 5 hr (0.200 hr^{-1}) and 4 hr (0.250 hr^{-1})

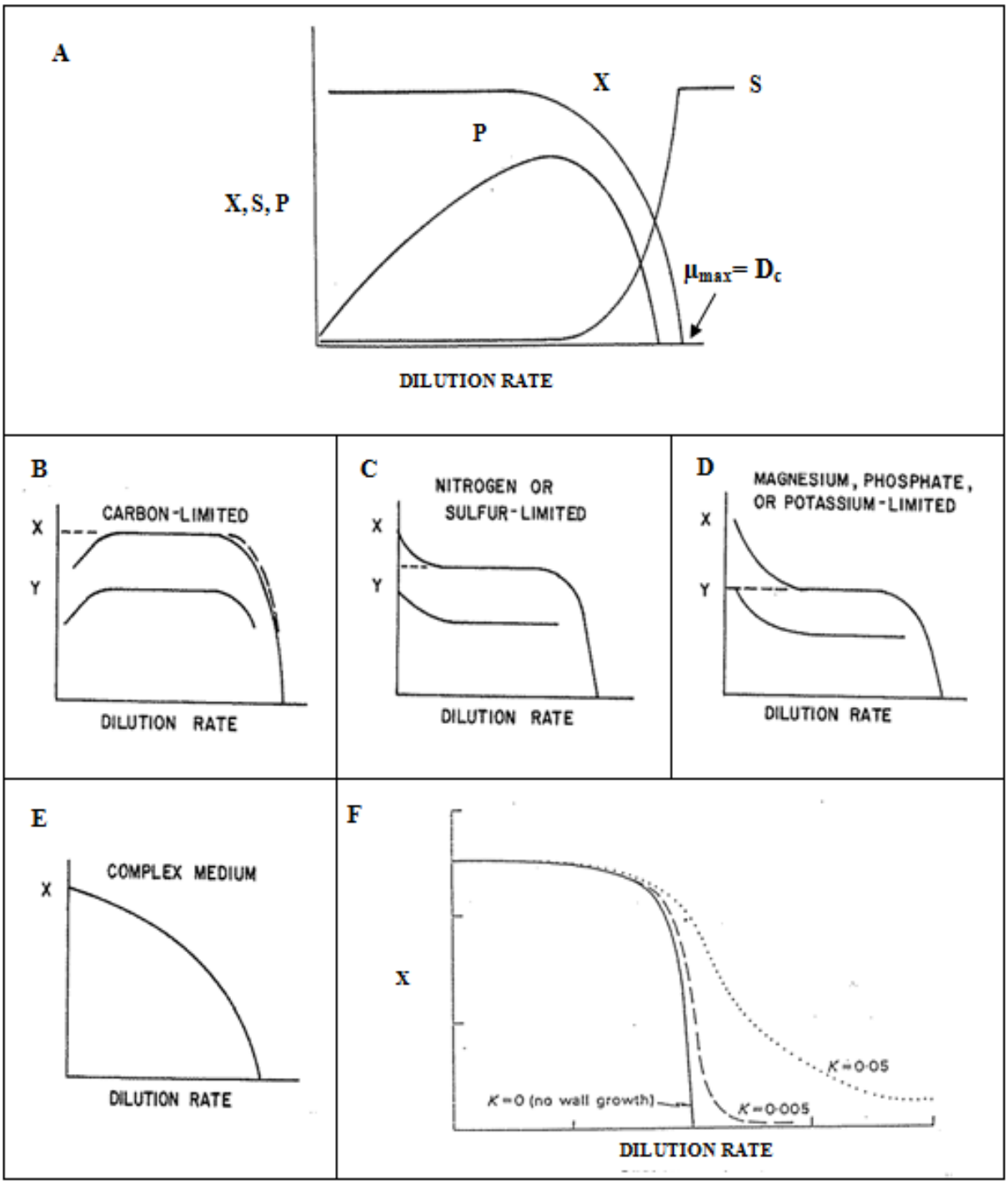

Figure 4-1: **A** - Theoretical continuous culture isotherms showing the relationship of cell concentration X, limiting nutrient concentration S (ferrous iron) and productivity P (Dilution rate x X) vs. the dilution rate. D_c is the critical dilution rate which in an ideal case equates to μ_{max} (adapted from Bailey and Ollis, 1977; Wang *et al.,* 1979). **B, C, D, E** and **F** are examples of non-ideal behaviour in a well mixed CSTR. **B** - Carbon limitations, **C** - nitrogen and sulphur limitations, **D** - potassium, magnesium or phosphate limitations, **E** - complex undefined media or trace element and oxygen limitations and **F** – wall growth. For illustrations **B-D**, dotted lines represent expected behaviour and in illustration **E**, dotted lines represent the deviation (du Preez, 1995; Pirt, 1975; Wang el al., 1979).

In reality, however there may be deviations from the Monod model possibly due to factors such as carbon limitations, nitrogen and sulphur limitations, potassium, magnesium or phosphate limitations, wall growth by cells and/or a complex undefined media (du Preez, 1995; Wang *et al.*, 1979). Figure 4-1 illustrations B-F, depict the expected trends for non-ideal culture behaviour in a CSTR. In ideal conditions, at steady state, the critical dilution rate (D_c) is equivalent to the maximum growth rate (μ_{max}) and wash out of microorganisms occurs at the critical dilution rate (D_c) because the microorganisms are unable to sustain themselves and their death rate exceeds the growth rate.

4.2.2 Culture behaviour in the continuous stirred tank reactor

Figure 4-2 presents experimental data showing the cell concentration of planktonic *Leptospirillum ferriphilum* and the redox potential in the CSTR at varying dilution rates.

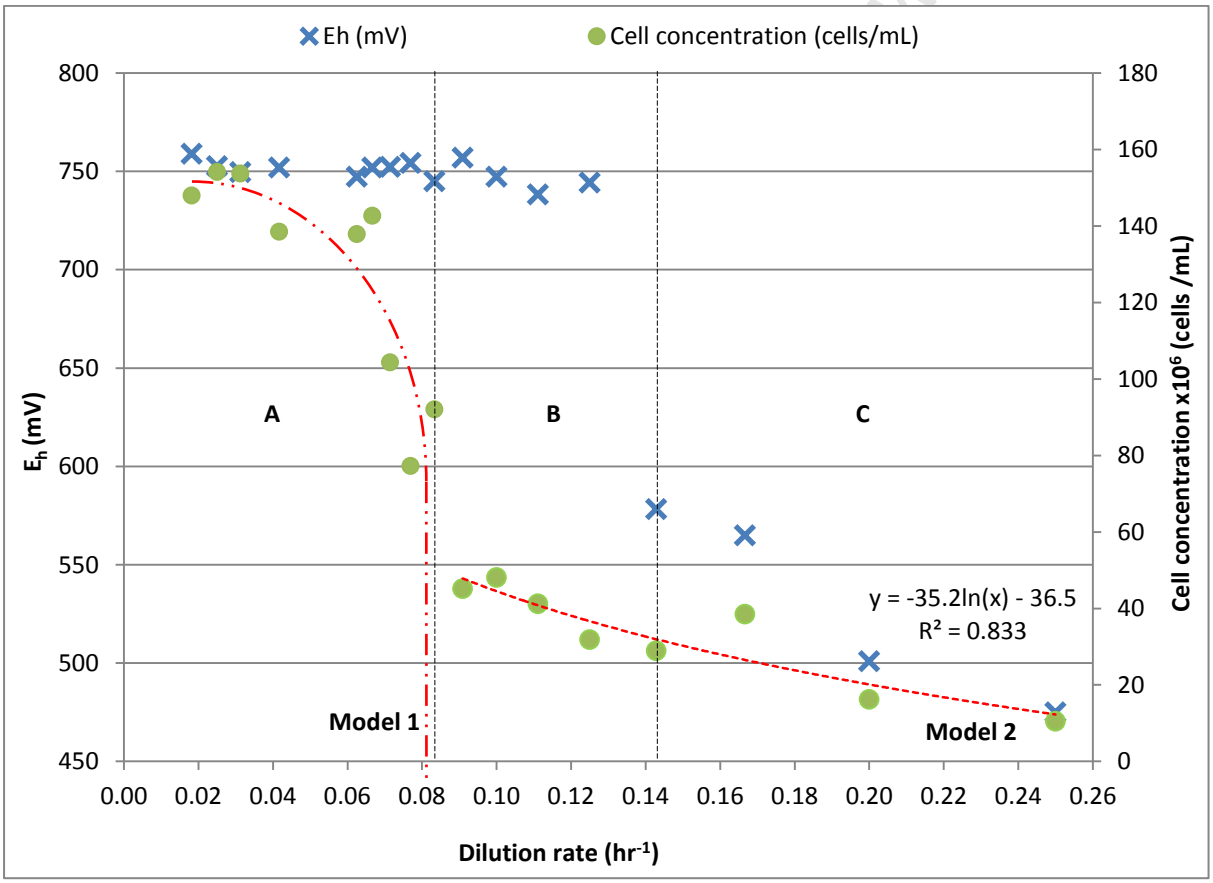

Figure 4-2: Redox potential (mV) and cell concentration vs. dilution rates (hr^{-1}). The figure is separated into three regions A, B and C for easier interpretation of data. Model 1 represents the trend of cell concentration vs. dilution rate from experimental data in region A which is then compared to the Monod model. In region B and C a trend in cell concentration of microorganisms eluted from the wall due to wall growth was observed and is represented by Model 2 which has a logarithmic relationship: cell concentration (cells/mL) = -35.2 Ln (dilution rate [hr^{-1}])-36.5.

The figure is split into three separate regions A, B and C (details of which are shown on Table 4-2) to simplify the interpretation of the data.

Table 4-2: Summary of results for regions A, B and C as observed from Figure 4-2

Region	Dilution rates (hr^{-1})	Residence times (hr)	Short description
A	0.0182 – 0.0833	55 – 12	-Consistent cell concentration between residence time 15-55 hr. -Drop in cell concentration between residence time 12-15 hr. - High and consistent redox potential.
B	0.0833 – 0.143	12 – 7	-Gradual drop in cell concentration. - High and consistent redox potential.
C	0.143– 0.250	7 – 4	-Gradual drop in cell concentration. -Gradual drop in the redox potential.

In region A, initially (dilution rates between 0.0183-0.0667 hr^{-1}) the cell concentration was consistent ranging between 143-154 x 10^6 cells.mL^{-1}. Thereafter (dilution rates 0.0667-0.0833 hr^{-1}), there was a gradual decrease in the cell concentration which continued to decline steadily between 45-11 x 10^6 cells.mL^{-1} in regions B and C. The redox potential in regions A and B was well above 700 mV which is expected for an active culture *of Leptospirillum ferriphilum* (Breed and Hansford, 1999; Rawlings *et al.,* 1999; Rawlings and Tributsch, 1999; Rawlings, 2002; van Scherpenzeel *et al.*, 1998). This indicates that in regions A and B most of the ferrous iron was oxidized to ferric iron and ferrous iron was therefore limiting. In region C, the redox potential dropped to 578 mV and continued to drop as the dilution rate increased. In this region ferrous iron was not limiting at dilution rates 0.200 hr^{-1} and 0.250 hr^{-1} and the conversion of ferrous iron to ferric iron moved from 99% to 85% and 67% respectively.

As mentioned in section 4.1, the growth of microbial cultures in CSTR systems has been studied extensively. Ideally, according to the Monod model, the expected trend from experimental work should resemble the theoretical continuous culture isotherm on Figure 4-1, illustration A. At lower dilution rates, the cell concentration in the CSTR is consistent and only drops rapidly on approaching the critical dilution rate (D_c) where the microorganisms are completely washed out of the reactor. On comparing the cell concentration vs. dilution rate isotherm from the experimental work (Figure 4-2) to the Monod model (Figure 4-1, illustration A), it was noted that initially in region A there was a positive correlation to the Monod model; however, in regions B and C a deviation from the Monod model was observed. There was no critical dilution rate (no rapid drop in the cell concentration) as

cells were not completely washed out from the reactor and the cell concentration was observed to tail off gradually. This deviation from the Monod model may have been caused by a number of possible limitations in the reactor system.

As discussed in section 4.2.1 deviations from the Monod model may be caused by carbon limitations, nitrogen and sulphur limitations, trace element and oxygen limitations, Mg^{2+}, K^{+} and PO_4^{3-} limitations and wall growth (see illustrations in Figure 4-1). The trend of the experimental cell concentration vs. dilution rate in Figure 4-2 corresponds to the deviation from the Monod model due to wall growth (Figure 4-1 illustration F), where the cell concentration was observed to tail off and the critical dilution rate was shifted such that wash out took longer to occur. Pirt (1975) reported that microorganisms were able to adhere to glass and metal surfaces in the event that a CSTR was run for a long period of time. This wall growth was reported to be rapid and persistent such that even after scraping the film off there was still rapid reformation of the film. Wall growth can vary from a light film of biomass to a massive accretion of biomass to the walls of the vessel. During wall growth formation, an adherent film constituting of bacterial cell layers coats the walls of the CSTR and builds up simultaneously with ferric oxyhydroxide (or jarosite) precipitate that helps bind the structure together. In most chemostat studies, to minimize wall growth build up, the culture is regularly transferred to a clean reactor. This however was not advisable in this study to avoid contamination of the pure culture which was very important.

Rossi (1990) reported that the effect of wall growth prevented wash out which could be advantageous in biohydrometallurgical processes. For this study, however, the presence of wall growth was a disadvantage. Wall growth in a CSTR also interferes with any observed system kinetics and physiological data (Rossi, 1990). The main objective of investigating the planktonic microbial population in this study was to determine the critical dilution rate of the reactor system at which wash out would occur and thereby allow conditions for the investigation of the activity of the sessile population only. Based on the experimental data shown in Figure 4-2, the critical dilution rate (D_c) of the continuous system could however not be determined as there was no complete wash out of cells for the range of dilution rates investigated (0.0182-0.250 hr^{-1}). Naik (2010) reported that the wash out of a *Leptospirillum ferriphilum* microbial culture occurred at 0.0714 hr^{-1} (14 hr residence time) although this probably referred to the initial decline observed at the end of region A in the present study, and did not account for or observe oxidation due to residual wall growth. The wash-out of cells from the present system however seemed to require a critical dilution rate greater than 0.250 hr^{-1} which was the highest dilution rate investigated. To further confirm the effect of wall growth in

the reactor system, the maximum growth rate (μ_{max}) was determined. In the event that there was wall growth in the CSTR; $D_c > \mu_{max}$ otherwise in ideal conditions (Monod model) $\mu_{max} = D_c$.

Figure 4-3 presents part of the microbial growth curve (exponential phase) for *Leptospirillum ferriphilum* microorganisms plotted from subsequent experimental work to determine the maximum growth rate. The experimental data was determined from an operating batch reactor containing 500 mL of an active culture and 500 mL of fresh feed medium at time = 0 hr (t_0). The cell concentrations were determined at 1 hour intervals for 10 hours and the natural logarithm of the cell concentration was plotted against time. During the first 2 hours, cells were in the lag phase (data points not shown; see Appendix C) thereafter, the cell growth was exponential. The gradient of the trend line shown in Figure 4-3 gives the maximum growth rate (μ_{max}) for *Leptospirillum ferriphilum* which was found to be 0.0831 hr^{-1} (12 hr residence time).

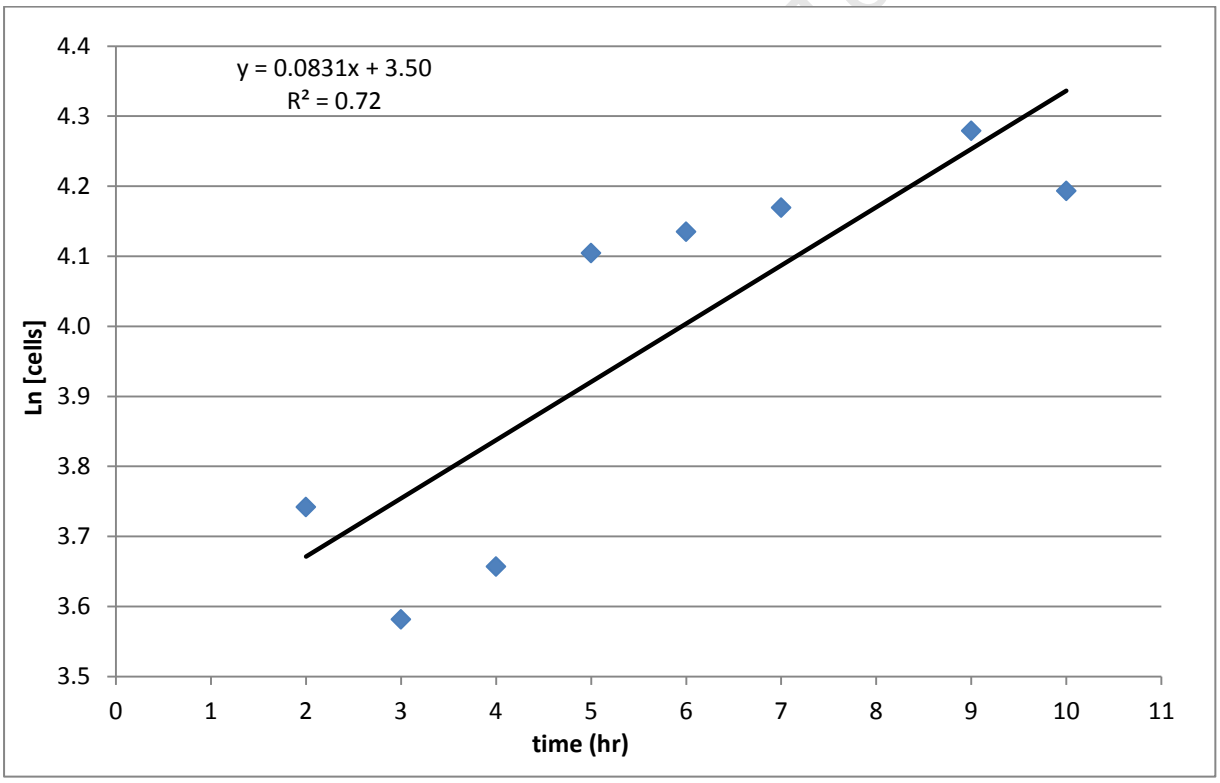

Figure 4-3: Microbial growth curve for *Leptospirillum ferriphilum* (exponential phase) showing the relationship between the natural logarithm of the cell concentration vs. time (hr). The maximum growth rate (μ_{max}) is the gradient which was found to be 0.0831 hr^{-1} (12 hr).

With reference to Figure 4-2, the apparent critical dilution rate for this system was a value greater than 0.250 hr^{-1} (4 hr residence time) $D_c > \mu_{max}$ (D_c>0.250 hr^{-1}>0.0831 hr^{-1}) which confirms that there was indeed wall growth in the reactor (du Preez, 1995; Rossi, 1999). In addition, the data in Figure

4-2 region A showed an initial correlation to the Monod model. The experimental data in region A was used to determine a model (Model 1) mimicking the Monod model, and is shown in Figure 4-2. According to Model 1, wash out would have occurred at a critical dilution rate of 0.0832hrs^{-1} (12 hr residence time). This critical dilution rate (0.0832 hr^{-1}) determined from Model 1 corresponds to the maximum growth rate (0.0831 hr^{-1}) determined from the growth curve on Figure 4-3. If wall growth was negligible, Model 1 was postulated to be the ideal model expected for the planktonic *Leptospirillum ferriphilum* culture in this reactor system. Where the dilution rate was high, associated with wall growth, the relative rate of re-inoculation from wall growth was negligible compared with wall growth.

In Figure 4-2 regions B and C, due to the effect of wall growth in the reactor, as discussed above, the occurrence of cells in the reactor in these two regions may have been due to cells eluted from the surface of the reactor wall. From the data, there appears to have been a logarithmic relationship in the cell concentration as the dilution rate was increased. The data in region B and C was extrapolated resulting in Model 2 shown in Figure 4-2 (equation 4-2): Model 2 was used to determine the rate at which cells were eluted from the reactor wall as well as also determine the critical dilution rate where complete washout of cells from this system would be expected to occur. This was calculated to be 0.35 hr^{-1} (2.9 residence times). Based on Model 2, it can be postulated that microorganisms attached to the reactor wall were eluted into the reactor medium at the rate of 0.35 hr^{-1}.

$$Cell\ concentration\ \left(\frac{cells}{mL}\right) = -35.2Ln\left(dilution\ rate(hr^{-1})\right) - 36.5 \qquad \text{Equation 4-2}$$

From the analysis thus far, it is evident that there was a deviation of the system from the Monod model due to the effect of wall growth. Initially (region A), the data corresponded to the Monod model, suggesting that the planktonic microbial population dominated the system at this point. On extrapolating the data in region A, Model 1 was determined. Based on Model 1, if the system had been ideal (Monod model) then the planktonic cells would have been washed out at a critical dilution rate of 0.0832 hr^{-1}. The maximum growth rate of *Leptospirillum ferriphillum* was subsequently found to be 0.0831 hr^{-1}, which confirms the accuracy of Model 1 as a model for the system were the system is ideal. Due to the effect of wall growth during actual experimentation, planktonic cells did not however wash out of the reactor completely and cells where continuously eluted from the reactor wall. This deviation is seen in regions B and C showing that there was a shift

in the system, and that the cells attached to the reactor wall (also a sessile microbial population) now dominated the system.

4.2.3 Ferrous iron oxidation rates, biomass and specific ferrous iron oxidation rates

Figure 4-4 presents the ferrous iron oxidation rates vs. the dilution rate obtained from the investigation of planktonic *Leptospirillum ferriphilum* in this study. 5 gL^{-1} ferrous iron feed was introduced to the reactor and the rate of addition controlled by varying the dilution rates. The rate of ferrous iron oxidation therefore was controlled relative to the amount of ferrous iron pumped into the reactor. Ferrous iron oxidation rates were calculated using the relationship shown by Equation 3-6 in Section 3.6.1. Ferrous iron tests at each dilution rate were conducted in triplicates. In regions A and B of Figure 4-4, it was observed that, generally, as the dilution rate increased the ferrous iron oxidation rate also increased. Ferrous iron was limiting in this range, and most of it oxidized to ferric iron.

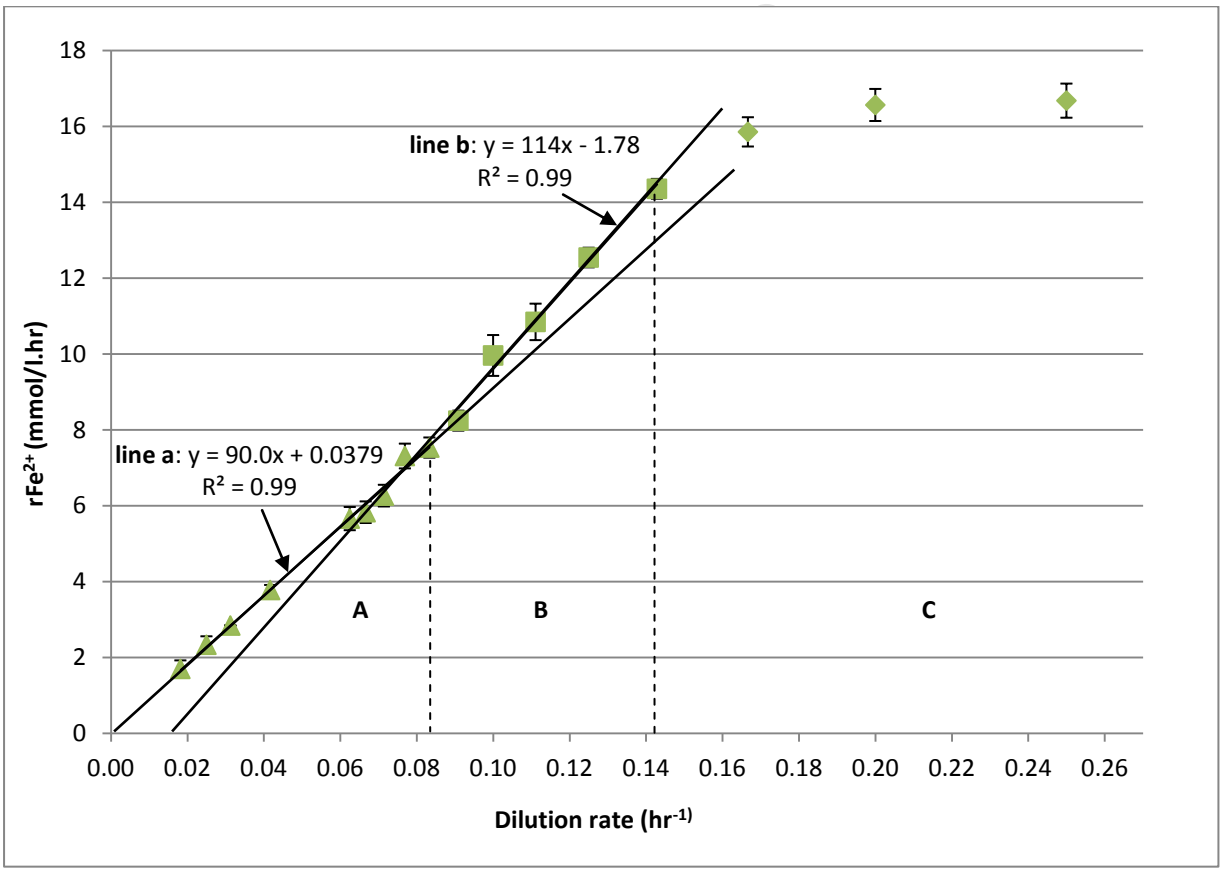

Figure 4-4: Rate of ferrous iron oxidation for *Leptospirillum ferriphilum* vs. dilution rate. The total ferrous iron concentration in the feed was 5 gL^{-1}. Ferrous iron tests for samples collected at steady state at each dilution rate were conducted in triplicates.

The limitation of ferrous iron in the system was confirmed by the redox potential measurements shown in regions A and B of Figure 4-2 which were found to be well above 700 mV, indicating that all the ferrous iron had been oxidized to ferric iron. In region C of Figure 4-4, the ferrous iron oxidation rate was observed to plateau indicating that ferrous iron was no longer limiting in the system. This was confirmed in Figure 4-2, where the redox potential in region C was observed to be at 578 mV and lower. It was calculated that whereas initially 99% of the ferrous iron was utilized in regions A and B, this declined to 85% and 67% at dilution rates 0.200 hr^{-1} and 0.250 hr^{-1} respectively in region C indicating that not all the ferrous iron was completely utilized. The rate of ferrous iron oxidation in region C was observed to approach a maximum ferrous iron oxidation rate of 16.7 $mmol.L^{-1}.hr^{-1}$.

Further analysis of the data in Figure 4-4, shows that there were two independent linear relationships of the ferrous iron oxidation rates relative to the dilution rates observed in region A and in region B. These relationships are defined in Figure 4-4 as line a and b. line a was extrapolated from the experimental data generated in region A and line b using experimental data in region B. In region A, at any fixed dilution rate, the ferrous iron oxidation rates (y-axis on Figure 4-4) of the system determined using line a were higher compared to the ferrous iron oxidation rates determined using line b. The opposite was observed in region B where at a fixed dilution rate, the ferrous iron oxidation rates of the system determined using line b were now higher compared to the ferrous iron oxidation rates determined using line a. The occurrence of two independent linear relationships (line a and b) may have been as a result of the existence of the two microbial populations in the system as discussed in section 4.2.2. It was mentioned that in region A, the planktonic microbial population was dominating thereafter moving onto regions B and C, there was a shift in the system and microorganisms attached to the reactor wall now dominated. line a represents the ferrous iron oxidation rates of the dominant planktonic population which was highest in region A and line b may be representive of the ferrous iron oxidation rates of the microorganisms attached to the reactor wall which was highest in region B.

4.2.4 Biomass and specific ferrous iron oxidation rates

Figure 4-5 and Figure 4-6 present the biomass, and specific ferrous iron oxidation rates respectively, of *Leptospirillum ferriphilum* in the system as a function of the dilution rate. Biomass data was obtained using two methods; off-gas measurements and dry mass analysis which are explained in Chapter 3 (Section 3.6.2 and 3.6.3). At steady state, all the carbon dioxide used up in the system (determined using off-gas measurements) was assumed to be converted to biomass and was used to

determine the off-gas biomass data. Dry mass biomass was determined by measuring the dry mass of 900 mL culture medium with a known cell concentration to then calculate the carbon equivalent for each cell in the system. Both methods were implemented to determine if they both yielded similar results on calculating the specific ferrous iron oxidation rates.

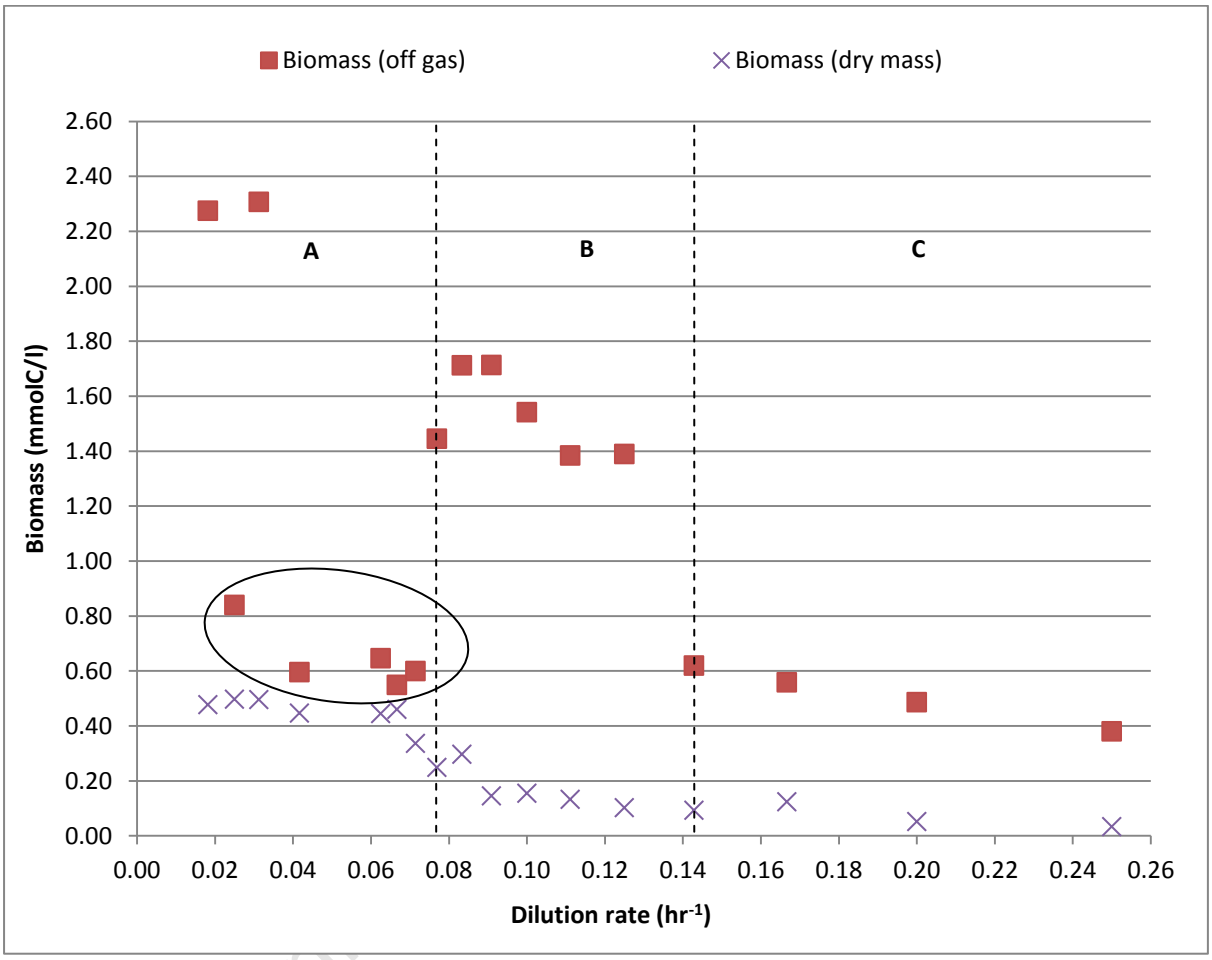

Figure 4-5: Amount of biomass vs. dilution rate. Biomass was calculated using two methods using off gas measurements and dry mass analysis. Data circled in region A may be assumed to be offset data due to technical errors.

Referring to Figure 4-5, biomass determined using off gas data was of a higher magnitude compared to the biomass determined using the dry mass method. There were limitations in measuring the biomass in the system. Off gas analysis and dry biomass measured different things with off gas analysis measuring biomass produced whilst dry mass accounted for planktonic biomass in the reactor. Neither method measured the total biomass concentration in the reactor which was therefore assumed. On comparing the trends of the biomass in the system, using both methods, there was no correlation between the two in region A. There were however similarities in the biomass trends in regions B and C. In region A, major fluctuations in the off-gas biomass were

observed which indicated the possibility of technical errors during measurements. The points enclosed in the circle in region A of Figure 4-5 were therefore considered to be offset data points resulting in a close correlation between the two methods in region A. The data points circled in region A of Figure 4-5 were therefore considered to be off-set data points in this study.

Off-gas biomass data was at its highest (approximately 2.30 mmolC.L^{-1}) in region A at dilution rates of between 0.0182-0.0313 hr^{-1}. This high amount of biomass may have been due to the combined effect of the growth of planktonic cells in the reactor and the growth of cells on the reactor wall. This changed between dilution rates 0.0313-0.0769 hr^{-1} with the amount of biomass dropping down to an average of 1.45 mmolC.L^{-1}. This drop in the biomass may have been as a result of the wash out of only the planktonic population from the reactor. It was determined in Section 4.2.2 that the maximum specific growth rate of *Leptospirillum ferriphilum* in this system was 0.0833 hr^{-1} (12 hr) therefore if the system were Monod type, this is the point where wash out would have occurred. Based on the off gas data, the drop in the biomass (washout of the planktonic cells) was at approximately 0.0769 hr^{-1} (13 hr) which is close to the maximum growth rate. The remaining biomass still present in the system in region A may have been as a result of the cells still growing on the reactor wall which were not washed out of the system. In region B, there was an increase in the biomass. The wash out of planktonic cells from the reactor system meant there was more ferrous iron available for the growth of cells attached to the reactor wall resulting in increased biomass. This growth was observed between dilution rates 0.0769-0.0909 hr^{-1} thereafter the biomass was observed to gradually decrease at higher dilution rates. This gradual washing out of cells from the reactor wall continued in region C.

Using dry mass analysis, the carbon equivalent was calculated to be 3.23E-15 ± 4.51E-16 gmolC.$cell^{-1}$. Since the cell concentrations of the planktonic cells in the system were accounted for (Figure 4-2), the biomass in the system could be determined. As already mentioned, there were similarities in the trends between the biomass data calculated from off gas measurements (off-set data not considered) and the biomass data calculated from dry mass measurements. The off gas biomass data was however of a higher magnitude. In dry mass analysis it was assumed that the carbon equivalent remained unchanged throughout the investigation but this was not true as shown from the off-gas measurements. Dry mass analysis overlooked the effect of wall growth and only accounted for the biomass of the planktonic population. Off-gas measurements however, accounted for the total amount of carbon dioxide used up in the reactor regardless of whether the culture was planktonic or sessile and therefore accounted for the total amount of biomass produced in the system. These

results showed inaccuracy in using dry mass analysis to determine biomass in the reactor system if wall growth was a factor. Off-gas data was therefore a more accurate method to use in this study to determine the biomass in the system.

On Figure 4-6, the specific ferrous iron oxidation rates from both methods (off-gas measurements and dry mass analysis) were compared. There was a correlation only in region A which can be clearly seen on Figure 4-7. Thereafter in region B and C, there were no similarities between the two sets of data. The specific ferrous iron oxidation rates determined using dry mass analysis was found to be much higher when compared to the specific ferrous iron oxidation rates determined using off gas measurements. This was because of the magnitude of the biomass measured in the system. A smaller amount in biomass meant higher specific ferrous iron oxidation rates.

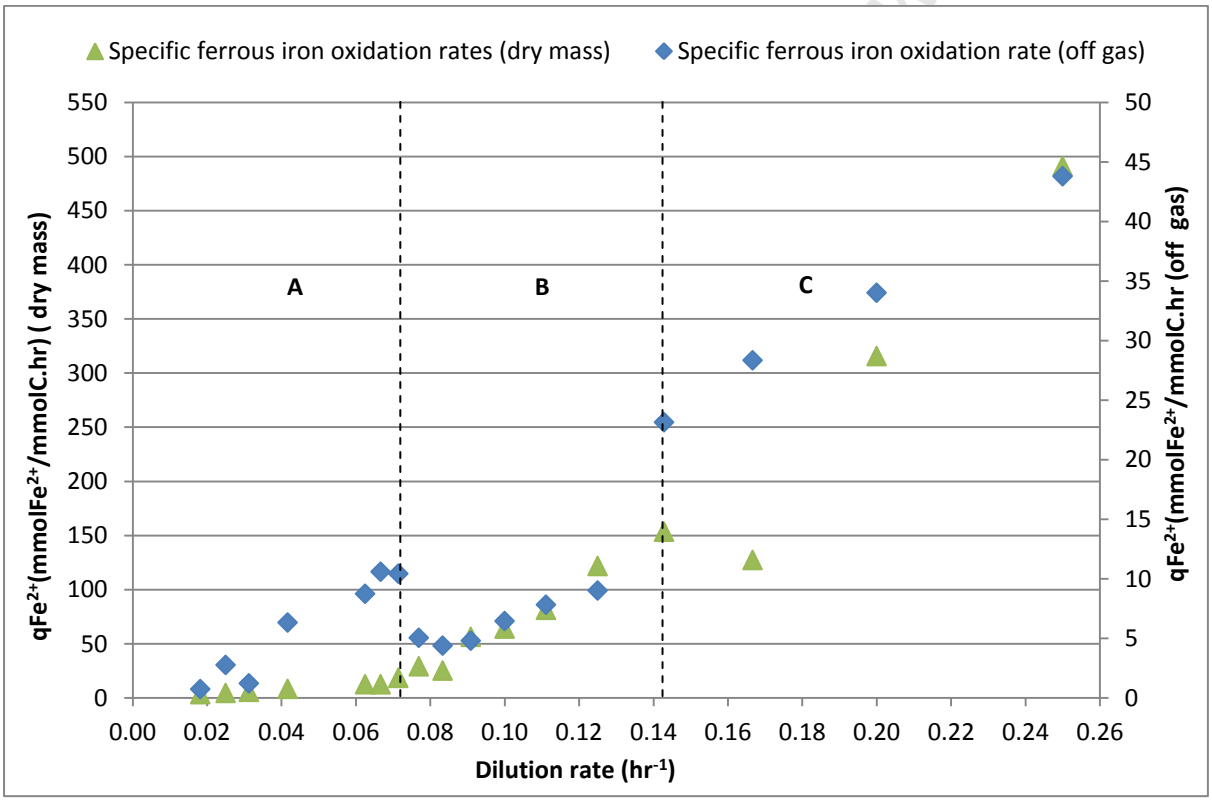

Figure 4-6: Specific ferrous iron oxidation rates of *Leptospirillum ferriphilum* vs. dilution rate. Data calculated from off gas measurements and dry mass analysis. Please note the scales on the y-axis as they are not the same.

Figure 4-7 presents the specific ferrous iron oxidation rates obtained from off gas measurements and dry mass analysis in region A. There was a linear relationship between the specific ferrous iron oxidation rates and the dilution rates. The carbon equivalent using dry mass calculations was found to be 3.23E-15 ± 4.51E-16 gmolC/cell and from off gas measurements it was found to be 7.78E-15 ±

1.93E-15 gmolC/cell which was more than twice greater than the carbon equivalent from dry mass analysis. The carbon equivalent using off-gas measurements was higher than the carbon equivalent determined by dry mass analysis because it accounted for biomass from both the planktonic culture and the cells attached to the reactor wall. The carbon equivalent obtained from dry mass measurements can only be used to determine biomass of planktonic cells in the system in region A.

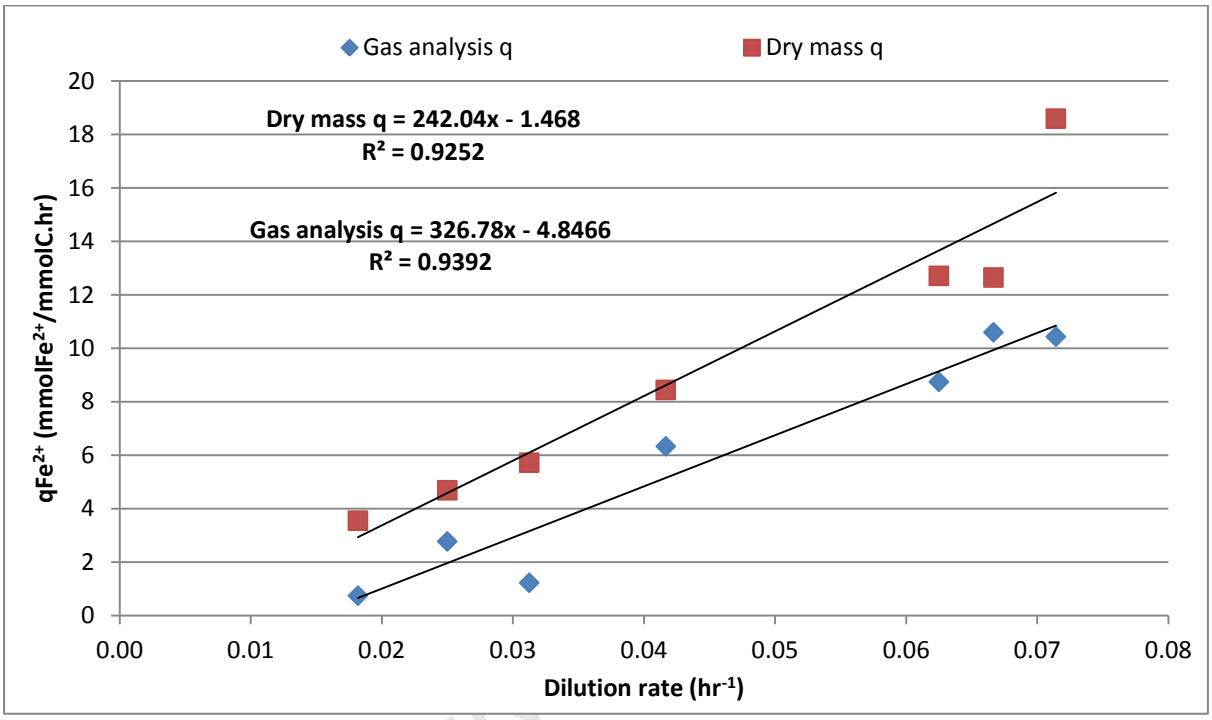

Figure 4-7: Specific ferrous iron oxidation rates obtained from the two methods (off-gas and dry mass). This is region A of Figure 4-6. Carbon equivalent by dry mass and off gas measurements was 3.23E-15 ± 4.51E-16 gmolC/cell and 7.78E-15 ± 1.93E-15 gmolC/cell respectively.

4.2.5 Comparison of Leptospirillum ferriphilum growth kinetics in sterile and non-sterile conditions

In this study, all experimental work was conducted under sterile conditions to prevent the contamination of the culture by other microorganisms. Contamination may interfere with microbial activity especially if the contaminants are ferrous iron oxidizers and behave differently if they possess different intrinsic properties. From a fundamental point of view, it was essential that the purity of the *Leptospirillum ferriphilum* culture be maintained so that the microbial kinetic data generated was relative to a single type of microorganism (*Leptospirillum ferriphilum* used in this study).

In Naik's (2010) study, which this work builds on, all experimental data on the microbial activity of *Leptospirillum ferriphilum* was generated from experimental work conducted in non-aseptic conditions (no filtration or autoclaving of the growth medium). In both Naik's (2010) and this study, prior to starting experiments the RNA gene was amplified using primers and sequenced to confirm homology. Thereafter, morphology checks were frequently done to ensure the culture was predominantly *Leptospirillum* and visual checks for fungus were also constantly performed.

Figure 4-8 compares the specific ferrous iron oxidation rates generated from Naik's work (non-sterile conditions) with specific ferrous iron oxidation rates from this study (sterile conditions) to observe if there were any significant differences in the microbial activity. Reactor conditions from both studies were identical although the type of bacterial strain of *Leptospirillum ferriphilum* used in the two studies differed. In Naik's study, the microbial species used was originally obtained from a vat-type two-stage (2x20 dm^3) continuous bioleaching mini-plant treating a pyrite-arsenopyrite concentrate, from Fairview, Barberton, South Africa. For this study, *Leptospirillum ferriphilum* of type strain ATCC 49881, originally isolated from a culture in the Centre for Bioprocess Engineering Research (CeBER) laboratory at the University of Cape Town was used.

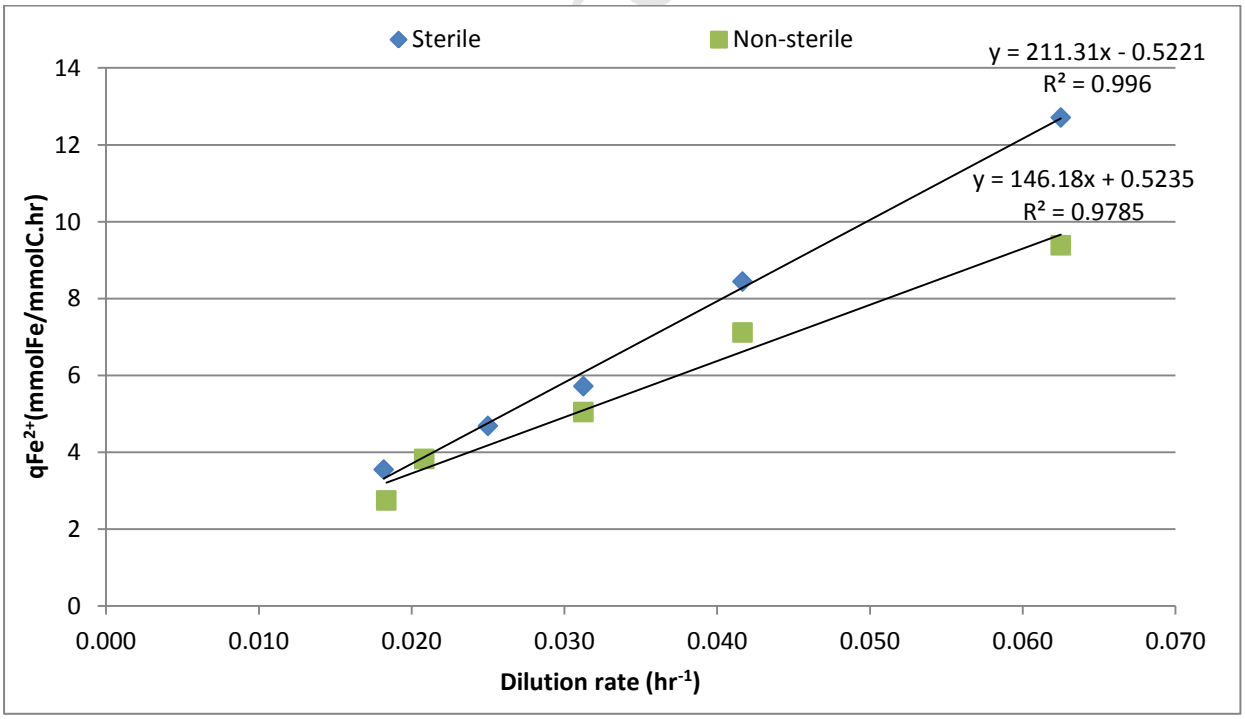

Figure 4-8: Comparison of the specific ferrous iron oxidation rates between sterile and non-sterile study

The maintenance and maximum growth yield of ferrous iron from both studies (shown on Table 4-3) were also compared. These were calculated by linearizing the Pirt equation (see Section 3.6.3 Equation 3-5). The specific ferrous iron oxidation rates from sterile experiments were only slightly higher than the specific ferrous iron oxidation rates from the non-sterile experiment; both studies had a similar linear trend of the specific ferrous iron oxidation rate. As the dilution rate increased, the specific ferrous iron oxidation rates also increased. Referring to Table 4-3, the yield from the non-sterile experiments was found to be higher showing more biomass was formed (31% more biomass). The maintenance was negligible for the sterile study. At total iron concentrations of less than 12 gL^{-1} the maintenance could not easily be determined accurately as it is small relative to the reciprocal of the yield ($1/Y_{SX}^{max}$) (Ojumu, 2008). The maintenance could therefore not be compared for the two studies due to possible inaccuracy.

Table 4-3: Results obtained for the maximum yield and maintenance

	$Y_{Fe^{2+}X}^{max}$ (x10^3) (mmolC/mmolFe)	Maintenance (mmolFe/mmolC.hr)
Non-sterile	6.84	0.524
Sterile	4.73	-0.522

From the comparison above, Naik's study had a higher maximum yield when compared to this study. This may have been because the two cultures were of different species. The trends in the specific ferrous iron oxidation rates were similar. As such although it was important to ensure that during investigation the purity of the culture was maintained for both studies, working under sterile conditions may have been unnecessary as there were no significant differences in the kinetic data generated from either study.

4.2.6 Conclusions

The investigation into the kinetic activity of planktonic *Leptospirillum ferriphilum* was conducted under sterile conditions. The purpose for planktonic experiments was to generate data specific to the reactor conditions in the laboratory which would be a benchmark for comparison with the activity influenced by the sessile microbial population discussed later in chapter 5. It was also necessary to investigate the activity of the planktonic *Leptospirillum ferriphilum* culture to determine the critical dilution rate of the system where there was complete wash-out of planktonic microorganisms from the reactor system. Determining the critical dilution rate of the system was essential as the investigation of the sessile microbial population was intended to be at wash-out conditions.

On analysis of the experimental data generated from the activity of the planktonic microbial population, it was found that there was a deviation from the Monod model in the reactor system. Based on theory, a correlation to the Monod model was expected where there was initially a consistent microbial population of planktonic cells then, at a critical dilution rate, the planktonic cells were completely washed out of the reactor. The experimental data, however, showed that for the range of dilution rates 0.0182-0.250 hr^{-1} (55-4 hr residence times), there was no complete washout of planktonic cells from the system. A close correlation to the Monod model was only observed at lower dilution rates (0.0182-0.0833 hr^{-1}). On extrapolating this data, Model 1 was postulated to represent the expected ideal behaviour in the event there had been no deviation. Based on Model 1, if the system were Monod type, then the critical dilution rate (D_c) would have been 0.0832 hr^{-1} (12 hr residence time). To confirm this, an experiment to determine the maximum growth rate of the culture was investigated. In an ideal situation, the critical dilution rate is equivalent to the maximum growth rate ($D_c = \mu_{max}$). The growth of the microbial population was monitored for 10 hr in a batch reactor in the laboratory and the maximum growth rate (μ_{max}) for *Leptospirillum ferriphilum* was calculated to be 0.0831 hr^{-1}. The critical dilution rate from Model 1 was found to be equivalent to the maximum growth rate calculated from the growth curve (0.0832 $hr^{-1} \approx 0.0831$ hr^{-1}). This confirmed that Model 1 possibly could have been the ideal trend (Monod model) if there had been no deviation.

If true wash-out eventually did occur in the system in this study, then the critical dilution rate would have been greater than 0.250 hr^{-1} (the maximum dilution rate investigated). This means that the critical dilution rate (D_c) would have been a value greater than the maximum growth rate (μ_{max}). According to literature, if $D_c > \mu_{max}$ and there is no complete wash-out of cells, leading to a gradual tailing off of the microbial population over a range of dilution rates, then this is an indication that there is wall growth in the system. The data in the region where there was a deviation (dilution rates ranging between 0.0833-0.250 hr^{-1}) was interpolated and a logarithmic relationship between the cell concentration and the dilution rates is indicated (Model 2). Based on Model 2, the critical dilution rate was calculated to be 0.350 hr^{-1}(2.9 hr residence times). It can be postulated that for this reactor system, wash-out should have been expected at the 0.350 hr^{-1} dilution rate. In summary of the findings mentioned above, it can be concluded that at dilution rates 0.0182-0.0833 hr^{-1}, the planktonic microbial population dominated the system. As the investigation progressed to higher dilution rates (0.0833-0.250 hr^{-1}) most of the microbial population (planktonic) was washed out of the system, however due to wall growth in the reactor a residual population remained in the reactor. There was therefore a shift in the system, and the cells attached to the reactor wall

continuously eluted cells to the liquid medium. At each dilution rate in this region, it is possible that the cells attached to the reactor wall released cells into the medium at the same rate they regenerate and therefore where the dominating microbial population in the system at the higher dilution rates.

Further analysis on the ferrous iron oxidation rates, confirmed the proposed deviation from the Monod model. There were differences in the ferrous iron oxidation rates relative to the dilution rates which depended on the dominating microbial population. Two distinct linear relationships line a (0.0182-0.0833 hr^{-1}) and line b (0.0833-0.143 hr^{-1}) were plotted each with different slopes using the data in the indicated regions. line a was representative of the planktonic population and line b was representative of the cells growing on the reactor wall. Ferrous iron oxidation rates determined from line a were higher in the region between 0.0182-0.0833 hr^{-1} when compared to ferrous iron oxidation rates determined from line b. The opposite scenario was observed in the region between 0.0833-0.143 hr^{-1} where ferrous iron oxidation rates determined from line b were now higher when compared to ferrous iron oxidation rates determined from line a.

Biomass in the system was determined using off-gas analysis and dry mass analysis. The specific ferrous iron oxidation rates were then calculated using the biomass calculated. Dry mass analysis depended on cell counting of planktonic microorganisms and did not account for wall growth. Off-gas data on the contrary measured the amount of carbon dioxide used up in the system which was then related to the biomass produced. Off-gas data therefore took account of the cells growing on the walls. On comparing results from the two analyses, it was discovered that there was plenty of biomass in the system even in the region where wall growth dominated. Dry mass analysis, however, was more accurate for quantifying the amount of biomass of planktonic microorganisms. This would be useful for determining the biomass of only planktonic cells in a system. Biomass data from off-gas analysis indicated that wash-out of planktonic cells was achieved at a dilution rate of about 0.0769 hr^{-1}. This critical dilution rate differs to the one postulated by Model 1 (0.0832 hr^{-1}) but both fall in the same region. Therefore it can be concluded that the critical dilution rate of the system could have occurred between the range 0.0769-0.0832 hr^{-1} if the system had been ideal.

A comparison of the experimental results from the study (operated under sterile conditions) and Naik's (2010) study (operated under non-sterile conditions) showed that there were similar trends in the specific ferrous iron oxidation rates, therefore working under sterile conditions may have been unnecessary.

Although there was no wash-out observed during the investigation of the planktonic microbial population, the investigation of the sessile population was therefore conducted at dilution rates 0.200 hr^{-1} and 0.250 hr^{-1}, where ferrous iron was unlimited and the planktonic microbial population was minimal. Based on Model 1, if the system was Monod type, then the complete wash out of planktonic cells would have occurred between 0.0769-0.0832 hr^{-1} (14 hr-12 hr). The result from investigating the sessile microbial population is presented in chapter 5.

5 Results and discussion (II)

5.1 Aim and approach

The activity of planktonic *Leptospirillum ferriphilum* microorganisms (results presented in chapter 4) was investigated with the purpose of obtaining results that would be used as a benchmark for comparison against the results determined from the investigation of the activity of sessile *Leptospirillum ferriphilum*. It was also necessary to determine the critical dilution rate where planktonic cells were washed from the system so that experiments on the sessile population were conducted independent of the planktonic population.

To begin with the sessile experiments, the sessile microbial population was firstly created. This was done by introducing a solid substrate (ceramic saddles) to a CSTR system containing an active culture of planktonic *Leptospirillum ferriphilum*. Naik (2010) showed that planktonic *Leptospirillum ferriphilum* easily attached to the surface of ceramic saddles. Ceramic saddles were ideal for this study because they were inert and did not provide nutrients or other energy sources (Naik, 2010). Prior to investigating the sessile population, understanding the nature of the attachment process was of importance to ascertain if attachment reached equilibrium or otherwise remained in a transient state in the CSTR + packed bed vessel system. Quantifying for initial number of attached cells during sessile experiments was essential as kinetic activity was relative to the microbial population. The results obtained from the attachment experiments conducted are reported in section 5.2. Once the attachment of microorganisms was established, the kinetic activity of the sessile microbial population followed and the results are reported in section 5.3.

5.2 Attachment experiments

5.2.1 Introduction

In literature, the attachment mechanism of microorganisms to a solid surface has been compared to the adsorption of atoms/molecules on the solid surface. A model by Zobell (1943) described attachment as a two stage process with free bacteria as the adsorbate B and the solid surface as the adsorbent substrate S (see equation 5-1).

$$B + S \leftrightharpoons [BS]^* \rightarrow BS \qquad \text{Equation 5-1}$$

The first reaction corresponds to reversible adsorption. When microorganisms get close to the surface, they experience attractive and repulsive forces. If the forces balance, then the complex

[BS]* may be formed. If there is no material bond between the surface and the microorganism there may be displacement resulting in the regeneration of free microorganisms and free active sites. Alternatively, in the event that there is a bond between the microorganism and the solid surface, then there is firm and permanent attachment to the surface represented by BS (Rossi, 1990; Rodriguez, 2003b). Bacterial attachment (initial and firm attachment) to metal sulphides can be modelled by equation 5-2:

$$K_a t = \frac{1}{\frac{1}{a}A_0 - X_{b0}} Ln\left[\frac{X_{b0}(\frac{1}{a}A_0 - X_{bs})}{\frac{1}{a}A_0(X_{b0} - X_{bs})}\right]$$ Equation 5-2

Where K_a is the attachment rate constant (mL/cell.hr); A_0 is the concentration of surface adsorption sites (cm^2/cm^3); a is the projected area per bacteria (cm^3/cell); X_{b0} is the initial concentration of free bacteria (cells/mL); X_{bs} is the concentration of attached bacteria on the solid surface (cells/mL) and t is the time (hr). The first stage has also been modelled using the Langmuir isotherm which allows for the effect of the concentration of planktonic microorganism in the system to adsorption and desorption. The concentration of planktonic microorganisms is a key parameter which affects both adsorption and desorption stages and has been found to be a limiting factor hugely influencing the rate and extent of attachment (Bromfield, 2011; Sohn, 2004).

The Langmuir isotherm equation for aqueous systems is:

$$\frac{X_e}{q} = \frac{X_e}{q_m} + \frac{1}{K_a q_m}$$ Equation 5-3

Where X_e is the concentration of the adsorbate at equilibrium, q is the amount of adsorbate absorbed per gram of adsorbent, q_m is the amount of adsorbate required to form a monolayer on the adsorbent (maximum adsorption capacity) and K_a is the Langmuir adsorption equilibrium constant. van Loosdrecht (1990) further modified the model by Zobell (1943) and described attachment as a four step process where microorganisms:

- are transported to the solid surface via diffusive transport, convective transport and/or active movement.
- initially adhere (reversibly or non-reversibly) to the mineral surface due to hydrophobic or electrostatic forces.
- firmly attach to the mineral surface and,

- colonize and form biofilms on the solid substrate surface.

Based on the four steps leading to attachment, Chiume (2011) reported that that the microbial population in heap systems may be categorized into three regions:

Category (I) Attached phase referring to:

- Loosely attached microorganisms to the mineral surface due to surface interactions.
- Strongly attached microorganisms to the mineral surface due to electrostatic forces thereafter EPS formation and biofilm formation.

Category (II) Planktonic phase:

- Refers to microorganisms found in solution and recovered in the pregnant liquor solution (PLS).

Category (III) Interstitial phase:

- Refers to microorganisms which accumulate in the stagnant fluid zones and pore spaces and can be categorized as 'attached'.

For this study, attachment was investigated in a closed system consisting of a 200 cm^3 glass vessel packed with 123 g of ceramic saddles (PBR) attached to a CSTR. The culture medium in the CSTR was then pumped upwards through the packed bed vessel (the recycle ratio-flow rate of culture out of the CSTR through the glass vessel: the flow rate of the fresh feed into the CSTR was 11.5). For all attachment experiments, the CSTR was operated at a fixed dilution rate of 0.0313 hr^{-1} (residence time 32 hr). Attachment was investigated for 6 separate time intervals (t=2, 4, 6, 8, 10 and 12 days) in triplicates to validate reproducibility. Quantifying the cell numbers of the sessile population was achieved via a detachment protocol formulated by Bryan *et al.* (2011) which allowed for the determination of interstitial cells, weakly attached cells and strongly attached cells from the surface of the ceramic saddles. Physical force such as hydrodynamic shear or from other types of stresses triggers the detachment of microorganism from the surface of mineral (Africa, 2009). During detachment, the liquid medium surrounding the ceramic saddles in the packed bed vessel was first removed and kept for cell counting. The saddles were then washed gently to recover interstitial cells. Shear force was then applied to the saddles to remove weakly attached cells. Strongly attached cells were recovered also using shear stress in a liquid with tween 20. The solution collected from each of these different steps was kept for cell counting to determine the microbial population (See Appendix B for a detailed description).

5.2.2 Attachment of microbial population

Figure 5-1 presents the results obtained from investigating the attachment of planktonic *Leptospirillum ferriphilum* to the surface of ceramic saddles.

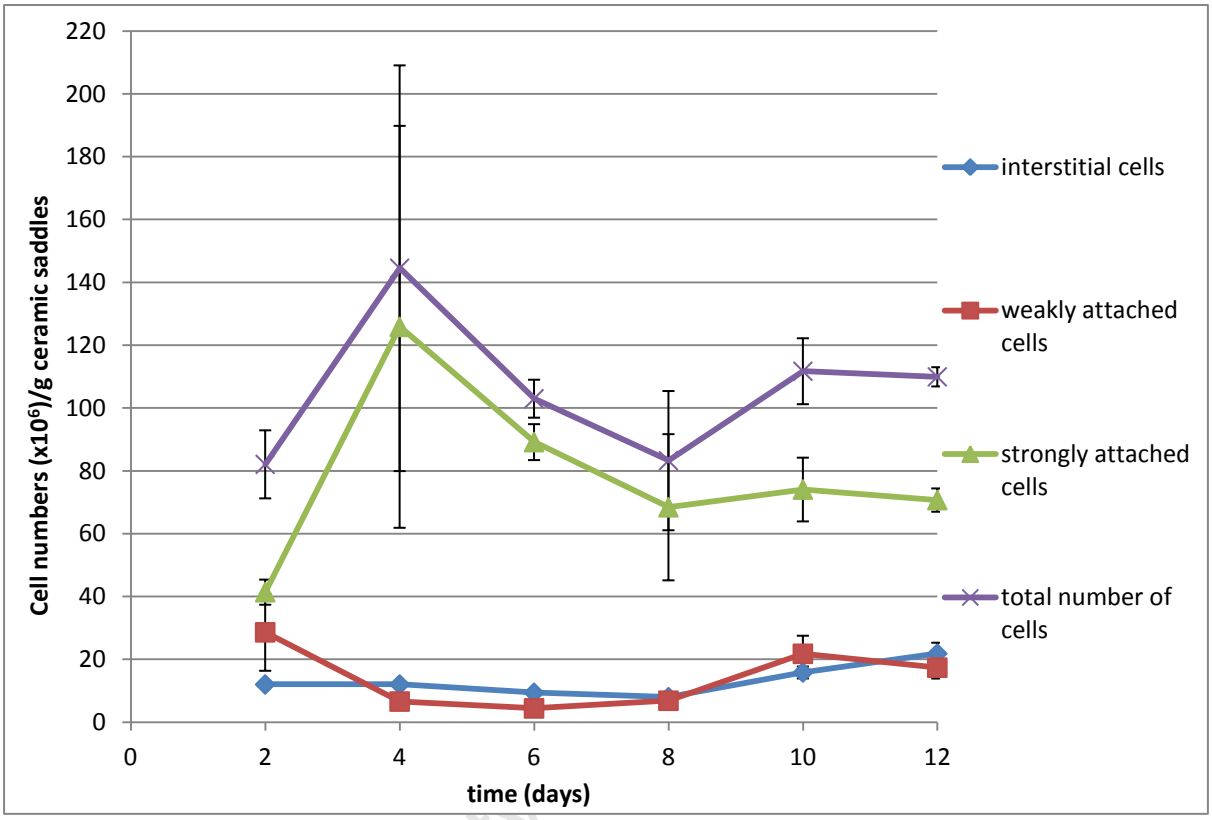

Figure 5-1: Attachment of a pure *Leptospirillum ferriphilum* culture to the surface of ceramic saddles packed in a glass vessel (PBR) and attached to a continuous stirred tank reactor as a closed system. The CSTR was operating at a 32 hr residence time (0.0313 hr^{-1}) and the recycle ratio was 11.5. Experiments were conducted in triplicates for each time interval (2, 4, 6, 8, 10 and 12 days) and at the end of every experiment microorganisms were detached using a detachment protocol to determine interstitial, weakly attached and strongly attached cells.

On average a total of 106 x 10^6 cells/g ceramic saddles attached to the surface of the ceramic saddles. By day 2, 77% of the microorganisms were already attached. In literature, attachment is reported to be rapid occurring within the first hours after contact (Rodriguez *et al.*, 2003). Bromfield (2011) in her attachment studies using *Metallosphaera Hakonensis* microorganisms found attachment to be rapid occurring within the first 10 minutes (shake flask experiments) and reaching equilibrium by approximately 20 minutes irrespective of mineral type and culture growth history. Africa (2009) investigated microbial attachment to sulphide minerals and reported that attachment was achieved after 20 and 30 minutes (shake flask experiments) for pyrite and chalcopyrite respectively. Based on these findings it was assumed that attachment was already established in the

first hour of contact. In this study, the aim of the attachment experiments was to investigate the nature of the growth of the microbial culture to the surface of the ceramic saddles by determining if steady state was established and to quantify the microbial population numbers. No experiments were therefore conducted at time intervals shorter than two days. There were small variations in the total number of attached cells over the individual time intervals. This can be seen in Figure 5-1, referring to the total number of attached cells counted where the error bars generally fell within the same range. There was therefore consistency in the number of attached cells between days 2-12 showing that attachment in the system reached steady state. Referring to Figure 5-1, up to 87% of the total numbers of microorganisms attached were firmly attached to the surface of the ceramic saddles. The remaining microbial population was either in the interstitial region or were weakly attached. Having the majority of the microbial population firmly attached meant the sessile population could not easily be washed out of the system during investigation as they were not just entrained in the medium in the PBR.

Figure 5-2 shows the cell concentration of planktonic *Leptospirillum ferriphilum* in the CSTR medium and in the PBR medium for the duration of the attachment experiments. Attachment experiments were conducted in triplicates for each time interval in the order of t=2, 4, 6, 8 and 10 days using one CSTR, with a fresh PBR being attached for each repeat experiment. A separate CSTR was used to investigate attachment at the 12 day period, therefore it was not included in Figure 5-2 as the cell concentrations differed significantly. At the end of each experiment, the PBR was detached from the CSTR and its contents were analysed. The detached PBR was immediately replaced with a new vessel packed with clean ceramic saddles and attached to the CSTR to start on a next experiment. The recycle ratio (the flow rate of culture out of the CSTR through the glass vessel: the flow rate of the fresh feed into the CSTR) was at 11.5 throughout. This high ratio ensured that the medium in the PBR was similar to the medium in the CSTR. This was of importance because sampling was done from the CSTR and each sample from the CSTR was representative of the conditions in the PBR. The two vessels could not be assumed to be one system if the conditions were different. Referring to Figure 5-2, there was generally a close correlation between the cell concentration in the packed bed vessel medium and the cell concentration in the CSTR, especially in the first 52 days, indicating that the conditions in both systems were uniform. The redox potential and pH were also measured and were found to be similar confirming uniformity of the conditions from both vessels.

There was a drop in the cell concentration of planktonic cells between days 6-52 due to the constant removal of the PBR at the end of the different experiments conducted.

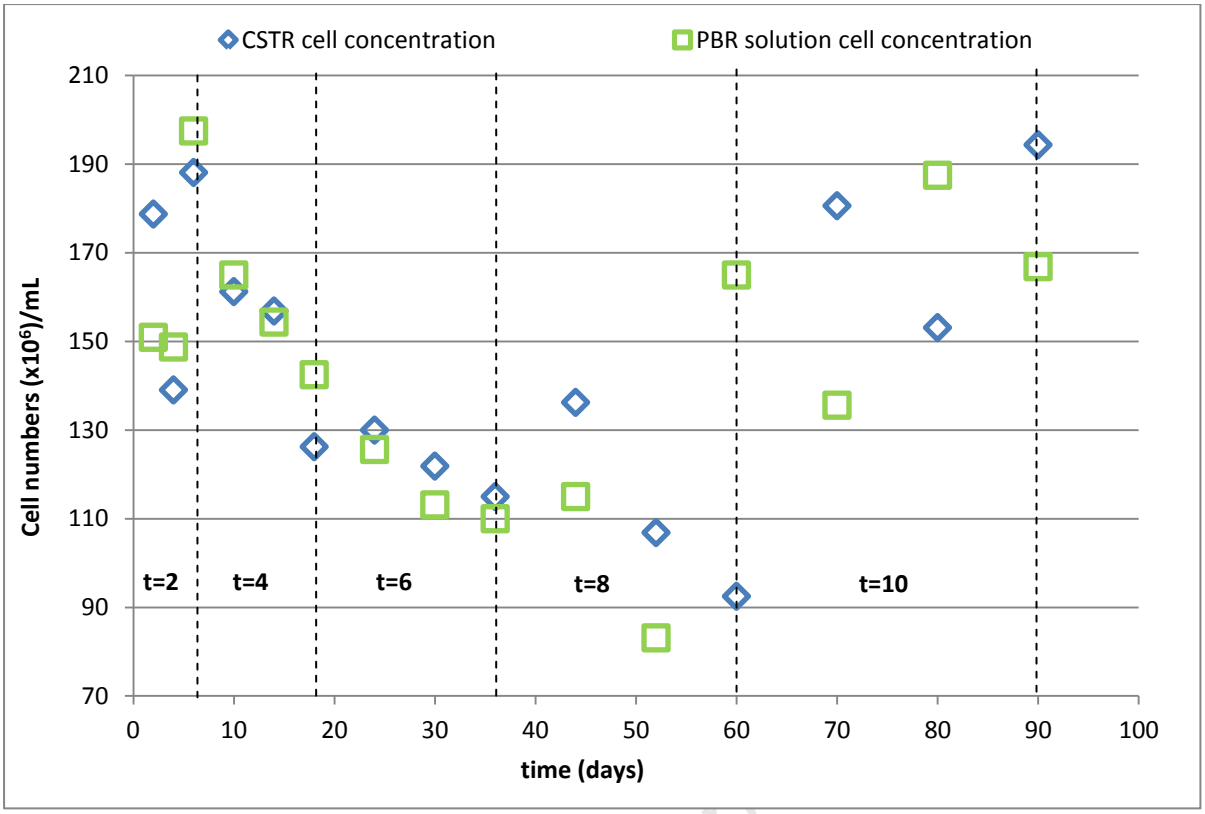

Figure 5-2: Cell concentration ($x10^6$) in the CSTR (Reactor 1) and PBR medium for the duration of the attachment experiments. It took 126 days to complete the attachment experiments (the first 90 days were conducted in CSTR (Reactor 1) and last 36 days in CSTR (Reactor 2)). Data on Figure 5-2 shows only the first 90 days. The last 36 days are not shown as a different CSTR was used for the investigation. The dotted lines separate the regions for each time interval investigated. For each time interval experiments were conducted in triplicates.

It was confirmed that the planktonic cells firmly attach to the surface of the ceramic saddles; therefore each time the PBR was detached from the CSTR planktonic cells were removed from the system as well, resulting in a decrease in the cell concentration in the CSTR. The system was not given enough time to recover from the loss of planktonic cells because the detached PBR with attached cells was immediately replaced with a new vessel containing fresh ceramic saddles and therefore could not reproduce fast enough to replace the cells removed from the system. The cell concentration in the CSTR therefore continued to drop as more cells were attached and were removed from the reactor system. The cell concentrations in the PBR and CSTR medium were also observed to be uniform. In the last 38 days, the planktonic cell concentration was observed to increase. This may have been because the PBR was attached to the CSTR for a longer period of time giving the system enough time to now reproduce and replace the lost microbial population previously removed from the system heading towards getting to a steady state. There were significant differences in the cell concentration of the planktonic cells in the CSTR compared to the

PBR medium observed in the last 38 days. As mentioned in section 5.2.1, the concentration of planktonic microorganisms is a factor that hugely influences the rate and extent of attachment. Comparing Figure 5-1 and Figure 5-2, an increase in the cell concentration in the mediums in Figure 5-2 between t=2 to t=4days corresponds to an increase in the total number of microorganisms attached to the ceramic saddles for the same time interval. A drop in the cell concentration in the mediums in Figure 5-2 between t=4 to t=8 days corresponds to a drop in the cell concentration of attached cells on Figure 5-1 for the same time interval. An increase in the cell concentration in the medium for t=8 to t=10 days also results in an increase in the number of attached cells on Figure 5-1 for the same time interval. This may confirm that the concentration of planktonic microorganisms indeed does affect the rate of attachment.

5.3 Sessile microbial culture experiments (I)

5.3.1 Introduction

In chapter 4, it was concluded that there was wall growth in the CSTR system during planktonic experiments, causing a deviation from Monod type behaviour. Due to wall growth, the critical dilution rate could not be determined from experimental data as there was no complete wash-out of planktonic cells. It was discovered that the system was possibly dominated by two different microbial populations. Initially, the planktonic population dominated the system and thereafter it was washed out, then there was a shift in the system where cells attached to the wall now dominated the system. Microorganisms attached to the CSTR wall were continuously eluted into the reactor solution, therefore planktonic cells were always present in the reactor (no wash-out). Ferrous iron was not limiting at dilution rates 0.200 hr^{-1} and 0.250 hr^{-1} (5 hr and 4 hr residence times) therefore for this study, the activity of the sessile population was investigated at these two dilution rates although the planktonic population was not completely eliminated from the system. The nature of attachment of planktonic cells (resulting in a sessile population) to the surface was discussed in section 5.2.2. It was discovered that by day two, most microorganisms were already attached to the surface of the ceramic saddles. On average, 87% of the attached microbial population were firmly attached. The number of microorganisms attached was also found to be consistent over the 12 day period showing that growth was not transient and reached a steady state at the given conditions (32 hr residence time).

The microbial oxidation rates of sessile *Leptospirillum ferriphilum* was investigated in a CSTR + PBR configuration. A 200 mL glass vessel was packed with 123 g of ceramic saddles and attached to a continuous stirred tank reactor (CSTR) with an active microbial culture of planktonic *Leptospirillum*

ferriphilum. The working volumes of the CSTR and the PBR was 1 litre and 180 mL respectively and the system was operated under sterile conditions. The PBR was coiled with tubing and water at 37°C was passed through the tubing to keep the temperature in the packed bed vessel at 37°C.

5.3.2 Data analysis of sessile population at residence times 4 hr and 5 hr

5.3.2.1 Results from the continuous stirred tank reactor (CSTR)

Figure 5-3 and Figure 5-4 show the cell concentrations and redox potential respectively determined during sessile experiments at residence times 4 hr and 5 hr. Sessile experiments were conducted once attachment (over 12 day period with CSTR operating at a 32 hr residence time) was established. The residence time was then switched to either 4 hr or 5 hr (at time = 0 days on Figure 5-3 and Figure 5-4). Generally for both experiments, by day 1, most of the planktonic cells were washed-out from the CSTR, and there was a huge drop in the redox potential. Thereafter, the redox potential and cell concentration were observed to gradually increase until a steady state was reached. At a 5 hr residence time, the redox potential dropped from 730 mV to 441 mV and the cell concentration from 168 to 11 x 10^6 cells.mL^{-1} by day 1.

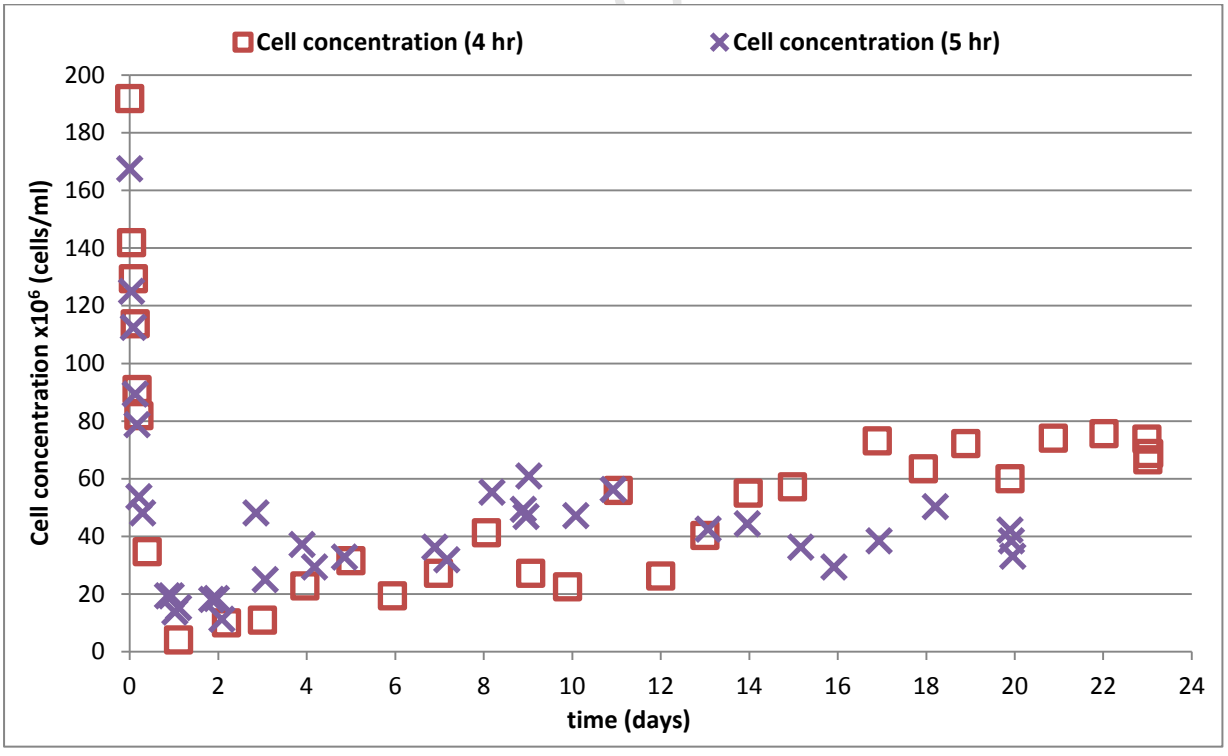

Figure 5-3: Cell concentrations of planktonic cells in the CSTR vs. time for residence time of 4 hr and 5 hr. At time=0 days, the residence time in the CSTR was switched from 32 hr to either 4 hr or 5 hr depending on the experiment being conducted.

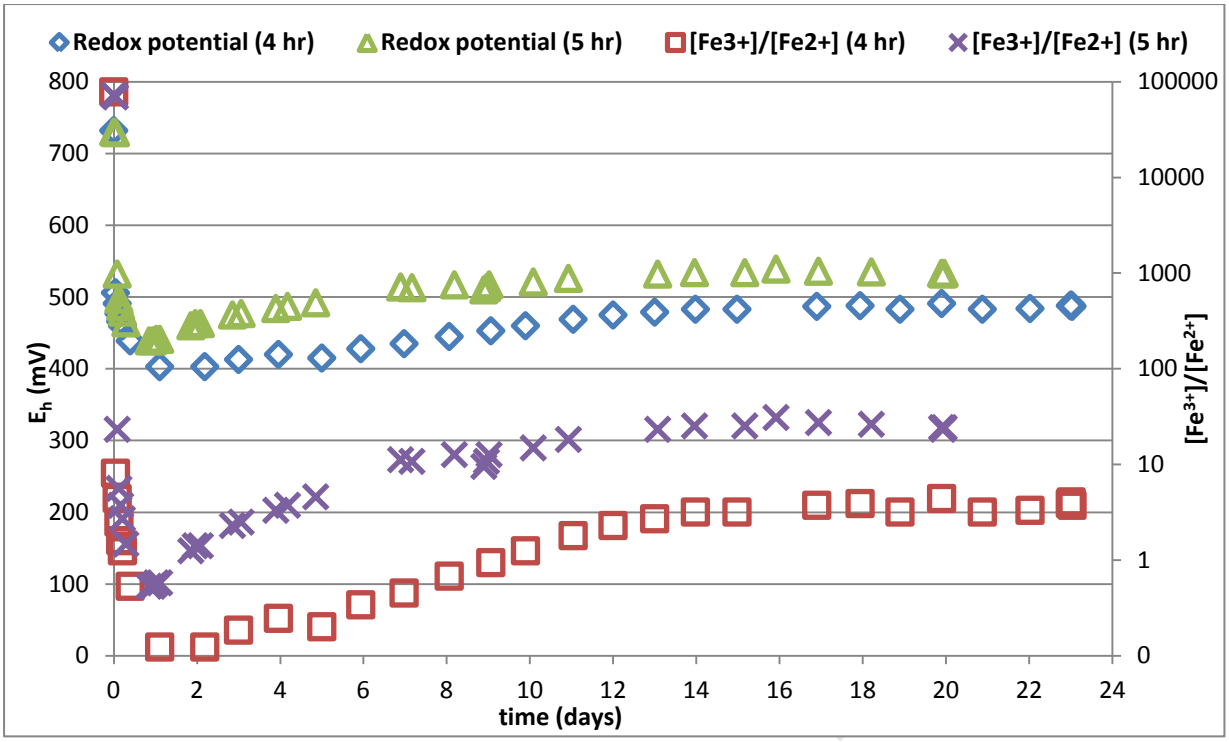

Figure 5-4: Redox potential (mV) and $[Fe^{3+}]/[Fe^{2+}]$ of planktonic cells in the CSTR vs. time for residence time of 4 hr and 5 hr. At time=0 days, the residence time in the CSTR was switched from 32 hr to either 4 hr or 5 hr depending on the experiment being conducted.

An immediate increase in the redox potential and the cell concentration was observed on day 2, and this continued until a steady state was reached. Steady state at a residence time of 5 hr was achieved after 13 days. This corresponds to 63 residence times which is a much longer time required to achieve steady state when compared to the planktonic experiments where steady state was achieved after 3 residence times. At steady state, the cell concentration was 38 x 10^6 cells.mL^{-1} and the redox potential was 533 mV at which 94% of ferrous iron would have been converted to ferric iron.

At a 4 hr residence time, the redox potential dropped from 732 mV to 403 mV and the cell concentration from 192 to 4 x 10^6 cells.mL^{-1}. There was a short lag phase between day 1 and day 5 where only small changes in the redox potential were observed, thereafter there was a gradual increase in the redox potential. An increase in the cell concentration was observed immediately after day 1. Steady state was achieved by day 17. This corresponds to 102 residence times which is a much longer time to get to steady state compared to the planktonic experiments where steady state was achieved after only 3 residence times. At steady state, the redox potential was 488 mV of which 76% of ferrous iron was converted to ferric iron and the cell concentration was 70 x 10^6 cells/ml. It took a

much longer time for the system at a 4 hr residence time to get to steady state compared to a 5 hr residence time.

Figure 5-5 shows the ferrous iron oxidation rates calculated for residence times 4 hr and 5 hr. At 5 hr residence time, the ferrous iron oxidation rate dropped from 18.5 to 7.90 mmolFe^{2+}.L^{-1}.hr^{-1} in the first day. Thereafter, there was an immediate increase in the ferrous iron oxidation rate until a steady state was reached on day 13 (17.4 mmol.L^{-1}.hr^{-1}). At 4 hr residence time, within the first day, the ferrous iron oxidation rate dropped from 22.8 to 0.60 mmolFe^{2+}.L^{-1}.hr^{-1} and then increased gradually until it reached steady state on day 17 (18.0 mmol.L^{-1}.hr^{-1}). This data corresponds to the cell concentration and redox potential data analysis shown in Figure 5-3 and Figure 5-4. On approaching steady state, the ferrous iron oxidation rates at a 5 hr residence time were generally faster compared to the ferrous iron oxidation rates at a residence time of 4 hr. This can be seen from the steepness of the graphs (The steeper graph - 5hr residence time - has faster ferrous iron oxidation rates).

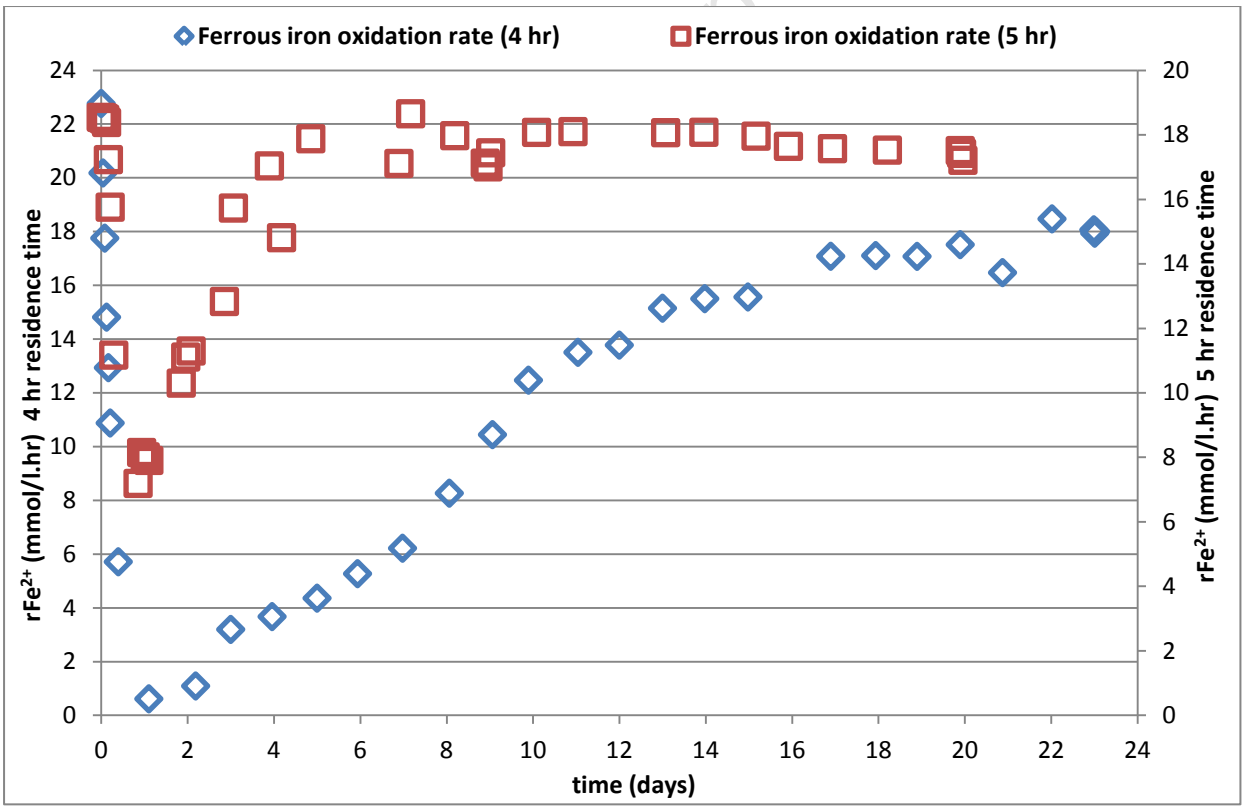

Figure 5-5: Ferrous iron oxidation rate at residence times 4 hr and 5 hr. At t=0, the residence time in the CSTR was switched from 32 hr to either 4 hr or 5 hr depending on the experiment being conducted.

Figure 5-6 shows the carbon dioxide uptake rates for both experiments. On illustration A (5 hr residence time) during attachment (t=0 to t=12 days), the carbon dioxide uptake rate was on average 0.015 mmol.L^{-1}.hr^{-1}. On switching the residence time in the CSTR from 32 hr to 5 hr, a rapid increase in the carbon dioxide uptake rate was observed. This rate climbed from 0.005 mmol.L^{-1}.hr^{-1} on day 12 to 0.11 mmol.L^{-1}.hr^{-1} where the system got to a steady state. It took 15 days for the off-gas data to reach steady state, which corresponds to 72 residence times. The rapid jump in the carbon dioxide uptake rate on switching the residence time from 32 hr to 5 hrs may have been due to the enhanced growth of microorganisms in the reactor system. Switching the residence time meant that more ferrous iron was pumped into the CSTR which in return promoted growth. At a 32 hr residence times there were ferrous iron limitations in the reactor system and a steady state was reached at the given conditions. Since there was wall growth in the CSTR, these cells may have immediately made use of the ferrous iron for their growth which can be translated to the immediate climb in the carbon dioxide uptake rate. It was also possible that the solubility of carbon dioxide to the reactor solution may have contributed to the jump in the carbon dioxide uptake rate. Using Henry's law the solubility of carbon dioxide in the reactor solution was calculated to be 3.43 x 10^{-4}, 2.20 x 10^{-3} and 2.75 x 10^{-3}mmolC.L^{-1}.hr^{-1} at 32 hr, 5 hr and 4 hr residence times respectively which was insignificant and was therefore assumed to be negligible.

On investigating the kinetics of sessile microorganisms at a 4 hr residence time Figure 5-6 illustration B, attachment (residence time of 32 hr) started on day 5 and was ongoing for 12 days. The residence time in the CSTR was switched to 4 hr on day 17. The carbon dioxide uptake rate was on average 0.023 mmol.L^{-1}.hr^{-1} for the planktonic culture and this remained consistent during attachment. After day 17, initially there was a drop in the carbon dioxide uptake rate from 0.023 mmol.L^{-1}.hr^{-1} to 0.006 mmol.L^{-1}.hr^{-1} over a two day period but this eventually picked up and the carbon dioxide uptake rate increased dramatically to a rate of 0.099 mmol.L^{-1}.hr^{-1} at steady state. It took 19 days to get to steady state which corresponds to 114 residence times. The drop in the carbon dioxide uptake rate on switching from a 32 hr residence time to 4 hr residence time corresponds to the lag phase observed in Figure 5-3 (cell concentration) and Figure 5-4 (redox potential). The lag phase took about 2 to 4 days and during this period the system adapted to the new conditions. There was enhanced growth in the CSTR thereafter and this was indicated by the climb in the carbon dioxide uptake rate.

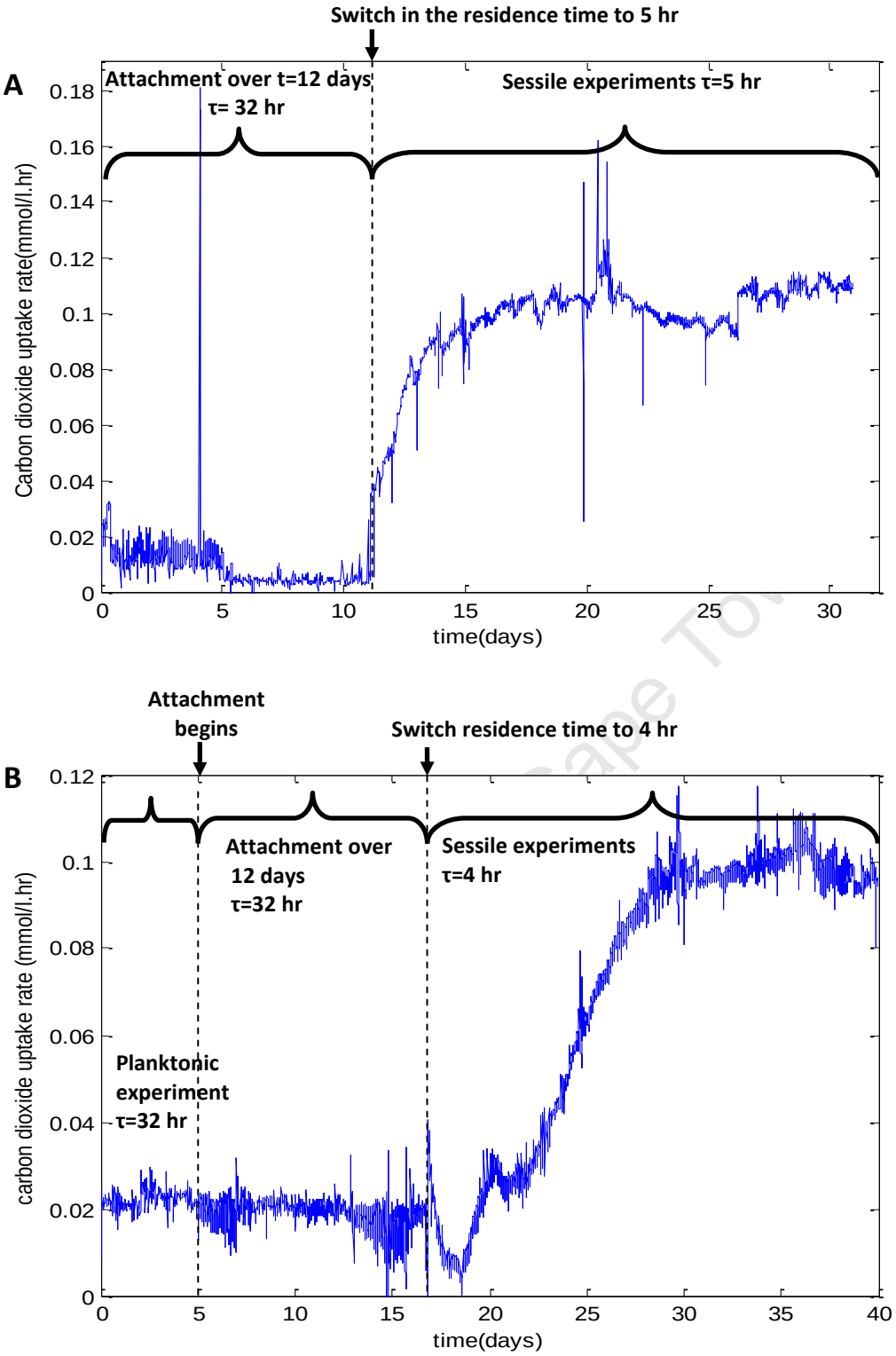

Figure 5-6: (**A**) Rate of CO_2 consumption for residence time (τ) of 5 hr. Data was captured over the attachment period (32 hr residence time) and during the investigation of the sessile population (5 hr residence time). The change in the residence time from 32 hr to 5 hr was on day 12. (**B**) Rate of CO_2 consumption for residence time (τ) of 4 hr. Data was captured over the planktonic period (32 hr residence time), attachment period (32 hr residence time) and during the investigation of the sessile population (4 hr residence time). The change in the residence time from 32 hr to 4 hr was on day 17.

5.3.2.2 Results from the PBR (sessile microbial population on detachment)

At steady state for both sets of experiments, the PBR was disconnected from the CSTR, and using a detachment protocol, the sessile microbial culture was stripped from the surface of the ceramic saddles for data analysis so that the microbial population in the system could be quantified. Figure 5-7 shows the actual numbers of the planktonic microbial population in the CSTR and PBR; and the total number of attached cells in the PBR. This data was obtained from attachment experiments at residence time 32 hr and from sessile experiments at 5 hr and 4 hr residence times.

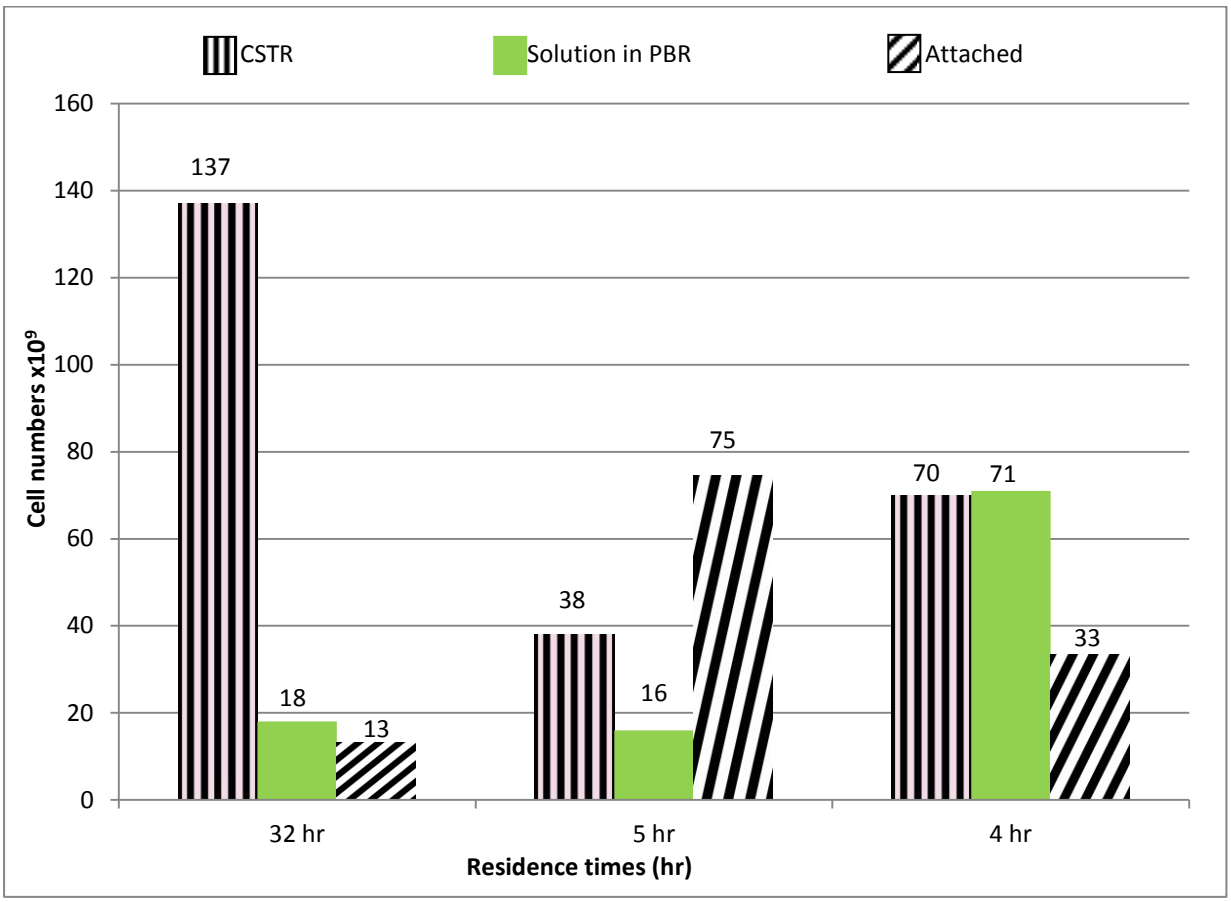

Figure 5-7: Planktonic microbial population in the CSTR and PBR solution; and sessile population attached to ceramic saddles in PBR at the end of experiments at residence times 32 hr, 5 hr and 4 hr.

Figure 5-8 shows the cell concentrations in the CSTR and PBR for residence times 32 hr, 5 hr and 4 hr. Figure 5-9, Figure 5-10 and Figure 5-11 show the % distribution of the microbial population in the CSTR medium, PBR medium and the attached cells in the PBR from sessile experiments conducted at 32 hr, 4 hr and 5 hr residence time.

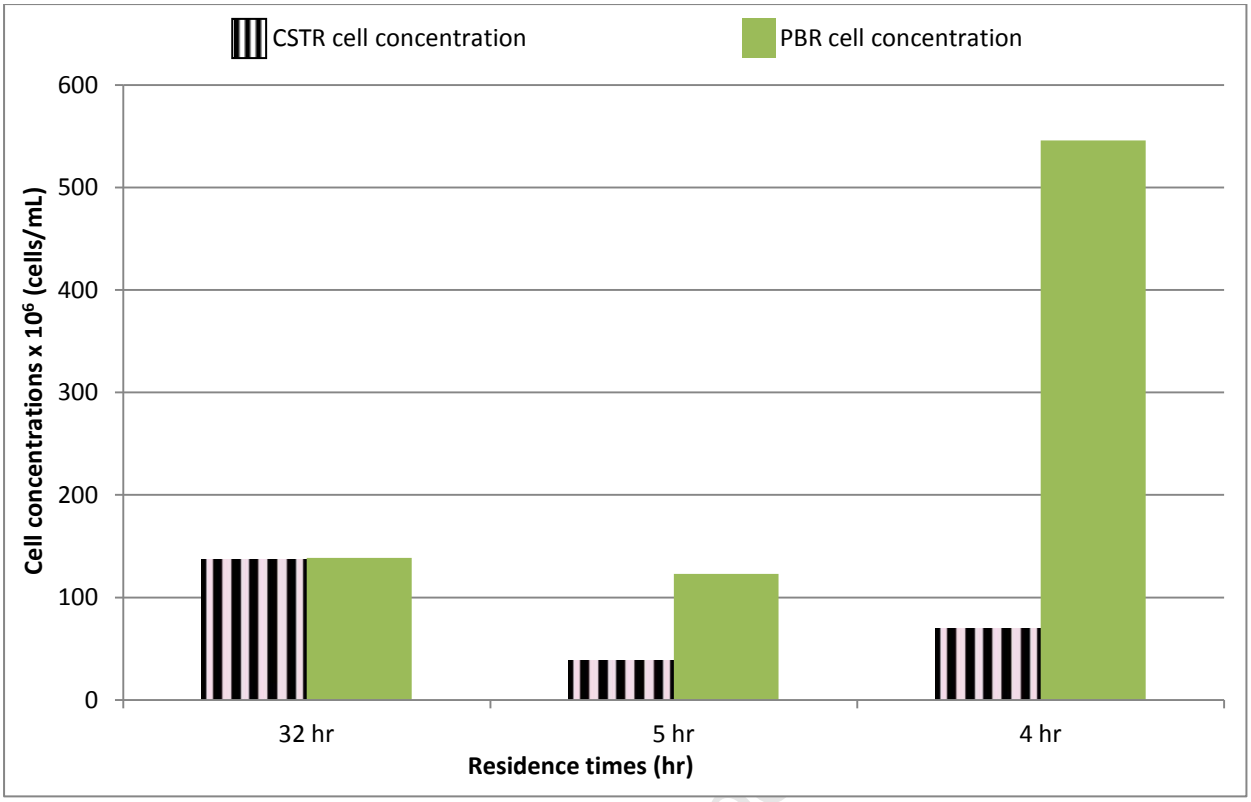

Figure 5-8: The planktonic cell concentrations in the CSTR and PBR medium for residence times 32 hr, 5 hr and 4 hr.

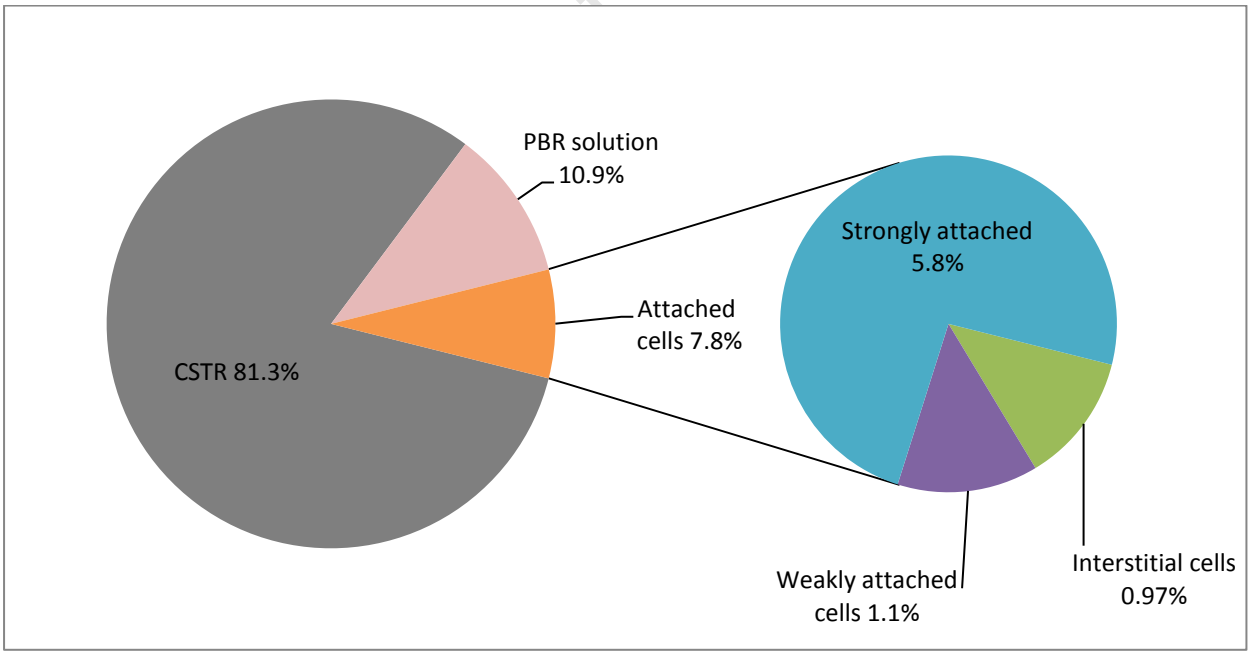

Figure 5-9: Percentage distribution of planktonic cells in the CSTR and PBR medium; and attached cells at the surface of the ceramic saddles in PBR. The packed bed vessel was connected to a CSTR operating at a 32 hr residence time. The total number of cells counted, both planktonic and sessile was 168 x 10^9 cells.

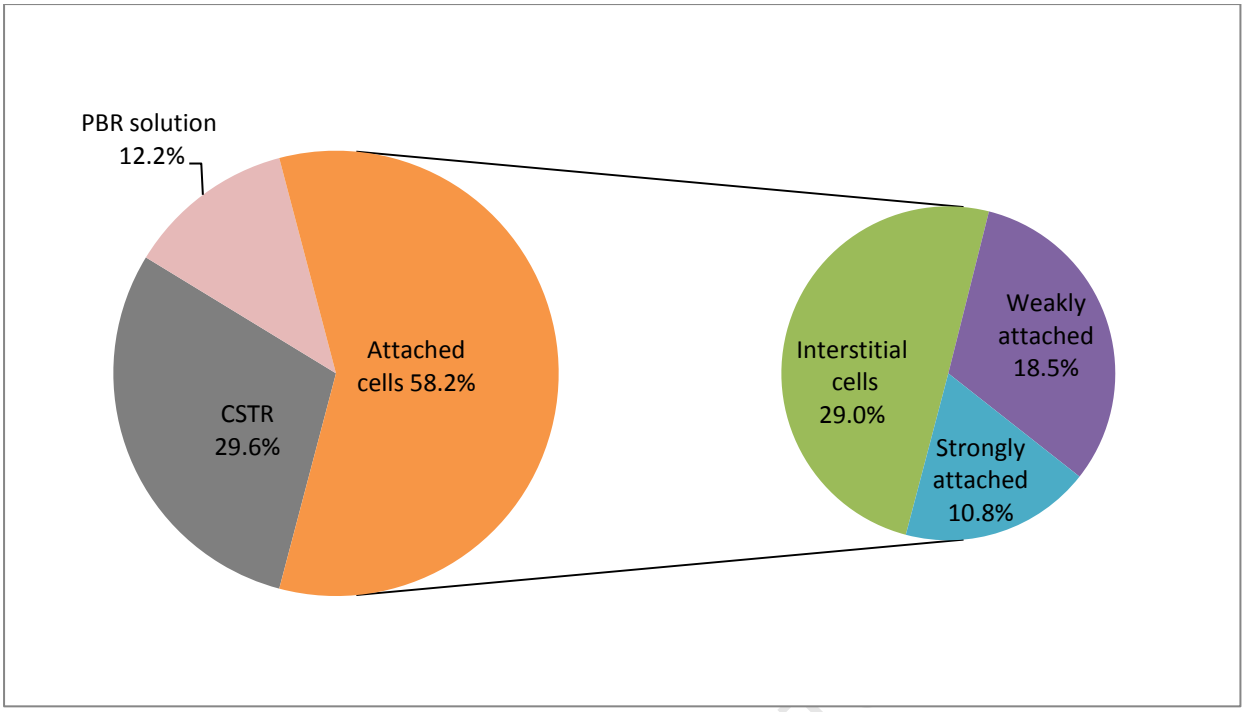

Figure 5-10: Percentage distribution of planktonic cells in the CSTR and PBR medium; and attached cells at the surface of the ceramic saddles in PBR. The packed bed vessel was connected to a CSTR operating at a 5 hr residence time. The total number of cells counted, both planktonic and sessile was 129 x 10^9 cells.

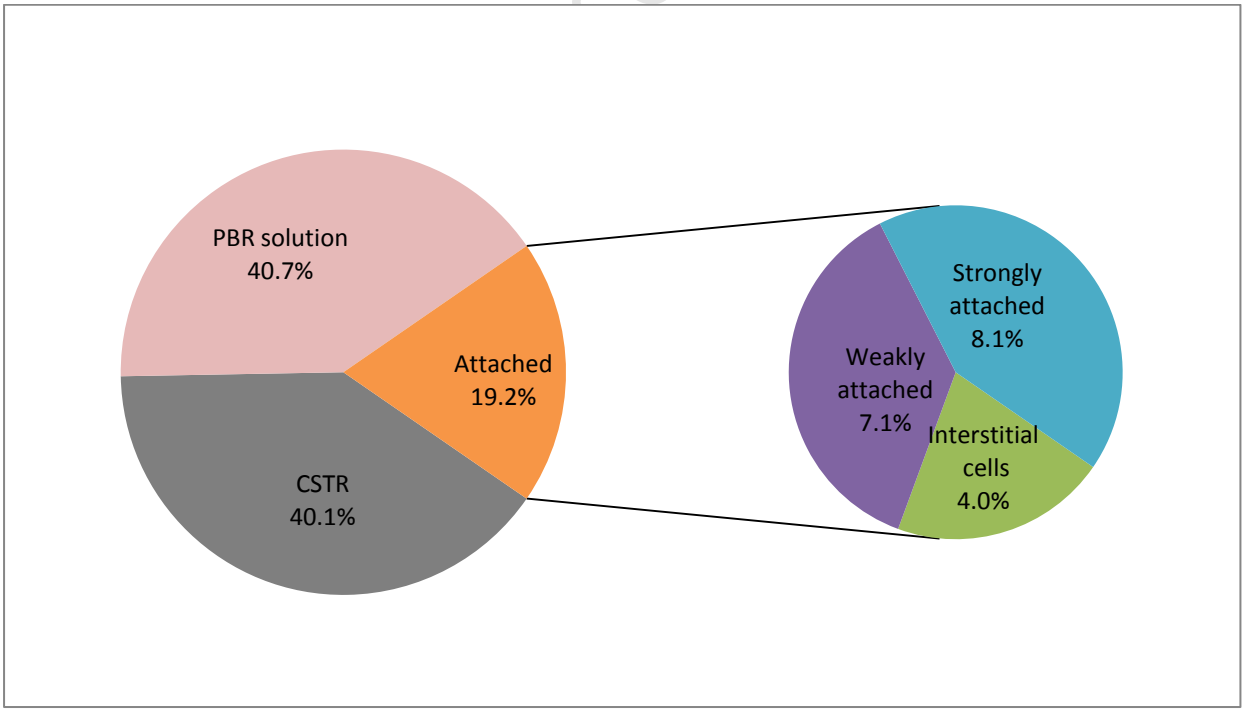

Figure 5-11: Percentage distribution of planktonic cells in the CSTR and PBR medium; and attached cells at the surface of the ceramic saddles in PBR. The packed bed vessel was connected to a CSTR operating at a 4 hr residence time. The total number of cells counted, both planktonic and sessile was 174 x 10^9 cells.

Referring to Figure 5-7, over 50% of the planktonic microbial population present at a 32 hr residence time was washed-out of the CSTR when the residence time was switched to either 5 hr (72% washed-out) of 4 hr (51% washed-out) residence time. On switching the residence time from 32 hr to 5 hr or 4 hr, the planktonic microbial population in the CSTR, dropped from 81.3% to 29.6% and from 81.3% to 40.1% of the total microbial population in the entire system respectively (See Figure 5-9, Figure 5-10 and Figure 5-11). The total number of cells (both sessile and planktonic) in the entire system at 32 hr, 5 hr and 4 hr residence time was 168 x 10^9, 129 x 10^9 and 174 x 10^9 cells respectively. There was no significant change in planktonic cell numbers in the PBR solution at a 5 hr residence times compared to the PBR solution at 32 hr residence time; however at a 4 hr residence time, a 75% increase in the planktonic microbial population numbers of the PBR solution was observed (see Figure 5-7). From this data it is evident that there was no complete wash-out of planktonic cells at residence times 5 hr and 4 hr as was expected due to the effect of wall growth. Generally there was an increase in the growth of attached cells in the PBR at 5 hr and 4 hr residence times. The sessile population increased by 83% and by 61% at a 5 hr and 4 hr residence time respectively.

During the investigation, a pump operating at its maximum (8.6 L.day^{-1}) was used to transfer the culture medium from the CSTR to the PBR. The recycle ratio (flow rate of culture out of the CSTR through the glass vessel: the flow rate of the fresh feed into the CSTR) was 11.5 at 32 hr residence time, 1.79 at 5 hr residence time and 1.43 at 4 hr residence time. It is important to keep this ratio as high as possible so that the conditions in the CSTR solution were similar to that in the PBR solution. This is a necessary condition for determining the microbial kinetics of the system as a whole. At uniform conditions, microbial kinetics from the PBR system could be determined using data captured from analyzing the CSTR samples. Given the low recycle ratios used, this was, however, not accurate for the experiments at residence time 4 hr and 5 hr. Figure 5-8 presents the cell concentrations in both the CSTR medium and the PBR solution at residence times 32 hr, 5 hr and 4 hr. At 32 hr residence time, the cell concentration of planktonic microorganisms in the in the PBR solution was similar to the cell concentration in CSTR solution (cell concentration in the PBR only 1% higher than cell concentration in the CSTR which can be assumed to be a negligible difference) because of a high 11.5 recycle ratio. At 5 hr and 4 hr residence times where the recycle ratios were smaller, the cell concentrations in the PBR solution were observed to be much higher compared to the cell concentrations in the CSTR. At 5 hr and 4 hr residence times, the cell concentration in the PBR increased by 69% and 87% respectively after the switch from a 32 hr residence time. A lower recycle ratio resulted in different conditions between the CSTR and the PBR solutions due to substrate

(ferrous iron) limitations in the system. Steady state in the PBR was different to the steady state in the CSTR. In the PBR solution, the redox potential was above 700 mV at both 5 hr and 4 hr residence times showing that ferrous iron was limiting. The redox potential in the CSTR on the contrary was 533 and 488 mV for the 5 hr and 4 hr residence times respectively showing that ferrous iron was still not limiting. More ferrous iron was required in the PBR to overcome the ferrous iron limitation and this could only be achieved by increasing the recycle ratio.

5.3.3 Discussion and conclusions

Table 5-1 gives a summary of all the results determined from investigating the kinetics of the planktonic microbial population vs. the kinetics of the sessile microbial population. There was no complete wash-out of planktonic cells from the CSTR due to the effect of wall growth. The activity of the sessile microbial population was investigated at residence times 5 hr and 4 hr where ferrous iron was not limiting.

At steady state for 4 hr and 5 hr residence times, the redox potential of the CSTR solution was 501 mV and 475 mV respectively during planktonic experiments. During sessile experiments, the redox potential in the CSTR increased slightly to 533 mV and 488 mV for 5 hr and 4 hr residence times respectively as a result of an extra 9% of ferrous iron being oxidized in the system. This confirms the growth of the microbial population in the system. Sessile experiments took longer to reach steady state compared to planktonic experiments. Steady state was reached after 3 residence times during planktonic experiments however, this varied in the sessile experiments. At 5 hr and 4 hr residence time, steady state was reached after 63-72 residence times and 102-114 residence times respectively.

During sessile experiments, the carbon dioxide uptake rates increased when the residence time was switched from 32 hr to either 5 hr or 4 hr residence times. At a 5 hr residence time, an instantaneous increase in the carbon dioxide uptake rate was observed and steady state was reached at 0.110 $mmolC.L^{-1}.hr^{-1}$. This sudden jump in the carbon dioxide uptake rate was as a result of microbial growth in the reactor system. More ferrous iron was pumped into the CSTR after the switch from a 32 hr residence time therefore there was more ferrous iron in the reactor system for growth. The jump was therefore as a result of the removal of the ferrous iron limitation. The growth of cells attached to the walls in the CSTR may have also contributed to this jump.

Table 5-1: Overall summary of results comparing kinetic data of planktonic experiments at steady state to kinetic data of sessile experiments at steady state (CSTR operating at 5 hr and 4 hr residence times). Note that the cell concentration of planktonic cells in the CSTR refers to free cells in the reactor only (does not account for wall growth); the total number of cells in the PBR includes the free cell in solution (planktonic), interstitial cells, weakly attached and strongly attached cells (the sessile population attached to the surface of the ceramic beads). Error was determined as the standard deviation vs. the sqrt (number of samples n) (error = standard deviation/√n).

	τ = 5hr Planktonic experiments	**τ = 4hr Planktonic experiments**	**τ = 5hr Sessile experiments**	**τ = 4hr Sessile experiments**
Dilution rate (hr^{-1})	0.200	0.250	0.200	0.250
E_h measured in CSTR (mV)	501	475	533	488
E_h measured in PBR (mV)	*	*	705	720
Residence times (τ) to steady state	3 τ	3 τ	63 - 72 τ	102 – 114 τ
Cell concentration of planktonic cells in CSTR ($cells.mL^{-1}$)	16.0×10^6	11.0×10^6	38.0×10^6	70.0×10^6
Cell concentration of planktonic cells in PBR solution ($cells.mL^{-1}$)	*	*	123×10^6	546×10^6
Total number of planktonic cells in CSTR	16.0×10^9	11.0×10^9	38.0×10^9	70.0×10^9
Total number of cells in PBR (both planktonic and sessile)	*	*	91.0×10^9	104×10^9
rCO_2 (off gas)($mmolC.L^{-1}.hr^{-1}$)	0.0914 ± 0.00028	0.0952 ± 0.00034	0.110 ± 3.8E-05	0.0990 ± 6.32E-05
rFe^{2+}($mmol.L^{-1}.hr^{-1}$)	16.6	16.7	17.4	18.0
q'Fe^{2+}ratio [rFe^{2+} : rCO_2] ($mmolFe.\ hr.\ mmolC^{-1}$)	182	175	158	182

*no glass vessel attached during experiment

The solubility of carbon dioxide was insignificant and did not contribute much to the jump in the carbon dioxide uptake rate during the switch. At a 4 hr residence time, there was a lag phase in the system in the first 2-4 days after the switch from 32 hr residence time. This may have been as a result of an initial wash-out of cells in the system during that period resulting in an initial decline in the carbon dioxide uptake rate. The system however recovered and the carbon dioxide uptake rate increased dramatically due to microbial growth.

During attachment experiments, the cell concentration in the CSTR at 32 hr residence time was found to be the same as the cell concentration in the PBR due to the high recycle ratio (11.5). The redox potential in both the PBR and CSTR solutions were also above 700 mV. The analysis of the samples obtained from the CSTR could therefore be assumed to represent activity in the PBR. At residence times 5 hr and 4 hr, the recycle ratios were much smaller (1.8 and 1.4 respectively) resulting in differences between the conditions (cell concentration and redox potential) in the CSTR solution to that in the PBR solution. Samples collected from the CSTR could therefore not be assumed to represent the conditions in the PBR and the kinetic in the PBR could therefore not be determined accurately. At a low recycle ratio the CSTR and the PBR were independent of each other and could not be assumed to be one whole system. Since the CSTR and the PBR were independent of each other the PBR had an insignificant effect on the kinetics of the entire system due to the low recycle ratios.

In order to use the relationship for determining the specific ferrous iron oxidation rate (qFe^{2+}) as reported in Section 3.6.3 (Equation 3-14), cell attachment in the reactor has to be negligible such that there is no accumulation of biomass. The biomass could be calculated using the carbon dioxide uptake rate and dilution rate. During sessile experiments, there was cell attachment and therefore accumulation of biomass in the system. Due to the effect of wall growth, the accumulation of biomass was also significant during planktonic experiments. qFe^{2+}could therefore not be calculated based on Equation 3-14 as the accumulation of biomass in the system could not be overlooked. For this study, the ferrous iron oxidation rate was therefore related to the carbon dioxide uptake rate as a ratio ($q'Fe^{2+} = rFe^{2+}: rCO_2$) for the purpose of comparing the data from the planktonic and sessile systems. Comparing the planktonic and sessile $q'Fe^{2+}$ratio (see Table 5-1) at a 5 hr residence time, there was 13% difference between the two systems. At a 4 hr residence time, the difference in the $q'Fe^{2+}$ratio was 4%. There was therefore a small difference in the $q'Fe^{2+}$ratio between planktonic and sessile experiments possibly because the PBR did not influence the CSTR significantly due to ferrous iron limitations caused by the low recycle ratio. An experiment at 5 hr residence times was

repeated at a higher recycle ratio to observe if there would still be any difference in the q'Fe^{2+}ratio. A high recycle ratio would decrease the residence time in the PBR and therefore allow for uniform conditions in the CSTR and the PBR. The results are reported in section 5.4.

5.4 Sessile microbial culture experiments (II)

5.4.1 Comparison of results of sessile experiments at 5 hr residence times using a low recycle ratio (1.8) and a high recycle ratio (21)

5.4.1.1 Results from the continuous stirred tank reactor (CSTR)

A sessile experiment with the CSTR operating at a 5 hr residence time was repeated using a higher recycle ratio (flow rate of culture out of the CSTR through the PBR: the flow rate of the fresh feed into the CSTR) of 21 from 1.8 (low recycle ratio). This was done by using bigger size tubing compared to the previous experiments on a pump operating at its highest capacity. Increasing the recycle ratio, meant the residence time in the PBR was shortened therefore allowing for similar conditions in the PBR and the CSTR. This was important to achieve so that the CSTR + PBR system were considered as one system. Samples for data analysis were taken from the CSTR and were representative of the solution in the PBR but this was true only in the event that the two vessels had uniform conditions. Figure 5-12 shows the cell concentration of planktonic cells in the CSTR from a system operating at both a low and high recycle ratio.

Generally, on switching the residence time, most of the planktonic cells were washed out of the CSTR by day 1. The cell concentration dropped from 168 to 11 x 10^6 cells.mL^{-1} at a low recycle ratio and from 123 to 28 x 10^6 cells.mL^{-1} at a high recycle ratio. There was an immediate increase in the cell concentration for both experiments after day 1 and a steady state was achieved by day 13 corresponding to 63 residence times when running at a low recycle ratio. This however was not the case at a higher recycle ratio. The cell concentration was observed to fluctuate significantly and did not appear to reach a steady state; however further analysis of the data, showed there was possible off-set data of which when eliminated line 'a' was determined. Assuming this was true, the system did reach a steady state after approximately 10 days. Planktonic microorganisms were never completely removed from the system during both experiments. This may have been contributed by the effect of wall growth as discussed in chapter 4 or due to the growth of microorganisms in the PBR that were being pumped continuously to the CSTR.

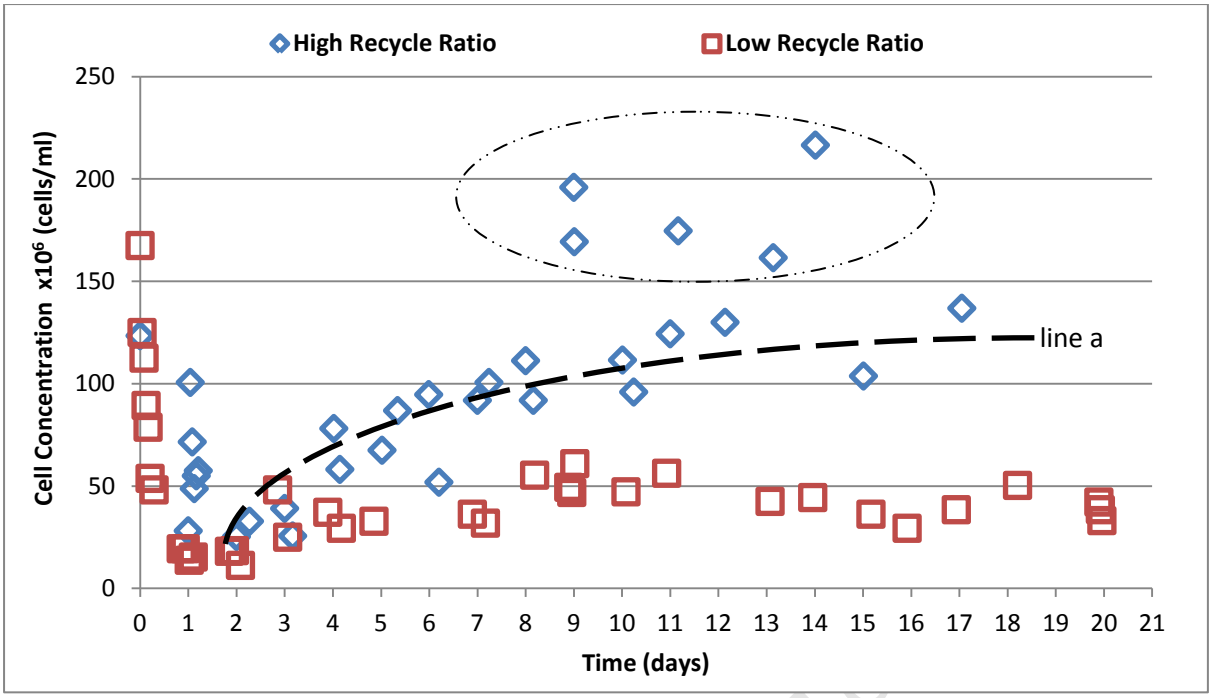

Figure 5-12: Cell concentration in the CSTR versus time at high and low recycle ratios. The residence time was switched from 32 hr to 5 hr and this switch was at t_0 on Figure 5-12. line 'a' ——— shows the proposed trend of the cell concentration which eliminates the offset data encompassed by the circle.

In section 5.3.2.2 it was reported that the concentration of microorganisms in the PBR was much higher than in the CSTR for operations at both 4 hr and 5 hr residence times (at low recycle ratios) but this did not have a significant effect on the cell concentration in the CSTR as the recycle ratio was too low. The availability of ferrous iron in the PBR was a limitation at a low recycle ratio. On increasing the recycle ratio however, the rate at which ferrous iron was pumped into the PBR increased which resulted in the increased number of cells in the system.

Figure 5-13 shows the redox potential and the ferric: ferrous iron ratio measured from experiments using both a low and high recycle ratio. The redox potential was observed to decrease to its lowest by day 1, a similar correlation to the cell concentration shown on Figure 5-12. This was from 730 mV to 440 mV at a low recycle ratio and from 729 mV to 439 mV at a higher recycle ratio. Steady state was achieved by day 13 when operating at the low recycle ratio and this decreased to 6 days at a higher recycle ratio. This corresponded to 63 residence times and 29 residence times respectively. At steady state, 94% of the ferrous iron was converted to ferric iron (533 mV) at low recycle ratio and 98% of ferrous iron was converted to ferric iron (566 mV) at a high recycle ratio.

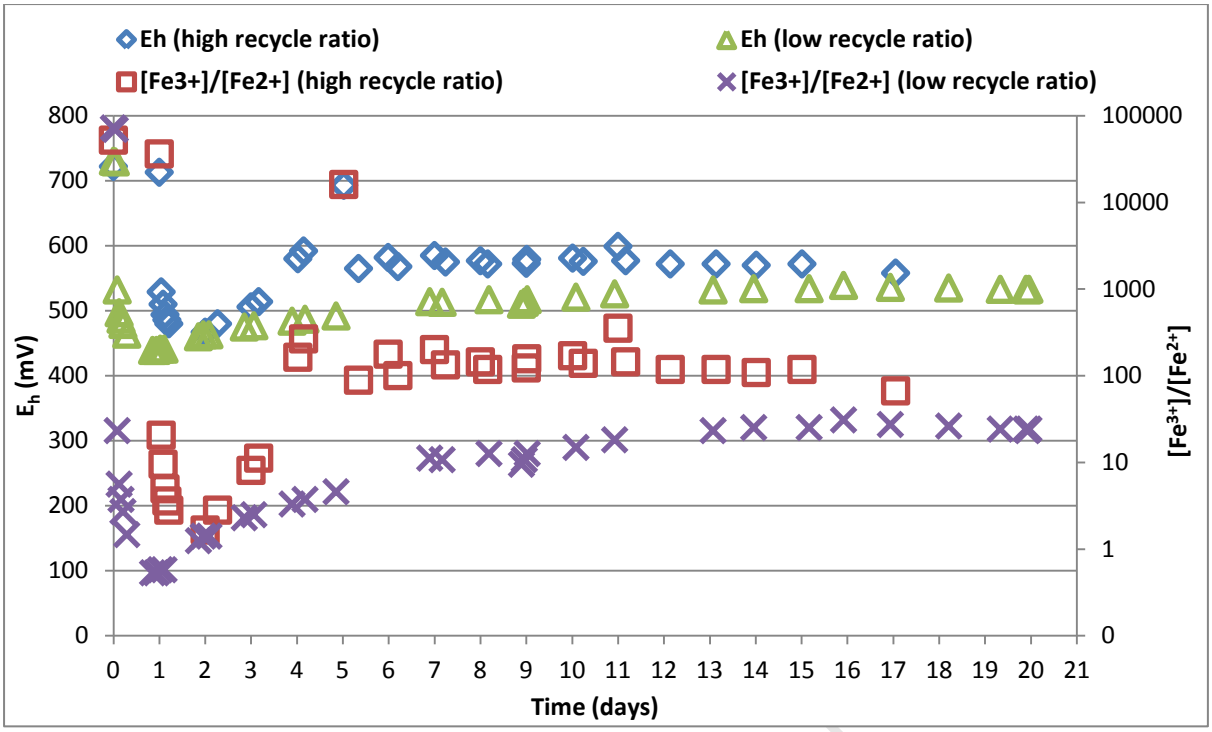

Figure 5-13: Redox potential and ferric to ferrous iron ratio measurements from the CSTR at high and low recycle ratios. The residence time was switched from 32 hr to 5 hr and this switch was at t_0 on Figure 5-13.

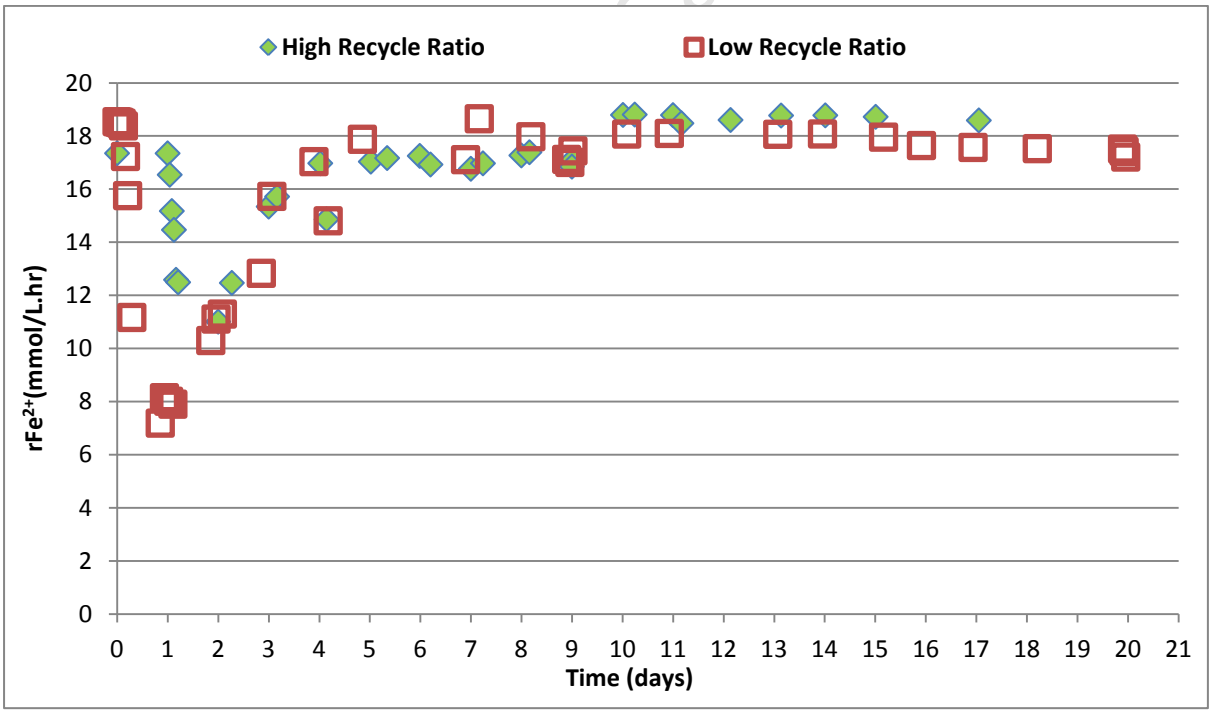

Figure 5-14: Comparing ferrous iron consumption in the CSTR versus time at high and low recycle ratios. The residence time was switched from 32 hr to 5 hr and this switch was at t_0 on Figure 5-14.

Figure 5-14 shows the ferrous iron oxidation rate. The rate decreased to 7.19 and 12.6 mmol $Fe^{2+}.L^{-1}.hr^{-1}$ by day 1 and steady state was achieved on day 13 (63 residence times) and day 10 (48

residence times) at a low and high recycle ratio respectively. At steady state, the ferrous iron oxidation rates were 17.7 and 18.7 mmol.L^{-1}.hr^{-1} at a low and high recycle ratio respectively.

The carbon dioxide uptake rates determined from both experiments using either a high (graph 1) or low (graph 2) recycle ratio are shown on Figure 5-15.

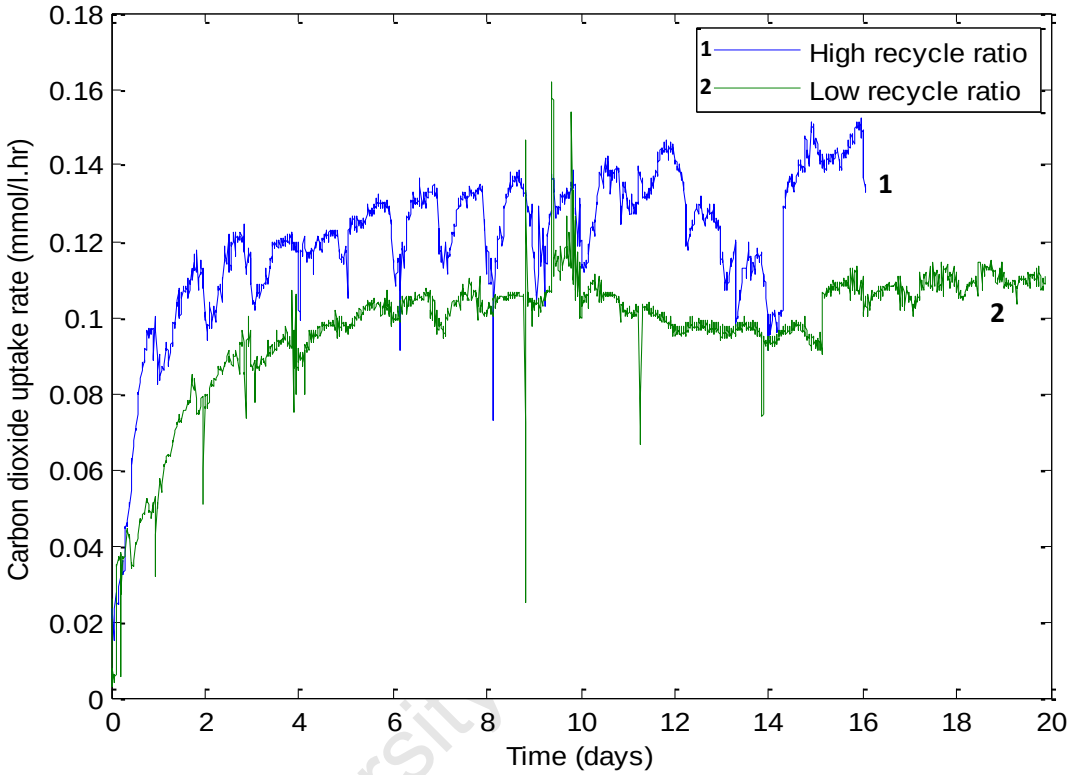

Figure 5-15: Carbon dioxide uptake in the CSTR versus time at high (1) and low (2) recycle ratios. The residence time was switched from 32 hr to 5 hr and this switch was at t_0 on Figure 5-15. Graph 1 represents the carbon dioxide uptake rate obtained using a high recycle ratio and graph 2 represents the carbon dioxide uptake rate obtained using a low recycle ratio.

On switching the residence time from a 32 hr residence time to 5 hr residence time, there was an instantaneous increase in the carbon dioxide uptake rates. The jump in the carbon dioxide uptake rate at a high recycle ratio was faster than at the low recycle ratio. At steady state, the carbon dioxide uptake rates were determined to be 0.110 mmol CO_2 $l^{-1}hr^{-1}$ at the low recycle ratio and 0.142 mmol CO_2 $l^{-1}hr^{-1}$ at the high recycle ratio. Once steady state was achieved in the CSTR for both experiments running at a low and high recycle ratio, the PBR was detached from the CSTR and a detachment protocol was followed to quantify the sessile microbial population from the surface of the ceramic beads. Section 5.4.1.2 presents the results obtained.

5.4.1.2 Results from the packed bed vessel (PBR)

Figure 5-16 shows a comparison of the microbial population (both planktonic and sessile) for both experiments using either a low or a high recycle ratio. Increasing the recycle ratio influenced the growth of both the planktonic and sessile microbial population (Growth tripled).

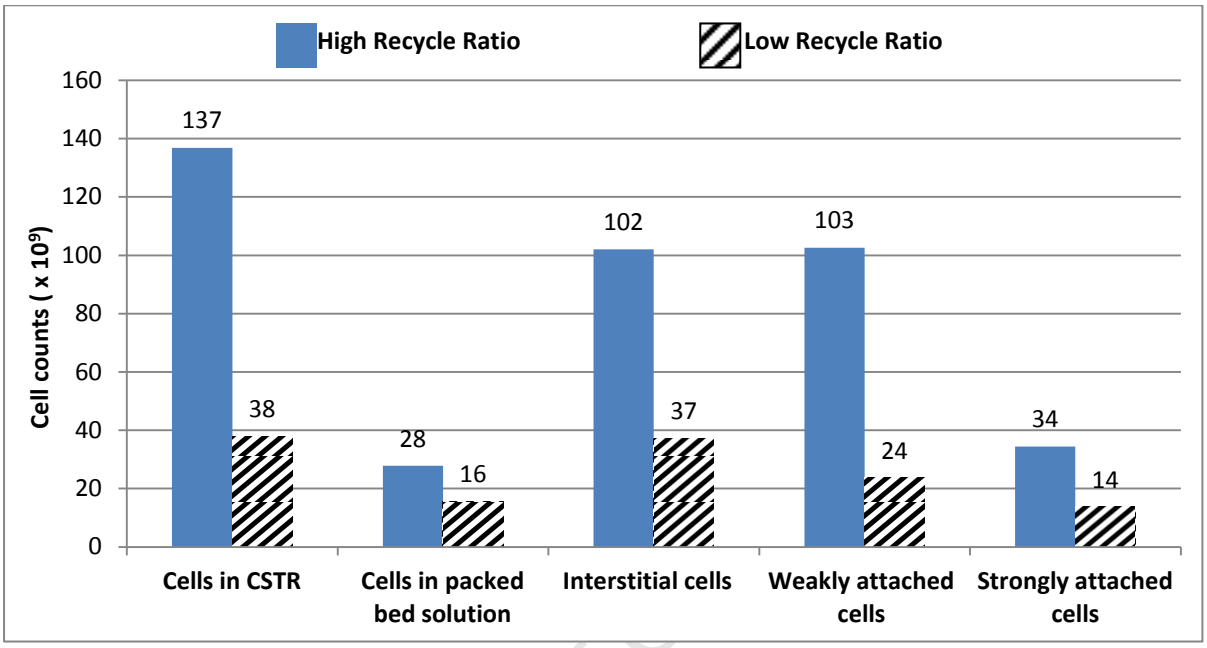

Figure 5-16: Total number of cells in the CSTR, PBR and cells attached to the surface of the ceramic beads (interstitial cells, weakly attached cells and strongly attached cells). Detachment was done at the end of the sessile experiments once steady state in the CSTR was achieved.

Figure 5-17 and Figure 5-18 show the percentage distribution of the microbial population in the CTSR, PBR and attached cells when using a high and low recycle ratio respectively. Despite a substantial increase in the microbial population when the recycle ratio was increased (see Figure 5-16), there were similarities in the distribution of microorganisms in the system for both experiments. The proportions remained almost the same with very few variations. 41-42% of the microbial population were planktonic and the rest of the microbial population in the system were sessile (58-59%). The majority of the sessile population, however, was not firmly attached (14-18%) with the remaining 82-86% being either weakly attached or in the interstitial phase.

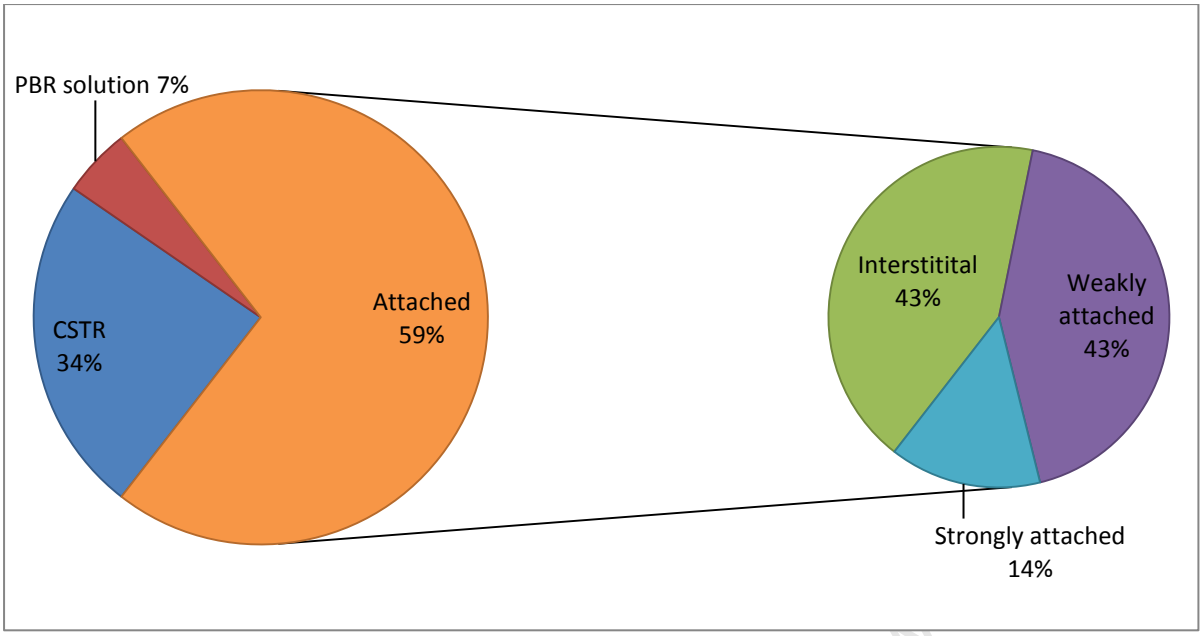

Figure 5-17: Percentage distribution of planktonic and sessile cells within the system at high recycle ratio. The total number of cells counted, both planktonic and sessile was 404 x 10^9 cells.

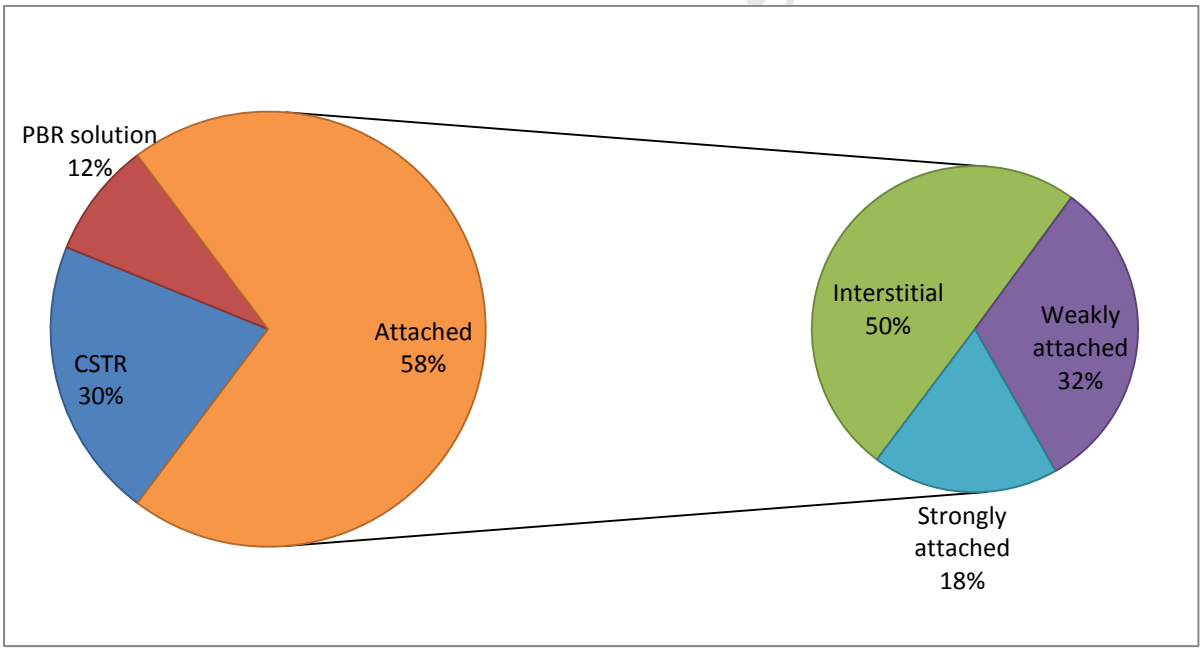

Figure 5-18: Percentage distribution of planktonic and sessile cells within the system at low recycle ratio. The total number of cells counted, both planktonic and sessile was 129 x 10^9 cells.

The increase in the microbial population explains the higher redox potential as well as the higher planktonic microbial population in the CSTR at a higher recycle ratio. Fluctuations of the cell concentration in the CSTR at the high recycle ratio may have been as a result of the many weakly

attached cells/interstitial cells now more easily being washed-out of the PBR due to the higher flowrates through the PBR.

Comparing the cell concentration of planktonic cells in the CSTR relative to the cell concentration in the PBR, there was a huge difference in the conditions between the two environments at a low recycle ratio. On increasing the recycle ratio, a significant difference was still observed, however, when compared to the lower recycle ratio there was an improvement. At a low recycle ratio the cell concentration was 3.2 times higher in the PBR than in the CSTR and this decreased to 1.6 at a higher recycle ratio. The redox potentials in the PBR for both experiments were much higher at 700 and 720 mV when compared to the redox potential in the CSTR; 533 and 566 mV at low and high recycle ratios respectively. The high redox potential values (above 700 mV) in the packed bed vessel are typically what should be expected of *Leptospirillum ferriphilum*.

5.4.2 Discussion and conclusions

Table 5-2 gives a summary of the results obtained from this study. Increasing the recycle ratio from 1.8 to 21 for sessile experiments at 5 hrs residence times did not achieve the goal of sustaining similar conditions between the CSTR and the PBR. The redox potential in the PBR differed to the redox potential in the CSTR and there was also a large population of microorganisms in the solution contained in the PBR relative to the liquid medium in the CSTR. The sessile population in the PBR may have reached a steady state due to ferrous iron limitations (ferrous iron was rate limiting again). The difference in cell concentrations however was narrowed down from 3.2 times to 1.6 times more cells in the packed bed vessel compared to the CSTR and it is possible that if an even much higher recycle ratio was used, then the two systems would eventually have had the same conditions and therefore be considered as one system.

The planktonic microbial population in the CSTR at steady after experiment using a high recycle ratio was three times higher than the microbial population from experiments using a low recycle ratio. The majority of cells in the PBR were either weakly attached or interstitial cells therefore they could easily be transferred from the PBR to the CSTR. This may have contributed to the higher planktonic microbial population in the CSTR at a high recycle ratio. The carbon dioxide uptake rate at a higher recycle ratio was higher (0.142 $mmolCO_2.L^{-1}.hr^{-1}$) than the carbon dioxide uptake rate at a lower recycle ratio (0.110 $mmolCO_2.L^{-1}.hr^{-1}$) as result of the increased microbial growth.

Table 5-2: Overall summary of results comparing kinetic data of planktonic experiments at steady state to kinetic data of sessile experiments at steady state (CSTR operating at 5 hr (**for both low and high recycle ratio**) and 4 hr residence times). Note that the cell concentration of planktonic cells in the CSTR refers to free cells in the reactor only (does not account for wall growth); the total number of cells in the PBR includes the free cell in solution (planktonic), interstitial cells, weakly attached and strongly attached cells (the sessile population attached to the surface of the ceramic beads). Error was determined as the standard deviation vs. the sqrt (number of samples n) (error = standard deviation/√n).

	τ = 5hr Planktonic Experiments	**τ = 4hr Planktonic Experiments**	**τ = 5hr Sessile Experiments (Low recycle ratio)**	**τ = 4hr Sessile Experiments**	**τ = 5hr Sessile Experiments (High recycle ratio)**
Dilution rate (hr^{-1})	0.200	0.250	0.200	0.250	0.200
E_h measured in CSTR (mV)	501	475	533	488	566
E_h measured in PBR (mV)	*	*	700	720	720
Residence times (τ) to steady state	3 τ	3 τ	63 - 72 τ	102 – 114 τ	29 - 48 τ
Cell concentration of planktonic cells in CSTR ($cells.mL^{-1}$)	16.0×10^6	11.0×10^6	38.0×10^6	70.0×10^6	137×10^6
Cell concentration of planktonic cells in PBR solution ($cells.mL^{-1}$)	*	*	123×10^6	546×10^6	214×10^6
Total number of planktonic cells in CSTR	16.0×10^9	11.0×10^9	38.0×10^9	70.0×10^9	137×10^9
Total number of cells in PBR (both planktonic and sessile)	*	*	91.0×10^9	104×10^9	267×10^9
rCO_2 (off gas)($mmolC.L^{-1}.hr^{-1}$)	0.0914 ± 0.00028	0.0952 ± 0.00034	0.110 ± 3.8E-05	0.0990 ± 6.32E-05	0.142 ± 6.32E-05
rFe^{2+}($mmol.L^{-1}.hr^{-1}$)	16.6	16.7	17.4	18.0	18.7
q'Fe^{2+}ratio [rFe^{2+} : rCO_2] ($mmolFe.\ hr.\ mmolC^{-1}$)	182	175	158	182	132

*no glass vessel attached during experiment

The q'Fe^{2+}ratio (see Table 5-2) at a 5 hr residence time with high recycle ratio, decreased by 27% compared to the planktonic experiment at a 5 hr residence time. Although during these experiments, the planktonic population was not completely eliminated from the system and no uniform conditions between the packed bed vessel and the CSTR were achieved, increasing the recycle ratio had an effect on the q'Fe^{2+}ratio. When the recycle ratio was increased the difference between the conditions in the CSTR and the PBR decreased. This change in the recycle ratio had an effect on the kinetics of the system. Increasing the recycle ratio from 1.8 to 21 decreased the q'Fe^{2+}ratio from 182 to 132 mmolFe.hr/mmolC which differed to what was determined from planktonic experiments. To achieve uniform conditions between the packed bed vessel and the CSTR, a bigger pump would be necessary to further increase the recycle ratio.

6 Overall discussion

This study set out to develop a strategy that would allow for the determination of ferrous iron oxidation kinetics catalysed by a sessile microbial population as a function of population size, availability of ferrous iron and culture conditions. In order to achieve this; three sets of experiments investigating the growth kinetics of a planktonic *Leptospirillum ferriphilum* microbial population, the attachment of these microorganisms and finally the growth kinetics of a sessile *Leptospirillum ferriphilum* microbial population were performed. Planktonic experiments were conducted using a continuous stirred tank reactor (CSTR) set-up and attachment and sessile experiments were conducted in a CSTR + PBR (packed bed vessel) set up. The advantage of using a CSTR was that the culture was well mixed and steady state could easily be achieved at specific conditons. The sessile population was contained in the PBR which was attached to the CSTR as a closed loop system. All samples for data analysis were collected from the CSTR, therefore in the case of the sessile experiments, it was important that the conditions in the CSTR were similar to that in the PBR for accurate results.

Data generated from the planktonic experiments was required as a benchmark for comparison to data obtained from investigating the activity of the sessile microbial population. It was also important to determine the critical dilution rate where planktonic microorganisms ideally, based on Monod type behaviour, were completely washed-out from the CSTR system. After the actual experimentation on data analysis, it was discovered that there was wall growth in the CSTR which caused a deviation from ideal Monod behaviour. Ideally, the maximum growth rate is the same as the critical dilution rate. In the event that there is wall growth in the system, the critical dilution rate tends to be greater than the maximum growth rate, therefore washout occurs at higher dilution rates. In this study, the washout of planktonic microorganisms was never achieved due to the effect of wall growth. It was however determined that if wall growth had been negligible then the wash-out of planktonic cells would have occurred between residence times of 12-14 hr. There were two microbial populations which dominated the CSTR system. The planktonic microbial population dominated between 55 hr to 12 hr residence times below which they were mostly washed-out. At lower residence times there was shift and the microorganisms growing on the CSTR walls took over to dominate the system between residence times 4 to 12 hr. It was postulated that if wash-out were to eventually occur in the system, this would have happened at a critical dilution rate of 0.34 hr^{-1}. Since there was no wash-out, sessile experiments were conducted at 4 hrs and 5 hrs residence times where ferrous iron was not found to be limiting – at least not initially.

Prior to carrying out sessile experiments it was important to understand the nature of attachment of the microbial population. From attachment experiments, it could be determined whether microbial growth reached a steady state or otherwise was in a transient state. The CSTR was operated at a 32 hr residence time and the recycle ratio (flow rate of medium cycled through the packed bed vessel: flowrate of medium through the CSTR) was 11.5 for all experiments. The high recycle ratio ensured that the conditions in the CSTR were similar to that in the PBR. From the investigation, the majority of the microbial population was attached to the ceramic saddles by day 2 and reached a steady state. On average 106 x 10^6 cells per g of ceramic saddles were attached of which 87% were firmly attached. Sessile experiments followed once attachment was achieved after a 12 day period at 4 hr and 5 hr residence times.

Sessile experiments were first conducted at both 4 hr and 5 hr residence times with recycle ratios at 1.4 and 1.8, respectively. There was generally increased growth of the microbial population in the system relative to the 32 hr experiment. During attachment experiments conducted at a 32 hr residence time, the recycle ratio was 11.5 and the planktonic cell concentrations in the CSTR and the PBR mediums were on average the same at 137 x 10^6 and 138 x 10^6 cells/mL respectively. At a 5 hr and 4 hr residence time with 1.8 and 1.4 recycle ratios respectively, the cell concentrations and redox potential measurements between the CSTR and PBR solutions differed (**5hrs** {CSTR-38 x 10^6 cells.mL^{-1} and 533 mV/ packed bed vessel-123 x 10^6 cells.mL^{-1} and 700 mV}; **4hrs** {CSTR-70 x 10^6 cells.mL^{-1} and 488 mV/ packed bed vessel-546 x 10^6 cells.mL^{-1} and 700 mV}). It was observed that there were ferrous iron limitations in the PBR and a steady state was reached at those conditions which differed to the steady state conditions in the CSTR. The two vessels could not be considered to be one whole system if there were differences in the solution conditions. Microbial kinetics of the sessile population therefore could not be accurately determined as samples from the CSTR were used as a representative of a sample in the PBR.

During planktonic experiment, there was wall growth in the reactor system and during sessile growth experiments, there was an accumulation of biomass in the PBR. The specific ferrous iron oxidizing rate, usually determined from a mass balance around the system could not be accurately calculated as there was an accumulation of biomass in all reactor systems. A q'Fe^{2+}ratio which is the rFe^{2+} : rCO_2 was therefore used in this study, to compare the kinetic data obtained from sessile experiments to that from planktonic experiments. Relative to planktonic experiments, the q'Fe^{2+}ratio decreased by 13% at a 5 hr residence time and increased by 4% at a 4 hr residence time (**5 hr** {planktonic-182 mmolFe.hr/mmolC / sessile-158 mmolFe.hr/mmolC}; **4 hr** {planktonic-175

mmolFe.hr/mmolC/ sessile-182 mmolFe.hr/mmolC}). These small differences between the q'Fe^{2+}ratio from planktonic and sessile experimental data indicated that the PBR had very little influence on the system.

An experiment at a 5 hr residence times was repeated, using a higher recycle ratio (recycle ratio was stepped up from 1.8 to 21) to remove the ferrous iron limitations in the PBR and therefore narrow the difference in the conditions of the CSTR and PBR. There was increased growth (69%) of the microbial population in the reactor system. Conditions between the PBR and CSTR were still observed to be different. At a low recycle ratio, the cell concentration in the PBR was 3.2 times more relative to that in the CSTR but this decreased to 1.6 on increasing the ratio. The q'Fe^{2+}ratio also decreased as a result of increasing the recycle ratio from 182 to 132 mmolFe.hr/mmolC (27% decrease). At a low recycle ratio the q'Fe^{2+} had decreased by 13%. This shows that although increasing the recycle ratio did not achieve homogenous conditions between the PBR and CSTR solution, it did have an effect on the q'Fe^{2+} ratio. Increasing the recycle ratio further would probably reduce on the differences between the PBR and CSTR by removing ferrous iron limitations and thereby allow for homogeneity between the PBR and CSTR solution conditions.

7 Overall conclusions and recommendations

7.1 Conclusions

This study was aimed at determining a strategy that allows the kinetics of ferrous iron oxidation catalysed by a sessile microbial population to be determined as a function of population size, availability of ferrous iron, and culture conditions. The conclusions drawn from this study are listed below and address the key questions in Section 2.5.3:

- Prior to investigating sessile microbial kinetics, it was important to carry out experiments on the planktonic population for use as a benchmark for comparison to the sessile experiments. It was also necessary to determine the critical dilution rate of the system where wash-out occurred so that sessile experiments were independent of the planktonic population. During planktonic experiments, the critical dilution rate of the system could not be determined as there was no complete wash-out of planktonic cells from the reactor system. This was due to the effect of wall growth. Based on the extrapolation of data of the cell concentrations, the maximum growth rate and biomass from off-gas data, it was shown that if the system followed a Monod type trend, then washout may have occurred around a 12 hr residence time. However, due to wall growth, the cells attached on the walls continuously eluted planktonic cells into the CSTR solution. The planktonic population therefore dominated the system until a residence times of about 12 hr thereafter the cells attached to the CSTR wall took over and were responsible for the reproduction of planktonic cells in the CSTR solution. There was a logarithmic relationship between the cells eluted and the dilution rate and from this the critical dilution rate was for this system was postulated to be at a 2.9 hr residence time. The critical dilution rate can be assumed to be system specific depending on the nature of the wall growth and re-inoculation.

- There were differences in the maximum yields of the cultures investigated under sterile conditions relative to unsterile conditions (sterile [4.73 x 10^3 mmolC/mmolFe] – non-sterile [6.84 x 10^3 mmolC/mmolFe]). This was possibly because the *Leptospirillum ferriphilum* cultures used during investigation were of different type strains. Trends in the specific ferrous iron oxidation rate were however similar. Therefore, on condition that the microbial culture was checked frequently for contamination and as long as there were morphology checks, visual checks for fungus and the culture DNA was extracted to confirm homology to ensure no contamination sterility may have been unnecessary. It would however be a prevention measure ensuring there is less probability of contamination.

- An investigation into the quantity of attachment of *Leptospirillum ferriphilum* microorganisms on the surface of ceramic saddles at a 32 hr residence time showed that attachment was largely established by day 2. Steady state was achieved during the attachment experiment therefore the cell concentration of attached cells was quantified (on average 106 x 10^6 cell /g ceramic saddles). Over 87% of the attached microbial population was firmly attached to the surface of the ceramic saddles. Attachment experiments showed that that the concentration of planktonic microorganisms affected the rate of attachment. Sessile experiments followed after attachment.

- Steady state for sessile experiments with a low recycle ratio at residence times 5 hr and 4 hr was achieved after 63 - 72 residence (1.79 recycle ratio) times and 102 – 114 (1.43 recycle ratio) residence times respectively. For planktonic experiments steady state was achieved by 3 residence times for both experiments at residence times 5 hr and 4 hr. Increasing the recycle ratio shortened the time it took to reach steady state. On repeating the sessile experiment at a 5 hr residence time, with a recycle ratio of 21, steady state was achieved after 29 – 48 residence times.

- During sessile experiments, at steady state, there was generally increased growth in the sessile microbial population in the PBR. Most cells were not firmly attached and varied between being weakly attached or interstitial or in the PBR solution.

- The cell concentration and redox potential of the solution in the PBR was not similar to that in the CSTR at a 5 hr and 4 hr residence time using a low recycle ratio (1.79 at 5 hr residence time and 1.43 at 4 hr residence time) hence the CSTR and PBR could not be considered as one system. There were ferrous iron limitations in the PBR which caused the PBR to reach a steady state relative to the given conditions. This steady state was independent of the steady state in the CSTR which was not necessarily ferrous iron limited. Since the CSTR was a separate entity to the PBR, on comparing the q'Fe^{2+}ratio [rFe^{2+} : rCO_2] (mmolFe. hr. $mmolC^{-1}$) there were small difference between q'Fe^{2+}ratio from planktonic experiments and sessile experiments. This was because the PBR did not influence the CSTR significantly due to ferrous iron limitations (in the PBR). The q'Fe^{2+}ratios from sessile experiments were 152 mmolFe.hr.$mmolC^{-1}$ (5 hr residence time, 13% decrease from planktonic ratio) and 182 mmolFe.$mmolC^{-1}hr^{-1}$ (4 hr residence time, 4% increase from planktonic ratio).

- Increasing the recycle ratio from 1.79 to 21 at 5 hr residence time resulted in huge growth of the microbial population. It also reduced the difference between the conditions in the CSTR and the PBR although there was still a significant difference. This was because more ferrous iron was fed to the PBR relative to the low recycle ratio experiments and a new steady state was achieved. At this new steady state in the PBR, ferrous iron was again ferrous iron limiting at the new conditions which was still different to the steady state of the CSTR. The $q'Fe^{2+}$ratios from sessile experiments at a high recycle ratio was 132 mmolFe.hr.mmolC^{-1} (5 hr residence time, 27% decrease from planktonic ratio).

  This study confirms that it is possible to develop a strategy that can be used to determine the ferrous iron oxidation rates of a sessile microbial population. In the context of trying to generate empirical data relative to only a sessile microbial population, studies should be conducted aiming towards avoiding wall growth in the CSTR so that planktonic microorganisms get washed-out and sessile microorganisms are in an independent reactor system (no planktonic microorganisms). This study also shows the importance of the recycle ratio in the reactor system so that the conditions in the CSTR are representative of that in the PBR. This can only be achieved at an appropriate recycle ratio high enough to prevent limitations in the reactor system especially in the PBR.

7.2 Recommendations

The following recommendations are suggested for further work:

- Wall growth was a significant factor that influenced the kinetics in the system. To try and reduce the wall growth effect, the agitation rate could be increased. Pirt (1975) reported that vigorous agitation rates prevented wall growth however splashes may cause the accumulation of biomass above the liquid level. Silicon grease can be used to temporarily prevent the adhesion of biomass on the reactor wall or a Teflon layer which is a permanent non stick surface can be applied. Dichlorodimethylsilane, a compound that deposits a silicon layer may be used temporarily to prevent the attachment of biomass to the reactor wall. Toxicity trials are included prior to using these chemicals. The reactor wall may also be scrapped frequently before starting each experiment to avoid the build up of biomass on the reactor wall (du Preez, 1995; Pirt, 1975). Several chemostat studies have handled wall growth by regular transfers to clean the reactor to avoid build up.

- To eliminate planktonic microorganisms from the system:

i. Either the measures mentioned above could be followed to avoid wall growth so that there is washout at a 12 hr residence time (Monod type behaviour). or

ii. Experiments may be conducted at 2.9 hr residence time where was-out is expected to occur as was shown in this study.

- The recycle ratio should be further increased using a faster pump and bigger tubing. This way the conditions in the PBR would be consistent to the conditions in the CSTR solution and more accurate measurements of the kinetics could therefore be deduced. Increasing the recycle ratio further, much greater than 21 might eventually achieve homogeneity in the conditions of the CSTR medium and PBR medium and thereby allow for accurate measurements of the kinetics of the sessile microbial population.

- More research needs to done to find a method that can be used to determine the amount of biomass (sessile population) that accumulates in the PBR through linking the microbial cell counts, carbon dioxide uptake rate and ferrous iron oxidation rates.

REFERENCES

1. Acevedo, F., Gentina, J.C. (**2007**). Bioreactor design fundamentals and their application to gold mining. In: Microbial Processing of Metal Sulphides (Eds. Donati, D.E. and Sand, W), Springer, 151-168.
2. Africa, C. (**2009**). Microbial attachment to sulfide minerals in a bioleach environment. MSc Thesis, University of Cape Town, South Africa.
3. Africa, C., Harrison, S.T.L., Becker, M., van Hille, R.P. (**2010**). In-situ investigation and visualisation of microbial attachment and colonisation in a heap bioleach environment: The novel biofilm reactor. *Minerals Engineering*, **23 (6)**, 486-491.
4. Akcil, A., Cifti, H. (**2007**). Role and contribution of pure and mixed cultures of mesophiles in bioleaching of a pyritic chalcopyrite concentrate. *Minerals Engineering, **20**(**3**)*, 310-318.
5. Alexander, B., Leach, S., Ingledew, W. J. (**1987**). The relationship between chemiosmotic parameters and sensitivity to anions and organic acids in the acidophile Thiobacillus ferrooxidans. *Journal of General Microbiology*, **133(5)**, 1171-1179.
6. Bailey, J.E., Ollis, D.F. (**1977**). Biochemical Engineering Fundamentals. 1st edition. McGraw Hill, New York.
7. Baker-Austin, C., Dopson, M., Wexler, M., Sawers, R.G., Bond, P.L. (**2005**). Molecular insight into extreme copper resistance in the extremophilic archaeon '*Ferroplasma acidarmanus*' Fer1. *Microbiology*, **151(8)**, 2637-2646.
8. Barreto, M., Jedlicki, E., Holmes, D.S. (**2005**). Identification of a Gene Cluster for the Formation of Extracellular Polysaccharide Precursors in the Chemolithoautotroph *Acidithiobacillus ferrooxidans*. *Applied and Environmental Microbiology*, **71(6)**, 2902-2909.
9. Blight, K., Ralph, D.E., Thurgate, S. (**2000**). Pyrite surfaces after bio-leaching: a mechanism for bio-oxidation. *Hydrometallurgy*, **58(3)**, 227-237.
10. Blight, K.R., Ralph, D.E. (**2008**). Aluminium sulphate and potassium nitrate effects on batch culture of iron oxidizing bacteria. *Hydrometallurgy*, **92(3-4)**, 130-134.
11. Boon, M., Heijnen, J.J. (**1998**). Chemical oxidation kinetics of pyrite in bioleaching processes. *Hydrometallurgy,* **48(1)**, 27-41.
12. Boon, M., Luyben, K.C.A.M., Heijnen, J.J. (**1998**). The use of on-line off-gas analyses and stoichiometry in the bio-oxidation kinetics of sulphide minerals. *Hydrometallurgy*, **48(1)**, 1-26.
13. Boon, M., Brasser, H.J., Hansford, G.S., Heijnen, J.J. (**1999**). Comparison of the oxidation kinetics of different pyrites in the presence of *Thiobacillus ferrooxidans* or *Leptospirillum ferrooxidans*. *Hydrometallurgy,* **53(1)**, 57-72.

14. Boon, M. (**2001**). The mechanism of 'direct' and 'indirect' bacterial oxidation of sulphide minerals. *Hydrometallurgy,* **62(1)**, 67-70.

15. Breed, A.W., Hansford, G.S. (**1999a**). Effect of pH on ferrous-iron oxidation kinetics of *Leptospirillum ferrooxidans* in continuous culture. *Biochemical Engineering Journal*, **3(3**), 193-201.

16. Breed, A.W., Hansford, G.S. (**1999b**). Studies on the mechanism and kinetics of bioleaching. *Minerals Engineering,* **12(4)**, 383-392.

17. Breed, A.W., Dempers, C.J.N., Searby, G.E., Gardner, M.N., Rawlings, D.E., Hansford, G.S. (**1999**). The effect of temperature on the continuous ferrous-iron oxidation kinetics of a predominantly *Leptospirillum ferrooxidans* culture. *Biotechnology and Bioengineering,* **65(1)**, 44-53.

18. Brierley, C.L. (**2001**). Bacterial succession in bioheap leaching. *Hydrometallurgy,* **59(2-3)**, 249-255.

19. Brierley, J.A., Brierley, C.L. (**2001**). Present and future commercial applications of biohydrometallurgy. *Hydrometallurgy,* **59(2-3)**, 233-239.

20. Brierley, J.A. (**2008**). A perspective on developments in biohydrometallurgy. *Hydrometallurgy,* **94(1-4)**, 2-7.

21. Brierley, C.L. (**2009**). Biohydrometallurgy: what is its future?. *Biohydrometallurgy: A meeting point between microbiology ecology, metal recovery processes and environmental remediation (IBS 2009, Bariloche Argentina)*, **18**(**71-73)**, 3-10.

22. Broadhurst, J.L. (**2007**). Generalized strategy for predicting environmental characteristics of solid mineral wastes- A focus on copper. Ph.D. Thesis University of Cape Town.

23. Bromfield, L. (**2011**). Factors affecting the attachment of *Metallosphaera Hakonensis* during the colonization of low grade mineral sulphide heaps. MSc Thesis University of Cape Town.

24. Bryan, C.G, Jones, G., van Wyk, N., Tupikina, O.V. (**2011**). The critical evaluation of techniques for the selective isolation and analysis of microbial populations involved in heap bioleaching. In press *Journal of Industrial Microbiology and Biotechnology*.

25. Chiume, A.R. (**2011**). The impact of irrigation conditions on the spatial development of microbial colonies in bioheaps. MSc Thesis, University of Cape Town, South Africa.

26. Clark, M.E., Batty, J.D., van Buuren, C.B., Dew, D.W., Eamon, M.A. (**2006**). Biotechnology in minerals processing: Technological breakthroughs creating value. *Hydrometallurgy.* **83(1-4)**, 3-9.

27. Córdoba, E.M. Munoz, J.A., Blazquez, M.L., Gonzalez, F., Ballester, A. (**2008**). Leaching of chalcopyrite with ferric ion. Part IV: The role of redox potential in the presence of mesophilic and thermophilic bacteria. *Hydrometallurgy,* **93(3-4)**, 106-115.

28. Cruz, R., Lazaro, I., Gonzalez, I., Monroy, M. (**2005**). Acid dissolution influences bacterial attachment and oxidation of arsenopyrite. *Minerals Engineering*, **18**, 1024-1031.

29. Daoud, J., Karamanev, D. (**2006**). Formation of jarosite during Fe^{2+} oxidation by *Acidithiobacillus ferrooxidans*. *Minerals Engineering.* **19(9)**, 960-967.

30. Davenport, W.G., King, M., Schlesinger, M., Biswas, A.K. (**2002**). Extractive metallurgy of copper. 4th edition. Elsevier Science Press, New York.

31. de Kock, S.H., Barnard, P., du Plessis, C.A. (**2003a**). Oxygen and carbon dioxide kinetic challenges for thermophilic mineral bioleaching processes. *Biochemical Society Transactions.* **32(2)**, 273.

32. de Kock, S.H., Naldrett, K., du Plessis, C.A. (**2003b**). Optimal oxygen and carbon dioxide kinetic challenges for thermophilic bioleaching archaea. *Biohydrometallurgy: A sustainable technology in evolution (IBS 2003, Athens Hellas)*, **15**, 319-328.

33. Demergasso, C. (**2009**). Microbial succession during a heap bioleaching cycle of low grade copper sulphides. *Biohydrometallurgy: A meeting point between microbiology ecology, metal recovery processes and environmental remediation (IBS 2009, Bariloche Argentina)*, **18**(**71-73)***, 21-27.*

34. Dempers, C.J.N., Breed, A.W., Hansford, G.S. (**2003**). The kinetics of ferrous-iron oxidation by *Acidithiobacillus ferrooxidans* and *Leptospirillum ferrooxidans*: effect of cell maintenance. *Biochemical Engineering Journal.* **16(3)**, 337-346.

35. Deveci, H., Jordan, M.A., Powell, N., Alp, I. (**2008**). Effect of salinity and acidity on bioleaching activity of mesophilic and extremely thermophilic bacteria. *Transactions of Non-ferrous Metals Society of China.* **18(3)**, 714-721.

36. Dopson, M., Baker-Austin, C., Kopinneedi, P.R., Bond, P.L. (**2003**). Growth in sulfidic mineral environments: metal resistance mechanisms in acidophilic micro-organisms. *Microbiology.* **149(8)**, 1959-1970.

37. Dopson, M., Halinen, A., Rahunen, N., Ozkaya, B., Sahinkaya, E., Kaksonen, A., Lindsrom, E.B., Puhakka, J.A. (**2007**). Mineral and iron oxidation at low temperatures by pure and mixed cultures of acidophilic microorganisms. *Biotechnology and Bioengineering.* **97(5)**, 1205-1215.

38. Du Plessis, C.A, Batty, J.D, and Dew, D.W. (**2007**). Commercial applications of thermophilic bioleaching, In: Biomining (Eds. Rawlings, D.E and Johnson, B.D)*,* Springer-Verlag, 57-78.

39. du Preez, J.C. (**1995**). Fundamentals of growth kinetics with emphasis on growth kinetics.

40. Ebbing, D. (**1993**). General chemistry. 4th edition. Houghton Mifflin company.
41. Ehrlich, H.L. (**2001**). Past, present and future of biohydrometallurgy. *Hydrometallurgy,* **59(2-3)**, 127-134.
42. Farah, C., Vera, M., Morin, D., Haras, D., Jerez, C.A., Guiliana, N. (**2005**). Evidence for a Functional Quorum-Sensing Type AI-1 System in the Extremophilic Bacterium *Acidithiobacillus ferrooxidans*. *Applied and Environmental Microbiology,* **71(11)**, 7033-7040.
43. Fowler, T.A., Holmes, P.R., Crundwell, F.K. (**2001**). On the kinetics and mechanism of the dissolution of pyrite in the presence of *Thiobacillus ferrooxidans*. *Hydrometallurgy.* **59(2-3)**, 257-270.
44. Franzmann, P.D., Haddad, C.M., Hawkes, R.B., Robertson, W.J., Plumb, J.J. (**2005**). Effects of temperature on the rates of iron and sulfur oxidation by selected bioleaching Bacteria and Archaea: Application of the Ratkowsky equation. *Minerals Engineering.* **18(13-14)**, 1304-1314.
45. Fu, B., Zhou, H., Zhang, R., Qiu, G. (**2008**). Bioleaching of chalcopyrite by pure and mixed cultures of *Acidithiobacillus spp.* and *Leptospirillum ferriphilum*. *International Biodeterioration Biodegradation.* **62(2)**, 109.
46. Gahan, C.S., Sundkvist, J., Sandström, Å. (**2009**). A study on the toxic effects of chloride on the biooxidation efficiency of pyrite. *Journal of Hazardous Materials.* **172(2-3)**, 1273-1281.
47. Gahan, C.S., Sundkvist, J., Dopson, M., Sandström, Å. (**2010**). Effect of chloride on ferrous iron oxidation by a *Leptospirillum ferriphilum*-dominated chemostat culture. *Biotechnology and Bioengineering.* **106(3)**, 422-431.
48. Garcia, O., da Silva, L.L. (**1991**). Differences in growth and iron oxidation among Thiobacillus ferrooxidans cultures in the presence of some toxic metals. *Biotechnology letters.* **13(8)**, 567.
49. Gericke, M., Neale, J.W., van Staden, P.J. (**2009**). A Mintek perspective of the past 25 years in minerals bioleaching. *Journal of the South African Institute of Mining and Metallurgy,* **109(10)**, 567.
50. Ghauri, M. A., Okibe, N., Johnson, D. B. (**2007**). Attachment of acidophilic bacteria to solid surfaces: The significance of species and strain variations. *Hydrometallurgy,* **85(2-4)**, p72-80.
51. Gupta, C.K., Mukherjee, T.K. (Eds). (**1990**). Hydrometallurgy in the extraction process. Florida, CRC Press.
52. Habashi, F. (**1999**). A Text book of hydrometallurgy. 2nd edition. Metallurgie Extractive Quebec, Canada.
53. Hansford, G.S., Vargas, T. (**1999**). Chemical and electrochemical basis of bioleaching processes. In: Process Metallurgy (Eds. Amils, R.R and Ballester, A), Elsevier. 13-26.

54. Hansford, G.S., Vargas, T. (**2001**). Chemical and electrochemical basis of bioleaching processes. *Hydrometallurgy.* **59(2-3)**, 135-145.

55. Harneit, K., Goksel, A., Klock, J.-H., Gehrke, T., Sand, W. (**2006**). Adhersion to metal sulphide surfaces by cells of *Acidithiobacillus ferrooxidans, Acidithiobacillus thiooxidans* and *Leptospirillum ferrooxidans*. *Hydrometallurgy*, **83**, 245-254.

56. Ingledew, W.J. (**1982**). *Thiobacillus ferrooxidans*: the bioenergetics of an acidophilic chemolithotroph. *Biochimica et biophysica acta (BBA) - Reviews on Bioenergetics.* **683(2)**, 89-117.

57. Jones, C., Kelly, D.P. (**1983**). Growth of *Thiobacillus ferrooxidans* on ferrous iron in chemostat culture: Influence of product and substrate inhibition. *Journal of Chemical Technology and Biotechnology.* **33B(4)**, 241.

58. Jordan, M.A., Barr, D.W., Phillips, C.V. (**1993**). Iron and sulphur speciation and cell surface hydrophobicity during bacterial oxidation of a complex copper concentrate. *Minerals Engineering.* **6(8-10)**, 1001-1011.

59. Kawabe, Y., Inoue, C., Suto, K., Chida, T. (**2003**). Inhibitory effect of high concentrations of ferric ions on the activity of *Acidithiobacillus ferrooxidans*. *Journal of Bioscience and Bioengineering.* **96(4)**, 375-379.

60. Kazadi, T.K., Petersen, J. (**2008**). Kinetic measurement of biological oxidation of ferrous iron at low ferric to ferrous ratios in a controlled potential batch reactor. *Hydrometallurgy.* **94(1-4)**, 48-53.

61. Kinnunen, P.H.-M., Puhakka, J.A. (**2005**). High-rate iron oxidation at below pH 1 and at elevated iron and copper concentrations by a *Leptospirillum ferriphilum* dominated biofilm. *Process Biochemistry.* **40(11)**, 3536-3541.

62. Kinzler, K. Gehrke, T., Telegdi, J., Sand, W. (**2003**). Bioleaching—a result of interfacial processes caused by extracellular polymeric substances (EPS). *Hydrometallurgy.* **71(1-2)**, 83-88.

63. Komadel, P., Stucki, J.W. (**1988**). Quantitative assay of minerals for Fe^{2+} and Fe^{3+} using 1,10-phenanthroline: III. A rapid photochemical method. *Clays and Clay Minerals*. (**36**), 379–381.

64. Lizama, H.M., Fairweather, M.J., Dai, Z., Allegretto, T.D. (**2003**). How does bioleaching start? *Hydrometallurgy.* **69(1-3)**, 109-116.

65. Lusinga, D. (**2011**). A multi criteria analysis and comparison of primary copper processing options. MSc Thesis University of Cape Town.

66. Maas, B., Paxton, J. (**2007**). Investigation into the microbial ferrous iron oxidation rates in a high surface area recycle reactor. BSc Chemical Engineering thesis University of Cape Town (unpublished).

67. Mathur, A.K. (**2005**). Biomining-A promising approach. *IANCAS Bulletin,* 10-15.

68. May, N., Ralph, D.E., Hansford, G.S. (**1997**). Dynamic redox potential measurement for determining the ferric leach kinetics of pyrite. *Minerals Engineering.* **10(11)**, 1279-1290.

69. Mignone, C.F., Donati, E.R. (**2004**). ATP requirements for growth and maintenance of iron-oxidizing bacteria. *Biochemical Engineering Journal.* **18(3)**, 211-216.

70. Morin, D.H.R. (**2007**). Bioleaching of sulfide minerals in continuous stirred tank reactors, In: Microbial Processing of Metal Sulphides (Eds. Donati, D.E and Sand, W), Springer, 133-150.

71. Naik, L. (**2010**). The effect of Carbon dioxide on the growth and activity of *Leptospirillum ferriphilum*. MSc Thesis University of Cape Town.

72. Nemati, M., Webb, C. (**1997**). A kinetic model for biological oxidation of ferrous iron by *Thiobacillus ferrooxidans*. *Biotechnology and Bioengineering.* **53(5)**, 478-486.

73. Nemati, M., Harrison, S.T.L., Hansford, G.S., Webb, C. (**1998**). Biological oxidation of ferrous sulphate by *Thiobacillus ferrooxidans*: a review on the kinetic aspects. *Biochemical Engineering Journal.* **1(3)**, 171-190.

74. Ojumu, T.V., Petersen, J., Searby, G.E., Hansford, G.S. (**2006**). A review of rate equations proposed for microbial ferrous-iron oxidation with a view to application to heap bioleaching. *Hydrometallurgy,* **83(1-4)**, 21-28.

75. Ojumu, T.V. (**2008**). The effect of solution conditions on the kinetics of microbial ferrous-iron oxidation by *Leptospirillum ferriphilum* in continuous culture. PhD Thesis University of Cape Town.

76. Ojumu, T.V., Petersen, J., Hansford, G.S. (**2008**). The effect of dissolved cations on microbial ferrous-iron oxidation by *Leptospirillum ferriphilum* in continuous culture. *Hydrometallurgy.* **94(1-4)**, 69-76.

77. Ojumu, T.V., Hansford, G.S., Petersen, J. (**2009**). The kinetics of ferrous-iron oxidation by *Leptospirillum ferriphilum* in continuous culture: The effect of temperature. *Biochemical Engineering Journal.* **46(2)**, 161-168.

78. Ojumu, T. V., Petersen, J. (**2011**). The kinetics of ferrous ion oxidation by *Leptospirillum ferriphillum* in continuous culture: The effect of pH. *Hydrometallurgy*. 106(1-2), 5-11.

79. Olson, G.J., Brierley, J.A., Brierley, C.L. (**2003**). Bioleaching review part B: Progress in bioleaching: applications of microbial processes by the minerals industries. *Applied Microbiology and Biotechnology,* **63(3)**, 249-257.

80. Ozkaya, B., Sahinkaya, E., Nurmi, P., Kaksonen, A.H., Puhakka, J.A. (**2007**). Iron oxidation and precipitation in a simulated heap leaching solution in a *Leptospirillum ferriphilum* dominated biofilm reactor. *Hydrometallurgy,* **88(1)**, 67.

81. Petersen, J., Dixon, D.G. (**2003**). The dynamics of chalcocite heap bioleaching. (IBS proceedings 2003, Vancouver Canada), 351-364.

82. Petersen, J., Dixon, D.G. (**2006**). Competitive bioleaching of pyrite and chalcopyrite. *Hydrometallurgy.* **83(1-4)**, 40-49.

83. Petersen, J., Dixon, D.G. (**2007a**). Modelling zinc heap bioleaching. *Hydrometallurgy*. 85(2-4), 127-143.

84. Petersen, J., Dixon, D.G. (**2007b**). Principles, mechanisms and dynamics of chalcocite heap bioleaching, In: Microbial Processing of Metal Sulphides (Eds. Donati, D.E and Sand, W). Springer, 193-218.

85. Petersen, J. (**2009**). Understanding and modeling of interactions in bioleach processes. Biohydrometallurgy: A meeting point between microbiology ecology, metal recovery processes and environmental remediation (IBS 2009, Bariloche Argentina), 18(**71-73**), 303-310.

86. Petersen, J., Minnaar, S.H., du Plessis, C.A. (**2010**). Carbon dioxide and oxygen consumption during the bioleaching of a copper ore in a large isothermal column. *Hydrometallurgy*. **104**, 356-362.

87. Pirt, J.S. (**1975**). Principle of microbe and cell cultivation. 1st edition.. John Wily and sons. New York.

88. Plumb, J.J., McSweeney, N.J., Franzmann, P.D. (**2008a**). Growth and activity of pure and mixed bioleaching strains on low grade chalcopyrite ore. *Minerals Engineering.* **21(1)**, 93-99.

89. Plumb, J.J., Muddle, R., Franzmann, P.D. (**2008b**). Effect of pH on rates of iron and sulfur oxidation by bioleaching organisms. *Minerals Engineering.* **21(1)**, 76-82.

90. Pogliani, C., Donati, E. (**1999**). The role of exopolymers in the bioleaching of a non-ferrous metal sulphide. *Journal of Industrial Microbiology and Biotechnology.* **22(2)**, 88.

91. Pradhan, N., Nathsarma, K.C., Rao, S.K., Sukla, L.B., Misha, B.K. (**2008**). Heap bioleaching of chalcopyrite: A review. *Minerals Engineering,* **21(5)**, 355-365.

92. Quatrini, R., Appia-Ayme, C., Denis, Y., Ratouchniak, J., Veloso, J., Valdes, J., Lefimil, C., Silver, S., Roberto, F., Orellana, O., Denizot, F., Jedlicki, E., Holmes, D., Bonnefoy, V. (**2006**). Insights into the iron and sulfur energetic metabolism of Acidithiobacillus ferrooxidans by microarray transcriptome profiling. *Hydrometallurgy.* **83(1-4)**, 263-272.

93. Ratledge, C., Kristiansen, B. (**2001**). Basic Biotechnology. Cambridge University Press.

94. Rawlings, D.E., Tributsch, H., Hansford, G.S. (**1999**). Reasons why '*Leptospirillum*'-like species rather than *Thiobacillus ferrooxidans* are the dominant iron-oxidizing bacteria in many commercial processes for the biooxidation of pyrite and related ores. *Microbiology,* **145(1)**, 5-13.

95. Rawlings, D.E. (**2002**). Heavy Metal Mining using Microbes. *Annual review of Microbiology,* **56(1)**, 65.

96. Rawlings, D.E., Dew, D., du Plessis, C. (**2003**). Biomineralization of metal-containing ores and concentrates. *Trends in Biotechnology,* **21(1)**, 38-44.

97. Rawlings, D.E., Johnson, D.B. (**2007**). The microbiology of biomining: development and optimization of mineral-oxidizing microbial consortia. *Microbiology.* **153(2)**, 315-324.

98. Reid, C. R., Prausnitz, J.M., Poling, B.E. (**1987**). The Properties of Gases and Liquids, 4th ed. McGraw-Hill, Boston.

99. Roberts, J.A., Fowle D. A., Hughes B. T., Kulczycki, E. (**2006**). Attachment behavior of *Shewanella putrefaciens* onto magnetite under aerobic and anaerobic conditions. *Geomicrobiology Journal*. **23**,631-640.

100. Rodríguez, Y., Ballester, A., Blazquez, M.L., Gonzalez, F., Munoz, J.A. (**2003a**). New information on the pyrite bioleaching mechanism at low and high temperature. *Hydrometallurgy.* **71(1-2)**, 37-46.

101. Rodríguez, Y., Ballester, A., Blazquez, M.L., Gonzalez, F., Munoz, J.A. (**2003b**). Study of Bacterial attachment during the Bioleaching of Pyrite, Chalcopyrite, and Sphalerite. *Geomicrobiology journal*. **20(2)**, 131-141.

102. Rohwerder, T., Gehrke, T., Kinzler, K., Sand. (**2003**). Bioleaching review part A: Progress in bioleaching: fundamentals and mechanisms of bacterial metal sulfide oxidation. *Applied Microbiology & Biotechnology.* **63(3)**, 239-248.

103. Rohwerder, T., Sand, W. (**2007**). Mechanisms and biochemical fundamentals of bacterial metal sulphide oxidation, In: Microbial Processing of Metal Sulphides (Eds. Donati, D.E and Sand, W). Springer, 35-58.

104. Rossi, G. (**1990**). *Biohydrometallurgy*. 1st edition. McGraw-Hill book company GmbH, Hamburg.

105. Sampson, M., Phillips, C.V. (**2001**). Influence of base metals on the oxidizing ability of acidophilic bacteria during the oxidation of ferrous sulfate and mineral sulfide concentrates, using mesophiles and moderate thermophiles. *Minerals Engineering,* **14(3)**, 317.

106. Sand, W., Gehrke, T., Jozsa, P.G., Schippers, A. (**1999**). Direct versus indirect bioleaching. In: Process Metallurgy (Eds. Amils, R and Ballester, A). Elsevier, 27-49.

107. Sand, W., Gehrke, T., Jozsa, P., Schippers, A. (**2001**). (Bio)chemistry of bacterial leaching—direct vs. indirect bioleaching. *Hydrometallurgy.* **59(2-3)**, 159-175.

108. Sand, W., Gehrke, T. (**2006**). Extracellular polymeric substances mediate bioleaching/biocorrosion via interfacial processes involving iron (III) ions and acidophilic bacteria. *Research in Microbiology,* **157(1)**, 49-56.

109. Sandström, Å. (**2008**). Hydrometallurgy. Division of process metallurgy, Department of Chemical engineering and Geosciences, Luela University of Technology.

110. Schippers, A., Jozsa, P., Sand, W. (**1996**). Sulfur Chemistry in Bacterial Leaching of Pyrite. *Applied and Environmental Microbiology.* **62(9)**, 3424-3431.

111. Schippers, A. (**2007**). Microorganisms involved in bioleaching and nucleic acid based molecular methods for their identification and quantification, In: Microbial Processing of Metal Sulphides (Eds. Donati, D.E and Sand, W). Springer, 3-33.

112. Shiers, D.W., Blight, K.R., Ralph, D.E. (**2005**). Sodium sulphate and sodium chloride effects on batch culture of iron oxidizing bacteria. *Hydrometallurgy.* **80(1-2),** 75-82.

113. Siddiqui, M.H., Kumar, A., Kesari, K.K., Arif, J.M. (**2009**). Biomining-A useful approach towards metal extraction. *American-Eurasian Journal of Agronomy*, **2(2)**, 84-88.

114. Sohn, S., Kim, D. (**2005**). Modification of Langmuir isotherm in solution systems-definition and utilization of concentration dependent factor. Chemosphere **58**, 115-123.

115. Sundkvist, J., Gahan, C.S., Sandström, Å. (**2008**). Modeling of ferrous iron oxidation by a Leptospirillum ferrooxidans-dominated chemostat culture. *Biotechnology and Bioengineering,* **99(2)**, 378-389.

116. Tributsch, H. (**2001**). Direct versus indirect bioleaching. *Hydrometallurgy.* **59(2-3)**, 177-185.

117. van Loosdrecht, M.C., Lyklema, J., Norde, W., Zehnder, J.B.A. (**1990**). Influence of interfaces on microbial activity. *Microbiology and Molecular Biology reviews,* **54(1)**, 75-87.

118. van Scherpenzeel, D.A. Boon, M., Ras, C., Hansford, G.S., Heijnen, J.J. (**1998**). Kinetics of ferrous iron oxidation by *Leptospirillum* bacteria in continuous cultures. *Biotechnology progress,* **14(3)**, 425-433.

119. Wang, D.I.C., Cooney, C.L., Demain, A.L., Dunnill, P., Humphrey, A.E., Lilly, M.D. (**1979**). Fermentation and enzyme technology. 1st edition. John Wiley and sons, New York.

120. Watling, H.R. (**2006**). The bioleaching of sulphide minerals with emphasis on copper sulphides — A review. *Hydrometallurgy,* **84(1-2)**, 81-108.

121. Witne, J.Y., Phillips, C.V. (**2001**). Bioleaching of Ok Tedi copper concentrate in oxygen- and carbon dioxide-enriched air. *Minerals Engineering.* **14(1)**, 25-48.

122. Zobell, C. (**1943**). Bacterial adhesion model. *Journal of Bacteriology*. **46**, 39-52.

Appendix A: Preparation of feed media and culture maintenance

Feed for the microbial culture was made in 10 litre batches. Each 10 litre batch required 8,800mL of deionised water, 200mL of 50X autotrophic basal salt solution (ABS), 10 mL of trace element solution and 1litre of 50 g/L ferrous iron solution at a pH of 1.1. (This makes a 5 g/L ferrous iron feed medium).

1) 50X Autotrophic Basal salt solution (g/L)

7.5 g $(NH_4)_2SO_4$

7.5 g $Na_2SO_4.10H_2O$

2.5 g KCl

25 g $MgSO_4.7H_2O$

2.5 g KH_2PO_4

0.7 g $Ca(NO_3)_2.4H_2O$

The pH should be adjusted to a pH of 1.1 using concentrated sulphuric acid (H_2SO_4), thereafter, the solution should be autoclaved. (Note that during feed preparation, the 50X concentrate was diluted first using deionised water).

2) Trace element solution (g/l) (used as 1 mL per litre of the complete medium)

The solution was prepared by dissolving the following salts in 800 mL of acidified distilled water (pH adjusted to pH of 1.1 using H_2SO_4); Salts were added in the order given below (each salt had to dissolved before adding the next).

10 g $ZnSO_4.7H_2O$

1 g $CuSO_4.5H_2O$

0.64 g $MnSO_4.H_2O$

1 g $CoSO_4.7H_2O$

0.7 g $CrK(SO_4)_2.12H_2O$

0.6 g H_3BO_3

0.5 g $Na_2MoO_4.2H_2O$

1 g $NiSO_4.6H_2O$

1 g $Na_2SeO_4.10H_2O$

0.1 g $Na_2WO_4.2H_2O$

pH was constantly checked and adjusted using H_2SO_4 to ensure it remained at 1.1. Once all the salts were dissolved, the volume of the mixture was topped up to 1litre with distilled water and the pH adjusted. The solution was also autoclaved and then chilled in a refrigerator operating at 4°C.

3) 50 g/L ferrous sulphate solution

248.92 g of ferrous sulphate heptahydrate ($FeSO_4.7H_2O$) was dissolved in about 700 mL of distilled water. The pH was constantly adjusted to 1.1 using H_2SO_4. Once fully dissolved, the solution was topped up to 1 litre using deionised water and the pH adjusted to 1.1. The solution was then filtered (sterilised) twice using 0.22 µm filter paper in a fume cupboard. (NB: $FeSO_4.7H_2O$ solution cannot be autoclaved as it precipitates). The filter unit used to sterilize the solution had to be autoclaved first before use to avoid contamination as much as possible.

4) Culture maintenance

Pure *Leptospirillum ferriphilum* - type strain ATCC 49881 was isolated from a culture in the Centre for Bioprocess Engineering Research (CeBER) laboratory at the University of Cape Town. The stock culture was maintained in a CSTR by feeding the culture with a 5g/l ferrous iron concentration at a 55hrs residence time. All feed solutions were sterilised and the entire system kept as sterile as possible. Sterilization was achieved by autoclaving and filtering all solution meant for feeding. DNA extraction by quantitative real time PCR (qPCR) of a sample from the reactor also confirmed the population of microbes in the reactor as purely *Leptospirillum ferriphilum*. The microorganism's morphology was checked regurlarly (everyday) under the microscope to ensure no contamination (*Leptospirillum ferriphilum* is generally spiral or comma shaped).Visual checks for any fungal infections were also investigated.

Appendix B: Analytical methods

1) Reagents used for determining iron concentrations

i) 1-10 phenanthroline indictor solution

2.1277 g of 1-10 phenanthroline (as $C_{12}H_8N_2$.H2O) was mixed in 100 ml of deionised water and poured into a 1000 ml volumetric flask. More deionised water was then added to make up to the 1000 ml mark and the solution left stirring overnight for 1-10 phenanthroline to completely dissolve.

ii) Ammonium acetate buffer solution

250 g of ammonium acetate ($NH_4C_2H_3O_2$) was dissolved in 150 ml of distilled water thereafter; 700 ml of concentrated glacial acetic acid was added to the solution.

iii) Ferrous iron stock solution (100ppm Fe^{2+})

Was made by slowly adding 20 mL of concentrated H_2SO_4 to 50 mL of distilled water and dissolving 497.629 mg of $FeSO_4.7H_2O$ to the solution. The solution was then topped up to 1000 mL with distilled water and mixed thoroughly. Standard solutions of lower concentration (10, 20, 30, 40 and 50 mg/L) were obtained by diluting the stock solution with deionised water as shown on the table below:

	Blank	**10mg/L**	**20 mg/L**	**30 mg/L**	**40 mg/L**	**50 mg/L**
Deionised H_2O	1000	900	800	700	600	500
Stock solution	0	100	200	300	400	500

2) Spectrophotometric analytical procedure for the determining of iron in samples

On testing ferrous iron and ferric iron concentrations it is important to know that when 3 molecules of 1-10 phenanthroline chelates with one Fe^{2+} ion, an orange red complex is formed that has an absorbance maximum of between 400 and 600nm. Also, Fe^{3+} gets reduced to Fe^{2+} using hydroxylamine according to the equation shown below:

$$2NH_2OH + 4Fe^{3+} \rightarrow N_2O + 4Fe^{2+} + 4H^+ + H_2O$$

Before determining the iron concentrations, the spectrophotometer was firstly calibrated. This was done by firstly preparing a blank solution containing 2 mL acetate buffer, 2 mL 1-10 phenanthroline solution and 1 mL of deionised water. The spectrophotometer was then set to 510 nm and calibrated to zero. A standard curve (shown below) was then generated by diluting the ferrous iron stock to 10, 20, 30, 40 and 50 mg/L.

mg/L	absorbance
10	0.472
20	0.835
30	1.232
40	1.753
50	2.014

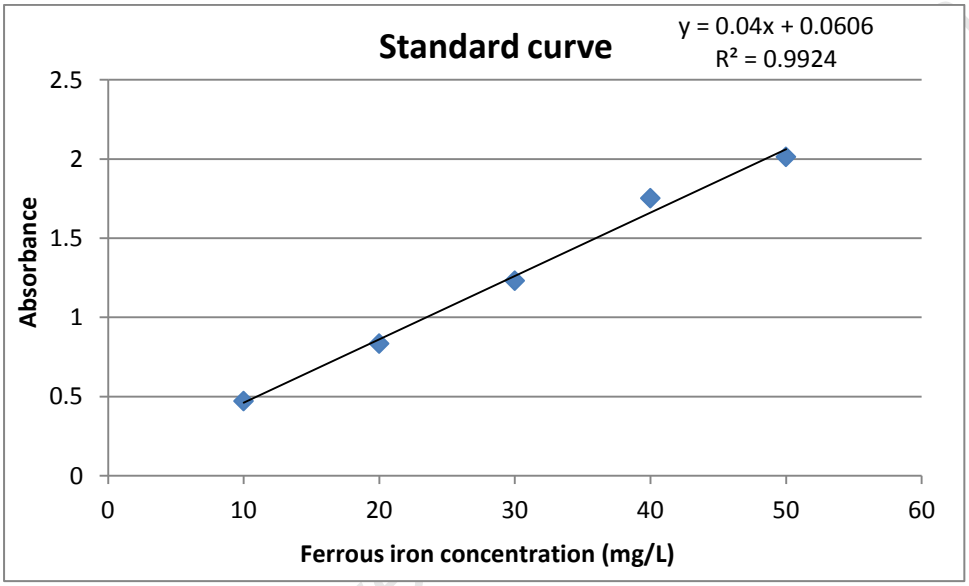

After calibrating the spectrophotometer, the measurement of iron from samples could be taken. A solution containing 2 mL acetate buffer, 2 mL 1-10 phenanthroline solution and 1 mL of deionised water and solution (depending on the dilution factor) was mixed together and the absorbance measured. Total iron concentrations were determined by adding one scoop of hydroxylamine and vortexing for 2 minutes then allowing the solution to stand for 5 minutes before determining the concentration spectrophotometrically.

3) Microbial cell counts

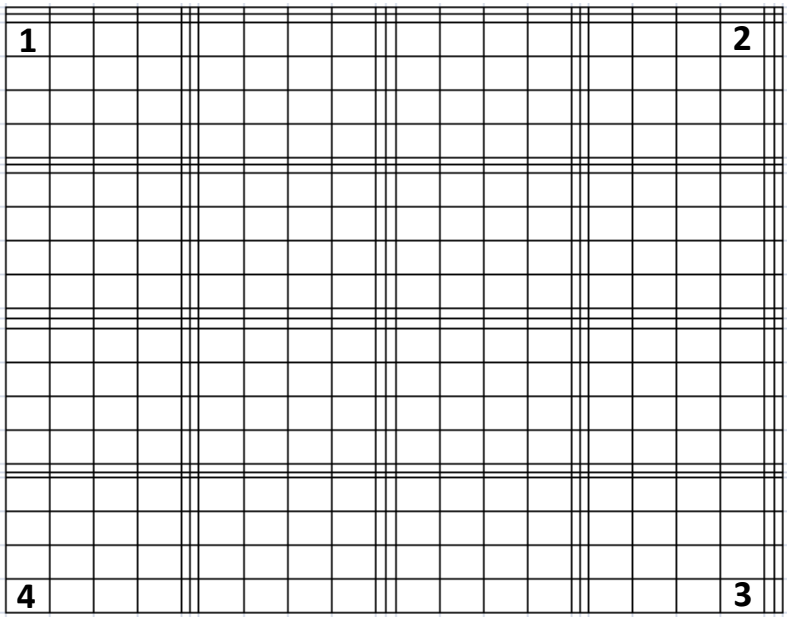

Area of Small Square: $\frac{1}{400}mm^2$ depth: 0.02mm

Area of 1 small square = $\frac{1}{400}mm^2$ = 0.0025mm^2

Depth = 0.02 mm

Volume of 1 square = $\frac{1}{400}mm^2$ * 0.02 mm = 0.00005 mm^3 =0.00000005 mL (**NB**: 1mL=1000 m^3)

Volume occupied by 64 (cells counted from 4 squares indicated above) = 0.0000032 mL

If x cells are in 64 squares x $\frac{1}{0.0000032mL}$ = 312500 cells/mL

Therefore; [cells] = Cells counted x 312500 cells/mL x Dilution factor

4) New detachment protocol

***Protocol is based on the UCT lab protocol and BHP-Billiton JTC protocol and was further developed by Dr C.G Bryan and Dr O. Tupikina *et al.*, 2009. The protocol includes the determination of the microbial counts of the interstitial phase liquid.**

Materials required:

1. Acidified detachment medium (no Fe^{2+}). The pH should be the same as for the feed without ferrous iron. Pure water leads to osmotic stress and could conceivably cause lysis and so should be avoided. The pH should be below 2.0 to avoid the precipitation of ferric iron.
2. Tween 20 at 0.4% v/v which is added to the two final washing steps.
3. Clean centrifuge tubes.

4. Large Erlenmeyer flasks for mixing and vortexing of ceramics and liquid.

Procedure:

1. Detach the glass vessel for the CSTR and collect the solution in the glass vessel surrounding the ceramic beads.
2. Place the 123 g of ceramic beads from the glass vessel to an Erlenmeyer flask and add 60 mL of the acidified detachment medium (note that the ratio of the detachment medium to ore is 0.5:1.0).
3. Gently invert or mix the interstitial liquid with the detachment medium whilst not detaching the cells from the solid phase.
4. Transfer the suspension to centrifuge tubes, record any volume added to balance the tubes and centrifuge for 1 min at 800*g*.
5. Carefully remove the supernatant and record the total volume recovered.
6. Add detachment medium to the vessel containing ore.
7. Vortex the ore and detachment medium thoroughly for two minutes.
8. Transfer the suspension to a centrifuge tube and, record any volume added to balance the tubes and centrifuge for 1 minute at 800*g*.
9. Carefully remove the supernatant and record the total volume recovered.
10. Repeat step 6-9 twice more (total of 3 washing steps).
11. Combine the liquid recovery from steps 6-10 and set aside.
12. Repeat step 6-9 twice more, but add 0.4 %(v/v) Tween 20 to the detachment medium.
13. Combine the liquid recovered from step 12.
14. You now have effectively four liquid phases:
    i. The solution in the glass vessel surrounding the ceramic saddles.
    ii. The interstitial or 'weakly associated' cell phase.
    iii. The attached or 'strongly associated' cell phase.
    iv. The attached or 'strongly associated' cell phase (detached with Tween 20)
15. When performing cell counts you should bear in mind that the cell counting has an intrinsic 30% margin for error.

5) Calibrating the E_h meter (adapted from the CeBER analytical methods handout)

- Prepare standard solutions of ferric and ferrous sulphate with suitable concentrations e.g. 3 g/l Fe^{3+} and 1 g/l Fe^{2+}.
- Adjust, at desired temperature, pH of the solutions to the desired value with sulphuric acid
- Take aliquots of ferrous sulphate solution and add to a constant volume of ferric sulphate solution, so that the different ratios of ferric and ferrous iron are in the range from 1 to 1000
- Measure the redox potential at each addition of the solution.
- Plot redox potential against ln(Fe^{3+} / Fe^{2+}) which gives a straight line.

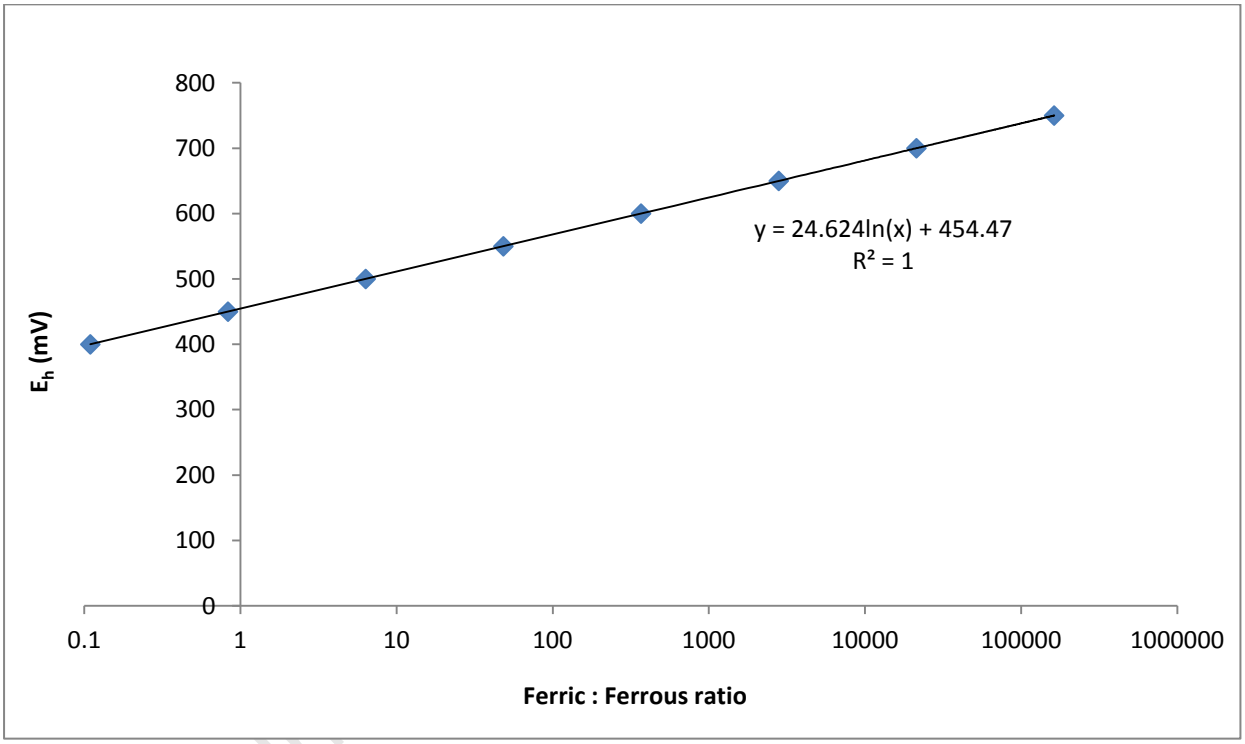

$$E_h = 454.47 + 24.624 \cdot ln\left(\frac{[Fe^{3+}]}{[Fe^{2+}]}\right)$$

Appendix C: Equations and sample calculations for data analysis

1) The stoichiometric equation and the degree of reduction balance:

Equation 1A is used to describe the bacterial oxidation of ferrous iron.

$$aCO_2 + bNH_4^+ + cO_2 + dFe^{2+} + eH^+ + 1CH_{1.8}O_{0.5}N_{0.2} + fFe^{3+} + gH_2O \quad \ldots\ldots\ldots \quad \text{Equation 1A}$$

$$-\frac{1}{d}r_{Fe^{2+}} = \frac{1}{1}r_x$$
$$-r_{Fe^{2+}} = dr_x \quad \ldots\ldots\ldots \quad \text{Equation 1B}$$

From an elemental and charge balance the following equations can be deduced:

C: a + 1 = 0 Equation 1C

H: 4b + e + 1.8 + 2g = 0 Equation 1D

O: 2a +2c + 0.5 + g = 0 Equation 1E

N: b + 0.2 = 0 Equation 1F

Fe: d + f = 0 Equation 1G

Z: b + 2d + e + 3f = 0 Equation 1H

Since there are 6 equations and 7 unknowns equation 1C to 1H were expressed as a function of d which is the coefficient of the limiting substrate. This results in the following:

a = -1

b = -0.2

c = $\frac{4.2+d}{4}$

e = 0.2 + d

f = -d

g = -0.6 - $\frac{d}{2}$

d can be expressed from the yield of biomass on ferrous iron therefore from equation 1A:

$$d = \frac{-r_{Fe^{2+}}}{r_x} = -\frac{1}{Y_{Fe^{2+}X}} \quad \text{Equation 1I}$$

Based on equation 1I the following equations representing constants a, b, c, e, f and g can be expressed as a function of the yield.

a = -1

b = -0.2

c = $-(\frac{1-4.2Y_{Fe^{2+}X}}{4Y_{Fe^{2+}X}})$

$$d = -\frac{1}{Y_{Fe^{2+}X}}$$

e = - $(\frac{1}{Y_{Fe^{2+}X}} - 0.2)$

f = $\frac{1}{Y_{Fe^{2+}X}}$

g = -$(-\frac{1}{2Y_{Fe^{2+}X}} + 0.6)$

Equation 1A can then be expressed as equation 1J which is the stoichiometric equation used to describe bacterial oxidation of ferrous iron:

$$CO_2 + 0.2NH_4^+ + \left(\frac{1-4.2Y_{sX}}{4Y_{sX}}\right)O_2 + \frac{1}{Y_{sX}}Fe^{2+} + \left(\frac{1}{Y_{sX}} - 0.2\right)H^+ \xrightarrow{bacteria} CH_{1.8}O_{0.5}N_{0.2} + \frac{1}{Y_{sX}}Fe^{3+} + \left(\frac{1}{2Y_{sX}} - 0.6\right)H_2O$$

Equation 1J

The **degree of the reduction balance** is an alternative way of expressing the conservation of electrons in the system (Ojumu, 2008).

$$\sum_{i=0}^{i} \gamma_i r_i = 0$$

Equation 1K

Table 1A: Degree of reductance of the relevant compounds (adapted from Ratledge and Kristianssen, 2001)

Compound	**Degree of reductance (γ)**
Carbon dioxide	0
Ammonium	0
Oxygen	-4
Ferrous iron	0
Hydrogen ion	0
Biomass	4.2
Ferric iron	0
Water	0

Based on equation 1K, table 1A and the stoichiometric equation (equation 1J), the degree of reduction balance can be deduces and is shown by equation 1L.

$$-r_{Fe^{2+}} = -4r_{Fe^{2+}} - 4.2r_{CO_2}$$

Equation 1L

2) Gas analysis

$$-r_j = \frac{C_{j,0}\tilde{v}_{in} - C_j\tilde{v}_{out}}{V_R}$$

$$\tilde{v}_{gas.in} \neq \tilde{v}_{gas.out}$$

$$\tilde{v}_{gas.out} = \tilde{v}_{gas.in}\frac{1-[O_2]_{in}-[CO_2]_{in}}{1-[O_2]_{out}-[CO_2]_{out}}$$

For oxygen,

$$-r_{O_2} = \frac{1}{V_R}([O_2]_{in}\tilde{v}_{gas.in} - [O_2]_{out}\tilde{v}_{gas.out})$$

$$-r_{O_2} = \frac{1}{V_R}([O_2]_{in}\tilde{v}_{gas.in} - [O_2]_{out}\tilde{v}_{gas.in}\frac{1-[O_2]_{in}-[CO_2]_{in}}{1-[O_2]_{out}-[CO_2]_{out}})$$

$$-r_{O_2} = \frac{\tilde{v}_{gas.in}}{V_R}\underbrace{([O_2]_{in} - [O_2]_{out}\frac{1-[O_2]_{in}-[CO_2]_{in}}{1-[O_2]_{out}-[CO_2]_{out}})}_{\text{dimensionless}}$$

Units for $\tilde{v}_{gas.in} = \frac{ml}{min}$ and $V_R = Litres$ need to convert the units to $\frac{mmol}{hrs.l}$;

Ideal gas law PV=nRT

$$\frac{\tilde{v}}{n} = \frac{T\times R}{P} = \frac{8.314\times 298}{101{,}325} = 24.45dm^3$$

To convert the units to $\frac{mmol}{hrs.l}$;

$\tilde{v}$ ml	mol	60mins	1dm^3	1	1000mmol
min	24.45dm^3	1hr	1000mL	V_R litres	1mol

$=\frac{\tilde{v}\times 60}{24.45}\frac{mmol}{hrs.l}$ hence;

$$-r_{O_2} = \frac{60\times\tilde{v}_{in}}{24.5\times V_R}\left\{[O_2]_{in} - [O_2]_{out}\times[\frac{1-[O_2]_{in}-[CO_2]_{in}}{1-[O_2]_{out}-[CO_2]_{out}}]\right\}$$

For carbon dioxide,

$$-r_{CO_2} = \frac{1}{V_R}([CO_2]_{in}\tilde{v}_{gas.in} - [CO_2]_{out}\tilde{v}_{gas.out})$$

$$-r_{CO_2} = \frac{1}{V_R}([CO_2]_{in}\tilde{v}_{gas.in} - [CO_2]_{out}\tilde{v}_{gas.in}\frac{1-[O_2]_{in}-[CO_2]_{in}}{1-[O_2]_{out}-[CO_2]_{out}})$$

$$-r_{CO_2} = \frac{\tilde{v}_{gas.in}}{V_R}\underbrace{([CO_2]_{in} - [CO_2]_{out}\frac{1-[O_2]_{in}-[CO_2]_{in}}{1-[O_2]_{out}-[CO_2]_{out}})}$$

$$-r_{CO_2} = \frac{60\times\tilde{v}_{in}}{24.5\times V_R}\left\{[CO_2]_{in} - [CO_2]_{out}\times[\frac{1-[O_2]_{in}-[CO_2]_{in}}{1-[O_2]_{out}-[CO_2]_{out}}]\right\}$$

$$C_x\left(\frac{mmol}{l}\right) = -r_{CO_2} \times residence\ time$$

3) Dry mass calculation

Biomass determined using the dry mass of a 900 mL culture collected from the CSTR overflow. This was done in triplicates. The dry mass per cell was first determined.

$$Dry\ mass\ per\ cell = \frac{dry\ mass\ (mg/L)}{cell\ concentration\ (cells/mL)}$$

Cell counting under a microscope was used to determine the cell concentration [cells.mL^{-1}], after which the 900 mL of culture was centrifuged and the biomass dried in an 80^{o}C oven before determining the dry mass [mg.L^{-1}].

Dry biomass is typically 50% carbon by weight (adapted from Naik (2010), Caracklis and Marshall (1990)) hence the carbon equivalent of each cell was calculated using Equation 3-12;

Cell $_{\text{carbon equivalent}}$ = 0.5 x Dry mass per cell = g_{carbon} per cell

4) Glass vessel (PBR) design calculations

Dimensions of glass vessel:

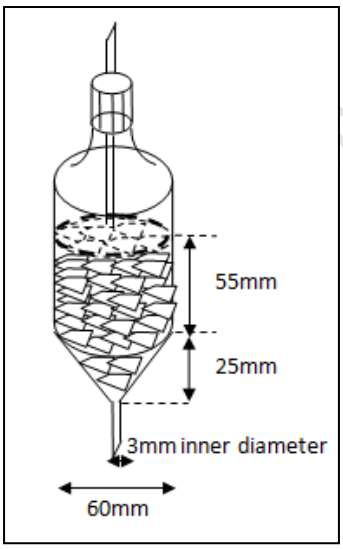

Volume occupied by ceramic saddles + voidage = Volume of frustum + volume of cylinder	
Volume of frustum	24.8 cm^3
Volume of cylinder	155cm^3
Total volume	180cm^3

Mass of saddles	123.04	g
Volume occupied by water in cylinder before adding ceramics	500	mL
Volume occupied in cylinder after adding saddles to water	550	mL
Volume occupied by saddles	50	mL
1mL=1cm^3		

From AceChemPack website for ceramics		
Normal size	12.0	mm
Surface area	647	m^2/m^3
V occupied by ceramics	180	cm^3
SA of ceramics	0.117	m^2
Mass of ceramics	123	g

Volume of a Frustum of a cone:

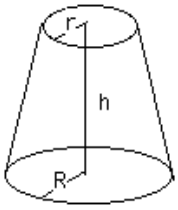

$$V = \frac{\pi h}{3}(R^2 + Rr + r^2)$$

Information obtained from:
http://jwilson.coe.uga.edu/emt725/Frustum/Frustum.cone.html (Date 08/11/2011).

Volume of a cylinder:

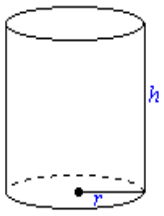

$$\mathrm{V} = \pi \mathrm{r}^2 \mathrm{h}$$

Information obtained from: http://www.mathsteacher.com.au/year9/ch14_measurement/18_cylinder/cylinder.htm (Date 08/11/2011).

Appendix D: Raw data

1) Pump calibrations

Pump for reactor 1 (Backup reactor)

Time in 10 minutes

Setpoint	Volume (ml)	Time (mins)	Flow (ml/h)
1.0	1.6	10	9.6
1.2	2.8	10	16.8
1.4	4.1	10	24.6
1.6	5.6	10	33.6
1.8	7.2	10	43.2
2.0	8.3	10	49.8
2.2	9.8	10	58.8
2.4	11.4	10	68.4

D (F/V)	F (ml/hr)	Res time (h^{-1})	Set point
0.018	18.18	**55.00**	1.23
0.021	20.83	**48.00**	1.29
0.029	28.57	**35.00**	1.47
0.042	41.67	**24.00**	1.78
0.063	62.50	**16.00**	2.28
0.077	76.92	**13.00**	2.62
0.100	100.00	**10.00**	3.17
0.125	125.00	**8.00**	3.77
0.167	166.67	**6.00**	4.76
0.250	250.00	**4.00**	6.74

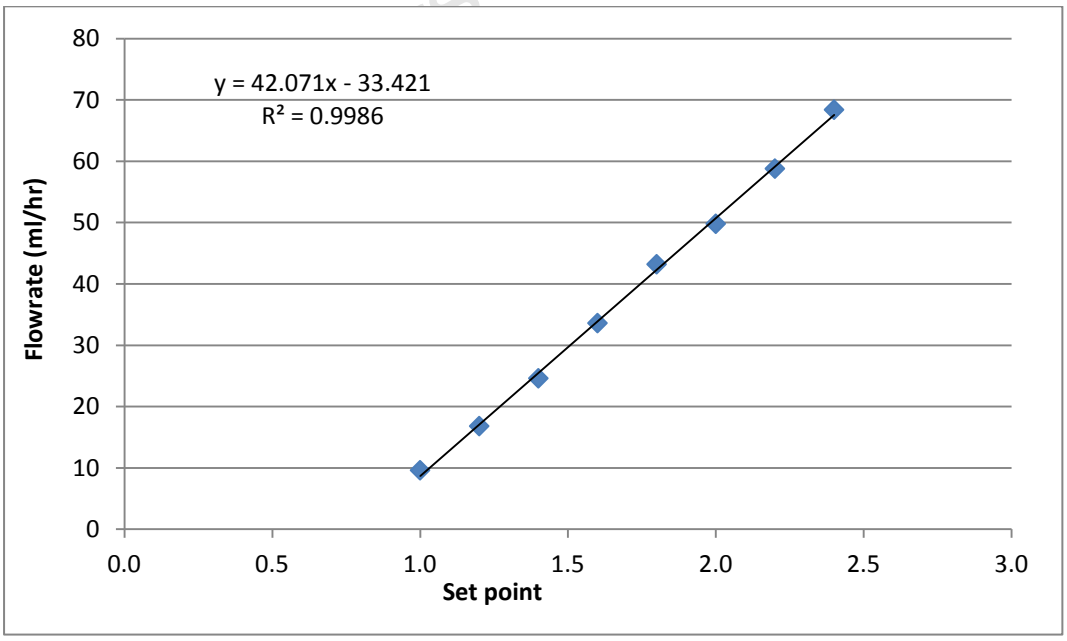

Pump for reactor 2

set pt	time (s) to fill 5mL	time hrs	flowrate mL/hr
1	1491	0.4142	12
1.4	622	0.1728	29
1.8	406	0.1128	44
2.2	298	0.0828	60
2.6	236	0.0656	76
3	190	0.0528	95
3.4	163	0.0453	110
3.8	145	0.0403	124
4.2	127	0.0353	142
4.6	115	0.0319	157
5	103	0.0286	175

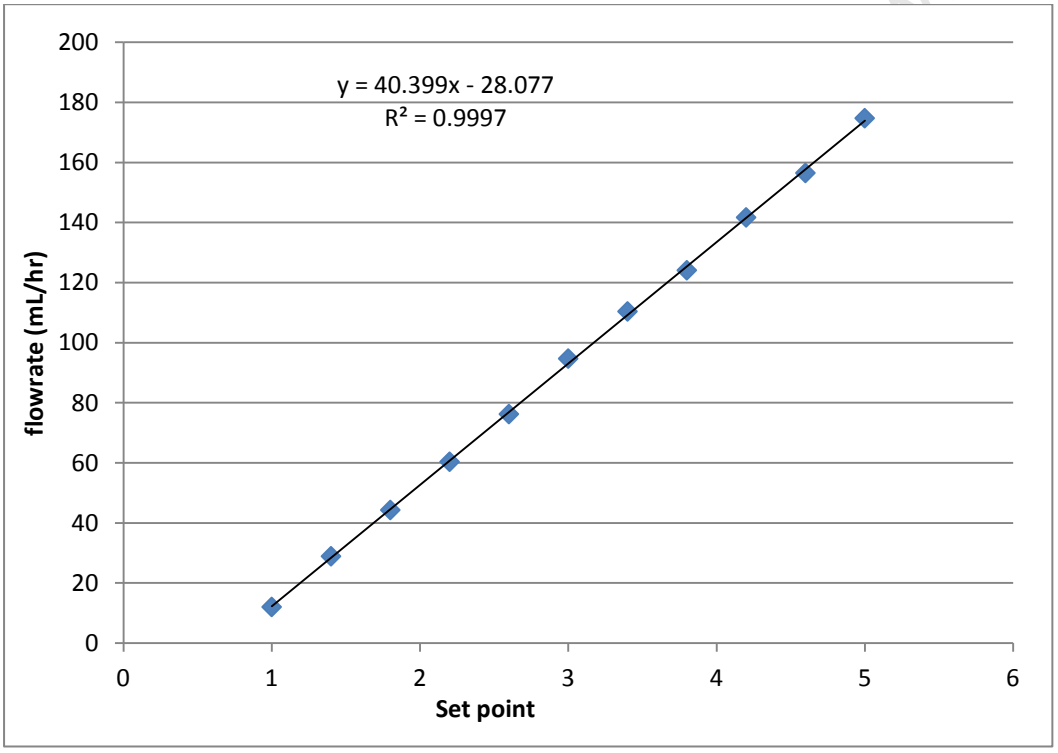

Pump for reactor 3

set pt	time (s) to fill 5mL	time hrs	flowrate mL/hr
1	1661	0.461	10.8
1.2	898	0.249	20.0
1.4	654	0.182	27.5
1.6	486	0.135	37.0
1.8	404	0.112	44.6
2	341	0.095	52.8
2.2	288	0.080	62.5
2.4	247	0.069	72.9
2.6	233	0.065	77.3
2.8	214	0.059	84.1
3	186	0.052	96.8
3.2	172	0.048	104.7
3.4	161	0.045	111.8
3.6	149	0.041	120.8
3.8	139	0.039	129.5
4	132	0.037	136.4

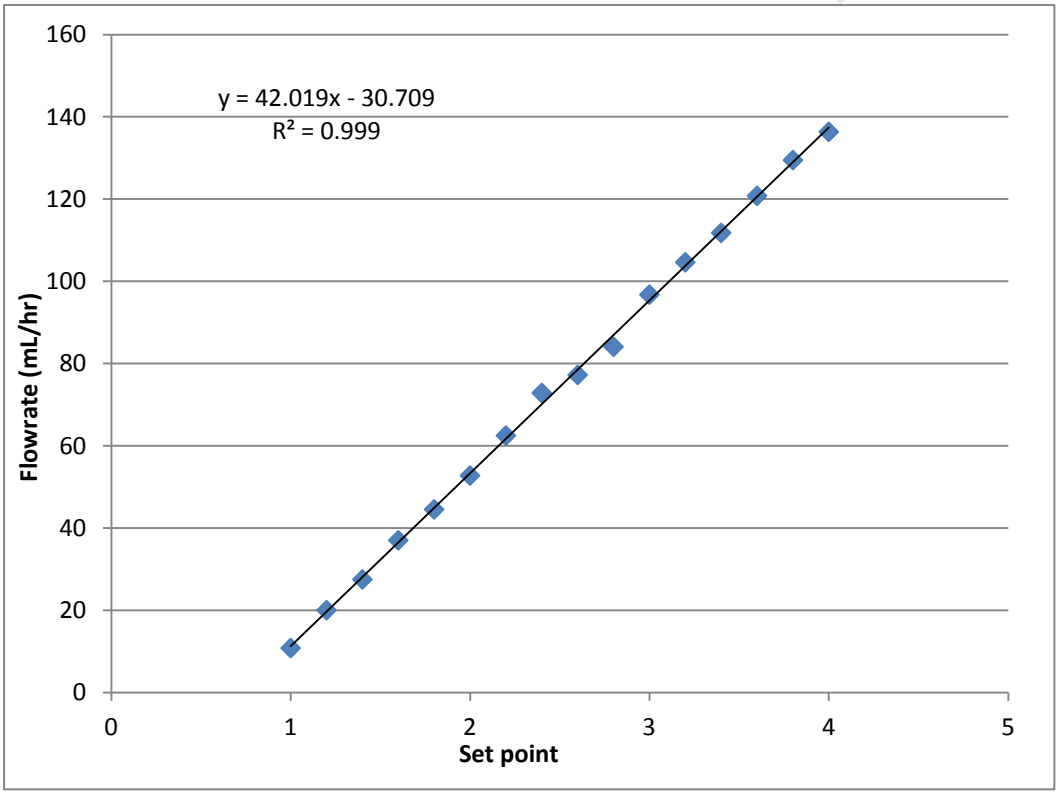

Pump for recycle loop to the PBR (glass vessel) at low recycle ratio

Set pt	vol (mL)	time (sec)	flow (ml/sec)	flow (ml/hr)
1.0	3	647	0.0046	16.69
1.2	3	422	0.0071	25.59
1.4	3	321	0.0093	33.64
1.6	3	259	0.0116	41.70
1.8	3	217	0.0138	49.77
2.0	3	183	0.0164	59.02
2.2	3	158	0.0190	68.35
2.4	3	140	0.0214	77.14
2.6	3	126	0.0238	85.71
2.8	3	115	0.0261	93.91
3.0	3	107	0.0280	100.93

	Set pt	Pump	Flow (mL/hr)	ratio	Flow (L/day)
	9	2	358	11.5	8.60
	1.47	3	31.3		0.75
4hrs	6.64	3	250	1.4	6.0
5hrs	5.29	3	200	1.8	4.8

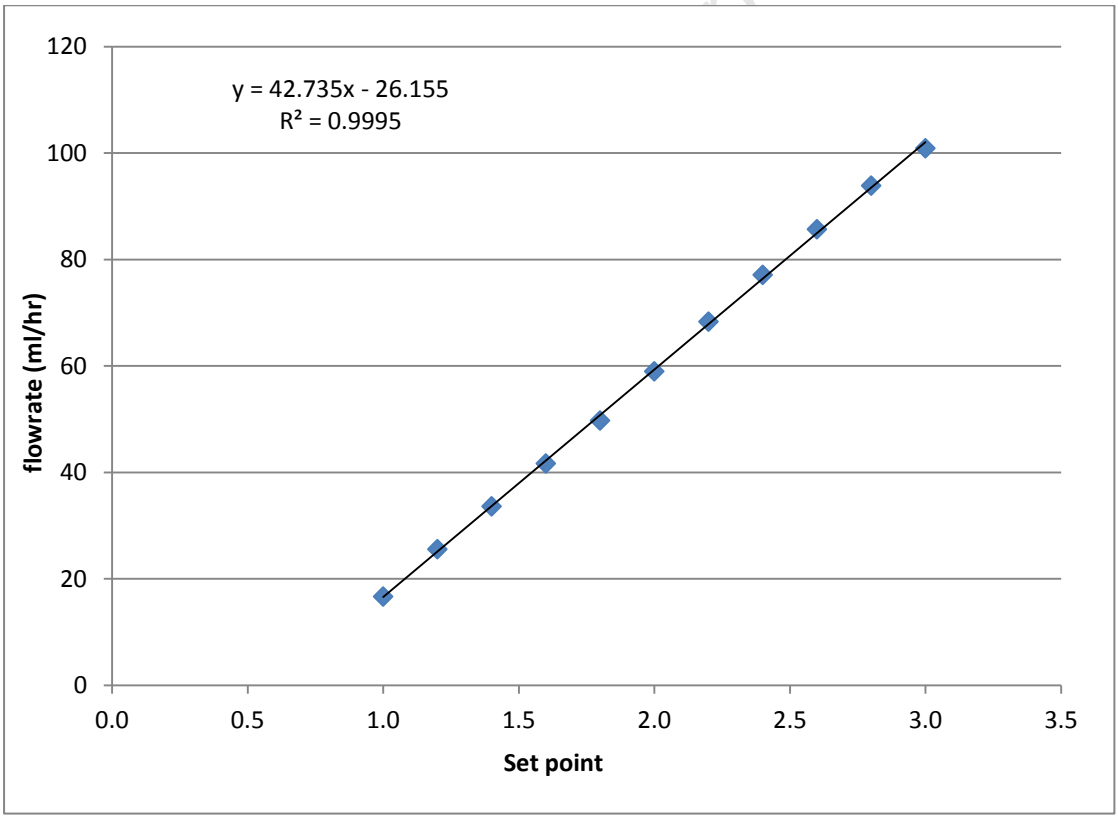

Pump for recycle loop to the PBR (glass vessel) at high recycle ratio

Set pt	Time	Time (s)	Time (hr)	Flowrate (ml/s)	Flowrate (ml/hr)
1	2.35	155	0.0431	0.065	232
1.2	1.43	103	0.0286	0.097	350
1.4	1.19	79	0.0219	0.127	456
1.6	1.03	63	0.0175	0.159	571
1.8	0.54	54	0.0150	0.185	667
2	0.45	45	0.0125	0.222	800
2.5	0.34	34	0.0094	0.294	1059
3	0.27	27	0.0075	0.370	1333
3.5	0.22	22	0.0061	0.455	1636
4	0.19	19	0.0053	0.526	1895
5	0.15	15	0.0042	0.667	2400
6	0.12	12	0.0033	0.833	3000
7	0.1	10	0.0028	1.000	3600

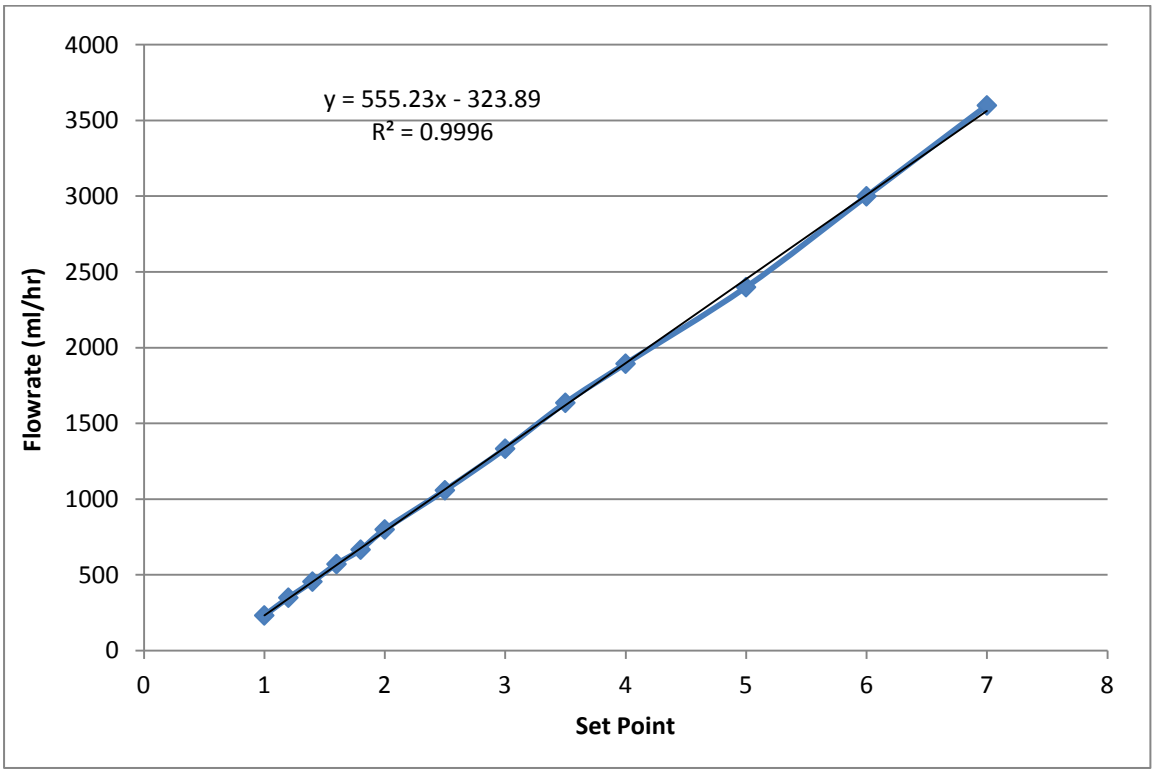

2) Maximum growth rate

	time	time (hrs)	cell counts				Eh (mV)	cell concentration x10^6	Ln [cells]
t_0	10h15	0	38	34	32	41	472	45	3.814
t_1	11h15	1	41	40	46	27	471	48	3.874
t_2	12h15	2	29	36	42	28	476	42	3.742
t_3	13h15	3	26	33	28	28	482	36	3.582
t_4	14h15	4	32	27	35	30	489	39	3.657
t_5	16h15	5	50	51	48	45	512	61	4.105
t_6	17h15	6	51	52	47	50	542	63	4.135
t_7	18h15	7	50	49	56	52	613	65	4.170
t_8	19h15	8	41	42	40	37	636	50	3.912
t_9	20h15	9	66	45	67	53	662	72	4.279
t_{10}	21h15	10	51	57	52	52	664	66	4.193

3) Solubility of CO_2

CO2 calculations

HCO2	0.0317	m3atm/mol		K1	5.01E-07
Ptot	1	atm		K2	5.62E-11
xCO2	3.50E-04				
CO2 aq	1.10E-05	mol/L	4.86E-01	mg/L	

pH	[H+]	[H2CO3]	[HCO3-]	[CO32-]	total
1	0.1	1.10E-05	5.53E-11	3.11E-20	1.10E-05
2	0.01	1.10E-05	5.53E-10	3.11E-18	1.10E-05
3	1.00E-03	1.10E-05	5.53E-09	3.11E-16	1.10E-05
4	1.00E-04	1.10E-05	5.53E-08	3.11E-14	1.11E-05
5	1.00E-05	1.10E-05	5.53E-07	3.11E-12	1.16E-05
6	1.00E-06	1.10E-05	5.53E-06	3.11E-10	1.66E-05
7	1.00E-07	1.10E-05	5.53E-05	3.11E-08	6.64E-05
8	1.00E-08	1.10E-05	5.53E-04	3.11E-06	5.67E-04
9	1.00E-09	1.10E-05	5.53E-03	3.11E-04	5.85E-03
10	1.00E-10	1.10E-05	5.53E-02	3.11E-02	8.64E-02
11	1.00E-11	1.10E-05	5.53E-01	3.11E+00	3.66E+00
12	1.00E-12	1.10E-05	5.53E+00	3.11E+02	3.16E+02
13	1.00E-13	1.10E-05	5.53E+01	3.11E+04	3.11E+04
14	1.00E-14	1.10E-05	5.53E+02	3.11E+06	3.11E+06

4) Planktonic experiments

Residence time	D (hr^{-1})	E_h (mV)	rCO_2	C_x off-gas	rFe^{2+}	qFe^{2+}	qFe^{2+} dry mass	C_x dry mass
55	0.0182	759	0.0414	2.276	1.70	0.75	4	0.478
40	0.0250	753	0.0210	0.841	2.33	2.78	5	0.498
32	0.0313	750	0.0721	2.308	2.84	1.23	6	0.496
24	0.0417	752	0.0248	0.596	3.78	6.33	8	0.447
16	0.0625	747	0.0404	0.647	5.66	8.75	13	0.445
15	0.0667	752	0.0367	0.550	5.83	10.60	13	0.461
14	0.0714	752	0.0429	0.600	6.27	10.44	19	0.337
13	0.0769	754	0.1112	1.446	7.31	5.06	29	0.250
12	0.0833	745	0.1428	1.713	7.53	4.40	25	0.297
11	0.0909	757	0.1558	1.714	8.24	4.81	56	0.146
10	0.1000	747	0.1542	1.542	9.96	6.46	64	0.155
9	0.1111	738	0.1539	1.385	10.85	7.83	81	0.133
8	0.1250	744	0.1738	1.390	12.54	9.02	122	0.103
7	0.1429	578	0.0886	0.620	14.35	23.15	154	0.093
6	0.1667	565	0.0932	0.559	15.86	28.35	127	0.124
5	0.2000	501	0.0974	0.487	16.57	34.02	316	0.052
4	0.2500	475	0.0952	0.381	16.68	43.80	491	0.034

Off-gas data (Example of the off gas data from planktonic experiments at a 4 hr residence time (steady state values)

Air In			Air Out				
Date	**Time**	**CO_2 (ppm)**	**Date**	**Time**	**CO_2 (ppm)**	**rCO_2**	**C_x**
2011/05/07	10:57:15 AM	323.24	2011/05/07	11:22:45 AM	291.34	0.041161	0.164643
2011/05/07	10:57:25 AM	325.22	2011/05/07	11:22:56 AM	291.22	0.043741	0.174965
2011/05/07	10:57:35 AM	327.49	2011/05/07	11:23:06 AM	291.21	0.046545	0.18618
2011/05/07	10:57:45 AM	329.41	2011/05/07	11:23:16 AM	291.19	0.048926	0.195705
2011/05/07	10:57:56 AM	331.44	2011/05/07	11:23:26 AM	291.10	0.051529	0.206117
2011/05/07	10:58:06 AM	333.46	2011/05/07	11:23:36 AM	290.70	0.054502	0.218007
2011/05/07	10:58:16 AM	335.37	2011/05/07	11:23:47 AM	290.36	0.057250	0.228998
2011/05/07	10:58:26 AM	337.31	2011/05/07	11:23:57 AM	290.23	0.059801	0.239205
2011/05/07	10:58:36 AM	338.78	2011/05/07	11:24:07 AM	290.17	0.061676	0.246703
2011/05/07	10:58:46 AM	340.77	2011/05/07	11:24:17 AM	290.15	0.064147	0.256588
2011/05/07	10:58:57 AM	342.33	2011/05/07	11:24:27 AM	290.15	0.066056	0.264224
2011/05/07	10:59:07 AM	344.08	2011/05/07	11:24:37 AM	290.14	0.068219	0.272875
2011/05/07	10:59:17 AM	345.62	2011/05/07	11:24:48 AM	290.14	0.070115	0.280458
2011/05/07	10:59:27 AM	346.98	2011/05/07	11:24:58 AM	290.08	0.071852	0.287407
2011/05/07	10:59:37 AM	348.47	2011/05/07	11:25:08 AM	289.99	0.073790	0.29516
2011/05/07	10:59:47 AM	350.09	2011/05/07	11:25:18 AM	289.83	0.075970	0.30388
2011/05/07	10:59:58 AM	351.11	2011/05/07	11:25:28 AM	289.58	0.077528	0.310112
2011/05/07	11:00:08 AM	352.55	2011/05/07	11:25:38 AM	289.44	0.079471	0.317885
2011/05/07	11:00:18 AM	353.76	2011/05/07	11:25:49 AM	289.30	0.081129	0.324517
2011/05/07	11:00:28 AM	354.94	2011/05/07	11:25:59 AM	289.13	0.082780	0.331122
2011/05/07	11:00:38 AM	355.72	2011/05/07	11:26:09 AM	289.13	0.083739	0.334958
2011/05/07	11:00:49 AM	356.87	2011/05/07	11:26:19 AM	289.10	0.085188	0.340751
2011/05/07	11:00:59 AM	357.98	2011/05/07	11:26:29 AM	289.07	0.086586	0.346345
2011/05/07	11:01:09 AM	358.77	2011/05/07	11:26:39 AM	289.07	0.087557	0.350228
2011/05/07	11:01:19 AM	359.52	2011/05/07	11:26:50 AM	289.02	0.088535	0.354141

2011/05/07	11:01:29 AM	360.56	2011/05/07	11:27:00 AM	288.98	0.089862	0.359447
2011/05/07	11:01:39 AM	361.49	2011/05/07	11:27:10 AM	288.87	0.091130	0.36452
2011/05/07	11:01:50 AM	362.21	2011/05/07	11:27:20 AM	288.75	0.092165	0.368662
2011/05/07	11:02:00 AM	362.85	2011/05/07	11:27:30 AM	288.62	0.093107	0.372426
2011/05/07	11:02:10 AM	363.66	2011/05/07	11:27:41 AM	288.42	0.094347	0.377387
2011/05/07	11:02:20 AM	363.88	2011/05/07	11:27:51 AM	288.30	0.094765	0.379059
2011/05/07	11:02:30 AM	364.66	2011/05/07	11:28:01 AM	288.31	0.095718	0.382874
2011/05/07	11:02:40 AM	365.19	2011/05/07	11:28:11 AM	288.19	0.096512	0.386047
2011/05/07	11:02:51 AM	365.83	2011/05/07	11:28:21 AM	288.23	0.097245	0.388979
2011/05/07	11:03:01 AM	366.44	2011/05/07	11:28:31 AM	288.28	0.097928	0.391713
2011/05/07	11:03:11 AM	366.89	2011/05/07	11:28:42 AM	288.23	0.098544	0.394176
2011/05/07	11:03:21 AM	367.33	2011/05/07	11:28:52 AM	288.17	0.099160	0.396639
2011/05/07	11:03:31 AM	367.93	2011/05/07	11:29:02 AM	288.19	0.099870	0.399482
2011/05/07	11:03:42 AM	367.96	2011/05/07	11:29:12 AM	288.15	0.099953	0.39981
2011/05/07	11:03:52 AM	368.15	2011/05/07	11:29:22 AM	288.11	0.100232	0.400929
2011/05/07	11:04:02 AM	368.84	2011/05/07	11:29:32 AM	288.08	0.101122	0.404487
2011/05/07	11:04:12 AM	369.11	2011/05/07	11:29:43 AM	288.03	0.101507	0.40603
2011/05/07	11:04:22 AM	369.60	2011/05/07	11:29:53 AM	288.03	0.102111	0.408442
2011/05/07	11:04:32 AM	370.05	2011/05/07	11:30:03 AM	288.02	0.102677	0.410708
2011/05/07	11:04:43 AM	370.10	2011/05/07	11:30:13 AM	288.02	0.102731	0.410923
2011/05/07	11:04:53 AM	370.22	2011/05/07	11:30:23 AM	288.02	0.102889	0.411556
2011/05/07	11:05:03 AM	370.73	2011/05/07	11:30:34 AM	288.02	0.103520	0.414078
2011/05/07	11:05:13 AM	371.08	2011/05/07	11:30:44 AM	288.02	0.103949	0.415795
2011/05/07	11:05:23 AM	371.16	2011/05/07	11:30:54 AM	288.01	0.104047	0.416187
2011/05/07	11:05:34 AM	371.20	2011/05/07	11:31:04 AM	288.02	0.104102	0.416407
2011/05/07	11:05:44 AM	371.43	2011/05/07	11:31:14 AM	288.03	0.104368	0.41747
2011/05/07	11:05:54 AM	371.87	2011/05/07	11:31:24 AM	288.03	0.104903	0.41961
2011/05/07	11:06:04 AM	372.12	2011/05/07	11:31:35 AM	288.04	0.105205	0.42082
2011/05/07	11:06:14 AM	372.22	2011/05/07	11:31:45 AM	288.03	0.105323	0.421291

2011/05/07	11:06:24 AM	372.22
2011/05/07	11:06:35 AM	372.22
2011/05/07	11:06:45 AM	372.22
2011/05/07	11:06:55 AM	372.22
2011/05/07	11:07:05 AM	372.24
2011/05/07	11:07:15 AM	372.33
2011/05/07	11:47:58 AM	340.14
2011/05/07	11:48:08 AM	342.05
2011/05/07	11:48:18 AM	344.09
2011/05/07	11:48:29 AM	345.94
2011/05/07	11:48:39 AM	347.46
2011/05/07	11:48:49 AM	349.31
2011/05/07	11:48:59 AM	350.79
2011/05/07	11:49:09 AM	352.37
2011/05/07	11:49:19 AM	353.75
2011/05/07	11:49:30 AM	355.01
2011/05/07	11:49:40 AM	356.02
2011/05/07	11:49:50 AM	357.36
2011/05/07	11:50:00 AM	358.47
2011/05/07	11:50:10 AM	359.41
2011/05/07	11:50:20 AM	360.36
		365.06

2011/05/07	11:31:55 AM	288.03
2011/05/07	11:32:05 AM	288.02
2011/05/07	11:32:15 AM	288.02
2011/05/07	11:32:25 AM	288.03
2011/05/07	11:32:36 AM	288.01
2011/05/07	11:32:46 AM	288.02
2011/05/07	12:13:29 PM	286.95
2011/05/07	12:13:39 PM	286.95
2011/05/07	12:13:49 PM	286.95
2011/05/07	12:13:59 PM	286.95
2011/05/07	12:14:09 PM	286.94
2011/05/07	12:14:19 PM	286.95
2011/05/07	12:14:30 PM	286.94
2011/05/07	12:14:40 PM	286.95
2011/05/07	12:14:50 PM	286.94
2011/05/07	12:15:00 PM	286.94
2011/05/07	12:15:10 PM	286.94
2011/05/07	12:15:21 PM	286.91
2011/05/07	12:15:31 PM	286.92
2011/05/07	12:15:41 PM	286.91
2011/05/07	12:15:51 PM	286.89
		289.13

	0.105337	0.421348
	0.105342	0.421369
	0.105341	0.421364
	0.105334	0.421338
	0.105375	0.421499
	0.105486	0.421944
	0.067283	0.269133
	0.069620	0.27848
	0.072129	0.288517
	0.074403	0.297613
	0.076266	0.305066
	0.078539	0.314156
	0.080352	0.32141
	0.082288	0.32915
	0.083982	0.335928
	0.085530	0.342119
	0.086783	0.347132
	0.088456	0.353825
	0.089809	0.359237
	0.090968	0.363874
	0.092163	0.368651
ave	0.09520	0.381
stdev	0.0141	0.0564
number	1755	1755
error	0.000337	0.001347

5) Dry mass data

Cell count of overflow cells/mL	Dry wt (mg/l)	Cell dry wt g/cell	Cell carbon equivalent gcarbon/cell	Cell carbon equivalent gmolcarbon/cell
185 x 10^6	10.4	5.65E-14	2.82E-14	2.35E-15
	17.1	9.25E-14	4.62E-14	3.85E-15
	15.4	8.35E-14	4.17E-14	3.48E-15
Average				**3.23E-15**
Standard deviation				**7.81E-16**
Error				**4.51E-16**

*Biomass concentration is the product of the carbon equivalent (gmolC per cell) and the cell concentration for each respective dilution rate

6) Attachment experiments

Eh	pH	cell counts in CSTR							PBR solution cell counts					
		a	b	c	d	$x10^6$conc (cells/ml)	$x10^9$cell no.	error $x10^9$	a	b	c	d	$x10^6$conc (cells/ml)	$x10^9$cell no.
759	1.336	136	141	152	143	178.8	178.75	168.65	124	130	115	114	151	20
742	1.392	105	110	112	118	139.1	139.06	26.05	126	132	108	110	149	19
763	1.313	138	156	153	155	188.1	188.13	**15.04**	161	163	138	170	198	26
755	1.273	148	126	116	126	161.3	161.25	148.13	130	128	122	148	165	21
748	1.379	134	94	128	146	156.9	156.88	19.07	146	106	130	112	154	20
758	1.367	112	100	82	110	126.3	126.25	**11.01**	114	116	118	108	143	19
751	1.404	96	132	90	98	130.0	130.00	122.29	90	120	86	106	126	16
757	1.474	92	106	94	98	121.9	121.88	7.51	92	78	94	98	113	15
755	1.434	88	94	98	88	115.0	115.00	**4.34**	88	84	86	94	110	14
753	1.368	116	108	116	96	136.3	136.25	111.88	98	92	94	84	115	15
751	1.364	82	72	106	82	106.9	106.88	22.30	66	64	63	73	83	11
750	1.330	84	77	60	75	92.5	92.50	**12.87**	146	112	142	128	165	21
755	1.374	160	148	132	138	180.6	180.63	176.04	116	106	104	108	136	18
746	1.271	146	132	80	132	153.1	153.13	21.00	142	156	156	146	188	24
740	1.432	152	178	126	166	194.4	194.38	**12.13**	156	128	122	128	167	22
748	1.392	50	43	39	50	56.9	56.88	96.67	80	86	90	86	107	14
746	1.407	84	64	62	88	93.1	93.13	41.68	138	122	94	120	148	19
747	1.435	110	118	114	106	140.0	140.00	**24.06**	110	106	78	112	127	16

Interstitial cell count							weakly attached cell count						
a	b	c	d	x10^{6}conc (cells/ml)	x10^{9}cell no.	error x10^9	a	b	c	d	x10^{6}conc (cells/ml)	x10^{6}cell no.	error x10^9
25	22	24	20	28	1.34	1.20	10	3	5	6	8	1058	2.86
18	17	24	16	23	1.10	0.12	27	33	27	31	37	5199	2.12
24	23	16	17	25	1.18	**0.07**	22	12	9	10	17	2335	**1.22**
20	19	19	23	25	1.19	1.20	4	4	3	1	4	529	0.66
25	13	20	17	23	1.10	0.11	14	4	1	1	6	881	0.19
27	16	27	20	28	1.32	**0.06**	6	2	2	3	4	573	**0.11**
17	15	13	13	18	1.09	1.16	6	4	0	1	3	619	0.54
16	14	16	12	18	1.09	0.12	3	4	1	1	3	506	0.06
22	14	19	14	22	1.29	**0.07**	5	2	2	0	3	506	**0.04**
10	12	8	12	13	0.79	0.98	6	3	2	0	3	619	0.84
17	13	12	15	18	1.07	0.17	4	2	3	0	3	506	0.49
15	14	13	16	18	1.09	**0.10**	10	5	6	4	8	1406	**0.28**
20	22	19	22	26	1.56	1.95	19	7	7	8	13	2306	2.68
32	33	30	31	39	2.36	0.40	27	17	16	12	23	4050	1.23
29	21	20	33	32	1.93	**0.23**	16	3	4	7	9	1688	**0.71**
30	24	26	23	32	1.93	2.69	16	10	12	9	15	2644	2.14
62	39	42	39	57	3.41	0.74	22	7	8	7	14	2475	0.74
39	32	32	42	45	2.72	**0.43**	14	2	3	4	7	1294	**0.42**

strongly attached cell count							x10^{6}Total cells	x10^6 cells per m^2	x10^6 cells per g	x10^6 cells per g average	error
a	b	c	d	x10^{6}conc (cells/ml)	x10^{9}cell no.	error x10^9					
34	28	12	13	27	4	4.14	6228	53226	62		
20	21	23	19	26	4	0.69	9958	85112	100	**82**	18.8
35	30	27	20	35	5	**0.40**	8445	72182	84		10.8
39	39	32	28	43	6	12.59	7799	66659	78		
200	146	132	98	180	25	11.08	27363	233870	274	**145**	111.8
45	44	25	29	45	6	**6.40**	8196	70048	82		64.6
54	59	54	48	67	12	10.97	13800	117949	112		
50	44	42	36	54	10	1.22	11269	96314	92	**103**	10.5
56	50	40	52	62	11	**0.70**	12938	110577	105		6.0
32	26	24	25	33	6	8.42	7425	63462	60		
38	24	22	167	78	14	4.96	15694	134135	128	**83**	38.4
26	21	24	20	28	5	**2.86**	7613	65064	61.89		22.2
67	53	45	41	64	12	9.11	15450	132051	125.61		
51	29	41	24	45	8	2.16	14569	124519	118.45	**112**	18.2
44	36	25	30	42	8	**1.25**	11213	95833	91.16		10.5
60	47	29	32	53	9	8.70	14025	119872	114.02		
50	36	31	23	44	8	0.79	13763	117628	111.89	**110**	5.3
46	50	21	39	49	9	**0.46**	12788	109295	103.96		3.1

7) Sessile Experiments (example using low recycle ratio data)

4hrs					
time (days)	E_h	[Fe3+]/[Fe2+]	pH	Concentration cells/mL	Rate (-rFe^{2+}) mmol/l.h
0.00	732	78489	1.33	191.9	22.8
0.04	506	8	1.32	141.9	20.2
0.08	491	4	1.325	129.4	17.8
0.13	477	2	1.26	113.8	14.8
0.17	466	2	1.28	90.9	12.9
0.21	460	1	1.48	81.9	10.9
0.40	439	1	1.3	34.7	5.7
1.10	403	0	1.31	4.1	0.6
2.19	403	0	1.29	10.0	1.1
3.00	413	0	1.23	10.9	3.2
3.96	420	0	1.201	22.8	3.7
5.00	415	0	1.242	31.6	4.4
5.94	428	0	1.245	19.4	5.3
6.98	435	0	1.253	27.2	6.2
8.06	445	1	1.243	41.3	8.3
9.06	453	1	1.3	27.2	10.4
9.90	460	1	1.353	22.5	12.5
11.04	469	2	1.28	55.9	13.5
12.00	475	2	1.296	26.3	13.8
13.00	479	3	1.327	40.3	15.1
13.98	483	3	1.386	55.0	15.5
14.98	483	3	1.347	57.2	15.6
16.90	487	4	1.311	73.1	17.1
17.94	488	4	1.392	63.4	17.1
18.90	483	3	1.341	72.2	17.1
19.90	491	4	1.34	60.0	17.5
20.88	483	3	1.357	74.1	16.5
22.02	484	3	1.399	75.6	18.5
22.99	488	4	1.395	73.8	18.1
23.01	489	4	1.364	66.6	17.9
23.03	487	4	1.365	68.8	18.0

5hrs					
time (days)	Eh	[Fe3+]/[Fe2+]	pH	Concentration cells/mL	Rate (-rFe^{2+}) mmol/l.h
0.00	730	72366	1.443	168	18.54
0.04	729	69486	1.517	125	18.52
0.08	532	23	1.526	113	18.48
0.13	497	6	1.517	89	18.38
0.17	487	4	1.511	79	17.23
0.21	479	3	1.498	54	15.75
0.29	464	1	1.579	48	11.17
0.85	439	1	1.303	19	7.19
0.94	439	1	1.288	19	8.15
1.02	441	1	1.304	14	8.01
1.10	441	1	1.283	15	7.90
1.85	460	1	1.255	18	10.30
1.96	463	1	1.233	18	11.11
2.08	463	1	1.272	11	11.30
2.85	475	2	1.285	48	12.83
3.06	477	2	1.276	25	15.73
3.90	484	3	1.24	37	17.04
4.18	487	4	1.211	29	14.81
4.85	492	5	1.295	33	17.88
6.90	514	11	1.268	36	17.11
7.17	513	11	1.292	32	18.65
8.19	517	13	1.307	55	17.97
8.90	510	10	1.317	49	17.12
8.96	513	11	1.246	47	17.01
9.02	517	13	1.305	61	17.44
10.08	521	15	1.417	47	18.07
10.93	526	18	1.567	56	18.10
13.07	532	23	1.359	43	18.06
13.96	534	25	1.328	44	18.08
15.17	534	25	1.32	36	17.96
15.92	539	31	1.372	29	17.64
16.94	536	27	1.347	38	17.57
18.21	535	26	1.361	50	17.52
19.90	533	24	1.348	42	17.51
19.93	532	23	1.356	38	17.42
19.96	533	24	1.346	33	17.21

8) Detachment data

		cell counts in reactor					
		a	b	c	d	x10^{6}conc (cells/ml)	x10^{9}cell no.
mine	5hrs	23	28	41	29	38	38
project students	5hrs	78	81	164	115	137	137
	32hrs	113	111	103	112	137	137
	4hrs	51	58	56	57	70	70

cell counts in glass vessel					
a	b	c	d	x10^{6}conc (cells/ml)	x10^{9}cell no.
60	149	88	87	120	16
216	140	122	206	214	28
118	113	108	114	141	18
400	455	485	400	544	71

interstitial cell count					
a	b	c	d	x10^{6}conc (cells/ml)	x10^{9}cell no.
512	532	496	440	619	37.13
1325	1385	1320	1410	1700	102.00
24.9	20.2	21.1	21.4	27	1.64
84	97	100	93	117	7.01

weakly attached cell count					
a	b	c	d	x10^{6}conc (cells/ml)	x10^{9}cell no.
100	125	100	95	131	24
444	450	468	462	570	103
13	6.9	6.2	5.8	10	1.8
61	50	57	51	68	12

strongly attached cell count					
a	b	c	d	x10^{6}conc (cells/ml)	x10^{9}cell no.
69	73	52	51	77	14
192	126	150	144	191	34
53	44	36	41	54	10
79	65	56	50	78	14

$x10^6$Total cells	$x10^6$ cells per m^2	$x10^6$ cells per g
74531	637019	605.95
239025	2042949	1943.29
13185	112696	107.20
33394	285417	271.49

Appendix E: Material safety data

1,10 - Phenanthroline monohydrate

Information obtained from: http://www.sciencelab.com/msds.php?msdsId=9927689 (08/11/2011)

Hazards

Can be harmful if inhaled, in contact with the eyes and if ingested. Toxic to lungs and mucous membranes.

Personal Protective equipment

Always wear safety gloves when handling the chemical

Ammonium acetate

Information obtained from: http://www.labchem.net/msds/75012.pdf (08/11/2011)

Hazards

May cause severe eye and skin irritation with burns. May also cause severe respiratory tract irritation with personal burns. Do not inhale or ingest as it is ma cause headaches, sore throats, vomiting, coughing or weakness amongst other symptoms.

Personal Protective equipment

Use in a ventilated area and wear protective clothing and gloves to prevent exposure to the skin. Wear splash proof safety glasses.

Ferrous sulphate heptahydrate

Information obtained from: http://www.sciencelab.com/msds.php?msdsId=9924057 (08/11/2011)

Hazards

Hazardous if in contact with the skin and eyes. It should not be ingested or inhaled.

Personal Protective equipment

Wear splash goggles, lab coat and safety gloves when handling.

Sulphuric acid

Information obtained from: http://www.ee.iitb.ac.in/~nanoe/msds/sulphuric%20acid.pdf 08/11/2011)

Hazards

Corrosive therefore should not be exposed to the eyes and skin. Should not be inhaled. May explode when in contact with other chemicals such as carbides or even water if not handled well.

Personal Protective equipment

Wear a lab coat, protective gloves, and closed shoes. Only use in a well ventilated area (i.e acid fume cupboard).

Hydroxylamine hydrochloride

Information obtained from: http://www.sciencelab.com/msds.php?msdsId=9927192 (08/11/2011)

Hazards

Do not expose to the skin, eyes and do not ingest. Decomposes violently or explosively when heated above 140^{o}C.

Personal Protective equipment

Wear splash goggles, boots and gloves.